TOWARDS THE DEVELOPMENT OF BIOSENSORS FOR THE DETECTION OF MICROBIOLOGICALLY INFLUENCED CORROSION (MIC)

A Dissertation

by

PRANAV KANNAN

Submitted to the Office of Graduate and Professional Studies of
Texas A&M University
in partial fulfillment of the requirements for the degree of

DOCTOR OF PHILOSOPHY

Chair of Committee,	Sreeram Vaddiraju
Co-Chair of Committee	M. Sam Mannan
Committee Members,	Arul Jayaraman
	Homero Castaneda
	Martin A. Wortman
Head of Department,	M. Nazmul Karim

August 2018

Major Subject: Chemical Engineering

ABSTRACT

Corrosion is one of the biggest concerns for mechanical integrity of infrastructure and infrastructural components, such as oil refineries, bridges and roads. The economic cost of corrosion is typically estimated to be between 1 to 5 % of the gross national product (GNP) of countries, of which the contribution of microbiologically influenced corrosion (MIC) is estimated to be between 10% and 50%. Current state-of-the-art approaches for detecting MIC primarily rely on *ex-situ* tests, including bacterial test kits (bug bottles); corrosion coupons, pigging deposits analysis and destructive analysis of MIC affected sites using SEM, TEM, and XRD. These *ex-situ* measurements do not capture the complexities and time sensitivities underlying MIC. This is owed to the fact that the proliferation of the microbial contamination is a dynamic and rapid process, and any delay can prove expensive as it is estimated that once the biofilm formation takes place the amount of biocides needed is magnitude of orders more as compared to when the bacteria are in planktonic form. Additionally, the field environment is a complex biotic and abiotic environment which is often difficult to replicate even in high fidelity laboratory models. Hence a real-time/pseudo real-time method of detection would greatly help reduce the costs and optimize biocide-based mitigation of MIC. To overcome the above-mentioned shortcomings associated with the state-of-the-art; this work is aimed at the development of a sensor substrate whereby highly specific detection can be carried out in the environment where the corrosion exists, in a real-time/pseudo real-time basis. More specifically, the research is aimed at the development of sensors based on a nanowire matrix functionalized with biomolecules which can perform this specific and real-time detection of MIC in the pipeline environment. Here, the detection of MIC is based on the binding of specific biomolecules

causing MIC to organic molecules anchored on top of the nanowires. These sensors also need to be inexpensive (made of low-cost, earth abundant materials), have low power consumption, and robustly deployable. The primary component of the detection platforms are copper oxide nanowire arrays (CuONWs with lengths of 25 to 30 μm, 50 to 100 nm in diameter) and silicon nanowires arrays (SiNWs with lengths of 5 to 8 μm, 45 to 100 nm in diameter). They are synthesized using facile and scalable techniques and are selected for their robust electrical and mechanical properties. Electrochemical degradation studies of the NWs were performed in 3.5 wt. % NaCl solution and simulated produced water using polarization and electrochemical impedance spectroscopy (EIS). The NWs systems showed robust resistance to degradation despite higher surface area (as compared to bulk counterparts), and both diffusion limitations and charge transfer resistance was observed on the analysis of the impedance response. The ability to immobilize a variety of moieties on the nanowire platforms gives them the ability to detecting a wide variety of MIC biomarkers. The Biotin-Streptavidin (SA) complex was used as a proof of concept to test the viability of the NW arrays as a substrate for sensing. A custom test bed was built for the functionalized NW thin films, and cyclic voltammetry studies revealed a stable current response with time for 10nM and 10,000 nM SA concentrations. The use of different probes such as aptamers to larger immunoglobulin probes provides the flexibility to detect the full spectrum of biomarkers. The development of these next generation sensor platforms along with the methodologies employed to stabilize them and assemble them into functional devices are explored in detail in this dissertation.

DEDICATION

This dissertation is dedicated to Mrs. Saroja Aravamuthan (*Roju Pati)* and Mrs. Ranganayaki Aravamudhan (*Rangi Pati),* Mr. P.K. Kannan (*Appa),* Mrs. Rama Kannan (*Amma),* and my brothers and sisters at the Process Safety Center.

ACKNOWLEDGEMENTS

I would like to express my sincere appreciation and gratitude to my co-advisors Dr. M Sam Mannan and Dr. S. Vaddiraju for the opportunity to perform research and learn from their expertise and wealth of knowledge and experience. Additionally, I would also like to acknowledge the members of my dissertation committee Dr. A. Jayaraman, Dr. M.A. Wortman and Dr. H. Castaneda, for their feedback and time through my doctoral program, and the multiple opportunities of collaboration and mentorship they have provided. Additionally, I would like to express my sincere thanks to Dr. C. Mashuga who volunteered his time as a committee member during my preliminary examination.

My time at Texas A&M University and at the Mary Kay O'Connor Process Safety Center was greatly and selflessly supported by the constant motivation and help provided by Ms. Valerie Green, Associate director of the Mary Kay O'Connor Process Safety Center who served both as a mentor and guide. I would like to thank and express gratitude to Capt. James Pettigrew and the Ocean Energy Safety Institute for his mentorship, support and countless opportunities for personal and professional development. I would like to acknowledge the Dr. Noor Quddus, Dr. Monir Ahammad, Dr. Hao Chen, Dr. Samina Rahmani, Dr. Bin Zhang, Dr. Sonny Sachdeva, Dr. Yogesh Koirala, Dr. Hans Pasman, Dr. Simon Waldram, Dr. Razia Sultana, and Dr. Easer Arafat Khan for their critical feedback through the years as research scientists and project managers.

I would like to express my sincere gratitude to the collaborators on the projects facilitated at the Mary Kay O'Connor Process Safety Center especially to Dr. S. Camille Peres (and the advanced procedures team), and Dr. R. Mehta who provided multiple opportunities for both personal and professional growth. In addition, I would like to acknowledge the graduate students and postdoctoral researchers of their laboratories for their time and support.

I am immensely grateful to the countless hours of patient support provided by Dr. Robert (Bob) Carter and the staff at student counseling services, as they helped me navigate through multiple crests and troughs. In addition, I would like to thank the opportunities provided by the Association of Former Students especially, the staff of campus programs, Ms. Kellie Malone, Ms. Kelli Hutka, and Ms. Allie Longoria, and all my peers at the Aggie Network Student Ambassadors. A special word of thanks to Mr. Dwain Mayfield and Mr. Kevin Andrews who has served as a beacon of inspiration and provided mentorship through my time at Texas A&M University.

I would like to express my incalculable appreciation and gratitude to the vision of Mr. Mike O'Connor and Dr. M. Sam Mannan at the Mary Kay O'Connor Process Safety Center. The 'community of learning' and their passion, served as a North Star and inspiration through graduate school, as I came upon to discover my passion in process safety.

I would like to thank my peers from Dr. Vaddiraju lab, the Mary Kay O'Connor Process Safety Center and Dr. Jayaraman lab for their support through the years of graduate school. In addition, I want to express sincere gratitude to Ms. Ashley Henley, Ms. Sheera Helms, Ms. Alanna Scheinerman, Ms. Toni Alvarado, Ms. Terah Cooper and Mr. Louis Muniz Jr. and all the administrative and business staff of the Artie McFerrin Department of Chemical Engineering and the Mary Kay O'Connor Process Safety Center.

Finally, everything I do is only possible due to the constant and untiring support provided by my parents Mr. P.K. Kannan and Mrs. Rama Kannan and I am eternally grateful to them.

CONTRIBUTORS AND FUNDING SOURCES

This work was supervised by a dissertation committee consisting of Professor Dr. S. Vaddiraju [Co-Advisor], Professor Dr. M. Sam Mannan [Co-Advisor], Professor Dr. A. Jayaraman of the Artie McFerrin Department of Chemical Engineering in Texas A&M University [Home department], Professor Dr. Homero Castaneda of the Department of Material Science & Engineering [Outside department] and Professor Dr. M.A. Wortman of the Department of Industrial and Systems Engineering in Texas A&M University [Outside department].

This work has been supported by funds from the Artie McFerrin Department of Chemical Engineering and the Mary Kay O'Connor Process Safety Center, Texas A&M University. The experiments in section 7 were supported in part by an Institutional Grant (NA14OAR4170102) to the Texas Sea Grant College Program from the National Sea Grant Office, National Oceanic and Atmospheric Administration, U.S. Department of Commerce (Grants-in-Aid of Graduate Research by Texas Sea Grant at Texas A&M University).

All work including the collaborative results conducted for the dissertation was completed by the student independently.

NOMENCLATURE

AFM	Atomic force microscopy
ASTM	American Society for Testing and Materials
CLSM	Confocal laser scanning microscopy
COD	Chemical oxygen demand
CPT	Critical Pitting Temperature
DGGE	Denaturing gradient gel electrophoresis
DSS	Duplex stainless steel
EDS	Electron Dispersive Spectroscopy
EET	Extracellular electron transfer
EIS	Electrochemical impedance spectroscopy
EN	Electrochemical noise
EPMA	Electron probe microanalysis
EPS	Exo-polysaccharides
FET	Field effect transistor
GC	Gas chromatography
GNP	Gross National Product
HDSS	Hyper Duplex Stainless Steel
HPLC	High performance liquid chromatography
IR	Infrared spectroscopy
LASCA	Laser Ablation and Solvent Capture by Aspiration
LPR	Linear polarization probe

MIC	Microbiologically influenced corrosion
M-MIC	Metabolite MIC
MIS	Microbiologically induced souring (Reservoir souring)
MPN	Most probable number method
MS	Mass spectroscopy
OCV	Open circuit voltage
PCR	Polymerase chain reaction
SCC	Stress Corrosion Cracking
SCCM	Standard Cubic Centimeter per Minute
SEM	Scanning electron microscopy
SRA	Sulfate reducing archaea
SRB	Sulfate reducing bacteria
SS	Stainless Steel
TEM	Transmission electron microscopy
UV-VIS	Ultraviolet/Visible light spectroscopy
XPS	X-ray photo electron spectroscopy
XRD	X-Ray Diffraction

TABLE OF CONTENTS

Page

LIST OF FIGURES

Page

Page

Page

LIST OF TABLES

Page

1. INTRODUCTION

Corrosion is one of the most systemic and historically amongst the most expensive problems for the many industrial sectors. These include petroleum refining [1], mining [2], transportation and food processing [3], nuclear industry [4], offshore oil and gas industry [5], industrial water systems[6], and many system and processes employing both metals and other engineered materials [7, 8]. Although estimates vary widely, it is estimated that the cost of corrosion is between 1 and 5 % of the gross national product (GNP) of countries across the world [9], which for the United States is estimated to be ~ 500 billion dollars [10]. A NACE International IMPACT study estimated the global cost of corrosion to be greater than $2 trillion in 2013 [11]. In MIC, the corrosion of a substrate is perpetrated and/or accelerated due to the presence of a wide variety of microorganisms on its surfaces, which include bacteria, algae, and fungi [9, 12-19]. MIC is estimated to directly or indirectly contribute to 10 % to 50% of the total cost of corrosion [20-22] with the NACE estimate at 20% of the total cost of corrosion [23].

MIC has been found in harbors, nuclear power plants, oil and gas industries [24, 25], process plants [26], geothermal plants, power plants, fuel reprocessing units [27], sanitary sewage drains [28], pipelines[29] and storage tanks [30], oil fields and process equipment associated with them (such as pumps, valves and vessels) [31], fire sprinkler systems [32], water-cooled heat exchangers, oil recovery injection systems [32], paper and pulp industry [33], radioactive disposal facilities[34], and even railroad systems [35].

An early reported incident was the 1977 Umm Said refrigerated propane tank explosion, where one of the proximate causes was suspected to be weld failure caused by MIC due to sulfate reducing bacteria in hydro-testing water. The estimated loss was $179 million due to the damage caused by the fire and explosion [36]. MIC has also been suspected to be a cause in the Prudhoe bay oil spill in the Alaskan North slope [37]. The oil spill resulted in an estimated discharge of 212,000 gallons of crude oil on the Tundra and was recorded as one of the largest oil spills on the North Slope [38]. Another significant incident where MIC was suggested as a cause for the internal corrosion was the natural gas pipeline leak and explosion in Carlsbad, New Mexico, United States and the 2015 Abkatun Permanente platform fire in the Gulf of Mexico [39, 40].

MIC activity is responsible for accelerated corrosion and failure in many engineering materials including mild steels [41-47], 1010 carbon steel [48, 49], 1018 Carbon steel[50-53], Q235 carbon steel [54, 55], API 5LX70 carbon steel [56], X80 pipeline steel [57], 304 SS [58, 59], 2304 DSS [60], 2707 HDSS [61], 2205 DSS [62-66], 316L SS [67, 68], 2507 DSS [69], aluminum alloys [70, 71],copper and copper alloys [67, 72], S32654 super austenitic stainless steel [73], which covers almost the entire spectrum of alloys used in both normal and critical applications (risers, blow out preventers and subsea pipelines) of the oil and gas industry.

Studies documenting the impact of MIC on daily operations in the oil and gas industry are limited. MIC studies in the Halfdan oilfield in the Danish sector of the North sea tracked corrosion activity on the topsides of oil platforms,[74] and the oil export spool [75]. However, the data available in the public domain is extremely limited for MIC. It is known heuristically that the microbiological diversity in observed in the oil-field environment is extensive and complex. The extent of this variation was explored in a study by Geissler *et al.* through

microbiological analysis of 4000 samples collected from the October 2009 to June 2013. More than 500 different bacterial and archaeal species were identified and specifically it was found that *Halanaerobium sp.,* was found in the onshore facilities in Texas, Gulf of Mexico and Northeastern South America [76]. The lack of a public database of MIC related incidents and accidents, as mentioned above, prevent the understanding of its full impact. MIC mitigation strategies have been extensively discussed including various organic and inorganic biocides, and more recently the use of quorum sensing biocides for biofilm dispersal in the following papers [77-83]. More recently, a bibliometric analysis of MIC utilized a dataset of 5,480 documents emphasize the primary challenge, namely the need for a real-time correlation of microbiology and corrosion data that goes beyond the limitations of subjective elucidation [22]. In addition, there has been significant advances in the application of molecular microbiological methods in the to manage MIC in upstream and downstream processes [84]. It is hence, important to understand the advantages and limitations of the current analytical tools in use at both the off-site and in the field. This provides an insight into the key requirements necessary in the development of next generation sensors.

1.1 Microorganisms and chemical microenvironment of MIC active sites

Wide varieties of microorganisms have been known to be responsible for MIC [9, 85-92]. A large volume of literature discussed SRB growth and metabolism in biofilms [9, 90] and its impact on corrosion [93-96]. The microenvironment on the surface of substrates formed with biofilms, with the metabolic activity of the microorganisms, promote flourishing biotic growth [97]. The organic and inorganic molecules [12, 18] in the biofilm, combined with variations in pH, flow rate, concentration, temperature and pressure [9, 19] lead to a generation of an environment where biota flourish. Beale *et al.* [18] analyzed metabolites in a system with copper

MIC corrosion found amongst others acetic acid, glycerol, adipic acid, terephthalic acid, palmitic acid compounds. In case of environments, such as sea water, additional factors including the total organic carbon, polycyclic aromatic hydrocarbons, chemical oxygen demand, inorganic compounds such as SO_4^{2-}, PO_4^{3-},NO_3^-,S_2^-,CN^-,NH_4^-,and heavy metals including Fe, Cr, Cu, Ni, Hg, Sn, and Zn [15] play a role in determining biota growth rates.

The environment encountered by microbiota determines their state. If they are in a nutrient deficient environment they stay in a "planktonic" state, whereas in a nutrient rich environment they sink onto surfaces and will try to "stick" on the surfaces thus rendering them "sessile"[98] [81, 99]. These sessile organisms predominate in most of the environmental, industrial and medical processes of interest. The bacteria and microbiota in the sessile state enclosed in a biofilm matrix have been observed to be in a state of stasis with circulatory and metabolic-cooperativeness, such that the microbiota react in fundamentally different ways with substrates compared to their planktonic counterparts [100].The biofilms are complex structures that exhibit spatial gradations of nutrient concentrations and structural complexities [92]. The biofilm's dynamic nature of growth [101] compounds the challenge of its detection and mitigation. The biofilms are characterized by the presence of extra-cellular polymeric substances (EPS), which are generally polysaccharides [102, 103]. The EPS provides a protective matrix for the microbiota by providing a physical barrier against environmental stressors, such as abrupt changes in pH, temperature, pressure, flow and toxic chemicals. The EPS also provides a static environment for the microbiota to adhere to the substrate and proliferate.

Sulfate reducing bacteria (SRB), are anaerobic microorganisms that thrive in anoxic environments and have been studied extensively for their impact on MIC. Muyzer and Stams (2008) have done an extensive review on their physiology, diversity and applications[104]. Even

at low H_2S concentrations of 0.5 mg/L [28] the action of H_2S is not isolated with a species of bacteria known as *Thiobacillus* providing the ability to oxidize sulfides to sulfates which then form sulfuric acid leading to aggressive localized corrosion. *Desulfovibrio vulgaris*, a SRB species with high potential to cause MIC, was found to survive up to 55 days even in the absence of an organic energy source [105]. When pH levels of 4 ~ 5 are reached these sulfate oxidizing bacteria tend to thrive producing sulfuric acid, [106] which is extremely detrimental to a wide variety of engineering materials. The impact of H_2S and MIC in waste water facilities was studied by Tator [28], which also elicited the consequences of the sulfur cycle.

In addition to bacteria, biofilms typically have a complex composite of microorganisms housed in the EPS framework [107-111]. As most studies of MIC are limited by culturable organisms, mainly bacteria, the role of other microbiota in causing MIC is often understated. Larsen *et al.* screened for microbiota responsible for pitting corrosion from an oil production facility. This yielded high levels of sulfate reducing archaea and methanogens [74]. A review of MIC in carbon steel pipes revealed the diverse group of autotrophic and heterotrophic microbes, which cause localized corrosion [112]. The microbes use organic matter as a carbon source and electrons sourced from oxidation of iron for cellular metabolism, ultimately yielding to accelerated corrosion. These microbes also form anaerobic microenvironments for SRB growth and galvanic couples, which reduce ferric iron. Furthermore, photosynthetic organisms such as cyanobacteria and algae can adsorb metals onto their cell walls and produce organic carbon for SRB and heterotrophic MIC microbes [112].Methanogens are typically archaea that reduce carbon-dioxide to methane. Larsen *et al.* focused on down-hole samples from an oil field with their qPCR studies indicated that the abundance of methanogens was 47–67 % of all the prokaryotes.

In addition, the abundance of sulfate reducing archaea led the authors to conclude that it is essential to go beyond SRB for a comprehensive MIC assessment [113]. A detailed study of microbiological communities in biofilms from an oil production facility indicated that apart from the expected domination of the *Desulfovibrio* species, bacteria such as *Pelobacter, Pseudomonas and Geotoga* and various methanogenic archaea were also present [110]. An assessment of the methanogen population of a skimmer pit by Conlette *et al.* revealed the dominance of acetotrophic and hydrogenotrophic methanogens in the skimmer pit along with massive methane production. The study was however not clear on the mechanistic relation between methanogen domination over SRB in low sulfate environments and corrosion [114]. Fungi have also known to affect metallic surfaces with a study of *Aspergillus Niger* on aluminum surfaces showing pitting and formation of 'hills and valleys' on the coupon surfaces following a 21-day exposure period. It was also observed that the fungus adhered to the surface and this led to the proliferation of the fungal hyphae [115]. The fungus *Aspergillus niger* has shown accelerated corrosion behavior on magnesium alloys (AZ31B). The preferential adsorption of corrosion products at the substrate interface and aggressive pitting corrosion were observed by Qu *et al.* [116]. Fungi have been also shown to promote degradation of fuels by functioning as an aromatic and aliphatic degrader resulting in the inclusion of oxygen and promoting ferric oxide formation [117, 118]. The fungi utilize the hydrocarbons as a carbon source for cellular metabolism and growth, which is assisted by the electrons from ferrous oxidation, forming the oxide inclusions. A recent study by Skovhus *et al.* based on the metagenomic analysis of corroded industrial metal samples and their residues has indicated presence of methanogens, such as *Methanothermococcus* and *Mehanocaldococcus*, apart from SRB and sulfate reducing prokaryotes [75]. Another widely implicated bacteria is *Pseudomonas aeruginosa*, a gram

negative motile rod-like bacteria that possesses the ability to generate extra-cellular polymeric substances (EPS) which creates differential aeration gradient for SRB proliferation leading to MIC[114]. Investigation conducted by Mansouri *et al.* used a co-culture of SRB and *Pseudomonas aeruginosa* and the results showed linear behavior between the weight loss of coupons being tested and the exposure time[119]. The expanding family of suspected MIC causing species was captured by Dinh *et al.* [120] who identified *desulfobacterium*, whose presence led to higher corrosion rates relative to that observed in the presence of *desulfovibrio* species. This suggested direct electron uptake mechanisms. A review [121] on the bio-deterioration of construction materials presents mechanisms for materials such as concrete in the presence of *Thiobacillus cretivorous* and other *Thiobacillus* species that have the ability to convert H_2S into sulfuric acid in the presence of oxygen. A sulfur uptake study on thermoacidophilic archaea was performed in the laboratory environment by Liu *et al.* The study revealed the existence of eroding pits and loose porosities which are symptomatic of biocorrosion [122]. Microbiological degradation of stone was found to be enhanced by the rapid growth of algae, cyanobacteria and fungi which bore into it by releasing extracellular enzymes and metabolites [123]. Romero *et al.* (2003) studied MIC by SRB on carbon steel by using hydrogen permeation [124], and they observed that the sulfate reducing bacteria *D.sulfuricans* induces carbon steel corrosion due to the biogenic H_2S released as the result of its metabolic processes.

In summary, a wide variety of microorganisms are known to utilize different metabolic pathways in affecting the corrosion of metal and other substrates. These include sulfide reducers (*Desulfovibrio* sp., *Desulfomonas* sp.), iron oxidizers/manganese oxidizers (Gallione*lla* sp., *Leptothrix* sp., *mariprofundus* sp.), iron reducers (*Pseudomonas* sp., *Shewanella* sp.,

Geothermobacter sp.), sulfide oxidizers (*Thiobacillus* sp.), acid producing bacteria and fungi (*Clostridium* sp., *Fusarium* sp., *penicillium* sp., *Hormoconis* sp.) and slime forming bacteria (*Clostridium* sp., *Bacillus* sp., *Desulfovibrio* sp., *Pseudomonas* sp.).

The organisms which cause MIC also have implications, such as microbiologically influenced souring (MIS) also known as reservoir souring [125], especially observed in reservoirs which use water injection for oil production[126]. The widespread use of secondary and tertiary oil recovery along with water-based enhanced oil recovery has increased the probability of introducing potentially harmful microorganisms into the reservoirs. Sulfate reducing prokaryotes (SRP), SRB and archaea have been implicated at the genetic, enzymatic and physiological level for sulfate reduction activity, which results in the accelerated souring in petroleum reservoirs [127]. The limited incubation time employed in laboratory studies of MIC and reservoir souring result in the fact that although laboratory scale studies are less expensive and easier to perform that field studies, their results may not validate field observations [128]. Traditional cathodic protection (CP) techniques are limited in combating MIC, with the application of even very negative potentials which would ideally lead to a highly negative over-potential at the anode proving ineffective as a method to control MIC [129].

1.2 Mechanisms of Microbiologically influenced corrosion

The mechanism of MIC has been of intense research over the last few decades. The main challenge with the determination of MIC mechanisms is the complexities associated with the microbiota and the biofilm, and the environment of operation[104]. Cathodic depolarization theory (CDT) [130, 131]proposes that the cathodic reduction of proton (H^+) into H_2 is catalyzed by the hydrogenase enzyme from the SRB. This results in reduction of sulfates to sulfides. The theory proposes that since the depolarization is kinetically unfavorable due to high activation

energy, the enzyme catalyzes the reaction. A limitation of the CDT is the lack of accounting for the biofilm's role in MIC.

The biocatalytic cathodic sulfate reduction (BCSR) [85, 132, 133] theory emphasizes the role of the SRB biofilm thus plugging one of the limitations of CDT. BCSR utilizes the Butler-Volmer equation to combine the charge transfer for the anodic and cathodic reaction, using classical electrochemical kinetics to account for mass transfer and charge transfer resistance [134]. The cathodic reaction of the BCSR theory assumes that there is a corrosive biofilm formed by SRB on the surface of the iron and the reaction are biocatalyzed.

To extend the influence of acidic metabolites and organic acids on the pit bottom, Gu and Xu also proposed proton and acid reductions which can cause additional corrosion. An additional reason, for the development of the BCSR theory was to explain the lack of correlation often found in field studies on the planktonic SRB cell count and MIC related pitting. This classifies MIC damage due to extracellular electron transfer (EET), where biocatalysis occurs in the cytoplasm, facilitated by electron transfer through bacterial biofilms. MIC driven by corrosive metabolites was attributed to the presence of species such as acid producing bacteria (APB). This is labelled as M-MIC (metabolite-MIC)[52]. The oxidant is reduced intracellularly in case of EET-MIC using a biocatalyst, whereas it is reduced extracellularly without a biocatalyst in the case of M-MIC[133]. A combined mechanistic model developed by Xu *et al.* [135] caused by SRB sulfate reduction and acid attack has been proposed based on BCSR theory and the proton reduction theory, and the model is based on the MIC pit covered with an SRB biofilm with an optional top biofilm/mineral film. BCSR theory has been supported by observation on experiments utilizing electron mediators that enhance electron transfer, increasing the corrosion [136, 137].

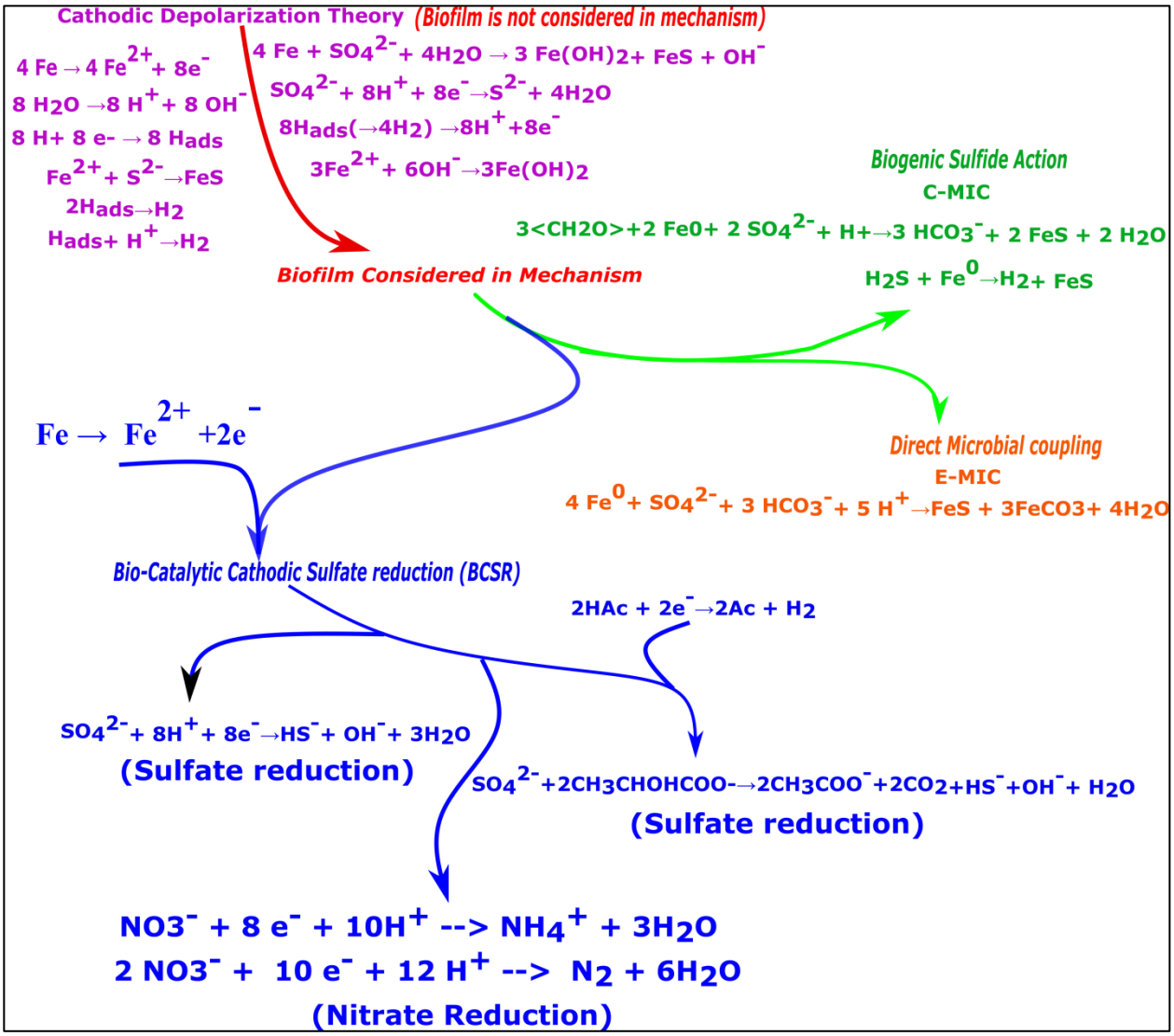

Figure 1. Schematic of the various mechanisms proposed for MIC primarily focused on electrochemical reactions facilitated or catalyzed by biota on the substrate.

The BCSR model has been used to explain MIC in studies with 1018 carbon steel under *desulfovibrio vulgaris* biofilm[52], *pseudomonas aeruginosa* biofilm[53] and nitrate reducing bacterium *Bacillus licheniformis[53, 138]*. Additionally, a study of carbon steel immersed in a ferrous-rich modified Baar's media found that Fe^{2+} aided SRB cells attachment in the early stages (< 60 minutes). However, there was no difference in the corrosion rate after 12 hours

between the Fe^{2+}- rich and -poor media [139]. An extensive review by Enning and Garrelfs [140] on the current state of the art of SRB's influence on MIC found that anoxic corrosion of iron is a slow process if only the proton reduction to H_2 was the predominant cathodic reaction, however proliferation of SRB could affect the rate of corrosion by 70 to 90 times as compared to that in sterile medium. There was a differentiation based on the chemistry of the attack with biogenic H_2S based attack on iron substrates classified as chemical microbiologically influenced corrosion (CMIC) and direct oxidation of the iron substrate by metabolic coupling classified as electrical microbiologically influenced corrosion (EMIC). This presents an alternate paradigm in understanding the mechanism of MIC as it decouples the direct and indirect corrosion mechanisms. A critical review [141] of anaerobic corrosion mechanisms found CDT did not appear significant in their studies. Their studies point towards production of volatile phosphorous intermediates which form black precipitates from the iron medium under study.

The biofilm's heterogeneity reveal the presence of anoxic and aerobic zones[123], which is realized in a complex array of electrochemical reactions as a consequence of the microenvironment. Figure 1 illustrates the evolution in the understanding of MIC mechanisms, including the dominant anodic and cathodic reactions for the various sub-mechanisms. Although MIC studies have primarily focused on anaerobic conditions, recent studies reveal the acceleration of corrosion even under aerobic conditions. A study of aerobic copper corrosion revealed a lower charge transfer resistance in a biotic environment possibly due to breakdown of the passive film by microbiological action [142]. Additionally, aerobic environments may undergo transformation into local anaerobic cells, due to the rapid microbiological growth which scavenge the oxygen[143]. Aggressive pitting-type corrosion accelerated by the presence of

aerobic *P.aeruginosa* biofilms has been found to accelerate corrosion of carbon, duplex and 304 stainless steels [65, 144-146].

Due to a large number of bench scale investigations of MIC, the surface preparation of substrates is important for reproducibility of results, since the area of attachment of the bacteria can be influenced by the underlying microstructure. There can be significant differences in the correlation between the exposure time and attachment to the surface as the study by Sreekumari *et al.* showed, where the area of attachment was inversely proportional to the grain size and also the base metal showed the least attachment as compared to the weld metal [147].Coupon preparation is most often carried out using ASTM standards such as ASTM G3 [148] which provides the guidelines for the preparation, cleaning and evaluating corrosion test specimens.

The challenges associated with determining precise mechanisms for MIC, combined with the complex biotic-abiotic interactions contribute towards the need numerous analytical tools for investigation. As an illustration, 77 case studies of MIC detection and investigation for materials utilized in the oil and gas industry are listed in Appendix C and Appendix D. A meta-analysis was performed with a focus on the analytical tools utilized by the studies. Figure 2(A) represents the frequency of usage of the analytical tools in MIC studies. An analysis of these selected cases shown in Figure 2(C) that 36% used 6 or more techniques, while 37% used 4 or 5 techniques to determine MIC causality. Further classification of the analytical tools in Figure 2B reveals that morphological (30%) chemical (24%) and electrochemical (28%) are used in equal proportion which indicates the prominence of the information gathered from these techniques.

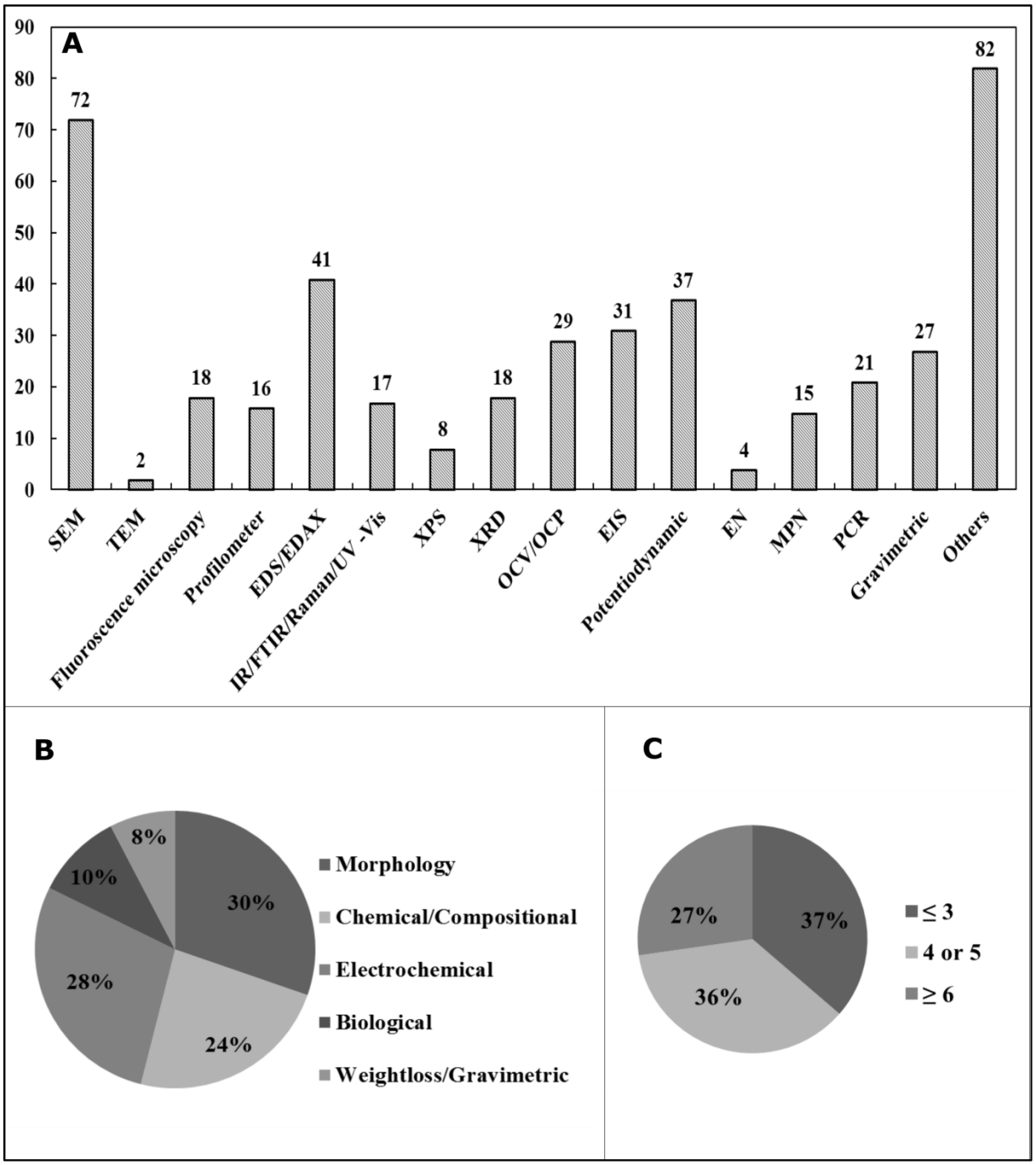

Figure 2. (A) Meta-analysis of analytical tools employed in 77 studies of MIC in the oil and gas industry. (B) Relative prominence of the types of analytical tools used to investigate MIC (C) Representation of the number of techniques used in each study for the characterization of MIC.

It should be noted that techniques which were used sparsely were classified as 'others', and is represented as a cumulative frequency in figure 2A. It is apparent that the economic cost and the skill demand required for the various tools revealed in the meta-analysis are considerably different. Sooknah *et al.* reviewed the MIC predictive models and [149] put forth three models, Checworks predictive model, Union electric callaway mic index, Lutey/stein MIC index. The discrete pieces of information are gathered from the analytical techniques, which are correlated with the existing literature or mechanistic understanding to devise mitigation strategies.

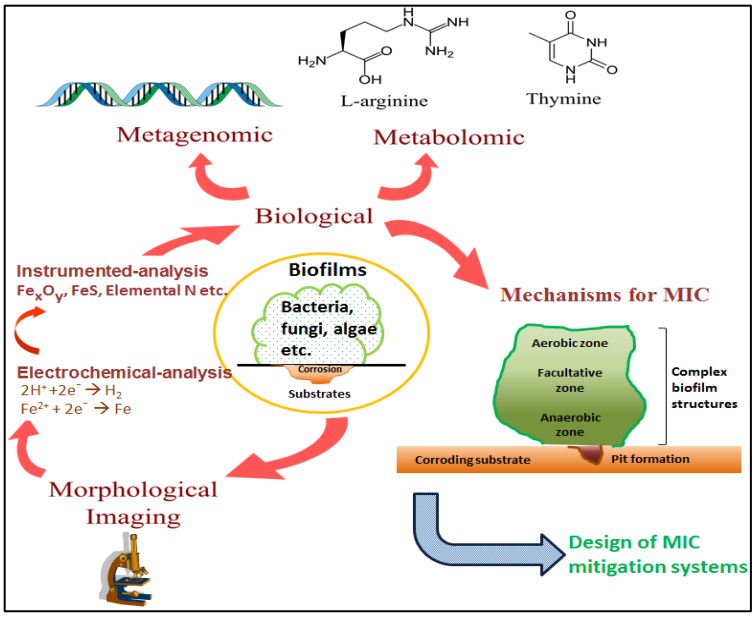

Figure 3. An overview of MIC investigation strategies. Information from morphology, electrochemistry, instrumented, and biological characterization provide the inputs necessary to understand degradation mechanisms.

Figure 3 is an illustration of MIC study lifecycle that are employed primarily offsite from facilities with MIC failures. The oil and gas industry is further challenged by the limitations placed by the remote location of the facilities, safety critical nature and limited redundancies in the components and the mitigation costs associated with managing MIC. The literature review utilizes the meta-analysis to elicit a complete and comprehensive understanding of the data gathered by each technique, the advantages and limitations and finally, present the motivation of the research to develop tools which can provide a single platform integrated monitoring tool.

2. OVERVIEW OF MIC DETECTION AND CHARACTERIZATION (LITERATURE REVIEW)

The monitoring and characterization of MIC can primarily be viewed as either online or offline modes. The first mode includes sampling or detection using qualitative and indirect methods. There are a few systems available currently used for corrosion monitoring of MIC by measuring biofilm activity and using baseline comparison such as the BioGeorge^{TM} [150] system. The probe is designed to promote the growth of microorganisms on the surface and then continuous monitoring of surface is conducted by measuring the current response. The second mode is offline detection methods being primarily achieved through off-site analysis of predetermined size corrosion coupons, pigging sludge, and fluid samples. The offline methods are classified based on the properties that are characterized or quantified; such as high-resolution imaging surface for the metallic substrate (morphological analysis) and potential formation of carbon or non-carbon based compounds, chemical compositional analysis of corrosion products or layering formation (including biofilm), chemical or bio activity (life cells or microorganisms), interfacial or electrochemical methods for corrosion assessment (electrochemical analysis), bioanalytical tools for bioactivity quantification (biological analysis).

Offsite analyses are conducted in laboratories, close to the sampling site or transported to centrally situated laboratories. A recent study [151] discusses the accuracy of this procedure, where oil field samples consisting of a consortia of SRB, acid producing bacteria (APB), general heterotrophic bacteria (GHB) were subjected to four storage conditions and were monitored over a seven day period. It was observed that samples preserved well at 4 ^{o}C, however there was a decreased microbiological concentration. Samples stored at 25 ^{o}C, 35 ^{o}C or cycled between 25 ^{o}C and 35 ^{o}C showed an increase in the concentration of the microbiota. This assumes great

importance since the phenomena under study has a component of microbiota (apart from substrate) which is temperature, time and microenvironment sensitive, and hence needs to be handled such that no erroneous information is obtained from the samples. A few existing reviews in literature discuss the use of some offsite tools used for the study of MIC. Chen *et al.* reviewed the use of instrumented tools to study MIC [19]. However, the review did not cover the usage of instrumented analysis in the context of microbiological and morphological analysis, which is essential to understand MIC in its entirety. A review by Sooknah *et al.* (2007) [152] gives a brief insight biological and instrumented tools. However, it is limited in description with minimal examples, but does provide an introduction to the next generation MIC detection, including biosensors.

2.1 Surface morphology identification and characterization

Microscopy is used to analyze the corrosion coupons, biofilms, fluid samples, and deposits to get a qualitative or quantitative visualization of changes in surface morphologies which may include the development of pits, distortions in grain boundaries, nature of deposits, and spatial distribution.

Techniques such as scanning electron microscopy (SEM), atomic force microscopy (AFM), environmental scanning electron microscopy (ESEM) provide visual information of the substrate morphology[153]. Cetin *et al.* investigated the effect of *Desulfotomaculum sp. (SRB)* isolated from an oil field sample on low alloy steel coupons. The SEM analysis could clearly identify the action of bacteria, which is isolated by exposing the differences in the extent of pitting between the sterile and active culture. Aggressive pit formation was observed in the active culture implicating the action of the SRB on the steel surface[31]. The heterogeneity of the biofilms, which may be multi-layered and have a complex spatial distribution of bacteria, fungi,

algae , diatoms and, protozoa [153, 154], make their study difficult with two-dimensional microscopy. A major drawback of using SEM with biofilms and soft matter samples is that the beam may damage the surface and the delicate structures of the biofilm. Adding to this difficulty is the requirement of an electrically conductive substrate for imaging samples using SEM. Making non-conductive sample conductive is possible by adding thin layers of metals to their surfaces using e-beam sputtering or similar techniques. Among EM techniques, ESEM is a tool which can overcome limitations involved in imaging biological samples under vacuum. In the case of ESEM, the use of low energy secondary electrons [154] helps protect the integrity of the biofilms, as the high energy electrons may cause their etching, thus ESEM is a use full tool especially for the concurrent study of the corrosion damage to the substrate with the biofilm matrix. A low cost but qualitative evaluation is optical imaging as seen in Figure 4(A).

Romero *et al.* [155] used SEM images to show that the biofilm development was efficient, and the combination of SEM and EDS provided insight into the surface modification post permeation and the formation of kansite. Similarly, Bairamov *et al.* [156] studied stainless steel 316 plugs in heat exchangers with SEM and EDS. The analysis showed the large presence of organic matter on the affected area in addition to deposits of iron and sulfide, a sign of MIC activity. Song *et al.* investigated the corrosion morphology in pipelines [157] and the morphological analysis suggested that three species of bacteria, SRB, iron oxidizing bacteria (IOB) and total general bacteria (TGB), were the causative species.

Confocal laser scanning microscopy (CLSM) utilizes a laser beam to scan a surface point-by-point without physical sectioning of the tissue to capture high resolution optical images[158]. CLSM are employed to give a three-dimensional visualization of biofilms. Neu and Lawrence (1997) utilized CLSM and analyzed the biofilm from river water samples [159]. They

found structural features, such as ridges, which were formed because of humic and detrital matter co-absorbtion. The ridges formed increased the surface area of the microhabitats for differential colonization in addition to possibly serving as additional sources of nutrients. A CLSM study of accelerated corrosion on 2205 Duplex stainless steel by Xu *et al.* [65] in the presence of marine *Pseudomonas aeruginosa* indicated a pit depth in inoculated media of 14 μm and in sterile media of 4.9 μm. Chen *et al.* [160] utilized CLSM to compare fluorescently tagged SRB with an abiotic sulfide-enhanced sterile culture. The cultures were exposed to 316L stainless steel and the CLSM images clearly indicated that bacteria accumulated in clusters on the surface, thus explaining the pitting observed on the surfaces of the coupons. CLSM images as seen in Figure 4(B) can clearly visualize and quantify biofilm thickness over time.

AFM offers a non-destructive and minimally invasive route for understanding the changes to surface [56, 131, 161, 162]. Profiling of a surface is performed using a tip mounted on a cantilever and high-resolution (angstrom scale) morphological characteristics of surfaces could be obtained. The functional characteristics of the material which can be inferred based on probe-surface interaction include the size, shape, friction, adhesion forces, cohesiveness, Young's modulus and chemical bond information of the surfaces [163]. A 1994 study on the bacterial degradation of stainless steel demonstrated the use of AFM to confirm the heterogeneity of the biofilms resulting from the presence of a mixed culture in them (*P.aeruginosa and D.gigas*) [164]. Silva *et al.* studied the effect of *Aspergillus Niger* on aluminum coupons using AFM to expose valleys and hills on the aluminum, including pits with mean dimensions of 80 nm in diameter in width and 9 nm in depth. The AFM allowed for imaging of discrete particle oxides on the surface and suggested that the biofilm had a larger contact area with the bulk liquid environment than with the substrate [115]. Fang *et al.* quantified

the bacterial adhesion forces and found the tip–bacterial surface force was -3.9 to -4.3 nN and the adhesion from the periphery to the cell substratum ranged from -5.1 to -5.9 nN, as compared to cell–cell interface which ranged from -6.5 to -6.8 nN. The higher adhesion forces could be attributed to the accumulation of the EPS [165]. AFM images allow for high resolution three dimensional imaging in a non-destructive manner as seen in Figure 4(D).

AFM allows of real time *in-vivo* visualization of surfaces in near physiological conditions with the entire topographic data obtained in Cartesian coordinates. It does not require pretreatment (pretreatment may generate artifacts), but lacks the capacity to image side wall features and is limited by the scanable survey area [166] [167]. Dong *et al.* found using AFM that surface roughness increased with the growth of the biofilm, ultimately reaching an apex value of 2596 nm, with eventual decrease to 2057 nm attributed to the sloughing of the aged biofilm from the base [42]. A study on stainless steel in the presence of the *Geobacter sulfurreducens* bacteria found a 10-fold increase in pit size in the biotic condition as compared to the abiotic condition, evidencing the impact of MIC [168].

Microscopy provides empirical evidence on the presence of microbiota and asset degradation. Real time analysis of ongoing corrosion is not possible by merely employing only microscopy. There are often delays due to the sample extraction and the need for destructive sampling such as the extraction of the pipe segment on which corrosion is suspected or is observed to have occurred, limits the uses of microscopy.

2.2 Chemical characterization of surface and corrosion products

The determination of corrosion products and the identification of the changes in the chemical composition of MIC-affected surfaces demand the use of multiple characterization techniques. These include Raman spectroscopy, X-ray diffraction (XRD), UV-Vis spectroscopy,

FTIR spectroscopy, X-ray photoelectron spectroscopy (XPS) and Auger electron spectroscopy (AES). Spectroscopic analyses have been beneficial in analyzing the chemical composition of the corrosion deposits to determine the nature of the corrosion.

2.2.1 Infrared (IR) and Fourier Transform Infrared (FTIR) Spectroscopies

Infrared (IR) spectroscopies are used to characterize the presence of organic functional groups (e.g., -COOH and -NH_2) in the corrosion deposits and on the surfaces of samples. The presence of organic functional groups may be indicative of MIC activity. The spectra are analyzed based on information of the process fluid the samples came into contact with, and in combination with microbiological assays. It is also useful to evaluate the changes in the biofilm by evaluating the metabolism within the biofilm. However, spectral information obtainable is limited by the presence of water, a strong absorber of IR frequencies. This problem is overcome using attenuated total reflection (ATR–FTIR), which reduces the path length of IR within the sample [152]. Nichols *et al.* [169] studied the use of FTIR for analysis of bacteria and biofilms identified spectral features for differentiation between microbiota in a consortia, and suggested that the potential exists for the differences to be quantified and used in the recognition of microbiological community structure. The use of diffused reflection infrared Fourier transform (DRIFT) spectroscopy allowed for the easy collection of data from metal disk surfaces and provided an avenue for the development of micro–FTIR probes for industrial deployment. The spectra provide data on the chemical composition of the metabolic and corrosion products, including chemical bonding information [170]. FTIR data is useful for both detection of MIC activity, and can be combined with other analytical tools utilized in fundamental studies for mechanistic evaluation of MIC. Rajasekar *et al.* used FTIR to study the effect of exposure of aluminum alloy 1100 and mild steel 1010 in urban coastal sites to airborne bacteria and found

FTIR peaks for mild steel at the exposure period higher at 90 days due to the possible accumulation of EPS. Peaks at 3380 cm^{-1} revealed the -NH bond stretch, while that at 1720 cm^{-1} indicated the existence of -SH. On the aluminum surface, the stronger intensity of the $-SO_4$ asymmetric stretching at 1107 cm^{-1} indicated a basic aluminum sulfate layer [41]. This indicated not only the involvement of airborne bacteria in MIC, but also a stronger corrosion resistance exhibited by aluminum compared to mild steel.

2.2.2 X-ray Diffraction (XRD), X-ray Photoelectron Spectroscopy (XPS), and Energy Dispersive Spectroscopy (EDS)

XRD and XPS studies are employed to obtain chemical composition information of the sub-biofilm corrosion deposits and the abiotic products of corrosion [171-175]. Huttunen-Saarivirta *et al.* studied the MIC in stainless steel heat exchangers using XPS. The analyses of the corroded substrate showed that there was preferential attack towards the ferrite phase [176], an important observation that would help in the preparation of the stainless steel. The XRD analyses also provide insights into the compositional and phase changes to the substrate under different conditions. El Hajj *et al.* investigated using XRD and Raman spectroscopy [177] sequential changes on carbon steel MIC subjected to aerobic and anaerobic conditions. XRD spectra of the corrosion layer revealed the presence of maghemite phase of iron oxide and limited quantity of magnetite for the sterilized coupon. It was observed that in an aerobic environment the iron (II) hydroxide oxidizes to form lepidocrocite (crystalline phase with rhombic structure), and depending on the activity of water this lepidocrocite isomerises into goethite (rhombic structure). Also, if the corrosion rate was low it was seen that the lepidocrocite was partially transformed into maghemite. In short, XRD data provided evidence of the mechanism of corrosion. The data also aided in determining the corrosion rates (using the

corrosion deposits seen on the surface). The form of phase differentiation was clearly elucidated as observed in Figure 4(F), where the relative abundance of the iron compounds and phases are clearly visible.

SEM/EDS analyses were used to identify deposits on coupons exposed to *Desulfovibrio capillatus* isolated from an oil field separator that faced severe corrosion in a study by Miranda *et al.*[178]. Two steel alloys (St-35.8) and (API-5XL52) were exposed for 45 days. EDS analysis of the samples revealed that the corrosion deposits contained Fe and S, which were suggested to indicate iron sulfide formation. The presence of iron sulfide is often used as a characteristic indicator of SRB activity on ferrous materials. lhan-Sungur and Cotuk studied microbiological corrosion in a simulated cooling tower system [179]. The EDS analysis of the corrosion deposits of the coupon exposed to sterile tap water for 10 months exhibited no Fe and S peaks observed indicating the lack of MIC activity. In coupons exposed to water (non-sterile) for 10 months and 11 days and peaks of Ca, Zn, Fe, O and Si was observed, but the sulfur peaks were indeterminate. Wide surface scans were carried out on SS 304 exposed to aerobic pseudomonas to investigate corrosion damage and changes due to biofilm formation. The relative atomic concentrations and their ratios were calculated based on the peak areas. The increased biofilm coverage was indicated by the increase in the C, O, N content represented by the increase in peak intensity and there was decrease in the Fe and Cr concentration after 28 days of exposure with Fe and Cr [145]. As seen in the overlaid SEM/EDS Figure 4(G), the relative abundance of the various atomic species is clearly demarcated and visible.

2.3 Biological Analysis

The usage of biological tools to characterize the microbiological community associated with MIC has been gaining prevalence over the last few decades. Traditional culture-based techniques can detect only 1% of the microbes in nature, [180] and microbiological tools provide an alternative for a more comprehensive assay. Novel approaches such as whole genome sequencing, stable isotope probing, use of functional gene markers, whole gene hybridization and meta-omics provide alleviation of issues such as small sample size, high throughput analysis and insight into metabolic pathways[180]. Although metagenomic and metabolomic techniques provide the distribution of microbiological communities in specific sample collection locations, the root cause of MIC, which is the combined effect of the microenvironment and the microbiological communities, is difficult to assess using them. These techniques also require highly trained personnel, sophisticated data analysis and robust feedback systems to ultimately impact MIC mitigation in applications. Biological analysis has traditionally been restricted to most probable number (MPN) methods or ATP-based activity assays, however, biological assays have been expanded to cover metagenomics and metabolomics analysis. The metagenomics analysis uses genomic information obtained through techniques, such as polymerase chain reaction (PCR) assays and gene sequencing. Metabolomic assays use combination of GC, HPLC and MS to analyze and identify chemical compositions in biological environments to access information on the metabolome[181, 182]. Combined metabolomics and metagenomic techniques as described earlier can be deployed to correlate MIC mechanisms with the microbiological community and identify essential MIC-causing chemical markers.

2.3.1 Metagenomic analysis

PCR-based characterization techniques have been widely used over the last century to understand the microbiological profile of any sample of microbiota [183, 184]. The inherent limitation in culturing wild type microorganisms in laboratories provides impetus for using molecular biology techniques to determine the presence of various species of microbiota in the samples [185-190]. The usage of PCR has also been coupled with techniques such as denaturing gradient gel electrophoresis (DGGE) where the 16S rRNA gene assays obtained after amplification of DNA from a mixture of uncharacterized microorganisms [191]. For the purposes of MIC, this is an extremely useful tool as the presence of a mixed species in a biofilm is a common occurrence in MIC affected systems. PCR coupled with DGGE was used by Teng *et al.* to identify the microbiological consortium in the investigation of the biofilm formed on a corroding iron pipe in a water distribution network [192]. DGGE fingerprinting was performed with the PCR products and the Shannon-Weiner index and the Simpson index was used to calculate the microbiological diversity. The coupled PCR-DGGE analysis have implicated the significant role of biofouling on the corrosion of cooling water systems using sea water [193]. Recent improvements include optimization of DNA staining technology with PicoGreen and SYBR green dyes, to improve automated evaluation of microbiological activity [194]. Also, focused 16s rRNA gene assays utilizing (flurogenic 5'-nuclease assay and SYBR Green I assay) allowed for increase in the speed of evaluation of critical sub-populations related to oil and gas corrosion. These methods allowed for quantification of the microbiological population distributions with an accuracy within 10% of the true value [195, 196]. These techniques have also been extended for the characterization of waters from hydraulic fracturing by Murali Mohan *et al.*, where there is tremendous proliferation of bacteria especially in produced waters [197].

16s rRNA sequencing was used with tag-encoded pyrosequencing and clone libraries to evaluate the relative abundance of the microbiota as seen in Figure 5(B). The taxonomic analysis identified the presence of facultative/anaerobic microorganisms possessing a wide range of metabolic abilities. The presence of multiple genomic lineages, which subsequently were capable of non-sulfate metabolism, indicating a need for better monitoring. The results also suggested that the produced water may have been seeded by the microbiological communities of the pre-fracturing fluid, and emphasized the need for better understanding of commercial disinfection of produced water for sustained reuse. Gonzalez *et al.* characterized the bacterial community in corroded oil pipelines [21] and found multiple species of SRB, including groups of *desulfobulbus, desulfobacter, desulfococcus-desulfonema desulfosarcina* bacteria.

Metagenomic tools have been employed to gather data on the phylogenetic diversity in biofilms for characterizing the corrosive characteristics [198-200]. The distinct presence of an acetotrophic and hydrogenotrophic methanogen indicated two mechanisms of corrosion, with the hydrogenotrophic group corroding the metals via cathodic depolarization and the acetotrophic group corroding the metals indirectly by syntrophic action with the SRB. The techniques have uncovered species of bacteria, which are thought to be more aggressively responsible to MIC related factors [43]. A quick PCR method is now available for in-field analysis [201] of corrosion deposits and pigging muck. DGGE along with random cloning of 16S rRNA gene were employed to identify the microbiological community in pipelines [202]. These have been done at specific sites including pipelines in Mexico [203], Alaskan North slope facilities [204], North Sea field [205], and coal beds in Canada [206] and from sour gas pipelines [207].

Skovhus *et al.* utilized DNA-based diagnostic kits on an oil field separator for the rapid enumeration of methanogens from pigging deposits [208]. The ability to use solid samples

reduced artifacts in the data attributable to oil induced auto-fluorescence and led to an increased ability of detecting MIC directly in the oil fields themselves.

Recent decrease in the cost of Next Generation Sequencing (NGS) systems, has led to rapid adoption in MIC genomic characterization [209-211]. NGS refers to the use of parallel computing and processing to sequences hundreds of thousands of DNA per run. Technological improvements and miniaturization have allowed for routine analysis using a single instrument [212]. A study of a brackish water pipeline used in bitumen production with steam assist, utilized samples from upstream and downstream of a sodium bisulfite injection point. The study utilized 454 and Illumina sequencing for metagenomic analysis. The taxonomic assignments revealed the abundance of *deltaproteobacteria and Archaea*. The microenvironment created by the brackish water with the bisulfite injection provided evidence for a potential role of the *Epsilonproteobacteria* in MIC [213]. NGS has been utilized to evaluate souring potentials of reservoirs by DNA analysis from core analysis of offshore reservoirs. A study of three cores from a high-temperature offshore reservoirs indicated the presence of *oxalobacteraceae, Pseudomonadaceae and Comamonodaceae families* which have been implicated in hydrocarbon degradation under anaerobic conditions[214]. The use of a system biology approach has been suggested for MIC, similar to approaches followed to study human diseases [215].

2.3.2 Metabolomic analysis

Metabolomics of biofilms involves gaining an understanding of the metabolites that participate in processes of the microbiological community in the biofilm for access to chemical signatures, which may be indicators of possible MIC activity. High-resolution MS provides the ability to differentiate between ions of nearly identical mass and also determination of mass of an ion with enough accuracy to determine the elemental composition of the ion [216]. MS is also

currently aided by laser ablation techniques that allow for efficient analyte capture and their efficient transport to (MS) devices. The laser ablation and solvent capture by aspiration (LASCA) system, where ablated materials in laser plumes are collected in a coarse aerosol and analyzed with electrospray ionization in a high mass resolution Quadrapole time of flight mass spectrometer. This method was used with amino acids test patterns and allowed for the detection and imaging of a large number of metabolites [217]. A Nd:YAG pumped optical parametric oscillator (OPO) laser was used to ablate *Serratia sp* colonies from an agar media. As mass spectra of the analytes could be obtained with very low laser fluencies, as low as one or two 1.5 mJ, 2.94 μm laser beam (wavelength of the beam providing an ablation size of 20 laser shots per pixel), this technique does not alter the analyte chemical compositions during the collection process [218].

Gutarowska *et al.* assessed the biodeterioration of materials and brick samples were used to extract organic residues. The organic residues were analyzed using high performance liquid chromatography system combined with a quadrapole time of flight (Q-ToF) spectrophotometer. The activation of metabolic pathways which result in primary and secondary metabolites was detected based on putative metabolites. A significant advantage of this method is the use of small quantity of samples to obtain information about species interaction[219]. The distribution of metabolites over the surface of the coupon including their relative abundance can be obtained as seen in Figure 5(C).

An extension of the LASCA technique to assess corrosion damage on 1018 carbon steel generated more than 1000 ions' metabolite profile and revealed heterogeneities within the biofilm. Strong correlation was observed between the biofilm metabolome and occurrence of corrosion in an anaerobic exposure study, and it was suggested that the spatial correlation of the metabolome may serve as a leading indicator of MIC[219]. These recent studies yielded a new perspective on MIC that focusses on the active constituents i.e., the metabolites rather than the source the microorganisms.

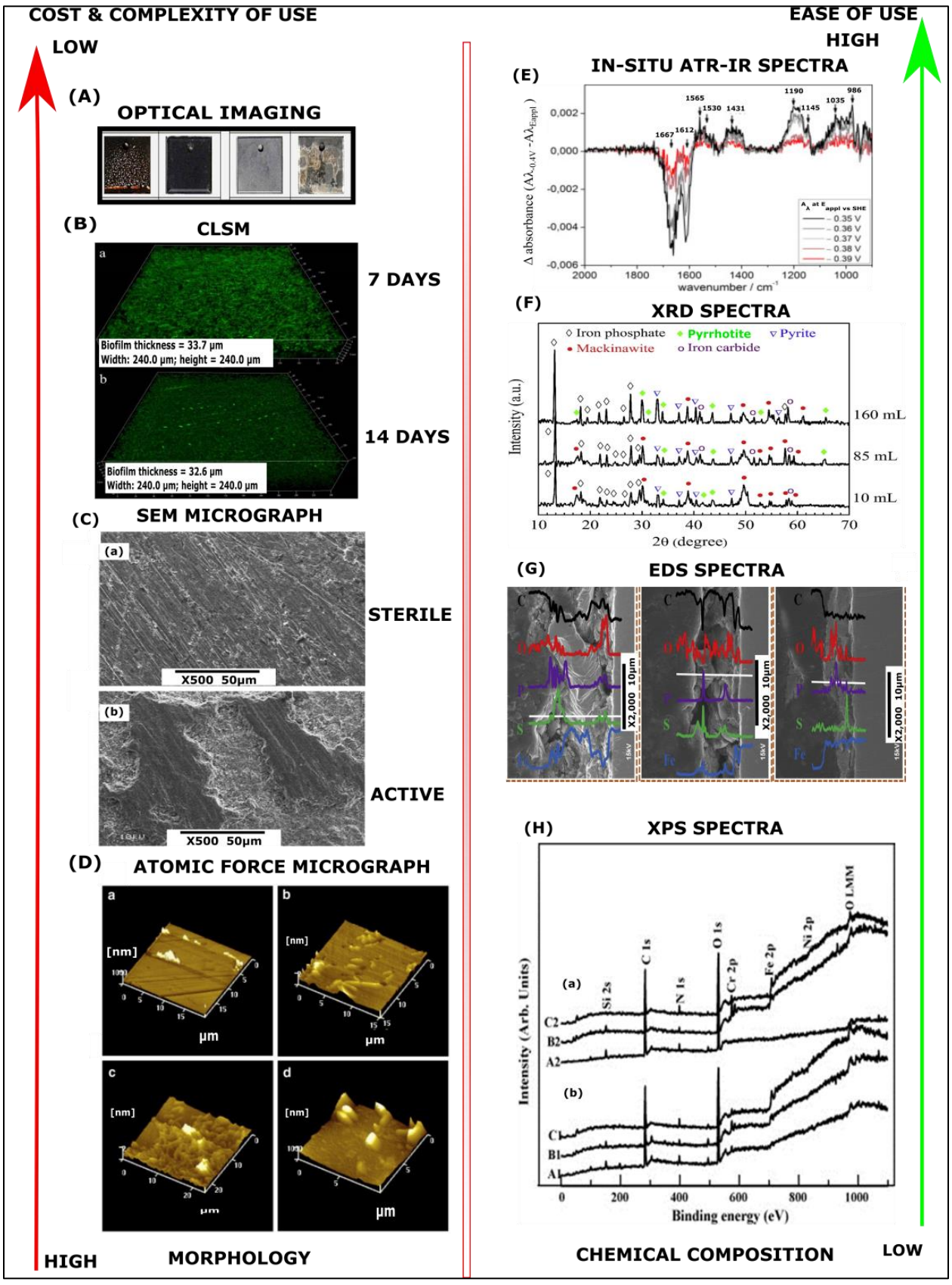

Figure 4. (A) Optical image of DH 36 alloy exposed to biotic and abiotic test media showing discoloration of surface with exposure [220], reproduced with permission from Elsevier (B) CLSM images of 304 SS coupon exposed for 7 and 14 days to biotic media containing *P.aeruginosa* showing biofilm coverage by live/dead stain [59], reproduced under creative commons license (C) The SEM micrograph of the surface of the steel coupon exposed to (a) sterile culture medium and (b) culture medium with *Desulfotomaculum sp*. [31], reproduced with permission from Elsevier (D) AFM image of SS coupons with *V.natriegens* after (a) 1-day (b) 3-day (c) 7 day and (d) 14-day immersion [221], reproduced with permission from Elsevier. (E) In-situ ATR-IR spectrum of in an active *Desulfopila corrodens* [222], reproduced with permission from Elsevier. (F) XRD spectra of C1018 coupon surface in *Desulfovibrio vulgaris* environment [52], reproduced with permission from Elsevier (G) SEM/EDS analysis with elemental composition of coupon surface following incubation in *Desulfovibrio vulgaris* environment [52], reproduced with permission from Elsevier. (H) Wide XPS spectra of surface film for SS 304 coupon sample (a) biofilm covered coupons and sample (b) coupons with biofilm removed [145], reproduced with permission from Elsevier

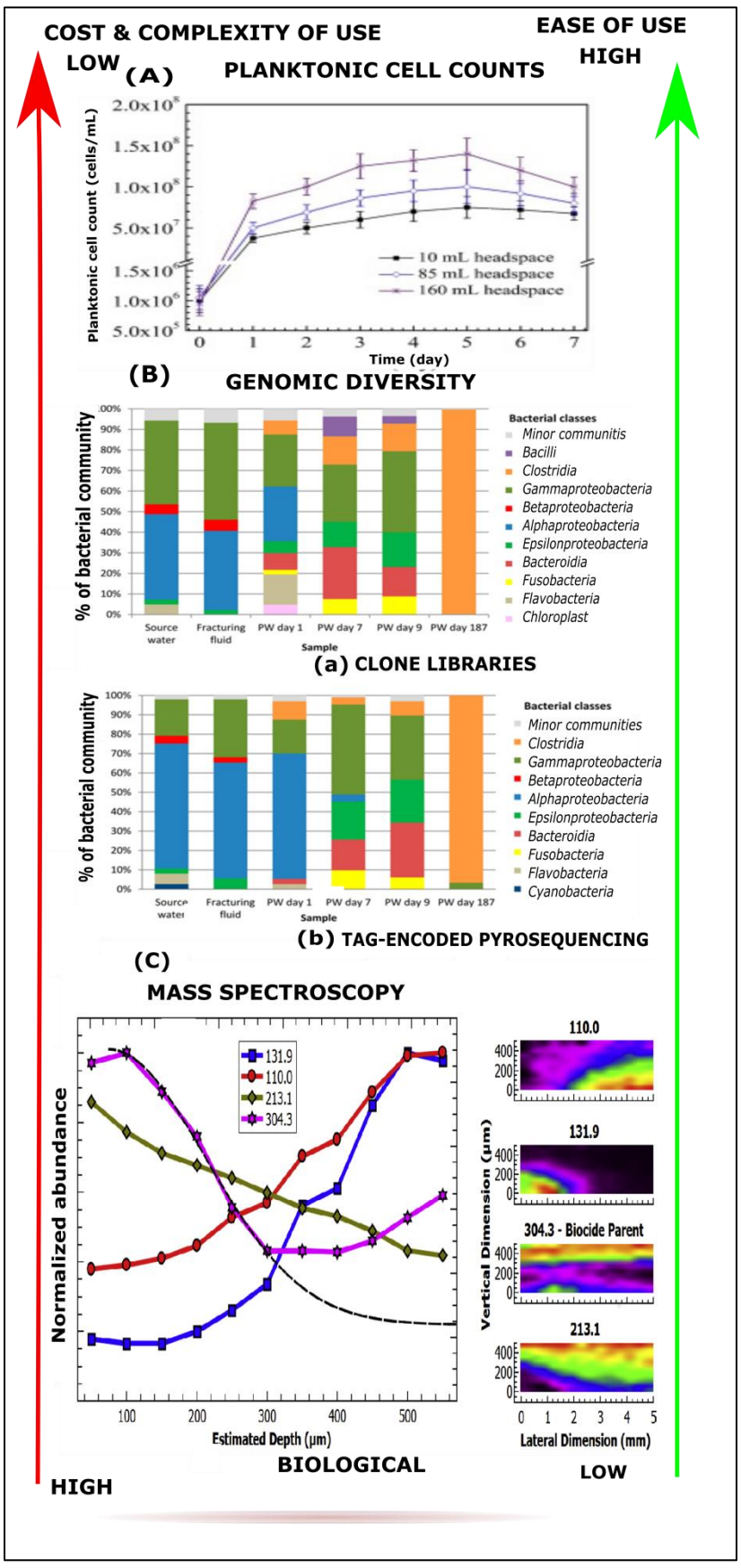

Figure 5. (A)The planktonic cell counts during a 7-day incubation of C1018 carbon steel in *Desulfovibrio vulgaris* [52], reproduced with permission from Elsevier (B)16S rRNA gene sequencing performed to characterize the microbial abundance water associated with fracturing fluid and the associated produced water (PW) with tests performed on days 1,7,9 and 187 using (a) tag-encoded pyrosequencing (b) clone libraries [197], Reproduced with permission from [197]. Copyright (2013) American Chemical Society (C) Depth profiles for ion concentrations with mass values and abundance of ion as function of depth after mass spectroscopic analysis of coupon surface [223], reproduced with permission from Elsevier

2.4 Electrochemical investigation and analysis

Electrochemical techniques have been used in corrosion research for more than four decades since the original Pourbaix studies, which gave an insight into the fundamentals of various corrosion mechanisms [224, 225]. These electrochemical techniques have been further extended into the realm of studying MIC with the aim of understanding its complexity. As discussed previously, there is no single comprehensive mechanism that can be used to explain the accelerated corrosion of materials subjected to MIC. Although multiple electrochemical techniques have been adapted to monitor MIC, it remains challenging to interpret the data and provide insight into the corrosion mechanisms due to the complexity and dynamic nature of environment created because of substrate-microbiota interaction. Very often, the use of appropriate electrochemical method needs to be coupled with careful experimental design, microbiological and metallurgical characterization of the system to provide even partial understanding of the mechanisms in MIC. In the following section, the common electrochemical techniques used for detection and monitoring the MIC will be discussed.

2.4.1 Electrochemical Noise (EN)

Electrochemical noise measures the fluctuations in potentials and currents caused by the spontaneous electrochemical reactions. Higher noise levels and larger fluctuations are mainly indicative of the onset of the localized corrosion processes, whilst a corroding metal undergoes uniform corrosion will be less noisy [226]. Investigation of the electrochemical noise signals can be carried out either in the time domain or frequency domain. Analysis of electrochemical noise signals in the time domain allows different statistical parameters such as localized index (LI) and electrochemical noise resistance (R_n) to be obtained[227]. Particularly, R_n which measures the ratio of standard deviation of potential noise signal to standard deviation of current noise signal

has been widely used to measure the rate of corrosion and is found to be comparable with polarization resistance [226-228].

Compared with the DC and AC techniques, electrochemical noise techniques are a non-destructive and non-interfering method and do not alter the system from the steady state [229-233]. These techniques are particularly advantageous for continuous monitoring without applying external perturbations [228, 230, 234, 235]. Electrochemical noise technique has been widely applied to differentiate between biological and non-biological corrosion and to evaluate the corrosion mechanism of MIC. It has also been used to distinguish between uniform and localized corrosion. Numerous researchers have utilized this technique to measure and monitor the onset of localized corrosion processes such as pitting, crevice corrosion and stress corrosion cracking [227, 234, 236, 237].

Meanwhile, analysis in the frequency domain using the maximum entropy method (MEM) or Fast-Fourier Transformation (FFT) method have been reported to be able to distinguish the type of corrosion [226, 235]. Homborg *et al.* has also reported that by applying mathematical analysis such as Hilbert spectra, the evolution of localized corrosion processes induced by MIC can be monitored using time-resolved instantaneous frequency information of electrochemical noise.[234, 236]. Studies by Men *et al.* of SRB corrosion on 304 SS utilized a back propagating neural network for identifying passivation, pitting induction and pitting successfully with an increased recognition of uniform corrosion [238].

2.4.2 Open circuit or corrosion potential measurement

Open circuit potential (or corrosion potential) of a corroding metal is the dynamic equilibrium potential at which the net current is zero. It is generally measured by comparing the potential difference between the metal immersed in corrosive medium and appropriate stable

reference electrode. The open circuit potential can be measured using a potentiometric circuit, and a high impedance voltmeter or an electrometer, without the need for applying external signals. Due to the simplicity of the measurement, the open circuit or corrosion potential measurement has been widely used both in the field and in the laboratories to assess the electrochemical behavior of the materials immersed in corrosive media.

It has been widely reported that the activity of the microorganisms in the biofilm can lead to potential ennoblement in various types of metals exposed to fresh, brackish and seawaters, including high alloyed stainless steel, platinum, gold, titanium, nickel and chromium [15, 239, 240]. Potential ennoblement is denoted by a shift of the potential in the positive direction as a result of living biofilm formation that provide an alternate oxygen reduction pathway leading to an increase in cathodic reduction rate [177, 241-245]. Numerous researchers have reported the ennoblement of stainless steels or other passive metals when exposed to natural seawater. Compared with the corrosion potential obtained in sterile or filtered seawater, an increase of 250-350 mV in corrosion potential was reported for conditions allowing microbiological activity [146, 244, 246]. An example is a study comparing the response of the carbon steel and low alloy steel to treated (T) and untreated seawater. The corrosion potential after 210 days immersion indicated that there were only limited differences between the treated and non-treated sea water. However, it was used to confirm the hypothesis, that the addition of an higher alloying element results in higher corrosion potential as seen in Figure 6(A) [177]. Potential ennoblement approaching 300 mV (vs. SCE) was observed in the first 7 days[177]. It is worthy to note that the main consequence of potential ennoblement is increase in the likelihood of the materials crevicing and the initiation and propagation of pitting corrosion, particularly in alloys with pitting potential close to the corrosion potential. A study of MIC ion Ni-free high nitrogen

stainless steel under the presence of *Pseudomonas aeruginosa* revealed open circuit potential (E_{OCP}) to be much higher in the inoculated medium, compared to that under controlled abiotic conditions confirming the acceleration of the cathodic reaction[114] . The corrosive nature of the *P.aeruginosa* biofilm was investigated in another study of 2304 duplex stainless steel where, it was found that the biotic pit depth was 11.0 μm, as to the 4.8μm depth observed under of the abiotic conditions [60].

Another important insight into MIC is provided by the fluctuations or noises in the OCP measurements. A study by Searson and Dawson [247] of OCP fluctuations for mild steel samples showed that these fluctuations exhibited a stochastic process with 1/f behavior. Although, it was concluded that the origin of the noise was not known, it was a reasonable method to identify the characteristics of the corrosion process. The stochastic process was mathematically correlated in terms of the standard deviation of the voltage fluctuations with respect to time and the corrosion rate calculated from the weight loss of the coupons. The correlation, standard deviation x 10^{-3} = corrosion rate (mpy), was devised from the frequency and corrosion rate data. It was noted that a roll over frequency of -20 dB/decade was observed for pitting attack and -40 dB/decade was observed for general corrosion. The two electrode system is also ideal for studying systems under the open circuit conditions, which include at least one anodic process and one cathodic partial process.

Although ennoblement has been observed for different metals subjected to various service environment with microbiological attack, it is not possible to determine the cause of ennoblement solely from the corrosion potential vs time curves. Furthermore, it remains complicated and challenging to compare the ennoblement data from different locations since the extent of ennoblement is site specific, depending on the microbiological population and the

chemistry of the surrounding water. Furthermore, it is also influenced by samples size, flow rate and temperature [15, 177, 239]. Hence, it can be inferred that ennoblement data by itself is insufficient for the diagnosis of MIC.

2.4.3 Linear Polarization Resistance (LPR)

Linear polarization resistance (LPR) is a relatively simple non-destructive method and frequently used to obtain information on the corrosion rate [248-252]. It is commonly used to continuously monitor the instantaneous corrosion rate of a material in the field, for example, buried pipeline. It requires a small signal perturbation in a narrow range (± 10 mV) relative to the corrosion potential, assuming the relationship between potential (E) and current (I) is linear. LPR is based on the Stern Geary relationship shown in the equation (16). The corrosion rate (CR) is inversely proportional to polarization resistance (R_p) at potentials close to the corrosion potential.

By determining the corrosion density (i_{corr}), the corrosion rate (CR) can be calculated using the equation listed below [177, 239, 240].

$$R_p = \frac{\Delta E}{\Delta I} \qquad \text{..... (1)}$$

$$I_{corr} = \frac{B}{R_p} \qquad \text{..... (2)}$$

$$CR = K \frac{i_{corr}}{\rho} EW \qquad \text{..... (3)}$$

where ΔE, ΔI, i_{corr}, B, CR, K, i_{corr}, EW corresponding to potential change, current change, corrosion current, Tafel constant, corrosion rate, conversion constant, corrosion current density, density of the material and equivalent weight respectively.

LPR is proven to be rapid response technique that enables corrosion engineers to evaluate changes in the process. It is frequently used to determine the effectiveness of inhibitors and optimize the concentration of inhibitors within a short period of time. Okoro *et al.* has studied the role of methanogens in the corrosion of pipelines transporting oil and water. In addition, the

effect of biocide addition was studied using LPR techniques. They found strong correlation between methane production and corrosion rate of mild steel coupons subjected to different biocides (NaCl, nitrite and tetrakis-hydroxymethyl phosphonium sulfate (THPS) of varying concentrations, as shown in Figure 6(B) [253]. It was found that an increase in methanogen production results in increased corrosion rate. Methanogens plays a predominant role in inducing microbiological corrosion in anaerobic environment.

LPR techniques generally result in steady state data, and assume that the corrosion process is uniform across the entire metal surface. As a result, it is not ideal to study localized corrosion, such as pitting and crevice corrosion. However, LPR studies it can be used as an indicator tools, if necessary, provided the rates of pitting and crevice corrosion are sufficiently high [177]. It should also be noted that β_a (Anodic) and β_c (Cathodic) values (Tafel slopes) which are calculated using polarization curves are known to be difficult to obtain and are known to vary through the study. This is attributed to the dynamic nature of MIC which results in non-homogenous biofilm activity on the surface [254]. In a study evaluating the resistance of 2205-Cu duplex stainless steel to MIC, it was found that the Tafel slope varied significantly during the incubation period, which was attributed to change in the biofilm thickness, coverage and activity[144].

Critical pitting temperature (CPT) techniques offer a reproducible, sensitive and efficient method to detect the propagation of pitting corrosion [255]. Due to similarities in pit morphology with pitting corrosion, CPT was employed to evaluate MIC. A study of MIC by *pseudomonas aeruginosa* biofilms in 2205 Cu-bearing stainless steel found and 220 (DSS) found that the latter exhibited larger CPT as compared with the former in the sterile medium. This indicated that the carbon content did not significantly influence corrosion resistance [144]. However, in a biotic

environment a higher MIC pitting resistance was found for Cu-DSS, but no significant change was observed in pitting potential and CPT [66].

2.4.4 Electrochemical Impedance Spectroscopy (EIS)

Similar to LPR, EIS requires a small external signal for perturbation. EIS technique is alternating current method, which involves the application of a sinusoidal potential onto a system, while measuring the corresponding current [256]. The impedance data was recorded over a wide range of frequencies from 10^{-3} 10^{3} Hz and above. EIS technique is widely used to distinguish various processes occurs at the interface between metal and electrolyte or between metal and a film, particularly for materials with non-conducting (i.e., organic coatings) and semiconducting surfaces (i.e., metal oxide films). Numerous researchers have applied this technique to study the disbonding, delamination or degradation of metal coating systems [115, 146, 243, 244, 246].

In MIC, most of the organic and microbiological films adhering to the surface of the materials immersed in natural aqueous environment are non-conducting in nature. Thus, this technique is useful to assess the electrochemical reactions occurring during MIC. Analysis of the EIS impedance is generally carried out with the aid of Bode plots or Nyquist plots to provide information on corrosion processes, such as diffusion, adsorption and capacitive control [73, 177, 257-262]. This can be achieved by fitting the EIS results with suitable electrochemical equivalent circuit (EEC) models to obtain electrochemical parameters related to the performance of the materials. A common example of an EEC used to represent the polymer/solution interface is shown in Figure 6(E)

Apart from measuring the capacitive and/or inductive component of the overall interfacial impedance, EIS technique is also capable of measuring the polarization resistance

(Rp), which is the inverse of the corrosion rate [15]. EIS can also provide useful information on electrochemical evolution of the material's interface exposed to biotic environment. Castaneda *et al.* have found that biofilm formation shifted the dominant process from active charge transfer reactions to a diffusion limited process. This is typically reflected through the change from semicircle behavior to straight line at low frequency as displayed in Figure 6(D) [263]. Luo *et al.* performed an experimental investigation in which the impedance spectra obtained from 316 stainless steel after exposure to oilfield-produced water over varying time periods exhibited differences, which were then correlated with the extent of corrosion. It was indicated that the presence of multiple time constants in Bode plots may be an indication of pitting. The phase angle plots generated to study the effects on carbon steel exposed to SRB biofilm culture in a study by Luo *et al.* investigating MIC in different immersion environments also exhibited differences which can be extrapolated and used in similar impedance plots to observe the differences in the rates of corrosion [44]. The increase in the phase angle at lower frequencies may also indicate a greater thickness of the as-formed biofilm. Sensors which employ EIS have been made to monitor the growth and degradation of biofilms. Interdigitated electrodes fabricated on printed circuit boards and low-temperature co-fired ceramics (LTCC) coupled with a 24-channel multiplexer were used to evaluate impedance response on a 24-well plate setup[264]. This demonstrates the potential of employing EIS as an in-field tool for corrosion detection.

The main disadvantage of EIS is its inability to quantify the electrochemical parameters directly from the impedance spectra. It requires a suitable electrical circuit model for the impedance analysis. Due to the complex interfaces involving partial coverage of biofilm, it is difficult to find a suitable model to quantification the electrochemical behavior of the materials

during MIC [14, 15, 41, 169]. Unlike an organic coating or metal oxide film, a biofilm formed on the metal surface is a dynamic entity and changes continuously owing to the organism's metabolism.

The use of external perturbation through current and voltage can disturb the system under study leading to erroneous corrosion rate data. EIS and LPR were found to inhibit cell growth of *pseudomonas aeruginosa* as compared to EN based monitoring[265]. Electrochemical frequency modulation (EFM) which utilizes current responses at harmonics and intermodulation of input frequencies allow for high sensitivity, with minimal interference from the current response [266]. The large effect of capacitive properties on the EFM analysis makes it a potential tool for MIC detection, especially with the large capacitive element produced by biofilms. This will subsequently lead to short term fluctuations in the electrochemistry. Depending on how fast the fluctuation occurs, these changes may or may not be detected while gathering the EIS data over a range of frequencies [177]. Thus, caution should be exercised during the EIS data interpretation. Similar to LPR technique, EIS techniques are generally employed under steady state condition and thus are not ideal to study localized corrosion.

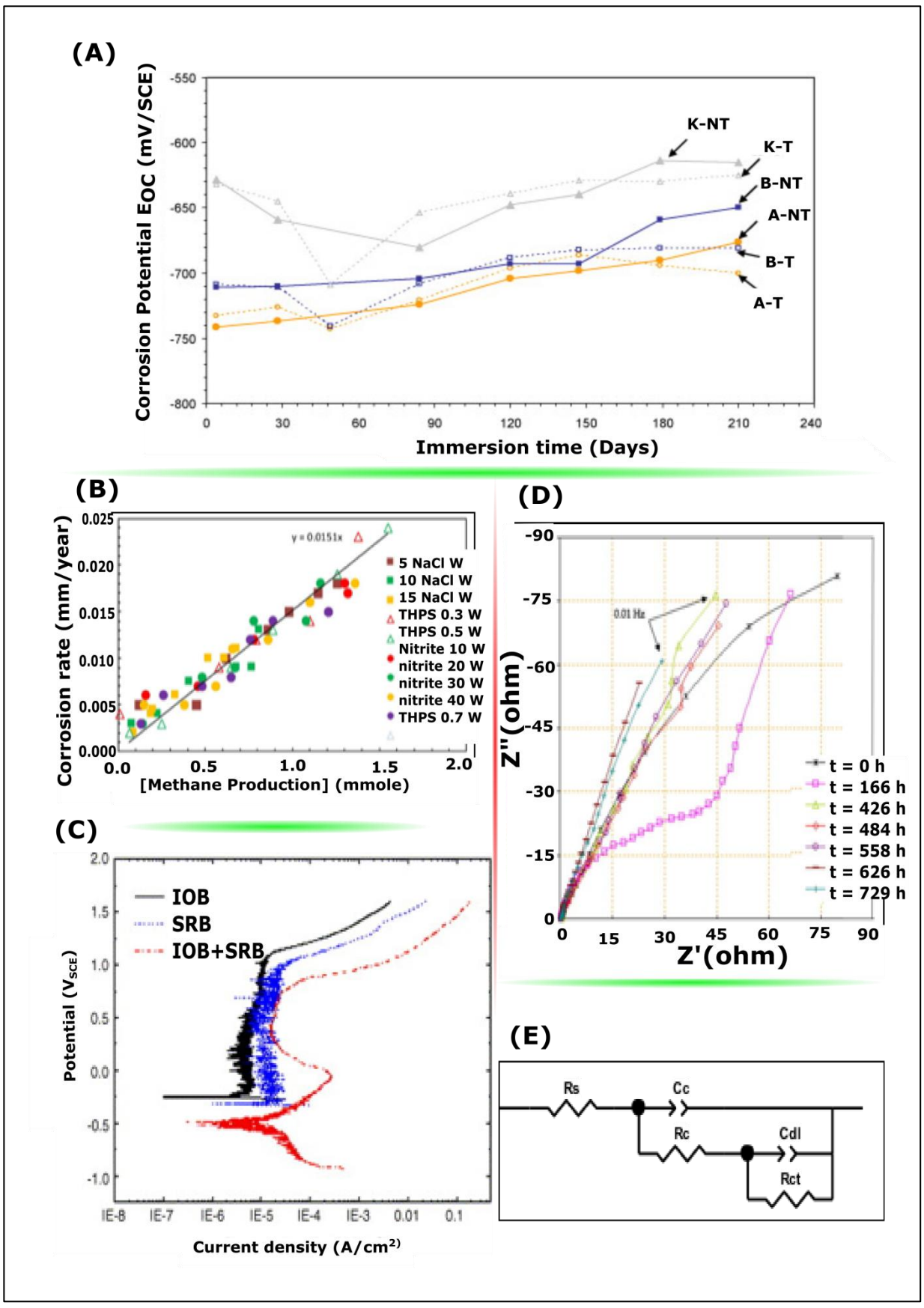

Figure 6. (A) The corrosion potential of two mild steels (A&B) and low alloy steel in treated (T) and non-treated seawater (NT) showing no significant difference with immersion time, with the corrosion potential of low alloy steel K higher than the mild steel in both conditions [267], reproduced with permission from Elsevier (B) The relationship between methane production and corrosion rate of mild steel coupons subjected to various inhibitor with different concentration (triangle: THPS; circle: Nitrite; Square: NaCl) [253], reproduced with permission from Elsevier (C) Polarization curves for 316L SS in three different biological solutions at 30°C, with IOB represents iron-oxidizing bacteria and SRB represents iron-oxidizing bacteria [268], reproduced with permission from ACS publications (D) Nyquist plot of carbon steel exposed to SRB biofilm culture media at different exposure times [263], reproduced with permission from Elsevier (E) circuit used to model the polymer/solution interface with R_s, C_C, R_c, C_{dl}, R_{ct} represent solution resistance, coating capacitance, coating resistance, double layer capacitance and charge transfer resistance respectively

2.4.5 Potentiodynamic polarization

Unlike LPR and EIS techniques, potentiodynamic scans are polarization scan techniques which involve potential perturbation relatively far from the steady state corrosion potential and the potential scan can range from several hundred mV to several V. The driving force for the reaction (potential) is controlled with the net change in the reaction rates being observed. The reaction rates are manifested in the form of the exchange currents (corrosion currents). Potentiodynamic polarization curves generally provide an overview of the reactions for a given corrosion system, including charge transfer and diffusion controlled reactions, passivity, transpassivity, pitting and protection potential. It is particularly suitable to evaluate susceptibility of materials to localized corrosion in different microbiological environments [53, 269-272]. Numerous researches have applied this technique to determine the effects of microorganisms on the corrosion behavior of materials, and compared them with the polarization curves obtained in abiotic environments. Xu *et al.* utilized the anodic polarization curves obtained from 316 type stainless steel in exposed to three different biological environments, which consisted of SRB, iron oxidizing bacteria (IOB) and a combination of both , as shown in Figure 6(C) [268]. The 316L SS exhibited pitting behavior in all the different environments. Nevertheless, the corrosion process was most severe and proceeded at the highest rates in the environment that had a combination of SRB and IOB in the inoculum. This was marked with a significant increase in the current density and a decrease in the width of the passive range of potential. Furthermore, a decrease in the breakdown potential also clearly showed that 316L SS was more prone to localized attack in environment composed of a combination of two species [268].

Although potentiodynamic polarization provides useful information on the electrochemical properties of metal surfaces in different environments, the major drawback of

this technique is irreversible changes occurring on the surfaces, which alter the properties of the metal. Additionally, changes in the structure of the biofilm are possible due to the use of a large signal perturbation that is required while conducting potentiodynamic polarization. A large number of samples are thus required to understand the electrochemical evolution over a certain period of time.

Table 1. Summary of advantages and limitations of the analytical tools deployed to study MIC in the Oil and Gas industry in the context of usability in field, specificity, and cost of analysis.

Techniques	Advantages	Limitations
Scanning Electron Microscopy	1. Rapid 2-D scans 2. High resolution 3. Suited for metallic/conductive surfaces 4. High-fidelity	1. Electron micrography requires vacuum increasing likely damage of biological structures 2. Bulky equipment 3. Offsite 4. Expensive
Atomic force microscopy	1. Quantitative pit/morphology evaluation 2. Sensitive	1. Offsite 2. Limited sampling area 3. Slow 4. High-skill level
Optical Microscopy	1. Rapid 2. usable in field	1. Nonspecific 2. Limited resolution

Table 1. Continued

Techniques	Advantages	Limitations
Transmission Electron Microscopy	1. High resolution 2. Fundamental evaluation	1. Offsite 2. Requires high skill 3. Expensive 4. Sample preparation challenging 5. Information limited due to scale
CLSM/Fluorescence microscopy	1. Limited sample prep 2. High resolution 3. 3D visualization of biofilm	1. Offsite 2. High skill requirement
X-ray diffraction	1. Rapid 2. Crystallographic evaluation (for phase/ composition)	1. Offsite 2. Limited resolution 3. Non-specific data
X-ray photoelectron spectroscopy (XPS)	1. Elemental analysis 2. Relative composition evaluation	1. Expensive 2. *Offsite* 3. Limited spatial coverage
Energy Dispersive spectroscopy (EDS)	1. Rapid 2. relative compositional analysis 3. Coupled with electron microscopy for morphological context	1. *Offsite* 2. Vacuum requirement 2. Expensive 4. Limited spatial resolution
Electrochemical Noise	1. Non-destructive 2. Continuous 3. Differentiation (pitting vs. crevice vs. SCC)	1. Complex data analysis 2. Noise and fluctuations

Table 1. Continued

Techniques	Advantages	Limitations
Open circuit potential	1. Low-cost 2. No external perturbation	1. Differentiation is limited 2. ennoblement is non-specific to materials
Polarization Studies	1. Determine susceptibility of substrates to corrosion 2. Corrosion rate evaluation	1. Large External perturbation2. Repeatability
Linear Polarization Resistance	1. Rapid response 2. Corrosion rate evaluation 3. Steady state data	1. External perturbation 2. Instantaneous corrosion rate 3. 'B' (Tafel slope) values unreliable
Electrochemical Impedance Spectroscopy	1. Mechanistic information 2. Differentiation	1. Complex data analysis 2. External perturbation3. High skill
MPN	1. Field deployable 2. Rapid 3. Low cost	1. Non-specific data
PCR	1. Specific 2. Field deployable kits	1. High skill 2. Expensive 3. Complex data analysis
16s rRNA and associated NGS	1. Highly specific 2. Metagenomic analysis	1. Expensive 2. High-skill 3. Offsite

Table 1. Continued

Techniques	Advantages	Limitations
MS	1. Highly specific 2. Bio-marker evaluation	1. Complex sample preparation 2. Complex data analysis 3. Offsite 4. High skill 5. Expensive 6. Custom method development
LASCA	1. Bio-compatible 2. Specific 3. Direct evaluation	1. Difficult sample prep 2. Complex data analysis 3. Offsite 4. High skill 5. Expensive

It is important to conduct holistic studies before concluding MIC activity at a site. Since, laboratory studies may be limited in terms of scope and simulated field environment, it is important to understand the advantages and limitations of the tools deployed to investigate MIC. The advantages and limitations from the perspective of the oil and gas industry are listed in Table 1. The current strategies for MIC detection are cost-prohibitive because of two different reasons: considerable training required for personnel and the large amounts of capital equipment required. Overall, next-generation methods for MIC detection that circumvent these limitations and have the following characteristics need to be developed: they should be mobile (should be able to detect MIC on-site), they should be non-destructive in nature, they should be cost-effective, and finally they need to be rapid (minutes~ hours). The last characteristic is owed to the economic cost of MIC mitigation, which may be enhanced because of improper and late

detection. Any existing knowledge from lab-scale studies should be used to corroborate observations from the field and identify phenomenological correlations.

2.5 Literature review conclusions

The current techniques employing only microbiological activity tracking have shown mixed results, owed to the difficulty in mapping only microbiological population density with the extent of their contribution towards MIC. The improved mechanistic understanding of MIC indicates that extracellular metabolites play a key role in its propagation. Therefore, the detection of these metabolites serves as a leading indicator for possible degradation activity. This demonstrates that there needs to be a unified platform capable of adapting to the evolving understanding of MIC for its effective early detection and prevention. Even high-throughput methods rely on the use of static microenvironments such as 96-well plates in which materials are exposed to corrosive microbiological consortia under investigation (for e.g., iron, carbon-steel), thus yielding limited applicability to real-time corrosion monitoring [273]. Multi-electrode array sensor systems (MASS) rely on similar changes in the microenvironment to generate a resistive response for characterizing the corrosivity [274]. Commercially available sensors such as the ALVIM system rely on the electrical response of the biofilm growth on a fixed location, offering a non-specific, albeit real-time monitoring of electrochemical activity[275].

The last decade has witnessed the rise of new detection platforms such as biosensors which have the potential of overcoming many of the limitations discussed. These biosensor architectures were primarily acquired from clinical chemistry, where they have been used for detection of moieties such as proteins and glucose [152, 276]. The use of nanowire-based architecture has been widely explored for the detection of both proteins and microbiological

species. A label-free detection technique was demonstrated [277], where silicon nanowires were surface functionalized using silane chemistry followed by characterization based on biotin-streptavidin interaction. Silicon nanowire-based sensing has been widely studied, s including the development of a Nano-Field Effect Transistor (FET) [278] for sensitive detection of chemical and biological moieties. These sensors were showed to be useful for detecting cardiovascular proteomic markers, [279] study of protein-protein interactions[280], and in FET-based biomolecule sensing [281]. Metal oxides (MO_x) nanowire-based sensors have also recently seen large research activity. For example, ZnO based sensors have been used for fabricating glucose-biosensor [282]. This involved the immobilization of glucose oxidase on a carbon-decorated ZnO nanowire array. Other examples, include DNA sensor applications [283], uric acid-biosensors [284], DNA Sequence detection [285], ZnO platelets-based antibody detection [286], and detection of specific protein residues to interpret and understand metabolic functions[287]. Specifically for MIC detection, the presence of SRB was determined by studying the chemical conversion of ZnO nanorods arrays into ZnS arrays[288].

In addition to nanowires, other transducing architectures have been explored for the purpose of sensing. This includes use of nickel foam combined with gold nanoparticles [86] immobilized with specific moieties for bioanalyte based impedimetric detection of MIC causing bacteria. Indirect detection utilizing temperature and H_2S sensing have been used in laboratory-scale for culturable microorganisms to yield binary classification of the possibility of MIC. A review [289] discussed the development and application of the nanowire sensors, various key results and mechanisms behind the operation of the sensors. Detailed reviews, specifically of microbiological biosensors and electrochemical biosensors can also be found in the literature where they are used for early detection based on biomarkers [290, 291].

Some examples of nanosensors are discussed further to detect various biomolecules. A study [292] of the degradation of concrete by *thiobacillus* utilized lipid biomarkers as indicators for the acid-producing bacteria. A study by Smith *et al.* [293] focusing on water networks utilized the polar lipid fatty acids in a biofilm to determine the nature of the biofilms which colonize the network. The study observed that the fatty acid composition did not significantly change with seasonal variations and oxirane fatty acids were identified as a possible marker for loss of biofilm viability. An example of a real-time study of a biofilm can be found in a study by White *et al.* [294], where a biofilm was studied using tryptophan fluorescence. Marker-free nano-sensors have demonstrated the ability of fast response and sensitivity up to 2.5 $\mu A/\mu M.cm^2$. A study utilized a PEDOT-PSS supramolecule functionalized on SW-CNT working electrode. This working electrode was utilized to detect changes in environment using the label-free surface and it exhibited stable and reproducible current response[295]. The studies summarized in this literature review do indeed attest to the fact that an a real-time MIC monitoring platform can be realized with a biomarker driven nanosensors approach. However, further research is required before wide scale adoption by the industry.

The development of a biosensor platform that supports the biomarkers itself needs further research. The sensor platform by itself should not react with any components of the environment inducing MIC. The platforms should have incorporated within them elements that make it anti-fouling. In addition, non-specific binding (NSB) of bioanalytes during sensing should also be avoided. As nanomaterials (such as nanowires) have high specific surface areas, they are highly desired for sensor platform fabrication. However, the high specific surface areas also make them unstable and lead to their fouling and the NSB of analytes and the reaction of the nanowire themselves with multiple species of the MIC-causing environment. Therefore, stabilization of

nanowire surfaces in a manner that makes them only react with specific analytes (or biomarkers) is essential. In addition, they should offer the possibility of detecting multiple analytes simultaneously. Taitt *et al.* [296] demonstrated the use of a single platform for nine analyte detection, giving impetus to the promise held by these emerging areas for MIC. This can be combined with high-throughput screening techniques such as bi-polar electrochemistry especially for complex substrate morphologies[297].Overall, the studies here demonstrate the need for a system of study and detection which provides the following characteristics.

- Scalability of detection strategy: Scalable strategies include the effort to mass produce detection platforms, include nanomaterials such as nanowires. This includes the large-scale production of the materials, but also the ability to assemble them into usable devices (such as sensors), in a cost-effective and reproducible manner. Although there has been research discussing nanomaterial mass production [298-301] there is a need to further these mass production strategies to produce nanomaterials that have degradation resistant [302] and modifiable-on-demand surfaces [299].
- Decreased capital costs: Offsite detection and study of MIC requires access to expensive resources of analytical equipment and reagents. Hence a low-cost method such as sensors fabricated with low-cost is necessary.
- Faster detection and higher spatial resolution: MIC is a phenomenon which displays a large amount of uncertainty in the spatial domain of occurrence. MIC sensors should have fast response time and high spatial resolution.
- Greater adaptability and reproducibility: MIC is a result of a complex consortium of microbiota, hence sensing technologies need to be modifiable to detect a wide array of

microbiota Also, the data produced using these methods need to be system independent and is reproducible.

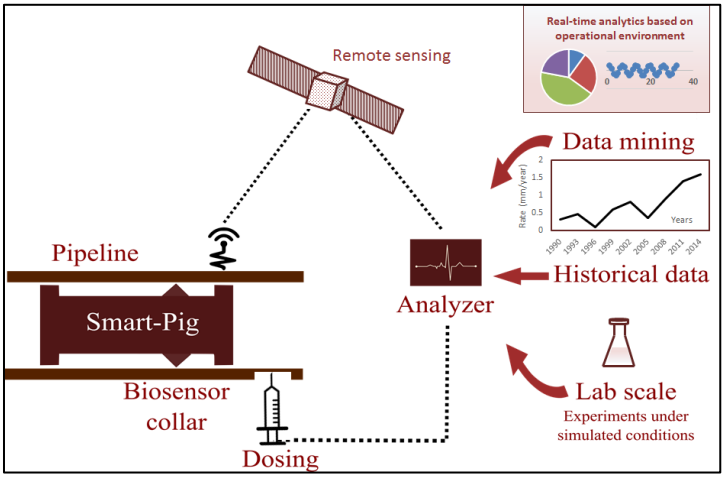

Figure 7. An integrated approach for remote and real-time MIC monitoring of MIC in the oil and gas industry.

Biosensors deployed on smart pigs as illustrated in 7 provide a possibility for spatial as well as temporal resolution of microbiological activity in real-time. The key is to combine existing information and prior art, with historical data from the affected site. This in conjunction with lab-scale studies which can be extrapolated to the conditions observed in the field, need to be utilized to determine a mitigation strategy. In conjunction with the use of wireless communication and data mining, this provides the ability for remote sensing and effective mitigation of MIC.

3. PROBLEM STATEMENT

MIC detection is currently performed utilizing morphological, chemical compositional, electrochemical and biological techniques. For effective diagnosis of MIC, the data from these tools need to be integrated, and often still requires expert elicitation. The current state-of-the-art is limited by a lack of online monitoring technique, with most high-resolution tools limited to off-site laboratories. Primarily industries rely on non-specific and qualitative techniques such as the use of corrosion coupons, bug-bottles and ATP tests on-site. Traditional culture-based techniques can detect only 1% of the microbes in nature and the use of selective media for detecting the presence or absence of bacteria may lead to faulty outcomes [303] [180]. Additionally, as revealed by the literature review, there is no comprehensive mechanism for MIC which is widely accepted and the mere presence of microbiota is not an indicator of MIC activity. It is also noted that the early detection of MIC is key to the effective mitigation, hence the delay caused by sample collection, and transfer may lead to erroneous conclusions. Metagenomic and metabolomic techniques provide the distribution of microbial communities and the metabolite profile in an oil field community, allowing for the identification of biomarkers. This is representative of the combined effect of the micro-environment and the microbial communities, however these techniques also require highly trained personnel, sophisticated data analysis and are limited by robust feedback systems to ultimately impact MIC mitigation in field applications. Unlike microbial assays, biosensors can be constructed to give outputs in scales of electric current, voltages or numeric scales such as the Callaway or the Stein-Lutey MIC index [149], which would allow the rapid assimilation of data in real time. Although biosensors utilizing nanomaterials such as nanowires offer an opportunity to detect these biomarkers in the process environment by their utilization as substrates has been limited by

challenges in synthesis and fabrication including lack of robust and scalable material synthesis and processing techniques. The nanowires provide advantageous material properties such as surface area to volume ratio, and an ability to functionalize and perform electrochemical measurements by using them as transducers. However, they are limited by their stability and useful nanomaterial candidates need to be studied in corrosive environments observed, for example in the chemical processing and oil and gas industry to evaluate their viability. The need of the hour is a real-time sensor which is stable, adaptable, mass-producible, reliable, reproducible, and selective. Overall, next-generation methods for MIC detection that circumvent these limitations and have the following characteristics need to be developed: they should be mobile (should be able to detect MIC on-site), they should be non-destructive in nature, they should be cost-effective, and finally they should have a fast response time.

4. GOALS

The goal of this thesis is to develop a path towards a sustainable and robust detection platform for the early detection of MIC. The current focus would be to identify substrate materials and morphology for biosensors, stabilization and characterization in industrial simulated environment and development of a proof of concept demonstration. The specific objectives are outlined below and detail the specific aims towards the development. Figure 8 demonstrates the target to be achieved with respect to the specific to MIC and the detection level that is aimed for with this approach.

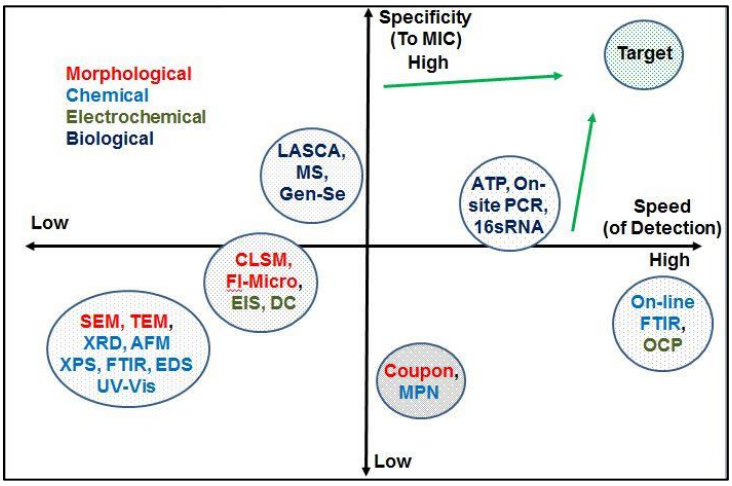

Figure 8. Target properties of the detection platform as compared to existing state of art.

The analytical tools discussed in the previous section have the ability to generate precise and accurate data in the morphological, chemical, electrochemical and biological domains, all of which are important for inferring the presence of MIC especially in laboratory investigation. For the development of the next generation of detection platform for wide scale deployment, it is important to evaluate existing platforms in the context of industrially relevant metrics of

specificity to MIC and speed of detection of MIC. Morphological and chemical investigation tools including SEM, TEM, XRD, AFM, FTIR and EDS provide information in off-site analysis and laboratory investigations. This information is at high-resolution, but the tools provide only limited scalability due to their size and cost limitations. Additionally, many of these tools require high levels of expertise and rigorous sample preparation which limits their application. The data generated can be utilized to provide both mechanistic insights and qualitative information which are useful for example to identify high-risk locations (by the evaluation of corrosion coupons from the field) for sensor deployment, and in incident investigations to establish MIC as a root cause. The techniques such as online FTIR and LPR provide real-time capability, but are limited by their specificity due to lack of the ability to differentiate between abiotic and biotic corrosion indicators. Techniques including such as next generation sequencing and mass spectroscopy can provide MIC specific information, however are off-site and lack the scalability for wide scale low cost deployment. They can however, be leveraged to identify potential bio-markers, high-risk microbiota and establish the biological markers of the system under investigation. This can be used to build chemical probes for the detection of these markers and functionalized onto the sensor substrate to yield a real-time platform for the detection of MIC. Hence, the goal of the sensor platform needs to be to overcome the speed and specificity limitations of existing tools as illustrated in Figure 8, and at the same time build on the high-resolution data provided by these tools in laboratory and off-site investigations.

4.1 Substrate identification, mass production and characterization

The first goal of the thesis is to identify a sustainable strategy for the development of a sensor platform. This entails the requirement of the ability to mass produce the substrate in a cost effective manner, with an additional requirement to assemble them in a usable device form. Mass

production exists for a few systems [298-301] but there is a need to further evaluate these mass production strategies for producing large quantities of materials. These nanowires also need to be made degradation resistant [302] and modifiable-on-demand surfaces [299]. The diameters of nanowires are comparable to the sizes of the biological and chemical species being detected and hence represent the possibility of being excellent transducers to ultimately interface with the macroscopic instruments. Concentration measurements have shown that detection can be carried out in the femtomolar range[304]].

The high surface area to volume ratios allow for increased sensitivity. For nanowires with a length of 10 μm and diameter ranging from 25 to 100 nm, the surface area to volume ratio varies between 10^8 m^{-1} to 2 x 10^8 m^{-1} [305]. It is estimated that a 1 cm^2 surface area of the bulk nanowire substrates, have an actual surface area (due to nano-structuring) of between 2 m^2 to 4 m^2. This provides a usable surface for chemical modifications required to perform sensing operations. For this goal two nanowire systems are chosen for evaluation. These are silicon nanowires (Si) and cupric oxide (CuO) nanowires. Silicon nanowires are widely known candidates as sensing substrates. They are semiconducting (and can be doped to manipulate bulk properties) and can be produced at large scale using facile techniques, and there exists the possibility of exploiting the surface chemistries of the passive SiO_2 layer to create semiconducting NWs which can be modified with receptors with the potential to perform sensitive detection of chemical and biological species in aqueous solutions, as has been demonstrated in clinical settings [278]. The silicon nanowires are proposed to be synthesized using a electroless etching process [306] and further characterized using SEM, XRD and Raman spectroscopy. Copper oxide nanowires (CuO NWs) provide a low-cost, highly scalable substrate which can provide micro/nanometer structures with properties such as modified wettability with

corrosion resistance and self-cleaning properties [307]. CuO NWs also have the potential to serve as self-sterilizing substrates, and provide fast response and recovery times [308]. As part of this goal, these nanowires will be synthesized utilizing a thermal route and characterized with SEM, TEM, Raman spectroscopy and XRD. Boron nitride, an inorganic ceramic material is known to provide degradation resistant properties to bulk and nanomaterials [309]. A CVD assisted route for further stabilization will be explored using two precursors, tribromoborazine and ammonia borane. The results are then characterized with SEM and Raman spectroscopy. The nanowires synthesized at the end of goal 1 are then utilized in goal 2 for their stability evaluation.

4.2 Electrochemical stability evaluation and study of degradation mechanism of the nanowires

The second goal of this thesis is to demonstrate the stability of the silicon and cupric oxide nanowires under simulated industrial environments. These environments are simulated utilizing a 3.5% NaCl solution [310] and simulated produced water [311, 312], both of which are used to perform corrosion and degradation testing of industrial materials at the laboratory scale [313].The stability would be evaluated utilizing DC and AC techniques. Potentiodynamic polarization measurements [314] would be utilized using a standard three electrode configuration with the nanowire substrates as a working electrode. A standard calomel reference electrode and platinum electrode are utilized with 200 mL of electrolyte, in a standard faraday cage. For the AC technique electrochemical impedance spectroscopy (EIS) is performed at open circuit conditions and to evaluate the impedance response of the working electrode [315]. Additionally, the Nyquist and bode plot are evaluated for the frequency response of the nanowire surfaces and equivalent circuit fitting is performed to explain the possible degradation mechanisms [316].

Based on these evaluations, the nanowires are then utilized to develop a proof-of-concept demonstration for goal 3.

4.3 Demonstration of proof-of-concept sensing using nanowire substrates

The third goal of this thesis is to develop and demonstrate the proof of concept by utilizing the nanowire based sensor substrate. Traditionally, nanowire substrates are utilized either as single nanowire devices[317] or nanowires in integrated circuits [318]. Although these serve as useful tools, industrial environments demand the use of mechanically robust setups to demonstrate their viability in the aggressive field environments. This work will however utilize the nanowires in their natively prepared form. Silicon nanowires are used in their as-prepared form, which is as etched epitaxial nanowires on silicon wafer. The nanowires would then be functionalized using Aminopropyltriethoxy silane (APTES) and N-hydroxysuccinimide biotin in a phosphate buffer solution [319]. This is achieved utilizing a combination of known biomolecule interaction using biotin and streptavidin (SA) [278]. The Silicon nanowires are exposed to streptavidin, a 60 kDA protein which has a high affinity to biotin (Rate constant ~ 10^{-14}). These two molecules exhibit a large affinity and irreversible affinity under a range of pH and ionic conditions. Finally, to perform the electrochemical analysis a custom thin-film device is built which utilizes the functionalized nanowire substrate as a working electrode in a three-electrode configuration. This would allow for the evaluation without the need for clean room of photolithography techniques to setup the substrate. The substrates are then exposed to 0.1M PBS solution of cyclic voltammetry characterization. The differences in the behavior of the SiNWs under 10 nM and 10,000 nM exposure of the SA analyte. The peak current responses at 0, 1, 2 and 3-hour immersion are used to evaluate the sensor response.

5. SUBSTRATE IDENTIFICATION, MASS PRODUCTION, AND CHARACTERIZATION

5.1 Introduction

The substrate compatibility with the scale of the target analyte allows for specific and sensitive detection of the target analyte [304] and this is an important factor in the selection of substrates for detection. As discussed in the literature review, these target analytes include large biomolecules for detection of specific microbiological species and smaller chain acids which are indicative biomarkers. The size of these molecules can vary from a few angstroms to few hundred nanometers, making nanomaterials an attractive platform for their detection since they offer a dimension ranging from angstrom to few hundred nanometers. Despite the attractiveness of nanomaterials as substrate, an important constraint to their wide-scale adoption is the lack of low-cost substrates which can be synthesized in relatively facile manner. Additionally nanomaterials may pose toxicological challenges during use and deployment which further reasons the use of substrates that have strong resistance against mechanical degradation and robust stability of sensor response in aggressive environments. Finally, as a sensor substrate, their electrochemical response needs to respond to the changes in external stimuli such as the change in the concentrations of the target analyte. Although it is possible to use non-targeted detection (where the substrate is used without further modification or chemical probes), calibrating the electrical response to microenvironment changes, the highly complex and fluid environment typically encountered in industrial systems such as crude oil and produced water pipelines present a challenge to this form of detection. The availability of self-assembled monolayers and aptamer based tools, provide the ability to deploy these molecular wires for the specific and sensitive detection of biomarkers such as volatile fatty acids and proteins.

Nanowires are an extensively studied nano-morphology owing to their size dependent properties such as optical electrical and magnetic properties [320], enhanced charge transport [321], wettability [307], minimum power consumption and surface area to volume ratio [304]. Nanomaterials of various morphologies such as quantum dots, nanowires, nanoribbons and nanorods have been synthesized using different materials including Group III—V elements, and co-block polymers [322] . They have also been used in gas sensors[323], thermoelectrics [299], biosensors [278], field-effect transistors(FET's) [324-326], solar cells [327] and nanoscale LEDs [328]. Nanowires have been synthesized using various material systems. This include elemental nanowires of silicon, Germanium, Copper, Iron and compound nanowires mainly, which are mainly semiconductors, which include ZnO, CuO, Cu_2O, GaAs, GaP, Zn_3P_2, InP, and Indium-tin oxide. Their wide-spread adoption in devices and end-user applications have been limited due to scalability constraints and limited understanding of their viability in aggressive environments. Some groups have attempted mass production of silicon nanowires [298], Zinc Phosphide [299] , Zinc Oxide [329] nanowire systems using chemical vapor deposition (CVD), hydrothermal, thermal and solution based synthesis methods [330]. However their study in industrial environments has been limited because of limited scale of production. However, with scalability and mass production of nanowires [331] being explored in recent time, it is important to understand their stability in commonly used industrial environments

Additionally, nano-materials suffer from easy gaseous and aqueous degradability, hence strategies have been proposed to enhance stability. This includes placing organic and inorganic coatings or surface enhancements by self assembled mono layer assemblies. Since the nanowires have an increased surface areas as compared to their bulk counter parts, it becomes necessary to study any additional protective strategies to reduce the degradation rate.

Two widely synthesized nanowires systems are silicon nanowires (SiNWs) and Cupric (II) oxide nanowires (CuONWs). Silicon is the second most abundant material on the earth, with high stability, low toxicity, good electrical properties and well established techniques for their fabrication [332]. SiNWs have been studied owing to the wide-spread interest in clinical applications for the detection of proteins, DNA, and enzymes[333]. Copper oxide nanowires have gained attention due to their low-cost and simple production techniques using thermal oxidation. CuONWs have been focused on thermal evaporation of copper in oxygen or air atmospheres at ambient atmospheres [334-338]. They have synthesized in the 300 to 900 ^{0}C at a variety of oxygen partial pressures [339, 340]. The thermal route has proven to be a facile viable route. CuONWs has been utilized for gas sensors, battery anodes, and even high temperature superconductors [341]. CuONWs have been investigated as an important p-type semiconducting material with applications in field effect transistors and thin-film based sensing devices [342].

5.2 Experimental methods and procedures

CuONWs are prepared using a thermal route based on a modified method described elsewhere [335]. Copper (industrial grade 99%, purity) is cleaned with acetone and deionised water and dried. It is then etched with 50% HNO_3 (by volume) to remove native oxides and rinsed multiple times with distilled water. It is then placed in a tubular furnace and heated at 500 ^{0}C for 8 hours. A ramp rate of 50 ^{o}C/min was used and air was used as the oxygen source. The copper oxide nanowires obtained were 25 to 30 μm in length and 50 to 100 nm in diameter and uniformly distributed as a mat of nanowires. The silicon nanowires were synthesized using a detailed procedure described elsewhere [306, 343]. Figure 9 and Figure 11 describes the process used to synthesize the SiNWs. <100> oriented silicon wafers were used, for the synthesis of the nanowires. A mixture of silver nitrate and hydrofluoric acid was used as the etching bath. After

the etching the mixture of nitric and hydrochloric acid was used to clean the wafer and they were rinsed thoroughly with DI water. The nanowires obtained were epitaxial and had diameters of between 45 and 100 nanometers and the lengths typically from 5 to 8 µm.

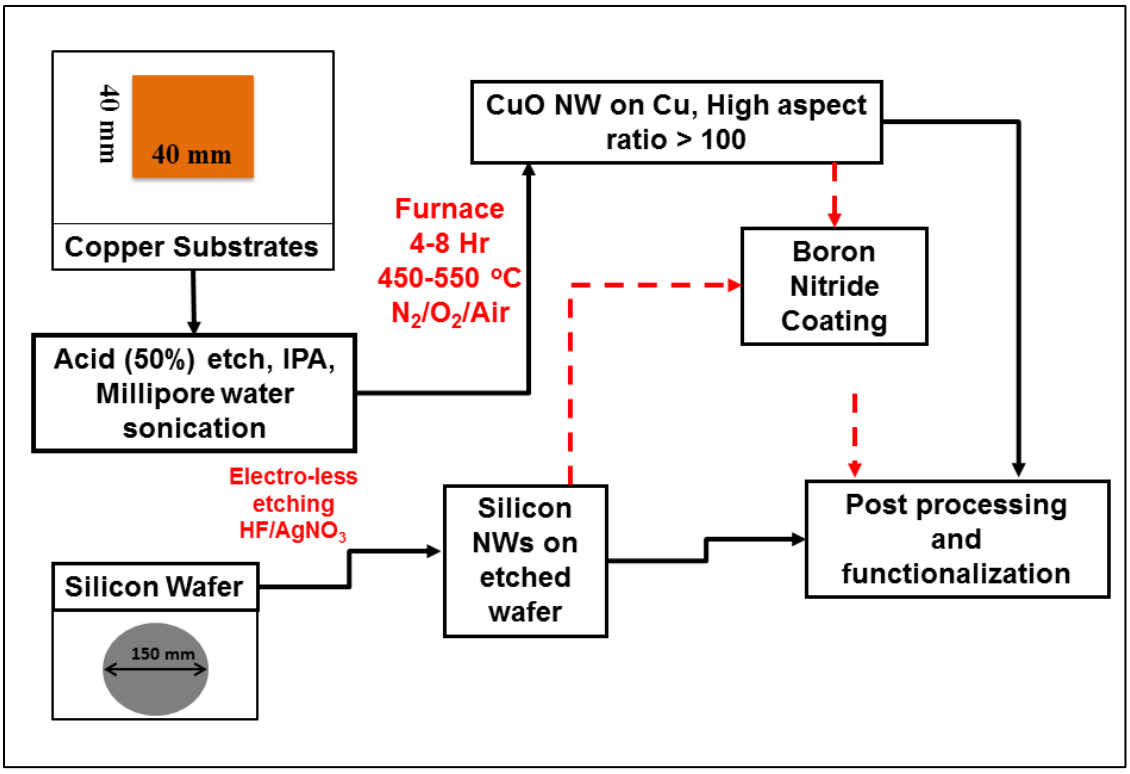

Figure 9. Synthesis scheme for the CuO NWs and SiNWs

Figure 9 demonstrates the synthesis scheme utilized in this approach. The synthesis methods allow for the reproducible and consistent low-cost production of the nanowire systems. This is because both the methods utilize relatively low-cost substrates and reagents. Additionally, all the steps are performed with the use of photolithographic tools and can be scaled with ease. For the silicon nanowires, the ability to have a continuous production line with silicon wafers

provide the scalability. In case of the copper oxide nanowires, the use of air as a source of oxygen with low-cost thermal furnace and inexpensive mass-produced feed stock of commercial copper, offer an excellent opportunity for scale up.

The as prepared CuONWs and SiNWs were then decorated with Boron Nitride (BN) using a thermally assisted chemical vapor deposition (CVD) [302]. The as-prepared nanowires are placed in a hot-walled CVD chamber in the presence of hydrogen as the carrier gas. B-tribromoborazine (~30 -40mg) is introduced into a decomposition zone at 600 ^{0}C. An alternative boron nitride coating strategy used ammonia borane through a stainless steel bubbler. Ammonia borane is heated to ~ 100 ^{0}C in a bubbler and introduced onto the substrate at a decomposition zone temperature of ~1000 ^{o}C under 20-80 sccm H_2 flow. The nanowires are characterized using scanning electron micrography (SEM) (JEOL JSM 6460), Raman spectroscopy (Horiba Jobin-Yvon, X-ray diffraction (Bruker powder diffractometer).

5.3 Results & Discussions

The SiNWs prepared using the electroless etching are in epitaxy with the substrate. This structure is a consequence of the etching process on the single crystalline silicon wafer which is along the dominant direction. The synthesis results in SiNWs that are adhered to the silicon wafer.

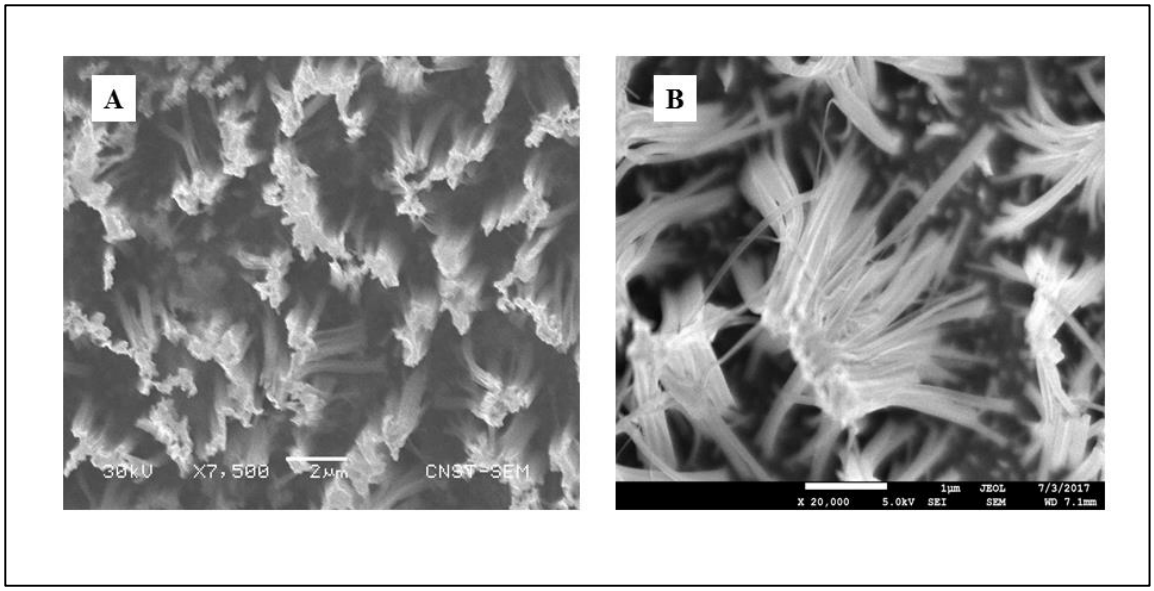

Figure 10. (A) SiNWs at as produced on silicon wafer (B) The bunching of SiNWs after formation as observed on the wafer

Figure 10 (A) shows the SiNWs which exhibit a typical size of 45 to 100 nm in diameter and 5 to 8 μm in length. The nanowires after formation bunch up as observed in Figure 10(B).This bunching up (bundle formation) is attributed to the capillary forces that are acting on the nanowires as they are pulled out of the etching bath [344] Although there was some variation observed of the nanowire density on the wafer, their synthesis yields relatively high reproducibility. The challenges include the sensitivity to even small changes in the procedures such as concentration of the silver nitrate, and temperature of the etching bath [344]. Figure 11 is a schematic representation of the process to make the SiNWs. It involves the synthesis step in the silver nitrate/hydrofluoric acid bath, followed by a cleaning step in an acid bath to remove silver precipitation from the silicon wafer.

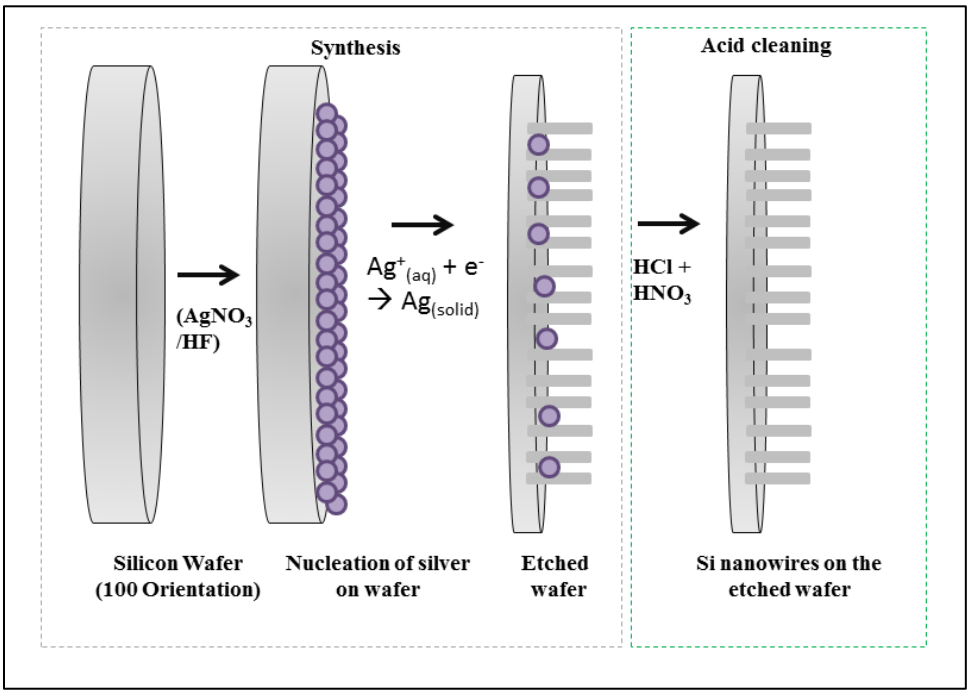

Figure 11. Schematic representation of the synthesis process of the silicon nanowires on the silicon wafer to yield the epitaxial nanowires

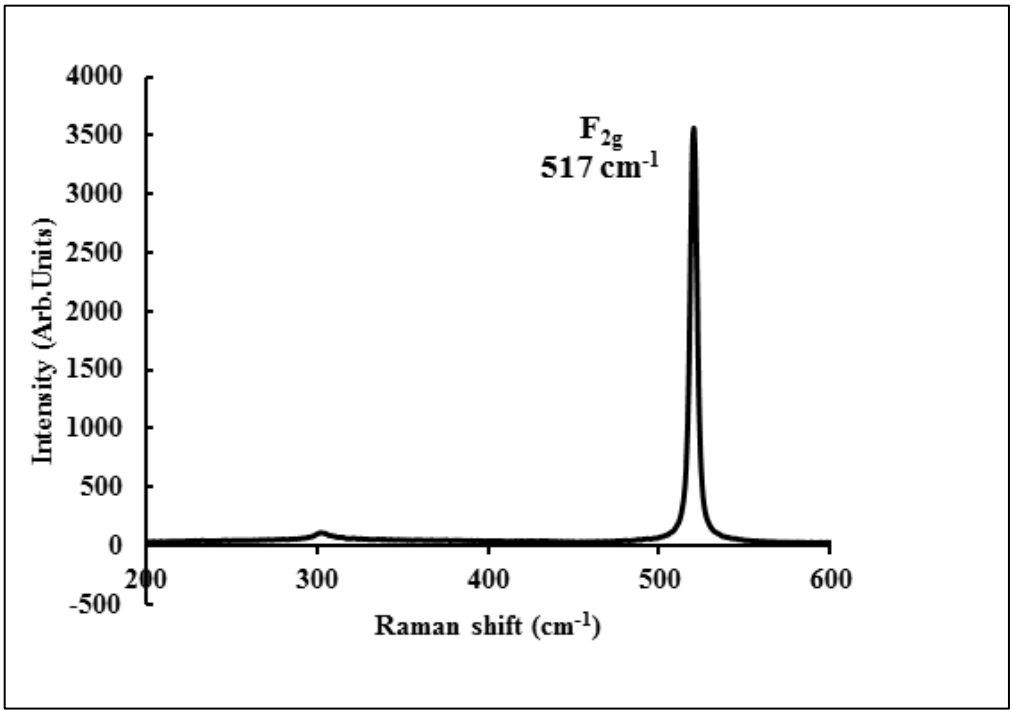

Figure 12. Raman spectra of as-prepared Si NWs

The nanowires were further characterized using Raman spectra to ensure that there was no residue remaining after the cleaning process. It was observed that the single silicon peak (Figure 12) with the Raman shift ~ 517 cm^{-1} was observed [345], indicating good residue free substrate (salts and any organic contamination) for the next steps in the processing. Figure 13(A) given below shows the as-prepared copper (II) oxide nanowires (CuONWs) with thermal heating route as described earlier. The 'mats' structure of the CuONWs can be observed clearly and dense coverage was observed over the copper substrate as seen in Figure 13(A) and Figure 13(B). The CuONWs synthesized had diameter of 50-100 nm as seen in the TEM image in Figure 13(C). The CuONWs had a length of 25-30 µm as seen in Figure 13(A).

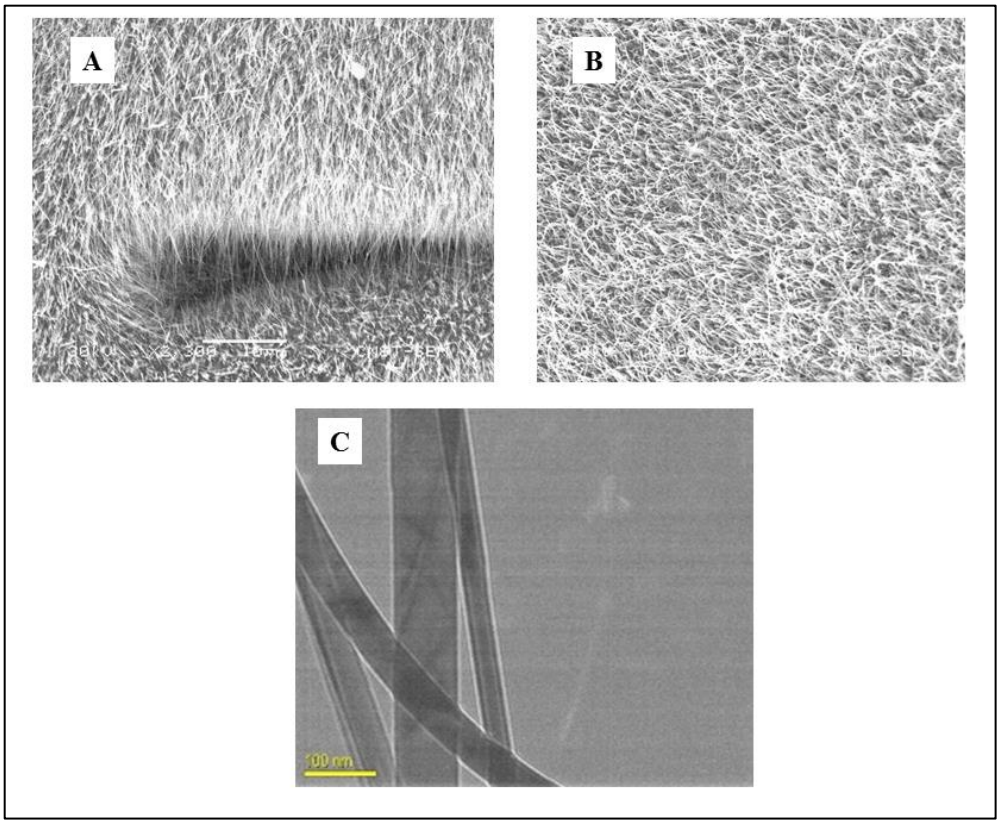

Figure 13. (A) Copper (II) oxide nanowires using facile thermal synthesis observed as a dense mat (B) High density CuO NWs coverage on copper substrate after thermal oxidation (C) HR-TEM image of CuONWs indicating a diameter of 50 to 100 nm

The CuO NWs synthesized by thermal oxidation were studied with Raman spectroscopy. There are 12 zone-center optical phonon modes of $4A_u + 5B_u + A_g + 2B_g$.[346]. Cu(II)O is a member of the C^6_{2h} space group with two molecules per cell [347]. The Raman active phonon modes are however only three and correspond to the A_g (296 cm^{-1}), $B_g^{(1)}$(346 cm^{-1}) and $B_g^{(2)}$(636 cm^{-1}). These three modes are however slightly displaced, with the A_g (297 cm^{-1}), $B_g^{(1)}$(348.5 cm^{-1}) and $B_g^{(2)}$(637.5 cm^{-1}) as seen in Figure 14. The displacement in the wave-number can be attributed to the size effects, which are a consequence of an increase in the crystal size [347].

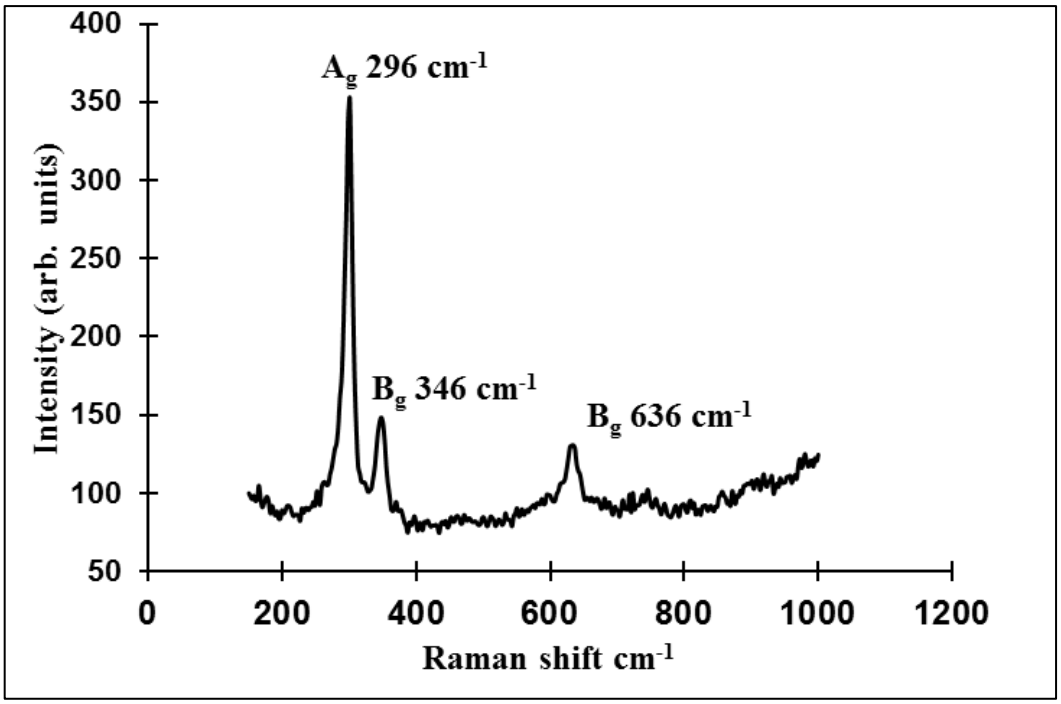

Figure 14. Raman spectra of CuO NWs exhibiting three Raman active phonon modes

The XRD spectra of the as-prepared CuO nanowires was obtained and it confirmed the presence of the Cu(II)O phase. However, the presence of remnants of the residual copper and

Cu(I)O phase was also detected. This is seen in the comparative XRD spectra as demonstrated in Figure 15.

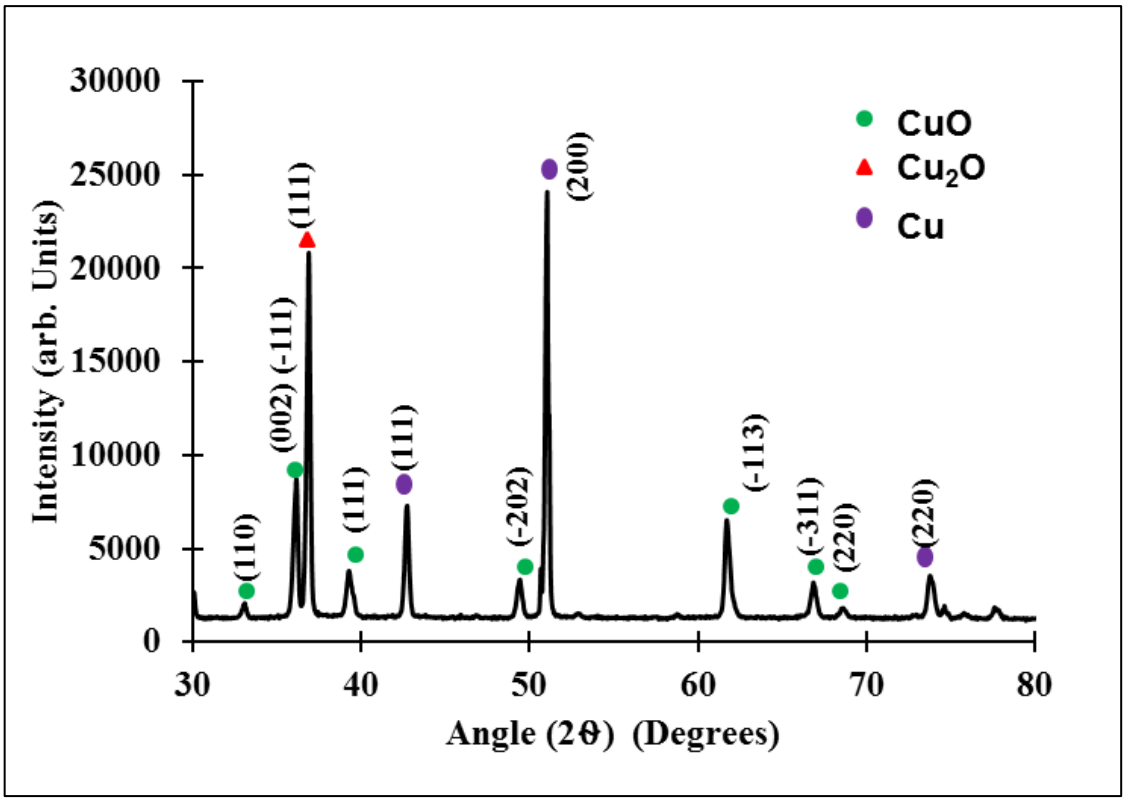

Figure 15. XRD spectra of CuO NWs synthesized using thermal synthesis on Cu substrate revealing CuO, Cu_2O and Cu phases

As seen in the cross-sectional SEM in Figure 16(A) and the XRD spectrum in Figure 15 we observe that the copper substrate after thermal oxidation reveals the presence of Cu, Cuprous oxide (Cu_2O) and Cupric oxide (CuO), The growth of the CuONWs are explained by the thermally assisted diffusion of copper ion to the surface and the counter diffusion of the oxygen from the surface to the cuprous oxide layer. The routes of this diffusion is proposed to be along the lattice or the grain boundary [348]. This is represented in Figure 16(A) and (B).

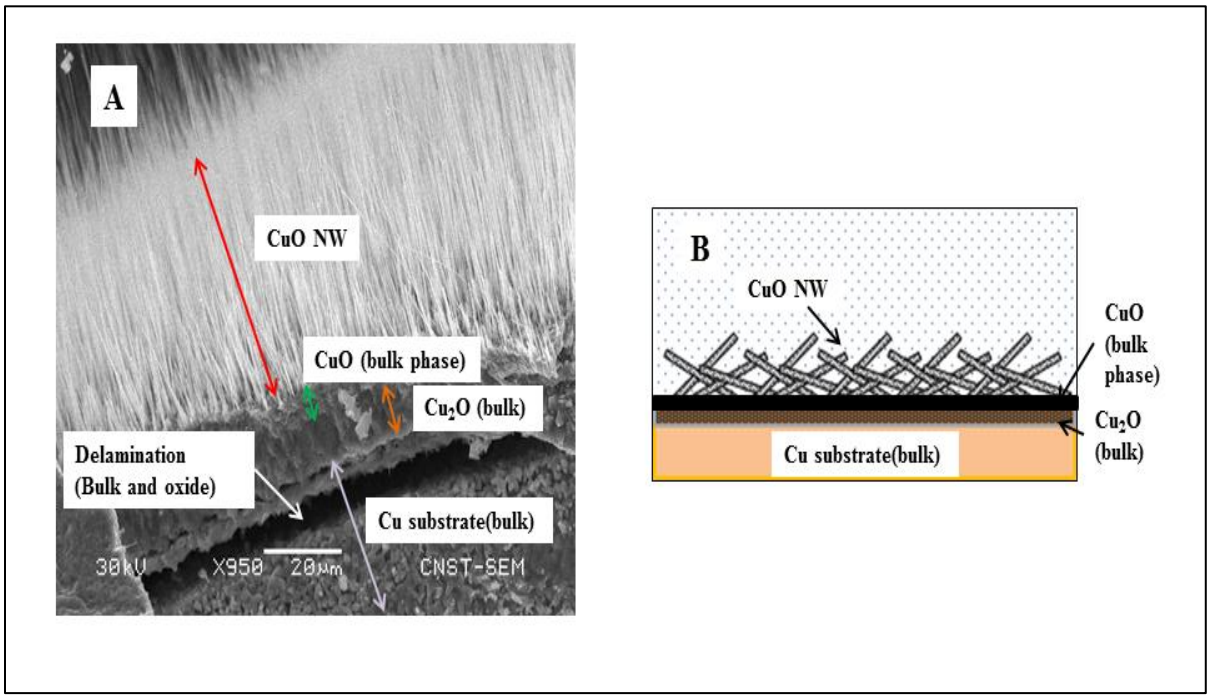

Figure 16. (A) Cross-section SEM of Cu-oxide thin-film exhibiting the oxide phases and the bulk substrate (B) schematic representation of the CuONWs mat

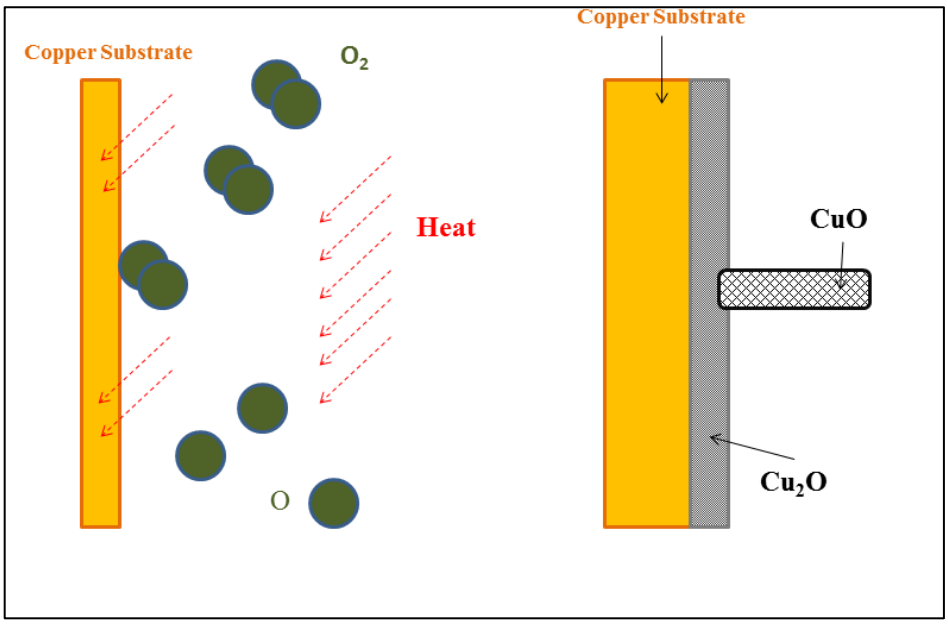

Figure 17. Schematic representation of thermal oxidation of copper substrate to form CuONWs [348]

A widely-accepted mechanism for the growth copper oxide nanowires is the metal oxidation process which involves the diffusion of copper ions from the bulk copper through the cuprous oxide layer with the oxygen diffusing in the opposite direction as illustrated in Figure 17 [348]. This presented with challenges especially with the CuONWs synthesis and utilization. As mentioned earlier, these nanowires are formed directly on the copper substrate surface, and tend to peel or form flakes which are easily removed from the surface due to mechanical stress placed during post processing on the surface. Additionally, it was also observed that as the CuONWs was synthesized using air as the supply of oxygen, local changes in concentration and air circulation had considerable effects on the uniformity of the nanowire coverage on the surface. In addition, it was observed that best coverage was obtained between 480 ^{0}C and 530 ^{0}C and at higher temperatures, there was stunting observed in the nanowire growth, and lower temperatures yielded poor coverage per run.

As discussed in the previous section, the nanowires are vulnerable to degradation in various environments. To attempt the further stabilization of the bulk nanowire systems two routes for the deposition of the boron nitride were utilized. The first route used tribromoborazine (TBB) as a precursor. TBB is a highly environmentally sensitive compound to oxygen and moisture (humidity). TBB is transferred to a silica crucible and introduced in the main chamber of the CVD reactor. For the second route, ammonia borane a relatively more environmentally stable precursor is used for the deposition of hexagonal-boron nitride (h-BN) onto the substrate. For the second method as mentioned in the experimental description a stainless steel bubble was setup externally to the main hot walled CVD chamber, and a relatively milder temperature of ~ 100 ^{0}C was used for the decomposition of the ammonia borane in the bubbler. Figure 18 and Figure 19 shows the Raman spectra of the silicon test substrates used to demonstrate the

deposition of the ammonia borane. The characteristic Raman shift of h-BN at the 1367 cm^{-1} is clearly observed. This mode is attributed to the E_{2g} vibrational mode of the B-N within the h-BN layers [349]. Additionally, it was also observed that on increasing the pressure in the chamber there was a change in the color density of the optical image as seen in Figure 20 and the and the SEM images in Figures 20(A) and 20(B) that the thin layers coalesce to form a thicker coating with the increasing pressure from 1.25 Torr to 2.5 Torr. Three Si samples were placed in the deposition chamber to study the variation in the coating quality with the location of within the tubular chamber.

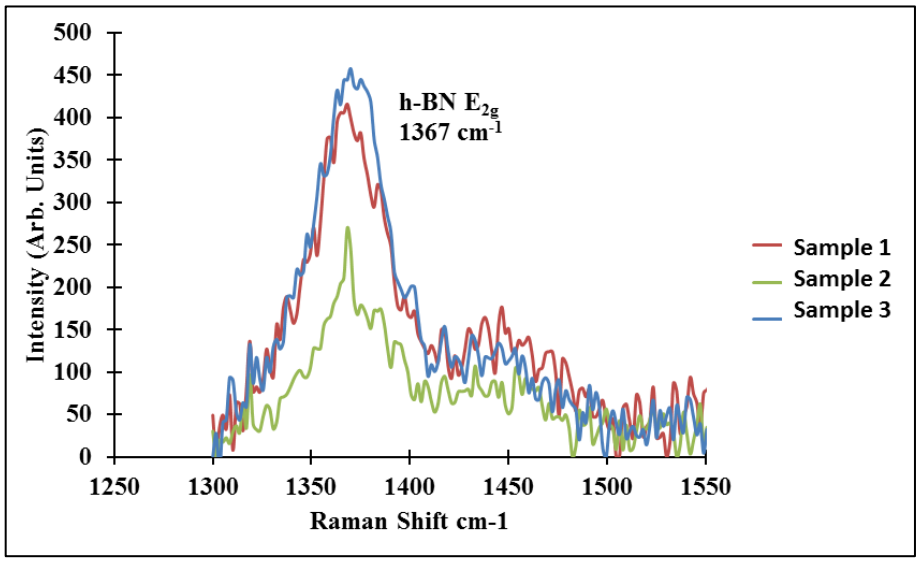

Figure 18. Raman spectra of silicon coated with boron nitride at pressure of 1.25 Torr using ammonia borane precursor exhibiting the characteristic shift at the 1367 cm^{-1}. Three replicates (silicon wafer) were labeled as Samples 1, 2, and 3.

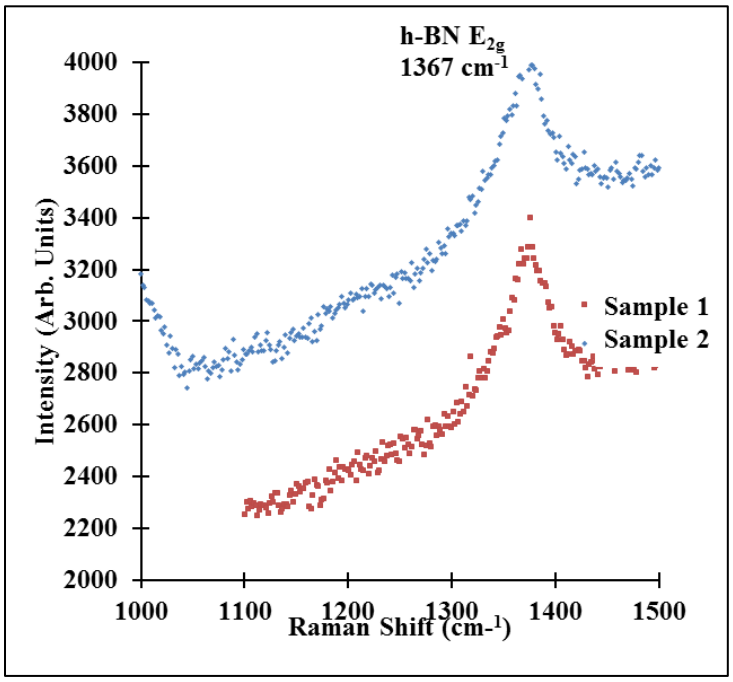

Figure 19. Raman spectra of boron nitride deposited at 2.5 Torr internal pressure of the CVD chamber with two replicates (Sample 1 and 2). The peak at 1367 cm^{-1} represents the characteristic shift of the h-BN Raman active phonon mode.

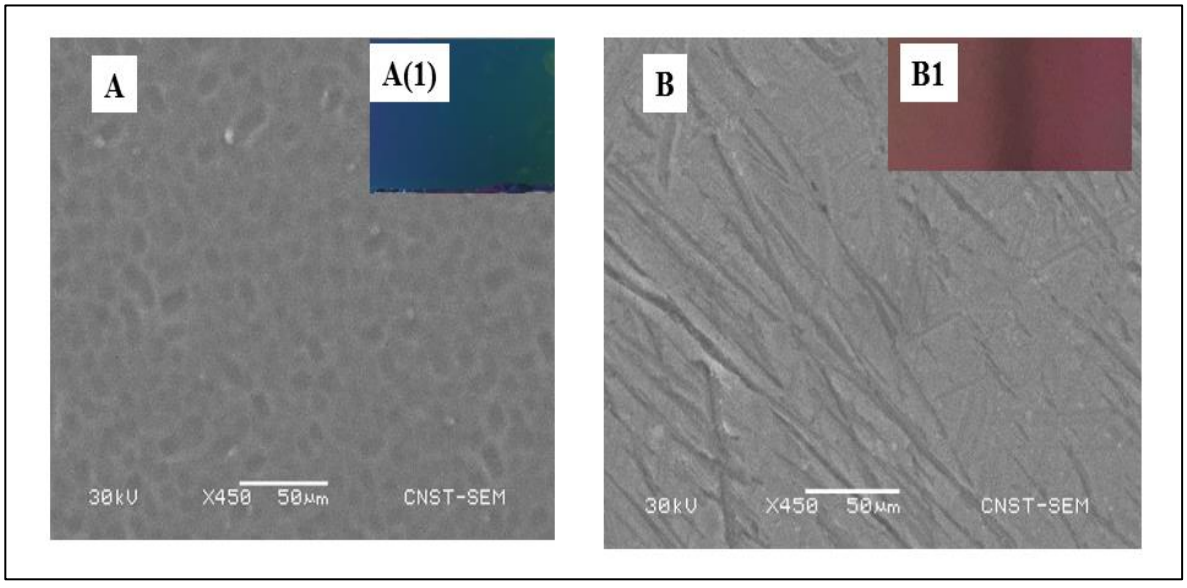

Figure 20. (A) SEM of h-BN deposited on silicon at a pressure of 1.25 Torr using ammonia borane precursor A(1) Optical image of the silicon wafer after the coating (B) with SEM of h-BN deposited on silicon at a pressure of 2.5 Torr (B1) optical image of wafer after the CVD

The difficulties in handling the TBN precursor led to the attempt to the use of relatively more stable ammonia borane precursor. It was observed that under low pressure vacuums of 1.25 Torr to 2.5 Torr consistent deposition could be obtained of the h-BN on the surface of the copper precursor. However, to consistently extend this approach to stabilize nanowires directly on the substrates requires further optimization. As demonstrated in the aging test in the pH 1.7 environments, the efficacy of the ceramic boron nitride (deposited with TBB) as an effective barrier to reduce was observed.

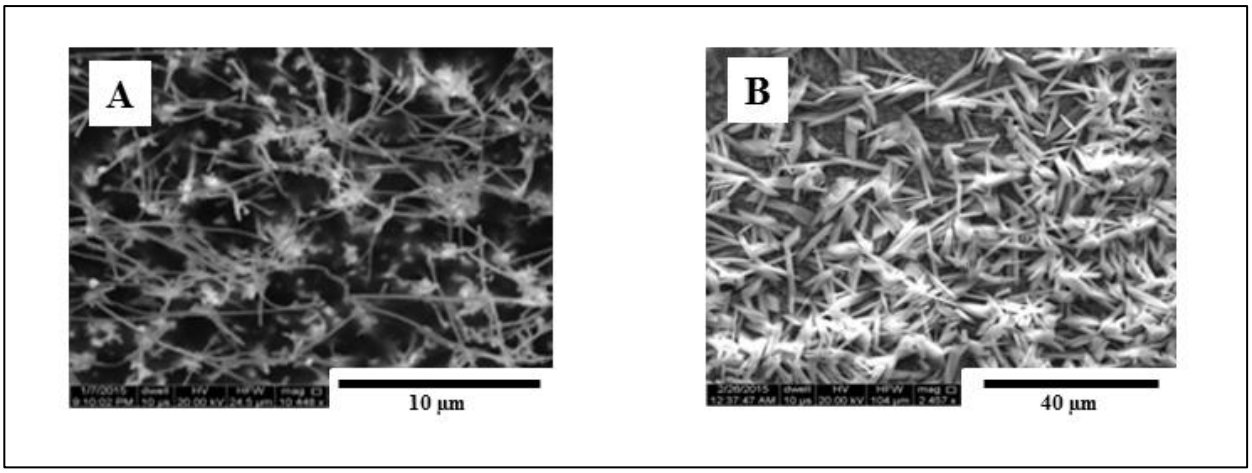

Figure 21. (A) SEM of BN decorated CuO NWs on a copper substrate, and (B) image of the nanowires after exposure to pH 1.7 acidic solution for 7 days

Figure 21 (A) illustrates a high magnification image of cupric oxide nanowires after the BN decoration. Specific changes are not seen as compared to the uncoated samples. The sample was exposed to a pH 1.7 solution prepared with Nitric acid and it is seen that on aggressive exposure to pH 1.7 environments, the nanowires do undergo etching to leave short residues; however, it is expected that such aggressive environments do not occur in typical service

environments. This is illustrated in Figure 21(B) where the nanowires are etched to form 'sharp ends' by losing their morphological integrity.

5.4 Conclusions

The methods utilized demonstrate the ability to produce nanowires at scale and reproducibly on low cost silicon wafers and copper plate bulk substrates. These nanowires are used in the next chapters to study the robustness in various electrochemical environments using polarization and impedance techniques and ultimately used to demonstrate a proof of concept sensing. The silicon nanowires are epitaxial to the surface and shorter in length as compared to the copper oxide nanowires. The thermal route of preparation yields the Cu(I)O phase as transition phase towards the preparation of the Cu(II)O nanowires. When copper oxide is synthesized then the major product is Cu_2O and CuO is formed slowly through the second step of oxidation [348]. The reactions are summarized as given below in equations 4 and 5:

$$4Cu + O_2 \rightarrow 2Cu_2O \ldots. (4)$$

$$2Cu_2O + O_2 \rightarrow 4\ CuO \ldots. (5)$$

Additionally, it is also observed that the distribution of the nanowires on the surface is markedly different for the silicon and copper oxide nanowires. This is attributable to the different methods of synthesis and mechanisms of formation of the NWs. Their synthesis techniques yield epitaxial nature of nanowires in the case of the SiNWs as against the mats that are formed in the case of CuONWs. The impact of the difference in the distribution of NWs and their sizes can be factors which affect their performance as substrates for sensing. The nanowires are used without destructive removal from the surface with the use of sonification or other nanowire removal technique.

6. STABILIZATION, FUNCTIONALIZATION AND ELECTROCHEMICAL STABILITY OF THE NANOWIRES

6.1 Introduction

The surface area to volume ratio and the susceptibility of the nanowires to chemical changes in the microenvironment render them vulnerable to degradation. In the sour environment often encountered in the oil and gas [311] and process industries, it is imperative that the sensor substrates offer robustness and be stable. The corrosive environments include H_2S and pH between 5 and 7 acetic acid, carbonates, sulfates and heavy sediments [350]. Nanowires have been shown to provide robust resistance to degradation even being added to coatings to provide corrosion resistance. Atomic layer TiO_2 on copper nanowires was demonstrated to be a reliable coating for rendering the nanowires stable in pure, hot de-aerated water systems (even after water immersion for 12 days at 150 ^{0}C) [351]. The TiO_2 imparts the copper nanowires the ability to stay degradation resistant even after exposure to the aggressive conditions. Further, atomistic decoration by using nano-octahedra morphology of $MnCr_2O_4$ has been utilized to improve pitting corrosion resistance in stainless steels [352]. Both silicon and copper oxide nanowires have been explored in literature for either direct or additive corrosion resistance. In a study of CuO NWs, the surfaces were modified using dodecane thiol to observe switchable wettability from super hydrophobic to super hydrophilic domain, due to the adsorption and desorption of this monolayer, thus dramatically improving corrosion resistance [307]. A two order magnitude decrease of the corrosion current was observed as compared to the bulk copper on the super hydrophobic copper oxide nanowire substrate possibly due to the lack of contact with the brine electrolyte, thus dramatically improving the corrosion resistance[307]. Silicon nanowires have been investigated as photo catalysts and battery anodes, both of which require robust mechanical

degradation stability in their respective environments. Although the presence of the silica layer, provides degradation resistance, it has been found that this resistance is limited in highly oxidative potential conditions [353] and in the case of micro capacitors, may need additional stabilization using compounds such as SiC to improve their stability [354]. Studies of the degradation of amorphous silica and quartz have indicated that the introduction of sodium chloride to a near neutral pH solution enhances the rate by up to 21 times as compared to deionized water [355]. The dissolution of silica in water is explained through the formation of silicic acid [356]. This part of the work aims to systematically understand the corrosivity of copper oxide and silicon nanowires in industrially simulated environments. Both the kinetic understanding of the corrosion current and further investigation into possible mechanisms of degradations are explored in detail using impedance spectroscopy.

6.2 Experimental methods

6.2.1 Solution preparation

A 3.5 weight % NaCl solutions were prepared using sodium chloride (BDH analytical, high purity and deionized water (Milli-Q water systems, 18.2 MΩ-cm resistivity at 25 ^{o}C). Simulated produced water [312] was prepared using the composition described in Table 2.

Table 2. Composition of the simulated produced water

Component	Content (g/L)
NaCl	16.61
KCl	0.35
Na_2CO_3	0.03
$MgCl_2$	1.66
$CaCl_2$	0.5
Na_2SO_4	1.1
$NaHCO_3$	3.06

6.2.2 Electrochemical tests

Electrochemical tests for corrosion were performed in a K0235 flat cell (Princeton applied research) using a platinum counter electrode and standard calomel reference electrode (E = 0.242V vs Standard Hydrogen Electrode (SHE) as shown in Figure 22. The working electrode was the modified CuONWs and silicon nanowires attached to the substrate of synthesis. The CuONWs film tend to delaminate from the substrate of synthesis, and hence for the electrochemical tests, the nanowire film was physically restrained to the surface using a transparent non-conductive tape to provide physical rigidity to the oxide layer during the

experiments. The corrosion cell was attached to a potentiostat (VersaSTAT 3, Princeton applied research), and the potentiodynamic scans are performed at +/- 300 mV from open circuit conditions. The scans were performed using a scan rate of 0.333 mV/s to ensure minimal disturbance of the electrode surface. The experiment was repeated with at least 3 replicates of the working electrode (NW thin film) in each environment. Electrochemical impedance spectroscopy is performed at open circuit conditions with no DC bias, at an applied current frequency of 100 KHz to 0.01Hz with amplitude of 10 mV/s. The EIS spectra were obtained at 0, 3, 6, 12, 18 and 24 hours. Figure 22 illustrates the setup during experimental operation. 100 to 150 mL of electrolyte was prepared and filled prior to every experiment. The electrolyte was sealed for the duration of the experiment. A dummy cell was used to verify the calibration of the EIS before the experimental run.

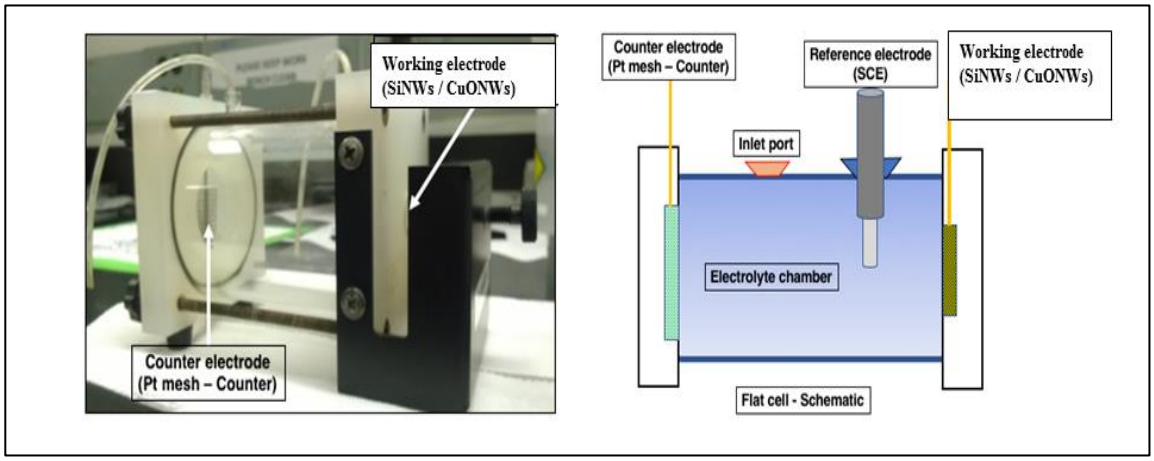

Figure 22. K0235 flat cell used in this work and a schematic of the cell indicating the platinum counter electrode, reference electrode and working electrode positions

6.3 Results

Figure 23 is an excerpt of a potentiodynamic scan that compares the current response a copper, CuO, and copper decorated with BN (using the TBB route of synthesis, explained in the earlier chapter) samples. An initial set of screening tests were carried out for coated and uncoated copper oxide and silicon nanowire samples to understand their responses under the 12-hour and 24-hour exposure to the brine solutions.

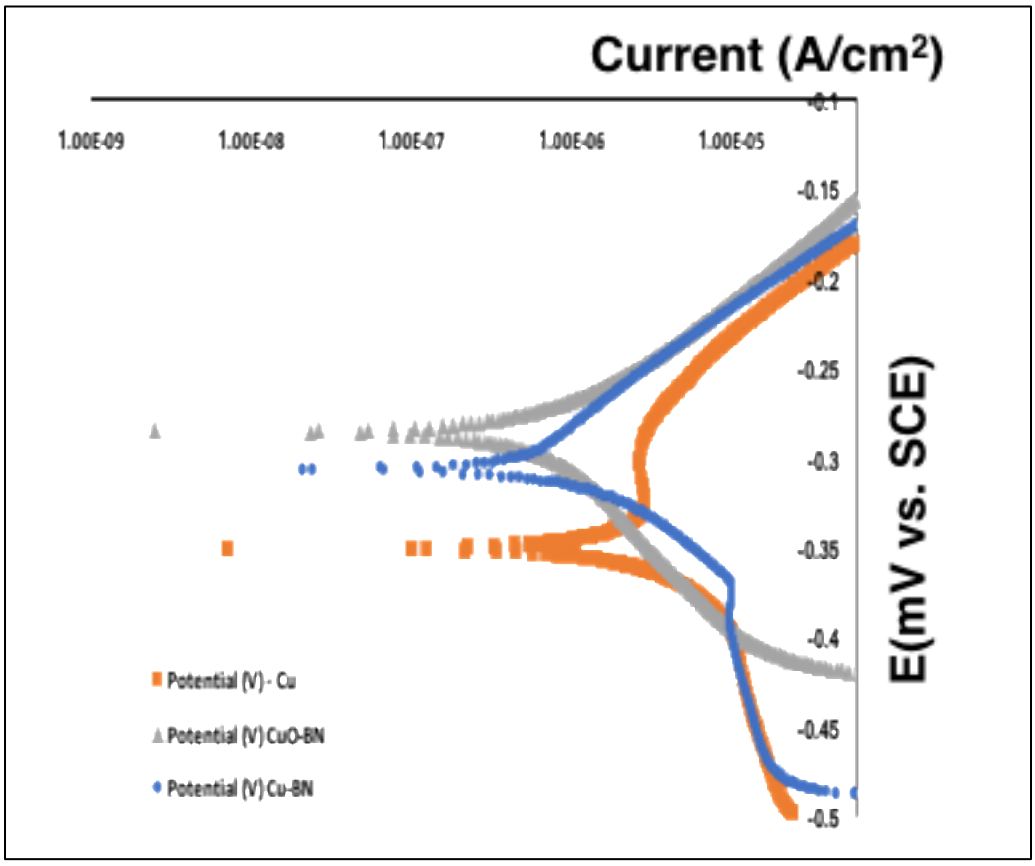

Figure 23. Polarization scan at 12-hour immersion in a 3-electrode setup using SCE reference electrode with Cu, CuO decorated BN and Cu decorated with BN as the working electrodes

Table 3. Corrosion potential and corrosion current density after a 12-hour immersion in 3.5% NaCl solution

Substrate	E (mV)	Current(A/cm^2)
Cu	-351.711	54.68 μA /cm^2
Cu-BN	-307.503	737.124 nA/cm^2
CuO-BN	-324.493	295.195 nA/cm^2

It is observed from Figure 23 that there is a slight increase in the corrosion potential in both the coated samples and the uncoated samples, which might be attributed to the formation of porous passive layer or the partial loss of coating causing the formation of active corrosion cells. For the BN decorated copper substrate, a possible break of coating in the cathodic region was observed, which was followed by an acceleration of the corrosion rate. The increase in corrosion potential of surface modified CuO films has also been observed in other systems where it was suggested that air pockets and capillary action could be responsible for the increased corrosion resistance of the films [357]. Based on the corrosion current at the 12 hour and 24-hour immersion, the nanowire substrates had exhibited higher resistance to degradation as compared to the other samples.

Table 4. Corrosion potential and corrosion current density after 24-hour immersion in 3.5 % NaCl solution

Substrate	E (mV)	Current
Cu	-338.891	31.697 μA /cm^2
Cu-BN	-315.07	1.967 μA /cm^2
CuO-BN	-271.812	1.586 μA /cm^2

Table 3 describes the corrosion potential and corrosion current observed after a 12-hour immersion in 3.5% aerated NaCl environment. The potentiodynamic scan was performed at +/- 300 mV as described in the experimental section. The Cu-BN and CuONWs-BN outperform the bare Cu substrate by an order of magnitude. This is evidenced by the decrease in the corrosion current from 54.68 μA /cm^2 to 737.124 nA/cm^2 for the copper decorated with BN and 295.195 nA/cm^2 for the CuO decorated with BN respectively. Further we observe that the corrosion potential varies by ~50 mV for the three materials indicating that the increased degradation resistance was primarily due to the modification of the surface, thus imparting a kinetic barrier (as indicated by the increase in the corrosion current density) to the corrosion [358]. At the 24-hour time point after immersion we observe as seen in Table 4, a decrease in the corrosion current for the bare Cu surface, which can be attributed to the formation of a passive hydrated hydroxide layer [359]. However, the coated samples (Cu-BN, and CuO-BN) show marginal increase in the corrosion current density as seen in Table 4, which may indicate a degradation of the coating because of the immersion.

Table 5 demonstrates the comparison of the corrosion current density between SiNWs and CuONWs. It is observed that the SiNWs offer higher resistance to degradation as compared to Cu and CuO as seen by their lower corrosion current density. SiNWs were also decorated with BN (using the TBB route) to generate SiNWs-BN. It is observed that after the coating, the corrosion current reduced by 60% as compared to the uncoated SiNWs. It is important to note that only the macroscopic surface area was used to calculate the corrosion rate and not the increased surface area obtained because of the nanostructuring of the surface. It is also seen that the in the presence of 5 wt. % NaCl solution and simulated produced water there is an increase in the activity on electrode potential. Similar trends are observed at the 24-hour time point after the

immersion of the nanowires as demonstrated in Table 6. The polarization scan plots performed are available in the Appendix A.

Table 5. Corrosion potential and current data after 12-hour immersion in 3.5% NaCl solution

Substrate	Environment	E (mV)	Current
Si	3.5% NaCl	-348.073	20.071 nA/cm^2
SiNWs	3.5% NaCl	-465.542	1.376 μA/cm^2
SiNWs-BN	3.5% NaCl	-303.01	330.615 nA/cm^2
SiNWs-BN	5% NaCl	-113.728	365.153nA/cm^2
SiNWs	Simpro	-134.6	244.759 nA/cm^2

Table 6. Corrosion potential and current data after 24-hour immersion in 3.5% NaCl

Substrate	Environment	E (mV)	Current
Si	3.5% NaCl	-338.176	14.717 nA/cm^2
SiNWs	3.5% NaCl	-470.945	1.468 μA/cm^2
SiNWs-BN	3.5% NaCl	-366.354	69.954 nA/cm^2
SiNWs-BN	5% NaCl	-253.734	1.205 μA /cm^2
SiNWs	Simpro	-69.136	40.374 nA/cm^2

After the initial exposure, detailed studies in replicates were carried out for the substrates of interest CuONWs and SiNWs in the two simulated environments of 3.5 % NaCl solution and

simulated produced water. Figure 24 illustrates the difference in the corrosion current of the CuONWs and the SiNWs on exposure to the solutions. It is observed that the highest corrosion current is shown by the CuONWs at the 12-hour exposure point. This can be explained by the hydrolysis of the copper oxide to copper hydroxide, which, is aggressive at the start due to the exposure of the new surface [360]. Additionally, the CuONWs form a porous mat on the copper substrate. The porosity may aid the diffusion of the chloride anions to the copper surface to generate copper chloride [361]. This provides another reason for corrosion on the surface, leading to a higher anodic current, yielding in a higher corrosion rate. It is seen that there is a steep decline in the corrosion current from the 24 hour to the 12-hour time point in the 3.5 wt. % NaCl solution. This is explained by the passive layer forming a physical barrier on the surface of the nanowires, preventing further action of the electrolyte. However, this hydroxide layer reduces the anodic current, this reflecting in the reduced corrosion potential. In the case of the simulated produced water we observe that CuONWs are slightly more resistant to degradation and this may be due to the presence of multiple ions screening the surface leading to a large diffusion limitation for the anodic current. However, we observe the same trend as related to the corrosion current with time, with a decrease observed at the 24 hour time point.

The SiNWs, at the outset have a three order of magnitude difference as compared to the cupric oxide nanowires in both the 3.5 wt. % NaCl solution and the simulated produced water environment. This can be attributed to both the presence of the passivating silicon layer and the nobility (as seen by the corrosion potential) because of this passivating layer. Further silicon is resistant to degradation to most weak acids, and the susceptibility of this layer is primarily to hydrofluoric acid attack. Slow silane hydrolysis possibly leads to a marginal increase in the corrosion current with time [355, 362], however it is marginal as compared to the CuONWs.

However, on comparing the results of both the CuONWs and SiNWs corrosion current density to the bulk materials, we observe significantly low corrosion current density for the silicon nanowires.

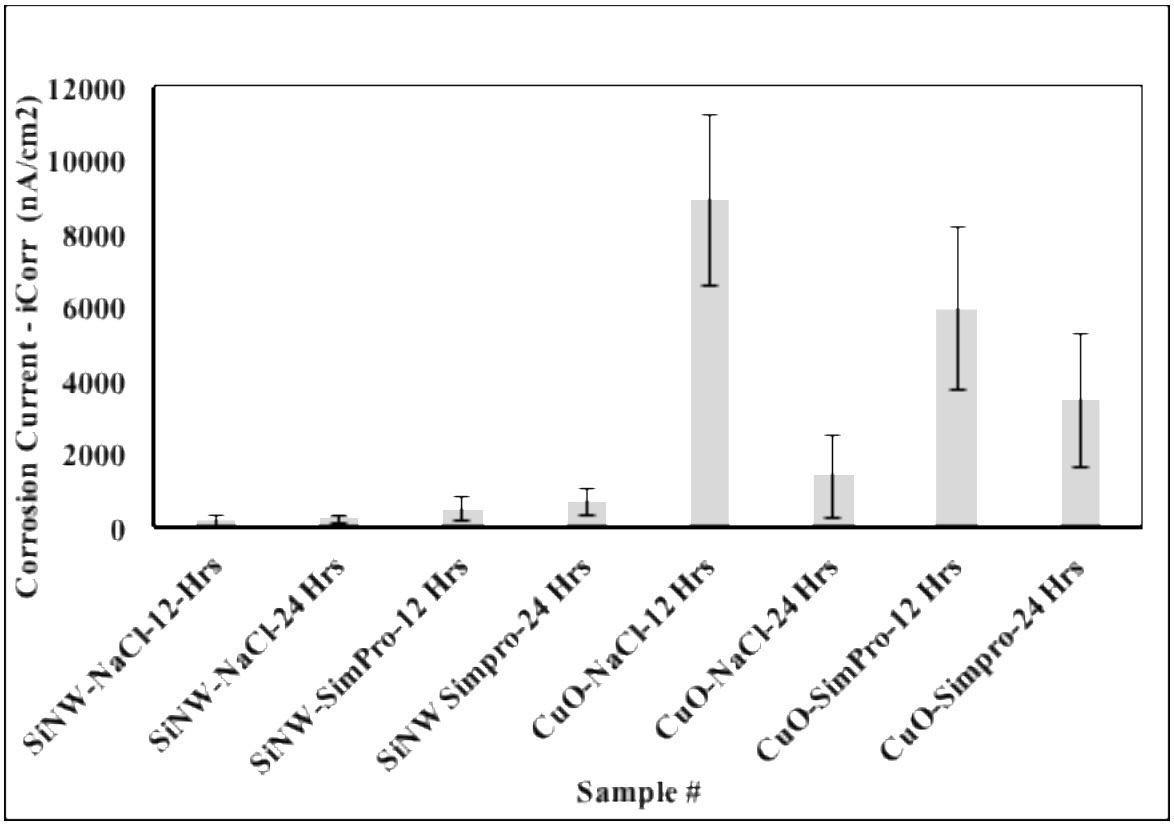

Figure 24. Corrosion current density of CuONWs and SiNWs in 3.5 wt. % NaCl solution and simulated produced water (SimPro)

Figure 25 illustrates the corrosion potential of the two substrates with time in the sodium chloride and simulated produced water environments. It provides a contrasting result to the corrosion current, with SiNWs showing more activity as compared to CuONWs. However, this observation is not in conflict with the earlier observation, since the corrosion potential is a

measure of the susceptibility due to the thermodynamics of the reaction whereas the corrosion current density is a measure of the rate of corrosion or the kinetics of corrosion. It is apparent from Figure 31 that SiNWs are showing higher susceptibility in both the environments as compared to the CuONWs. Interestingly, there the corrosion potential with time is relatively stable for both the nanowire systems with time, indicating that the systems are in relative equilibrium with their environments. Further AES and XPS studies may be used to illustrate the specific chemistry of this higher activity exhibited by the SiNWs. Additionally, we see that in the complex brine mixture with multiple ionic components the corrosion potential observed can be as much as -500 mV (vs SCE). This is an indication that despite having low kinetic susceptibility there is a low thermodynamic barrier for corrosion.

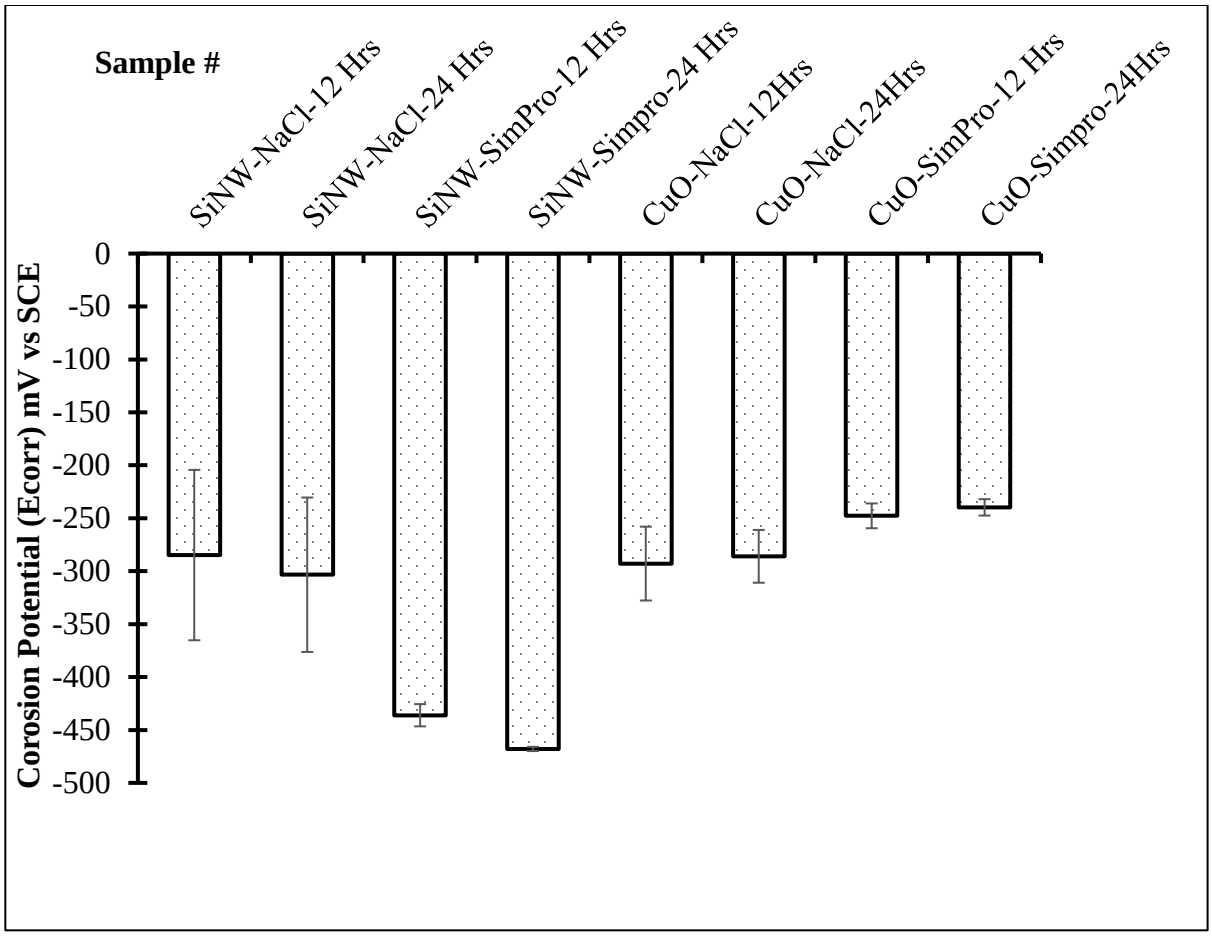

Figure 25. Corrosion potential of CuONWs and SiNWs in 3.5 wt. % NaCl solution and simulated produced water (SimPro)

To further investigate the kinetic processes on the surface of the working electrode that is the SiNWs and CuONWs, impedance studies were performed with the methods outlined earlier and their Nyquist and bode plot (phase and magnitude) were studied. Additionally, to get further quantitative insights the data was fitted using Zsimpwin3.60 software to equivalent circuits to yield quantitative insights.

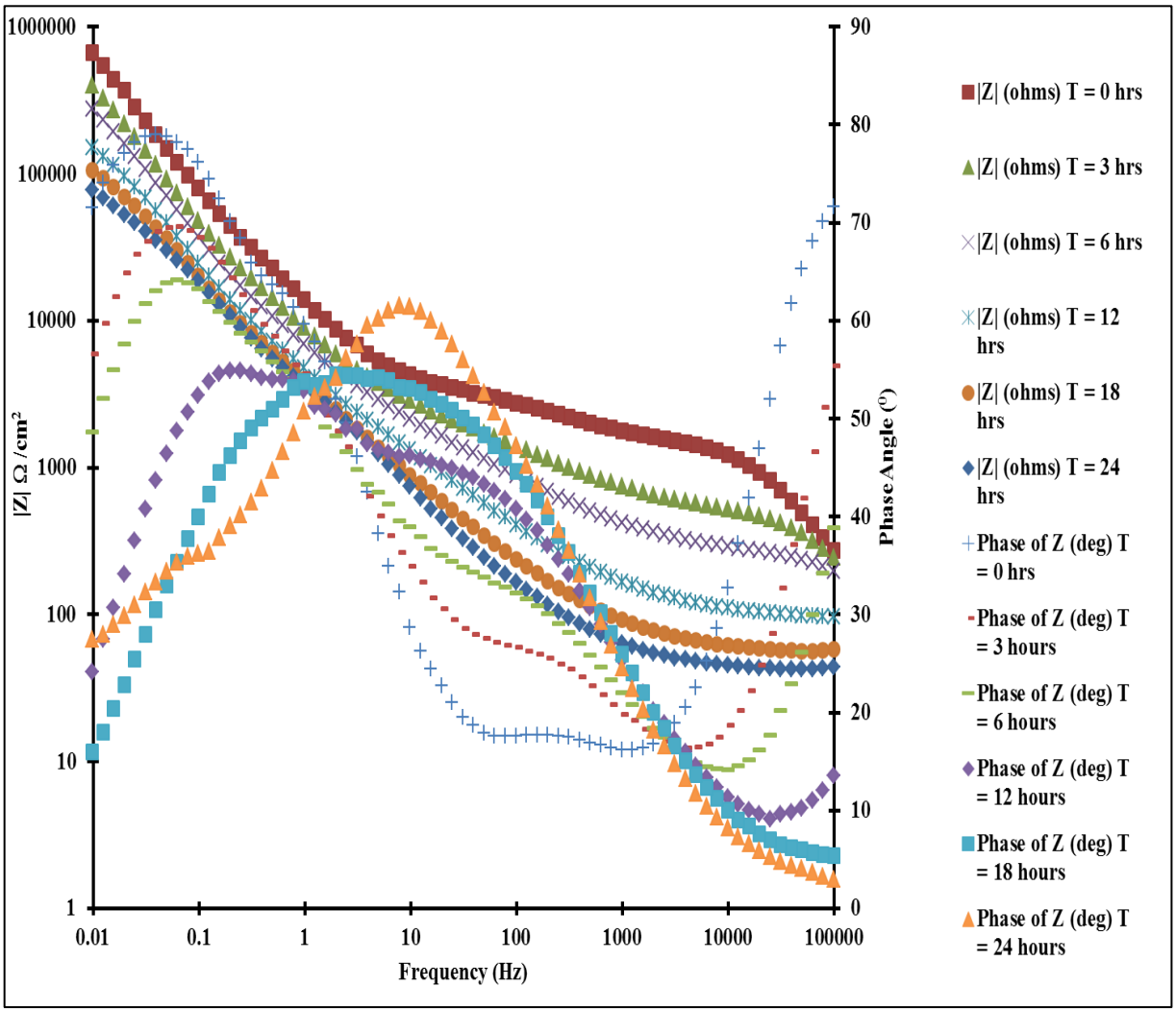

Figure 26. Bode magnitude and phase plot of SiNWs immersed in simulated produced water for 24 hours

In Figure 26 we observe that at high frequency there are several regions of impedance observed at the initial time points of immediate immersion and 3 hours, however, as the system stabilizes we observe that an approximately constant impedance of the order of ~ 100 Ω/cm^2 is reached. At low frequencies, we see impedance of the order of ~ 100KΩ/cm^2 which is in line with the low current densities observed and the high resistance to degradation observed for the silicon nanowires. Figure 27 illustrates the same in the Nyquist plot, where we see a very high

charge transfer resistance starting at immersion which stabilizes with the progression of time. This is observed empirically by the large diameter semicircle formation >250 KΩ/cm^2 radius which implies > 500 KΩ/ cm^2 in charge transfer resistance at immersion. This may be due to the dual effects of the silica surface and the presence of a pronounced double layer at the beginning of the immersion.

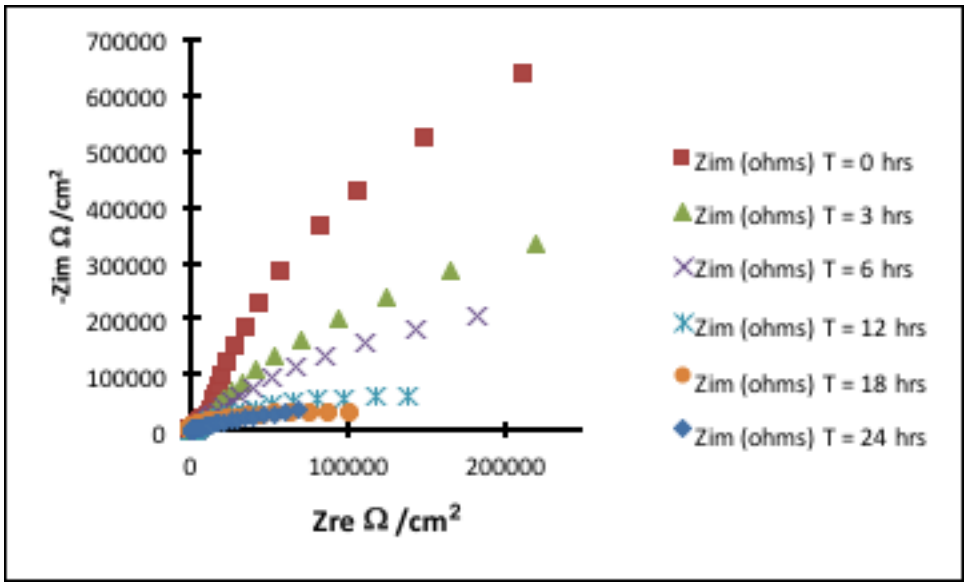

Figure 27. Nyquist plots of SiNWs immersed in simulated produced water for 24 hours

The Figure 28 illustrates the behavior of the SiNWs working electrode in 3.5% NaCl. We observe a similar behavior with instability at high frequency at the initial time points and then a stable impedance behavior observed with the progression of time. This may indicate that there may be mass transfer limitations due to either, the native charges on the surface or due to disturbance of the ionic medium. Since the detection principle in a biosensor is the modification of the surface potential this may present a challenge to the detection paradigms. As time

progresses a stable interface is obtained with defined characteristics. Additionally, it should be noted that all the experiments were performed under static conditions; hence the effect of turbulence is unknown at this point. Given the charge transfer barrier observed, the impact of turbulence would be expected to be minimal over time; however, it is possible that turbulence may reduce the initial impedance barrier observed after immersion. Hence, it can be inferred that the native charges on the surface and the highly ionic medium result in charge and mass transfer resistances. Additionally, the lack of turbulence in the system implies diffusion as the primary hydrodynamic consideration.

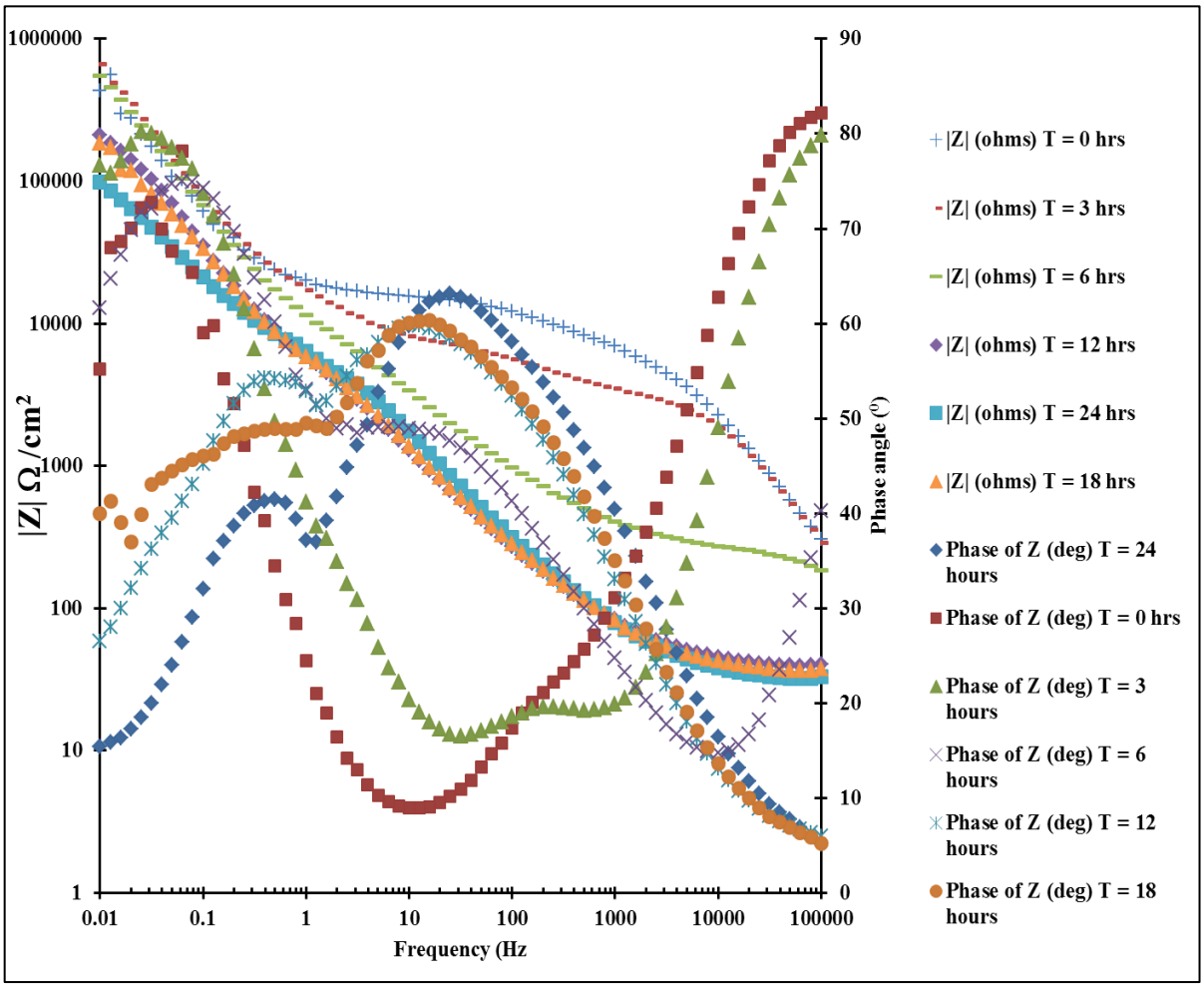

Figure 28. Bode magnitude and phase plot of SiNWs immersed in 3.5 wt. % NaCl solution for 24 hours

Figure 29 illustrates the Nyquist plot and we observe that immediately after immersion, at low frequencies there is noise observed in the data. This may be because of issues with the contact or movement, causing noise. Additionally, we see that there is increase in charge transfer resistance briefly with time, before returning to the trend as observed before of decreasing to the 150 KΩ/cm^2 value. This aberration in the trend may be due to residual impurities at the nanowire surface that may have acted as a resistance to charge transfer that over time are etched or diffused away thus revealing the nanomaterial surface. It is important to note that the expansive

surface area provided by the nano-morphology also present challenges to keep the surface native and pristine under non-experimental conditions due to affinity to electrostatic charges and the resultant contamination by organics and particulate matter.

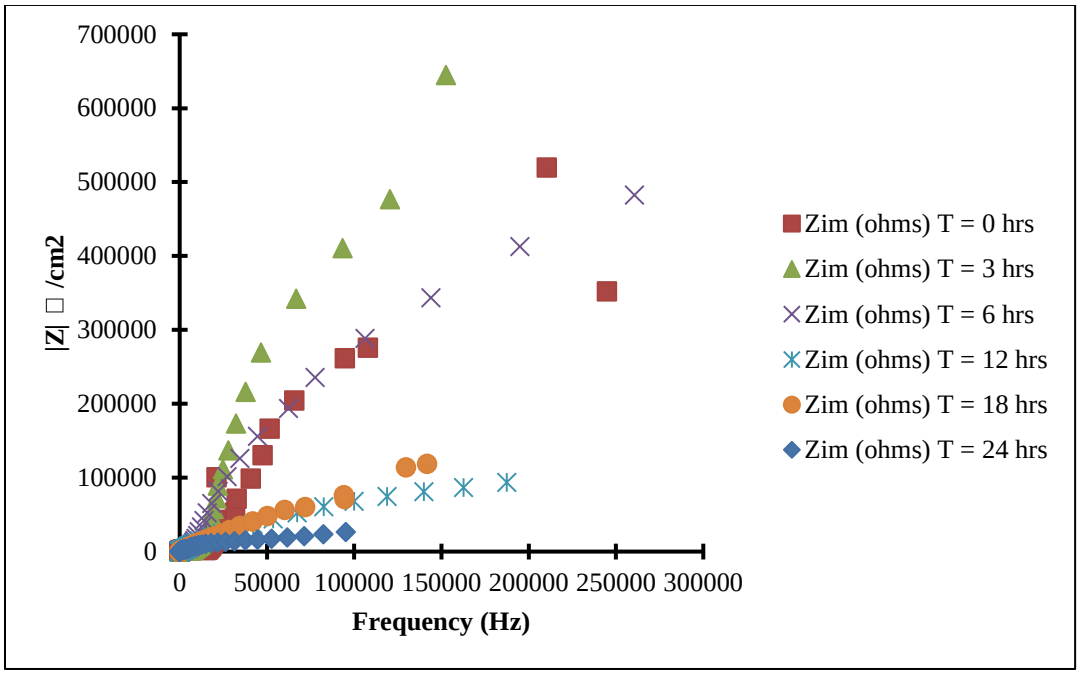

Figure 29. Nyquist plot of Si NWs immersed in 3.5 wt. % NaCl solution for 24 hours

Figure 30 illustrates the behavior of CuONWs in 3.5 % NaCl. We see that there is a presence of a pronounced charge transfer resistance of ~ 8 KΩ /cm^2 followed by a possible diffusion controlled resistance. Additionally, we see that there is a diffusion limitation to the charge transfer forming with increasing time as the charge transfer resistance decreases from about 15 KΩ /cm^2 to 8 KΩ /cm^2 and then stabilizes after the 18 hour time point. This diffusion limitation is inferred from the ~ 45^o linear profile at the low frequencies a seen in Figure 30.

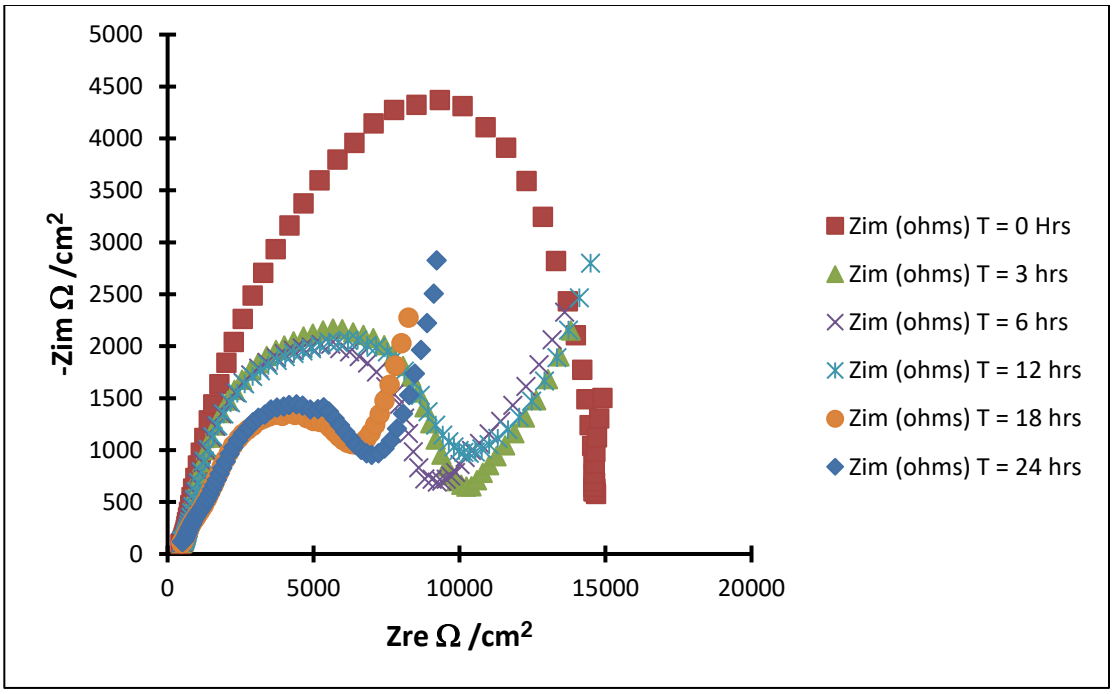

Figure 30. Nyquist plot of CuO NWs immersed in 3.5% NaCl for 24 hours

We also observe in Figure 31 that the initial impedance is high at ~ 1 KΩ / cm² which are consistent through the duration of the experiment. This can be explained by the earlier experimental observation of the "flaky", peeling off characteristic of the nanowire film of CuO. This may cause porosity between the NW film and the copper substrate. This may lead to poor contact with the external circuit lead of the working electrode, which is reflected in the relatively high impedance observed. Further we observe that at low frequency the charge transfer resistance is high initially and then lowers to a stable value. This can now be clearly inferred as the slow diffusion of the electrolyte into the porous nanowire film, which ultimately results in the decrease in the resistance leading to higher anodic current and degradation.

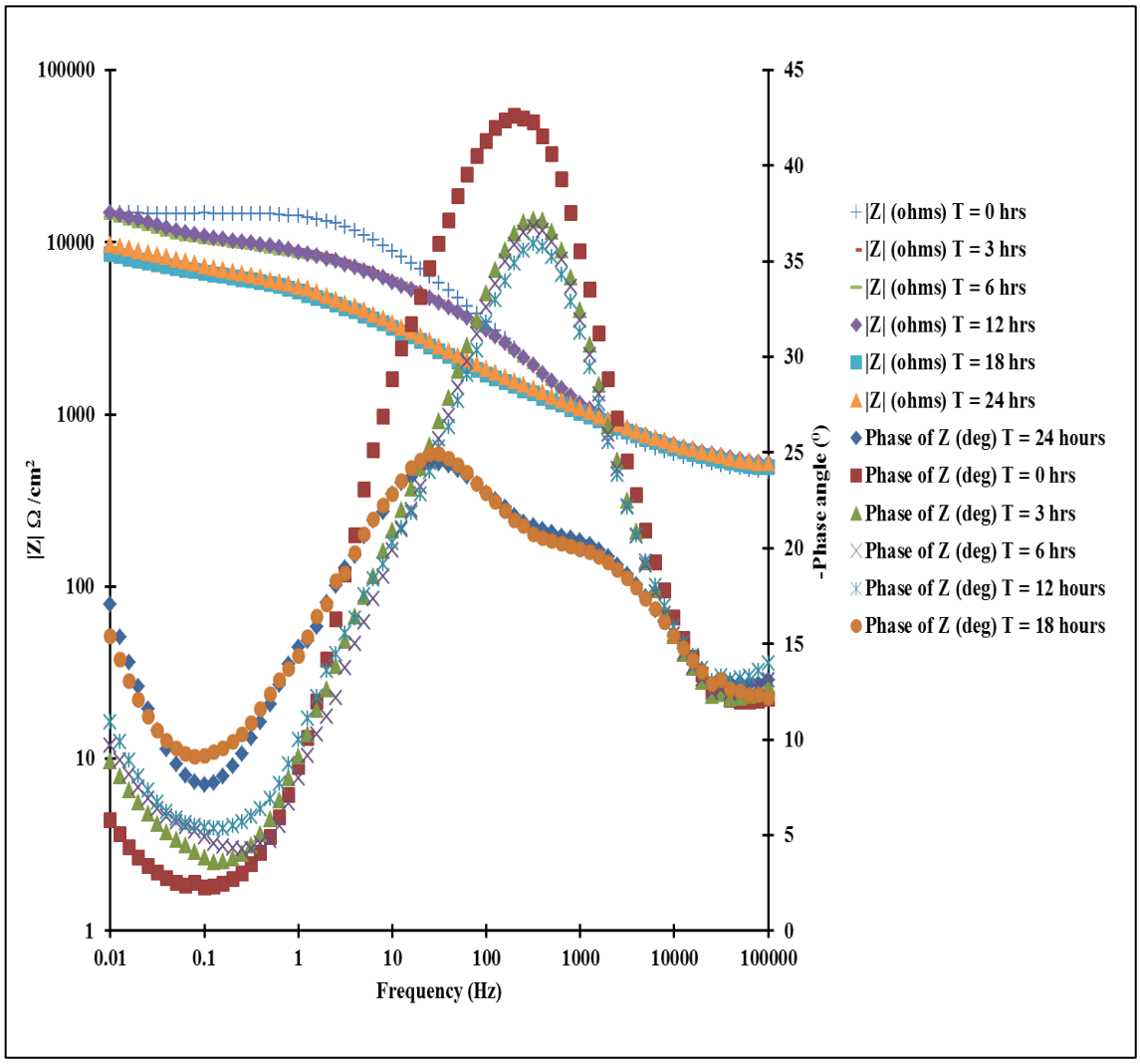

Figure 31. Bode magnitude and phase plot of CuONWs immersed in 3.5% NaCl for 24 hours

Figure 32 illustrates the behavior of the CuONWs thin film in simulated produced water. We observe that as compared to the brine solutions used earlier, the charge transfer resistances are smaller after the initial immersion and reach a stable value faster at ~ 5 KΩ /cm^2 which is lower than in 3.5 wt.% NaCl solutions. This can be explained with the composition of the simulated produced water which consists of higher levels of aggressive anions such as sulfates

and carbonates in addition to the chloride. This may lead to multiple reactions with the copper oxide to yield the passive film less resistant and hence leading to higher anodic currents.

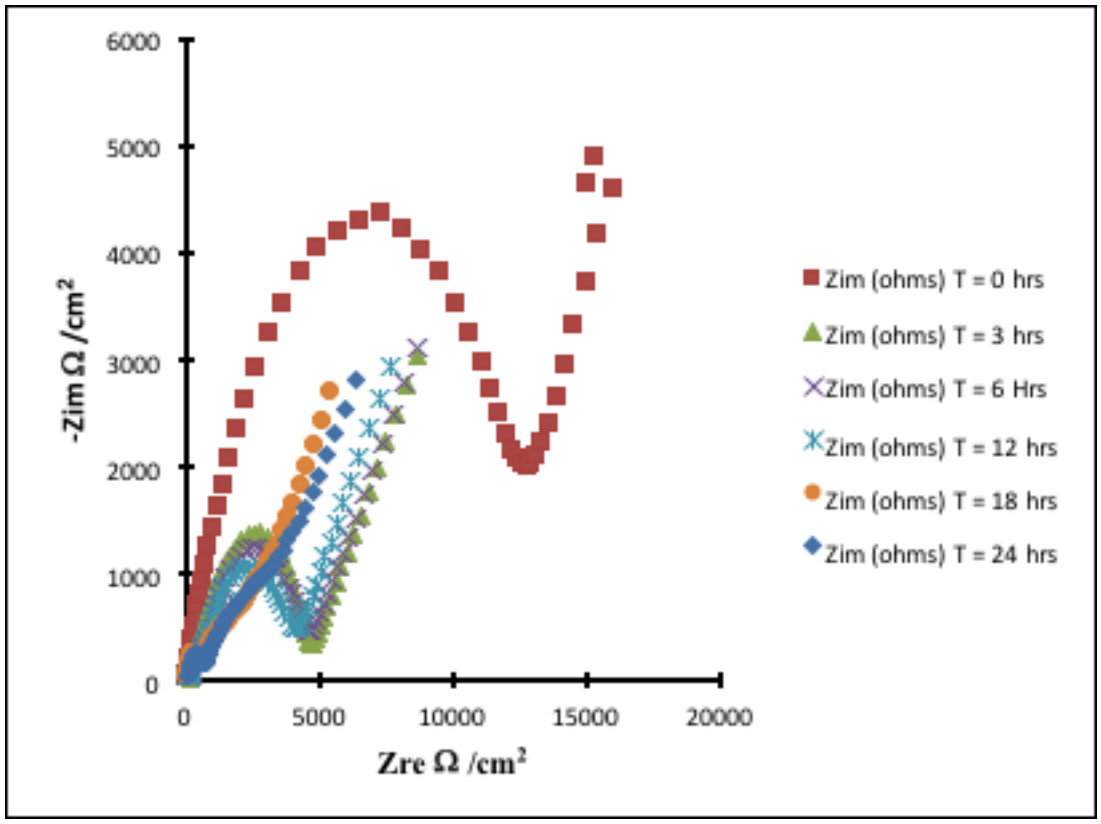

Figure 32. Nyquist plot of CuONWs immersed in simulated produced water for 24 hours

We observe in the bode plot shown in Figure 33 that the initial impedance at high frequency is an order of magnitude lower in the case of simulated produced water as compared to the 3.5 wt.% NaCl solution. This can be attributed to the micro dissimilarity in the samples, which may lead to an increase in initial charge transfer resistance, which then is averaged as the system reaches steady-state. Additionally, we observe that there is a pronounced difference in the

impedance at the higher and lower frequency illustrating the possible effects of charge transfer resistance and diffusion resistance. Additionally, it also possibly indicates the presence of multiple charge transfer resistance, especially from the electrode to the nanowire film (small ~0.1 KΩ /cm^2), and the nanowire thin film to a passive layer and then from the passive layer to the electrolyte itself. This is utilized in the fitting of the equivalent circuit as illustrated in the next sections.

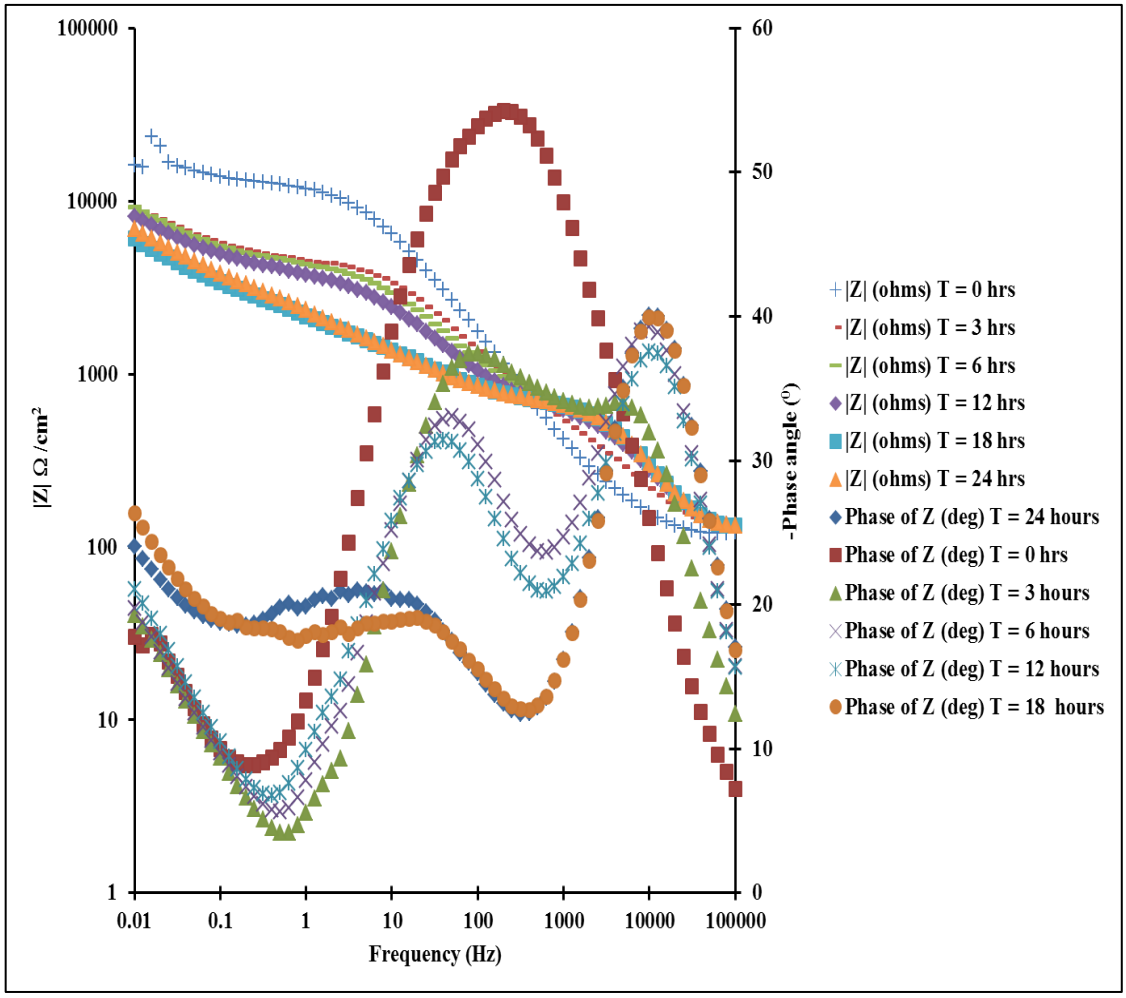

Figure 33. Bode magnitude and phase plot of CuO NWs immersed in simulated produced water for 24 hours

To further understand the underlying mechanistic limitations an iterative process was utilized to fit the circuits to the impedance data obtained earlier. The process was using a Randles and modified Randles circuit as the starting point. However, with the observations as noted earlier from the Nyquist and bode plot, the introduction of multiple capacitive double layers and the presence of a diffusion limitation was introduced (using a Warburg impedance element). Finally, as noted in Figure 34 circuit (1) was chosen based on the fit for the Si NWs system and circuit (2) was chosen for the CuO NWs system.

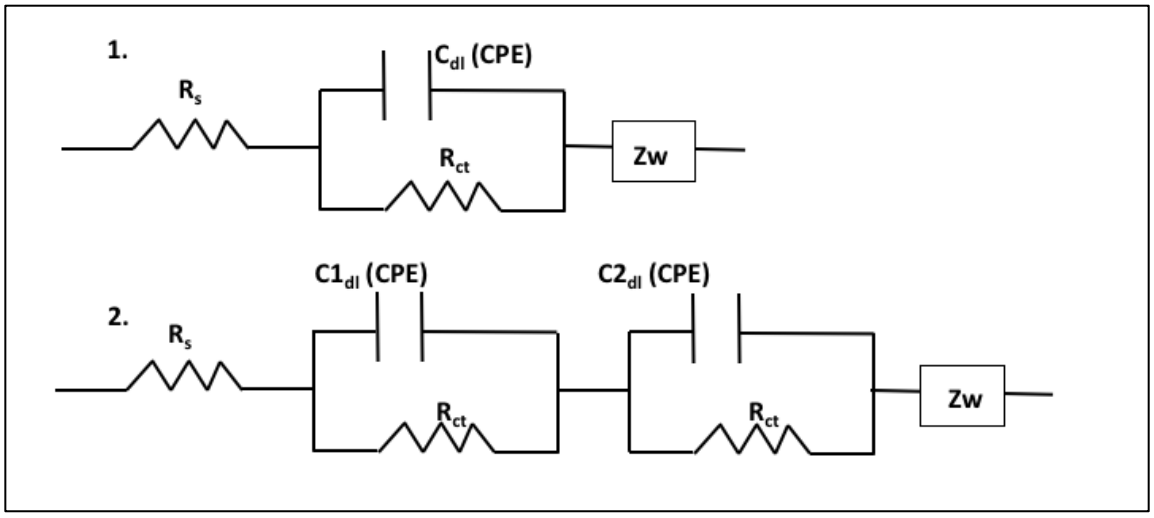

Figure 34. Equivalent circuits for the Si NWs and CuO NWs systems

Table 7 illustrates the equivalent circuit parameter values after fitting for the CuONWs system. Assuming the two-layer capacitive resistance between the passive layer and the nanowires and the nanowires and the bulk substrate, we observe that there is a higher resistance at the first charge transfer layer as compared to the second later. Additionally, the double layer capacitance observed is also higher in both the cases of the simulated produced water and the

3.5% NaCl solution. This is not surprising since both the substrates are immersed in highly ionic solutions and although the experiment is performed in the open circuit mode there is always the possibility of a strong ionic double layer due to the presence of highly mobile counter ions.

Table 7. Equivalent circuit parameters for CuO NWs system

Sample	R_S (Ω /cm^2)	$C1_{dl}$ (F/cm^2)	$R1_{ct}$ (Ω /cm^2)	$C2_{dl}$ (F/cm^2)	$R2_{ct}$ (Ω /cm^2)	Z_W (Ω /cm^2)
CuO NWs in 3.5 % NaCl	92.07	3.13E-05	5.42E+02	1.15E-06	1.48E+02	4.45E-03
CuO NWs-Simulated Produced Water	5.31E+01	2.18E-05	3.56E+02	1.03E-07	3.56E+02	1.55E-03

Table 8. Equivalent circuit parameters for Si NWs system

Sample	R_S (Ω /cm^2)	C_{dl} (F/cm^2)	R_{ct} (Ω /cm^2)	Z_W (Ω /cm^2)
Si NWs in 3.5 % NaCl	5.08E+01	5.17E-06	5.843E+004	N/A
Si NWs in Simulated Produced Water	3.47E+01	6.53E-05	4.09E+04	2.72E-04

For the SiNWs system in the 3.5 wt. % NaCl environment there is a poor fitting of the equivalent circuit with the diffusion limitation (Warburg element) as seen in Table 8. This is explained by the observations in the Nyquist plot, where the main limitation is observed as charge transfer. In the case of simulated produced water, we see the recurrence of a diffusion limitation at the nanowire surface. This is attributed to the complex ionic action (since there are multiple anionic and cationic compounds as seen in the composition) of the sulfate and carbonate counter ions on the NW system.

6.4 Conclusions

An iterative process using an increasing complexity in the models was used to fit the data to explain the behavior of the CuONWs and SiNWs in the aggressive salt solutions. EIS allows for the estimation of the contribution of the various sensing elements to the response of the system. The Nyquist plot allows for the relationship between the real and the complex part of the complex impedance to be demonstrated. The bulk corrosion resistance can be estimated by the interception of the semi-circle with the real axis [363]. Theoretical models were evaluated to explain the behavior of the surfaces. A simplistic model (Randles circuit) followed by multiple layer of (resistance – capacitance) and finally a dual diffusion controlled and polarization control model was also simulated.

It was observed that the simple Randles circuit based model could not adequately fit the experimental data. The impedance element conjugated diffusion state (RCRCRW) model, fit the data adequately at higher frequencies, however some amount of divergence was observed at the lower frequencies. Similar models fitted to explain SiNWs as working electrode in batteries have found to fit impedance observations [364]. It was observed that there was a decrease in the corrosion resistance with time (as observed in the Nyquist plot). On fitting of the data, it was observed that the best fit was obtained for the RCRCRW to explain the impedance behavior of the CuONWs and RCR and RCRW equivalent circuits for the SiNWs. The presence of Warburg impedance is also observed on the Nyquist plot.

7. DEMONSTRATION OF PROOF-OF-CONCEPT USING NANOWIRES SUBSTRATES

7.1 Introduction

The use of nanowires as biosensors and electrochemical sensors has been reviewed by multiple authors, apart from the preparation of these nanowires and fabrication of the sensors. A review [289] discussed the development and application of the nanowire sensors, various key results and mechanisms behind the operation of the sensors. Detailed reviews, specifically of microbial biosensors, can also be found in the literature [290]. The use of electrochemical biosensors also hold a large opportunity towards point of care diagnostics of life threatening diseases, such as cancer, where early detection can be a matter of life and death and vastly improve the economics of the situation. A review of these studies could also be found in the literature [291].

The use of a biosensor-based platform requires a robust platform for immobilizing multiple chemical 'markers' indicative of MIC. The surface functionalization of the nanowires necessary for this purpose can be achieved through conventional self-assembled monolayers and the formation of amine terminated surfaces allowing for the bonding of the N-terminus molecules such as biotin [277]. Nanowire array-based biosensors have also shown excellent stability and reproducibility when used in complex biological environments such as human plasma, where it has been applied for determining glucose levels. In presence of competing analytes such as ascorbic acid and dopamine, it was still observed to give reproducible results, further the loss of electro activity was found to be marginal even after ~ 1 month of storage [365].

To demonstrate the viability of an aggregate nanowire based sensor, a biotin streptavidin based proof of concept could be used, and on further identification of biomarkers responsible for

MIC, this approach can be extended to the other biomarkers. Initially, the biotin streptavidin interaction are studied *ex-situ* and functionalization are carried out using existing chemistries in literature[366]. The use of nanostructured arrays of silicon nanowires have been demonstrated using the antibody-antigen interaction [367]. In this study, it is attempted to use large scale nano-array directly grown on silicon wafers to study the interaction and viability on the sensor substrate. This study utilizes the biotin modified SiNWs directly as the working electrode without further modification to conduct sensing experiments. It has been observed in experiments, that the macroscale CuONWs films show a higher level of brittleness as compared to the as-grown silicon nanowires wafer. Nanowire functionalization is carried out using a sandwich assay consisting of aminopropyltriethoxysilane (APTES) linker followed by a biomolecule moiety. The detection principle is illustrated in Figure 35. Although it is expected that this linker based approach would yield strong covalent bonding between the nanowires and biomolecule, a weakening of the sensor response is also expected due to charge screening [304].

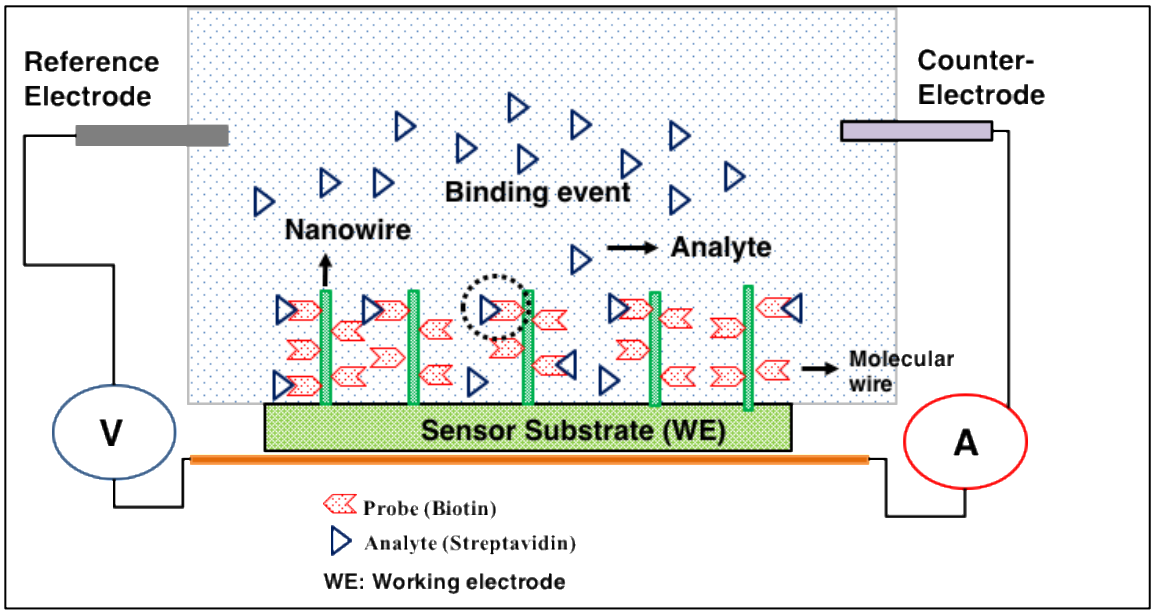

Figure 35. Detection principle for the binding event (Biotin – SA) interaction on the silicon nanowire arrays

Functionalization of the surface reduces the current due to the charge screening and this forms an important design consideration [368]. The functionalization scheme should try and limit the level of charge screening for improving sensitivity of the response. The Debye length ensures that the specific binding of macromolecules contribute to the sensor response and this length is calculated based on the electrostatic species in the solution [304]. Analyte detection must take into account factors such as employing ionic strength feedback control [369]. N-terminated SiNWs that are synthesized in this work using the APTES linker that are modified using biotinlyation with NHS Biotin in PBS buffer solution. It is noted in literature that devices with this functional arrangement can be stored without degradation for a period of up to 12 hours [277]. The response can be gathered as a resistance change across the terminals and the technique has been investigated in CuO based chemical sensors[370]. The usage of two-step functionalization using a electroactive monolayer of hydroquinone followed by cyclopentadiene

or a thiol group (based on regions of hydroquinone oxidation) allow for spatially selective bio-functionalization [371]. This setup (with functionalized SiNWs) is exposed to a biomarker-rich liquid environment and the electrical response is characterized with cyclic voltammetry.

7.2 Experimental methods

7.2.1 Setup of sensor test bed

A custom sensor test bed was fabricated to assist with the rapid use of nanowire substrates. The test bed was fabricated using a modular technique. A three-layer setup as demonstrated in Figure 36 was made using polypropylene blocks. These were selected due to their biocompatibility and ease of use. Ports were fabricated to introduce the environment (electrolyte), the counter and reference electrodes and additionally a substrate holder was fabricated to hold the thin film substrate. Additionally, the availability of an analyte injection port allows for the continuous injection of the analyte into the holder. The substrate holder allows the electrical isolation and direct connection to the working electrode lead of the potentiostat. The chamber for the electrolyte is fabricated using a borosilicate glass and sealed using Teflon gaskets. The chamber is fabricated in two different sizes allowing for one with a volume of 50 mL and another with a volume of 150 mL. The overall setup allows for leak proof long-term exposure of the substrate and minimizes the contamination of the electrolyte or surface of the working electrode from the environment. The whole setup is placed in a faraday cage for minimal interference from any external electrical fields during the experiment.

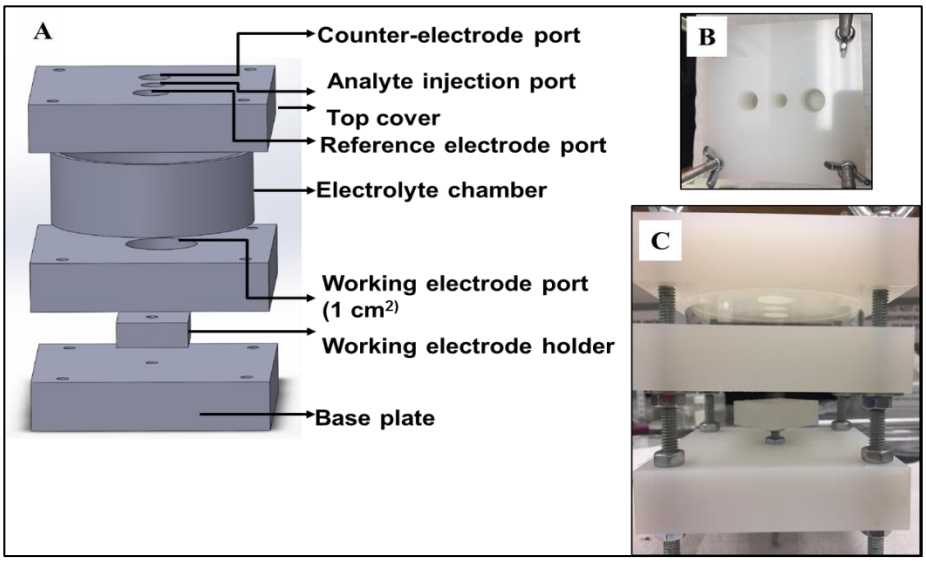

Figure 36. (A) Schematic of nanowire-thin-film sensor test bed (B) Top cover of the test bed and (C) Front-view of the fabricated test bed indicating the location of the working electrode holder

7.2.2 Solutions preparation

Stock solutions of sodium phosphate buffer was made using Stock Solution A (0.2 M Sodium Phosphate Monobasic): 27.6 g $NaH_2PO_4*H_2O$ (FW: 137.99g/mol) in 1L H_2O and Stock Solution B (0.2 M Sodium Phosphate Dibasic): 53.62g $Na_2HPO_4*7H_2O$ (FW: 268.07) in 1L H_2O. These two phosphate buffer solutions were prepared with deionized water (Milli-Q water systems, 18.2 MΩ-cm resistivity at 25 ^oC) and stored at ambient conditions. Streptavidin solutions of two concentrations, 10nM and 10,000 nM were prepared in 0.01M phosphate buffer solutions (PBS).

7.2.3 Functionalization

A 1% and 2% solution by volume of APTES was prepared in hexane/toluene and exposed in a stepwise manner to the nanowire substrates. The biotin functionalization was carried out in a 0.01 M PBS solution (~ pH = 7.4) at 0.5 mL of biotin, at a concentration of 5

mg/mL in 0.01 mol/L phosphate buffer (pH= 7.4). The exposure of the Streptavidin (SA) was conducted in a phosphate buffer of 0.01 M for 2 hours ex-situ.

7.2.4 Cyclic voltammetry

CV characterization was performed using a three-electrode setup with a standard calomel reference electrode and a graphite counter electrode. The system was connected to a high internal resistance potentiostat (Versastat 3, Princeton applied research) and CV was performed with the modified silicon nanowires as the working electrode. The studies were performed under DC voltage with no AC frequency and the measurements were carried out at -0.8 V to + 0.8 V at a scan rate of 100 mV/s.

7.3 Results

The Figure 37 illustrates the current response for the CV carried out for the bare Si NWs to the functionalized Si NWs at 10000 nM concentration. It should be noted that two concentrations of the primary molecular linker of APTES are utilized as a method to investigate the surface coverage effects of the molecular probes biotin in this case. 1% and 2% concentrations of the APTES are utilized. It is observed that there is a clear difference between the bare Si NWs and the coated Si NWs and hence this indicates its sensitivity to even small changes on the surface. Additionally, we observe that as the density of molecules increase on the surface because of functionalization the current response at maximum voltage decreases. This is as expected because of the resistance to charge transfer and the diffusion barrier. After exposure to the streptavidin and the formation of the immuno-complexes we observe a stable response at ~150 μA at 10,000 nM SA concentration and ~64 μA at 10 nM SA concentration. Additionally, we observe that there is a difference in the response to the peak loadings of 10 nM as against the three-fold higher 10,000 nM of SA.

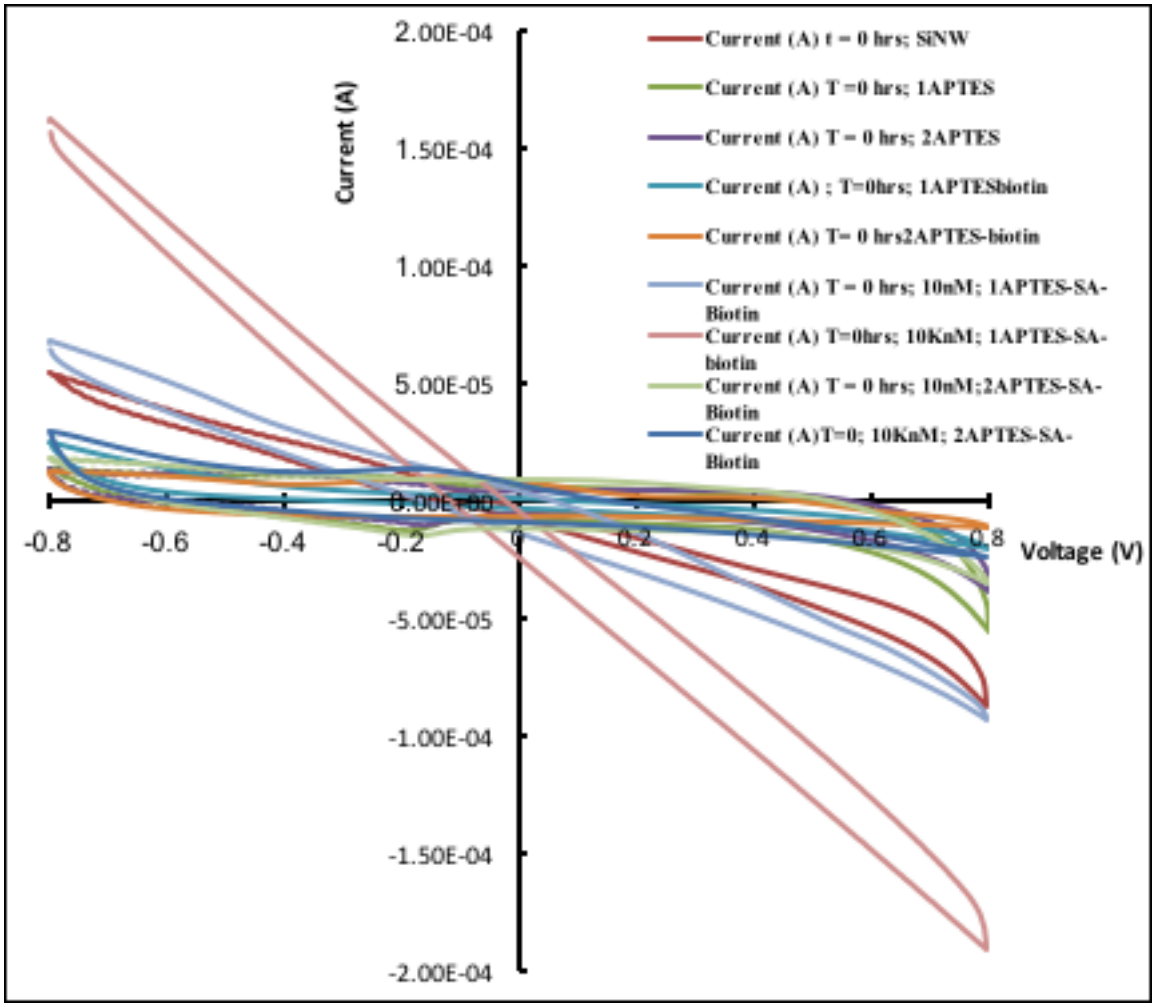

Figure 37. Variation of CV response with change in working electrode at time of initial immersion

Additionally, to investigate the effect of the exposure time on the response, the substrates with the full functionalization of APTES-biotin and the SA probe exposure were investigated at four time points after immersion until 3 hours. It was observed as seen in Figure 38 that at low loadings of the current at peak voltage increases slowly with time and stabilizes after 2 hours. This may be explained to the equilibrium achieved by the system, which is static (no stirring induced turbulence). Additionally, it should be noted that the experiments are performed at room

temperature and hence there is a potential of degradation of SA with time which is the case of large proteins [372]. This might release more counter-ions in the solutions allowing for a decrease in solution resistance. The time dependent behavior is a consequence of multiple factors which may not be completely captured using only CV.

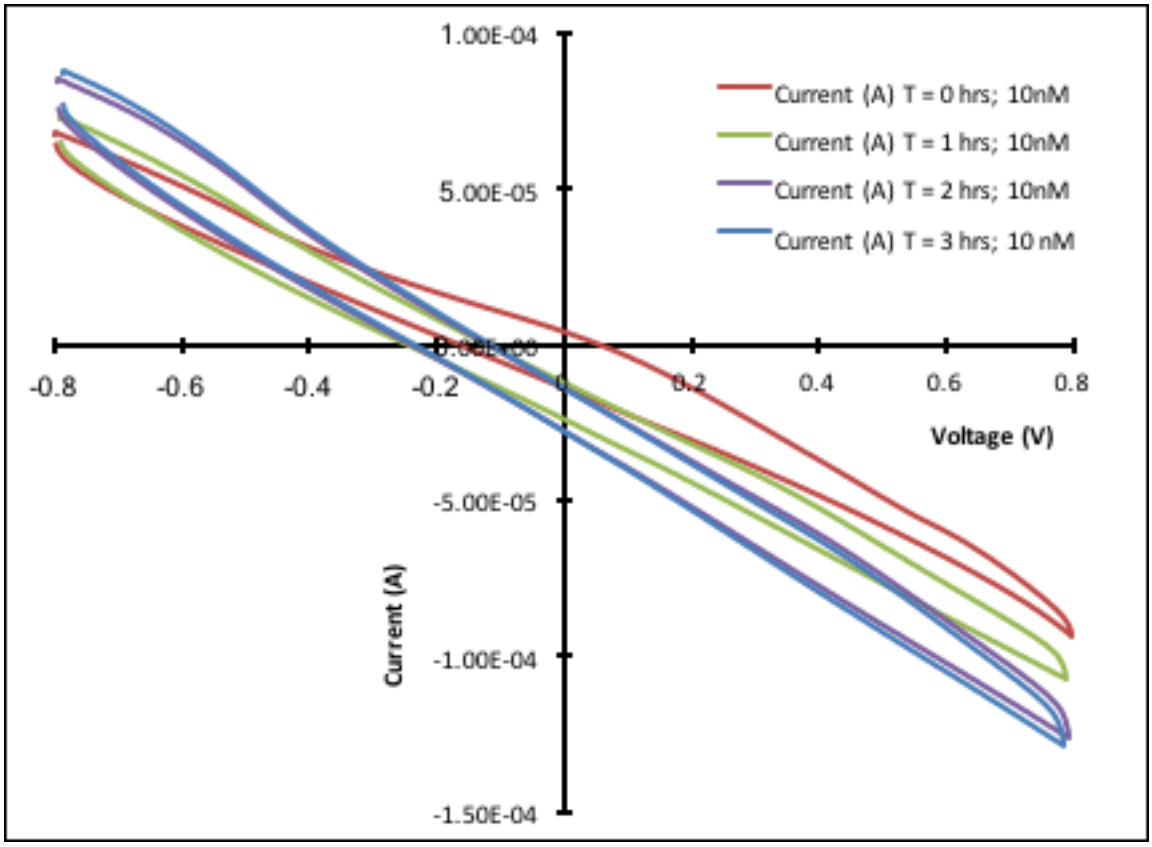

Figure 38. CV results at 10nM exposure of functionalized Si NWs to SA

Figure 39 illustrates that at higher loading the response is more stable with time. This is a consequence of exhaustion of all probe sites, hence the change in the response might be due to

externalities such as degradation of excess protein. Additionally, we observe that other than immediately after immersion, the current response is extremely stable.

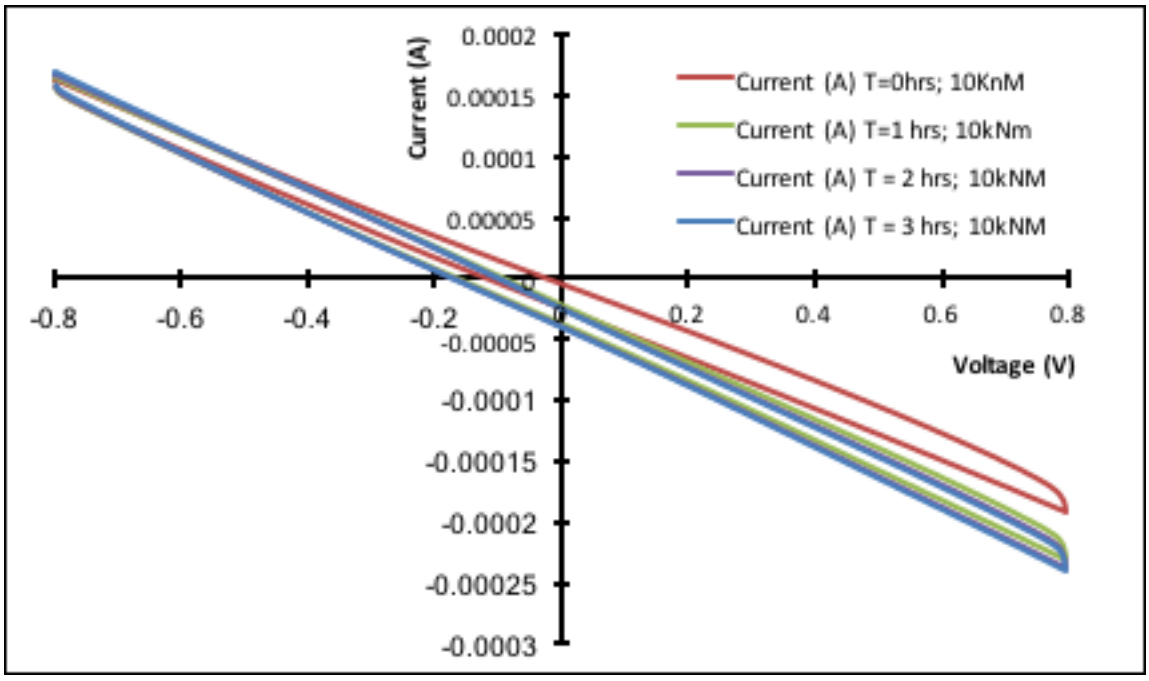

Figure 39. CV of exposure of functionalized NW-Biotin-SA substrate to 0.1 PBS at 10knM loading

Figure 40 illustrates the combined response of the sensor substrate with time and concentration. We observe that there is a joint variation of the current at peak voltage with time and with SA loading. This illustrates the need for a further investigation into the response range and the sensitivity limitation of the SiNWs substrate. Although the NWs provide large and robust surface area for functionalization, this also leads to challenges of NSB even under controlled conditions. The binding in the current case can be due to the affinity of the SA to directly block some charge transfer pathways on the SiNWs. Additionally, there may be un-reacted SA which

provides additional challenges of noise and interference with the electrochemical measurements. The nanowires are typically more effective at detection of low concentrations of analyte (species to be detected) due to linear dose-response observed.

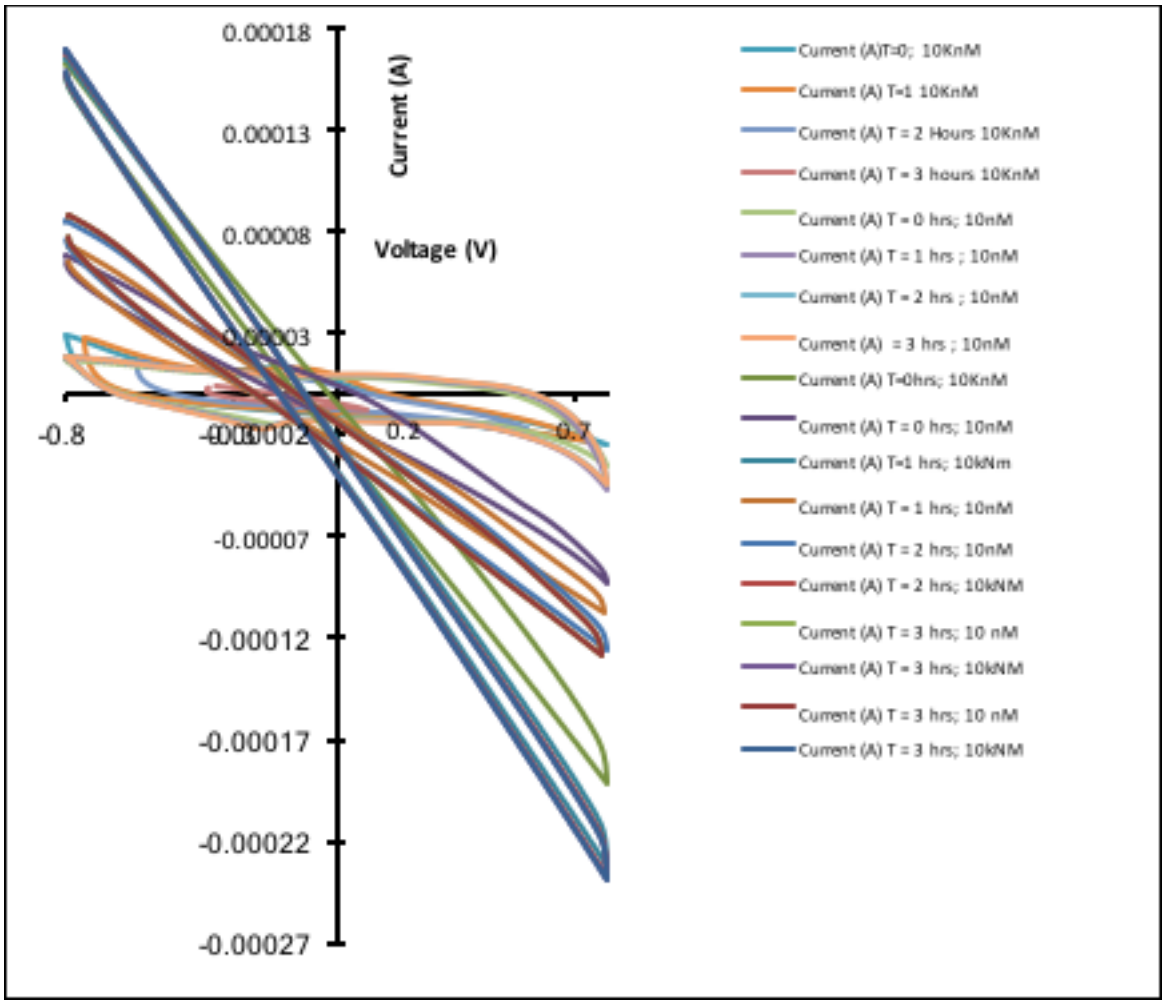

Figure 40. Combined response with time of CV of functionalized SiNWs substrate in 0.1 M PBS for 0,1,2,3 hours of exposure.

Figure 41 shows the current response at the peak negative voltage of ~-790 mV over the 3-hour period of exposure of the working electrode to the 0.1 M PBS. We find a stable response over time with minimal degradation in terms of the current. For the 10000 nM SA concentration, it is observed that the current response is stable at ~ 150 μA over the time. For the 10 nM concentration, it is observed that the response is initially ~64 μA increasing to 80 μA at hour 3. This difference can be attributed the changing ionic concentration of the solution due to degradation of the SA, and excess SA that may be remaining on the surface (Due to saturated binding sites).

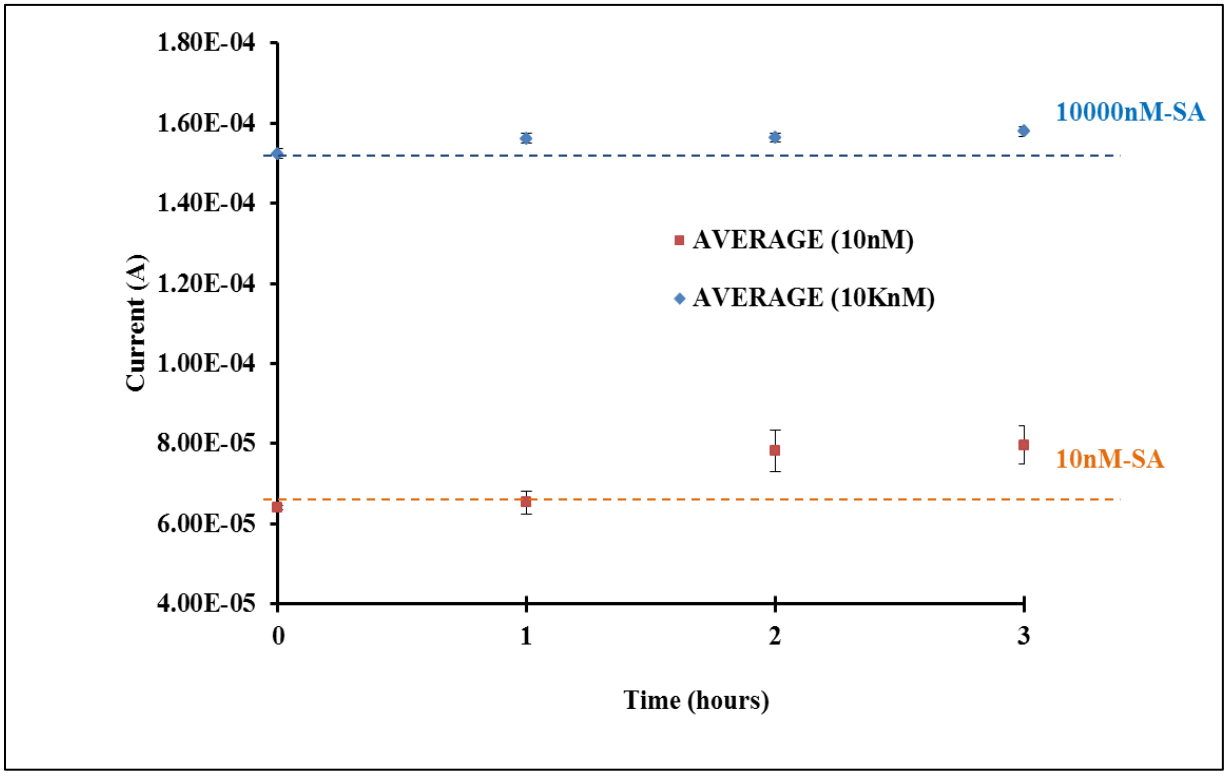

Figure 41. Current response at peak voltage negative voltage over time for SiNWs functionalized with 1%APTES-Biotin and exposed to SA

7.4 Conclusions

The proof of concept studies were performed using a SiNWs array synthesized on a Si wafer using the electroless etching synthesis process discussed in section 5. This is one of the few studies in which the nanowires are used directly after synthesis without the need for clean-room based fabrication or metal deposition for contacts. A custom nanowire-thin film test bed was fabricated using polypropylene sheets and coupled with a three-electrode probe setup. To test the viability of the substrate for sensing, a model system was selected with biotin as the probe and streptavidin as the analyte. This selection was made because of the low dissociation constant (irreversibility) observed for the biotin-streptavidin couple. Streptavidin was chosen as a demonstration probe (biomarker), due to the presence of multiple binding sites for biotin [373]. The functionalized silicon nanowires were used as the working electrode. The SiNWs were functionalized using a one-pot, three-step process. A molecular wire was built through first, a covalent functionalization of APTES followed by a buffer based functionalization of NHS-biotin.

On exposure of the functionalized substrate with the biotin probe to two concentrations of SA of 10 nM and 10,000 nM clear changes at peak negative voltage of ~-790 mV were observed for both the loadings. The current response was observed to be at ~150 μA at 10,000 nM SA concentration and ~64 μA at 10 nM SA concentration. Additionally, the functionalized nanowires showed higher charge transfer resistance as compared to their non-functionalized counter parts. This was explained due to the blocking of charge transfer sites by the covalently bonded APTES molecules and the NHS biotin. In addition, effects of both time and concentration were observed in the case of the functionalized substrates. This may be due to the artefacts presented by the degradation of the protein at ambient temperature, or may be a consequence of a steady state reached over time in the static system. It was observed that over time, stable current response was seen for the 1%APTES-NHS-biotin functionalized SiNWs and this optimized configuration of the model system can be further evaluated for non-specific binding and dose-response calibration studies.

8. CONCLUSIONS

The following are the conclusions of the study. The meta-analysis of 77 studies of MIC from the literature elicits the general methodology of the combined use of morphological, compositional analysis, electrochemical analysis, and biological analysis for its detection. 27% of the studies used 6 or more analytical tools to determine and analyze MIC. The tools used currently require expertise to integrate into a MIC assessment and management program [374-376]. The studies require the use of dedicated offsite facilities, limiting any on-site deployment for rapid evaluation and are often prohibitively expensive and use simulated environments, which lacked the fidelity of field environments.

Furthermore, the analysis also shows that mere presence of microbiota in a system does not necessarily imply MIC activity. Therefore, traditional culture-based techniques that depend on the use of selective media for detecting the presence or absence of bacteria may lead to erroneous results [303]. Microbiological assay techniques, such as the metagenomic and metabolomic techniques, provide a way of moving to a more robust determination of MIC. This has been corroborated in several studies which seek to use biological assays as a rapid tool to evaluate microbiological communities from industrial samples [377]. In addition, even at the laboratory scale it is challenging to accurately and precisely simulate field conditions for reproducible results [378]. A key to rapid detection of MIC in pipelines includes characterization of the microbiological diversity from possible affected sites in the field directly on-site, without transporting them to off-field characterization facilities. In such instances, on-site samples include pipeline debris, produced water and crude oil.

This thesis provides several novel advances to the state of understanding of nanowire use in industrial scale sensors and their application as a technology for the detection of MIC. The

thesis advances three areas (1) Use of aggregated nanowires as a scalable sensor substrate, fabricated using facile (simple) techniques (2) Electrochemical characterization study and stabilization of nanowires in simulated industrial environments (3) Extension of nanowire-based substrates in modified flat corrosion cell as a sensor for the detection of biomarkers as a proof of concept for MIC detection. The conclusions of the studies in the three areas are as follows:

(1) Copper (II) oxide (CuONWs) and silicon nanowires (SiNWs) were synthesized in facile and at relatively large scale (wafer scale for SiNWs, and commercial scale copper sheets) to yield high aspect ratio NWs. The CuO NWs synthesized were 25 to 30 μm in length and 50 to 100 nm in diameter and the Si NWs were 5 to 8 μm in length and 45 to 100 nm in diameter. Additionally, two routes for stabilization with BN using ammonia borane and tribromoborazine were used.

(2) The electrochemical degradation studies showed that the SiNWs had much lower corrosion current density in extremely corrosive environments of 3.5 wt. % NaCl and simulated produced water. Additionally, CuONWs showed 1-fold higher corrosion current density, however demonstrated stability. Both the nanowire systems showed robust resistance to degradation despite, their considerably higher surface area as compared to bulk counterparts. The mechanistic investigation revealed the presence of two double layers and a diffusion limitation in the case of CuONWs and a single double layer and diffusion limitation in the case of the SiNWs. The two double layers can be attributed to the resistance provided by the passive films and the porous nanowire mats formed in the synthesis process. The SiNWs demonstrated extremely high charge transfer resistance > 50 $K\Omega/cm^2$ (based on equivalent circuit fittings) indicating their robustness even in aggressive environments. Equivalent circuit with a single double layer-element

was fit for the SiNWs. For the CuONWs we observe a charge transfer resistance of ~ 8 KW /cm^2 and an increasing diffusion limitation to charge transfer with time of immersion. Equivalent circuits with two double layer elements and a Warburg element for the diffusion limitations were used to explain the electrochemical impedance behavior of the CuO nanowires.

(3) The use of biotin-streptavidin (SA) complex was chosen to demonstrate the viability of the substrate for sensing. A custom test bed was built to easily and reproducibly introduce functionalized substrates to bulk solutions. Cyclic voltammetry studies revealed a stable current response at peak negative potential of ~-0.79 to be ~150 μA at 10,000 nM SA concentration and ~64 μA at 10 nM SA concentration for SiNWs functionalized with a SA sensitive molecular wire.

9. SUMMARY AND FUTURE WORK

Generation of dose response calibration curves to evaluate the linear response range of the sensor substrate. The current study focused on the evaluation of the response at two discrete concentration levels (10 nM and 10,000 nM) of the model analyte (Streptavidin). Hence, the future work needs to evaluate response of the substrates over a wider range of analyte concentrations. Such data would provide the range of operating conditions for the sensors and sensitivity range. The calibration curves should also be generated to study the effect of the sensor substrate‘s response to variations in time, pH, ionic strength and temperature. This study also needs to be repeated for other nanowire substrates, and the data set will establish the region of sensitive response to allow for selection of sensor substrates for field deployment. Table 9 provides the variables for evaluation and a range of the parameters to perform a design of experiment for the generation of the dose response curves.

Study of NSB under increasing complexity in the sensing environment is critical to evaluate the scalability of the substrate to the industrial scale. The current work focused on obtaining a proof of concept in a controlled buffered (PBS) environment and using a model system of biotin and streptavidin. The next step would be to evaluate the sensor response in varying buffer concentrations (to raise the ionic strength) and generate response curves for the model system. Following this steps, the next step is to test the sensor response with the presence of possible interfering biomolecules, which either compete with SA for the biotin probe, or present a degradation risk to the biotin probe. Additionally, the evaluation of a terminal methyl based blocker on NW surfaces to reduce the risk of NSB needs to be evaluated. Following the complete characterization under abiotic scheme, the next step would be to evaluate the sensor response in the presence of single species, co-cultures and the finally diverse microbiological

environment. The biomarkers can initially be introduced *ex-situ* to the environment, and ultimately an *in-situ* biomarker can be detected. The final step before pilot scale testing is the introduction of oil and water mixtures to evaluate consequences of fouling presented by oily residues in combination with the biotic environments. Table 9 provides some examples of variables that can be tested to evaluate non-specific binding.

Equivalent circuits obtained from the impedance studies and the sensitivity and specificity of the sensor response are two areas which provide opportunities for further investigation. The equivalent circuits revealed the presence of charge transfer and diffusion resistances, which may be intrinsic to the nanowire systems, or may be a time dependent consequence of the action of the brine electrolytes. By designing experiments to systematically investigate the evolution of these circuit elements and in parallel to the sensor response studies in these environments, it is possible to identify design parameters for optimal sensor response. These include impedance studies in a step-wise manner of the molecular wire (surface functionalization), and the dose-response studies under a variety of external stressors (change in pH, salt concentrations). Ultimately, these studies need to progress towards the introduction of initially controlled biotic environments (single, and co-cultures) and progress towards naturalistic environments such as field produced water and oil-water-biota mixtures.

Table 9. Future work direction with parameter and range of evaluation of variables

#	Future work	Parameter	Range
1	Dose response calibration curves	Analyte concentration (Proof-of-concept-Streptavidin)	1, 2, 5, 10, 100, 1000, 10000nM
		Temperature	25 to 50 ^{o}C
		Ionic Strength	0.01 M PBS to 1 M PBS / Simulated produced water
		pH	5.5 to 8.5
2	Non-Specific Binding evaluation	Presence of Streptavidin degraders	
		Proteins, amino acids	
		Long chain fatty acids	
		Produced water residues	
		Biotic environment (single species and co-culture, laboratory based)	
		Oil Field water mixture	

Table 9. Continued

#	Future work	Parameter	Range
3	Degradation mechanism	Elemental composition change at nanowire surface	
		Equivalent circuit parameters change with time	
		Oil-water mixtures	
		Biotic environment (single species and co-culture, oil-field water)	

Extensive characterization of both the substrate and the electrolyte microenvironment are required to explain the fundamental mechanisms of degradation of these nanowire substrates. This would allow for the development of better functional chemistries which utilize the electronic and chemical properties yielded by these materials. A continuing challenge is the scale up of the nanowire system to a bulk scale without loss of properties. Industrial systems require more robust, and fouling resistant architectures [302], which need to be explored to bring nanowire/and nanomaterial systems to scalable sensing in process industries.

Data mining on microbiological community data can yield insights into organisms which show the highest proliferation and largest possible impact to MIC, and biosensors specifically targeting these can be deployed in field. Biosensors can overcome the limitations of size using embedded and lab on chip architectures to give outputs in scales of electric current, voltages or numeric scales which would allow the rapid assimilation of data [379-382]. The possibility to

couple the active sensing element with wireless transmitters using radiofrequency (RF)[383] promise reliable tool for non-destructive and real-time monitoring. This can be combined with risk-based inspection methods [384] such as fuzzy-logic and probabilistic techniques for improved MIC threat assessment [385].This can lead to intelligent process control and mitigation systems.

Identification of biomarkers is the key to the development and deployment of such biosensors. This includes the exploration of aptamer chemistry for more robust probes [386, 387], as compared to the immunosensors (or ELISA) based chemistries. This would render them much more resistant to degradation and allow for long term storage. Current efforts include the improvement in the biomonitoring standards which promise to yield more complete data sets of the microbiological community. This ultimately yields key performance indicators and actions for consistent reporting across the industry [388].

The advent of nanomaterial-based platforms [389-393] provides an opportunity to use this data and achieve reduction in costs related to MIC and the improvement in the asset integrity management programs [394, 395]. There is a major opportunity for research aimed at mass producing reliable technologies for detecting MIC in dynamic environments such as crude oil pipeline, storage tanks, water networks, offshore oil platforms and others. If realized, they provide large economic benefits to many industries affected by MIC. The impact of research in this area would be the reduction of incidents in an environment of increasing economic pressures due to oil process fluctuations and reduction in maintenance budgets, thus increasing the possibility of failures and lapses.

REFERENCES

1. Gaylarde, C.C., F.M. Bento, and J. Kelley, *Microbial contamination of stored hydrocarbon fuels and its control.* Revista de Microbiologia, 1999. **30**(1): p. 01-10.

2. Tang, K., V. Baskaran, and M. Nemati, *Bacteria of the sulphur cycle: an overview of microbiology, biokinetics and their role in petroleum and mining industries.* Biochemical Engineering Journal, 2009. **44**(1): p. 73-94.

3. Lee, A. and D. Newman, *Microbial iron respiration: impacts on corrosion processes.* Applied microbiology and biotechnology, 2003. **62**(2-3): p. 134-139.

4. Cattant, F., D. Crusset, and D. Féron, *Corrosion issues in nuclear industry today.* Materials today, 2008. **11**(10): p. 32-37.

5. Battersby, N., D. Stewart, and A. Sharma, *Microbiological problems in the offshore oil and gas industries.* Journal of applied bacteriology, 1985. **59**(s14): p. 227S-235S.

6. Cloete, T.E., L. Jacobs, and V.S. Brözel, *The chemical control of biofouling in industrial water systems.* Biodegradation, 1998. **9**(1): p. 23-37.

7. Iverson, W.P., *Microbial corrosion of metals.* Advances in applied microbiology, 1987. **32**: p. 1-36.

8. Holdom, R.S., *Microbial spoilage of engineering materials.* Tribology International, 1977. **10**(3): p. 155-162.

9. Javaherdashti, R., *Impact of sulphate-reducing bacteria on the performance of engineering materials.* Applied microbiology and biotechnology, 2011. **91**(6): p. 1507-1517.

10. Bank, W. *Gross Domestic Product data from Worldbank.* [cited 2014 7th July]; The Gross National Product of the countries are Tabulated.]. Available from: http://data.worldbank.org/indicator/NY.GNP.MKTP.PP.CD.

11. Koch, G., J. Varney, N. Thompson, O. Moghissi, M. Gould, and J. Payer, *International measures of prevention, application and economics of corrosion technologies study*. 2016, NACE International: Houston, Texas.

12. Tribollet, B., *Electrochemical sensors for biofilm and biocorrosion.* Materials and Corrosion, 2003. **54**(7): p. 527-534.

13. Borenstein, S., *Microbiologically influenced corrosion handbook*. 1994: Elsevier.

14. Little, B., P. Wagner, and F. Mansfeld, *An overview of microbiologically influenced corrosion.* Electrochimica Acta, 1992. **37**(12): p. 2185-2194.

15. Little, B.J., F.B. Mansfeld, P.J. Arps, and J.C. Earthman, *Microbiologically influenced corrosion*. 2007: Wiley Online Library.

16. Videla, H.A. and L.K. Herrera, *Microbiologically influenced corrosion: looking to the future.* International microbiology, 2005. **8**(3): p. 169.

17. Li, K., M. Whitfield, and K.J. Van Vliet, *Beating the bugs: roles of microbial biofilms in corrosion.* Corrosion Reviews, 2013. **31**(3-6): p. 73-84.

18. Beale, D.J., M.S. Dunn, and D. Marney, *Application of GC–MS metabolic profiling to 'blue-green water'from microbial influenced corrosion in copper pipes.* Corrosion science, 2010. **52**(9): p. 3140-3145.

19. Chen, G., R. Palmer, and D. White, *Instrumental analysis of microbiologically influenced corrosion.* Biodegradation, 1997. **8**(3): p. 189-200.

20. Heitz, E., H.-C. Flemming, and W. Sand, *Microbially influenced corrosion of materials: scientific and engineering aspects*. 1996: Springer-Verlag.

21. Neria-González, I., E.T. Wang, F. Ramírez, J.M. Romero, and C. Hernández-Rodríguez, *Characterization of bacterial community associated to biofilms of corroded oil pipelines from the southeast of Mexico.* Anaerobe, 2006. **12**(3): p. 122-133.

22. Hashemi, J., N. Bak, F. Khan, K. Hawboldt, L. Lefsrud, and J. Wolodko, *Bibliometric Analysis of Microbiologically Influenced Corrosion (MIC) of Engineering Systems.* CORROSION, 2017.

23. Skovhus, T.L., D. Enning, and J.S. Lee, *Microbiologically Influenced Corrosion in the Upstream Oil and Gas Industry*. 2017: CRC Press.

24. De Turris, A., M. de Romero, S. Papavinasam, and W.D. Gould. *Synergistic Effect of Sulphate-Reducing Bacteria And CO2 On the Corrosion of Carbon Steel In Synthetic Produced Water*. in *CORROSION 2012*. 2012. Salt Lake City, Utah, USA: NACE International.

25. Xu, D. and T. Gu, *The war against problematic biofilms in the oil and gas industry.* J Microb Biochem Technol, 2015. **7**: p. 124.

26. Festy, D., R. Marchal, and N. Monfort. *Parametric Study of Localized Corrosion Artificially Initiated: Application to a Carbon Steel Biocorrosion Sensor*. in *CORROSION 2001*. 2001. Houston, Texas, USA: NACE International.

27. Festy, D., M. Keddam, B. Tribollet, and N.M. Moros. *Detection and Mapping of SRB Influenced Corrosion of C-Steel*. in *CORROSION 2002*. 2002. Denver, Colorado, USA: NACE International.

28. Tator, K.B. *Hydrogen Sulfide and Microbiologically Induced Corrosion of Concrete Steel and Ductile Iron in Waste Water Facilities*. in *CORROSION 2003*. 2003. San Diego, California, USA: NACE International.

29. Vanaei, H., A. Eslami, and A. Egbewande, *A review on pipeline corrosion, in-line inspection (ILI), and corrosion growth rate models.* International Journal of Pressure Vessels and Piping, 2017. **149**: p. 43-54.

30. Rajasekar, A., B. Anandkumar, S. Maruthamuthu, Y.-P. Ting, and P.K. Rahman, *Characterization of corrosive bacterial consortia isolated from petroleum-product-transporting pipelines.* Applied microbiology and biotechnology, 2010. **85**(4): p. 1175-1188.

31. Cetin, D. and M.L. Aksu, *Corrosion behavior of low-alloy steel in the presence of Desulfotomaculum sp.* Corrosion Science, 2009. **51**(8): p. 1584-1588.

32. Bsharat, T.K., *Detection, Treatment, and Prevention of Microbiologically Influenced Corrosion in Water-Based Fire Protection Systems*. 1998: National Fire Sprinkler Association.

33. Blanco, M., C. Negro, I. Gaspar, and J. Tijero, *Slime problems in the paper and board industry.* Applied microbiology and biotechnology, 1996. **46**(3): p. 203-208.

34. Flitton, M.K.A. and T.S. Yoder. *Twelve Year Study of Underground Corrosion of Activated Metals*. in *CORROSION 2012*. 2012. Salt Lake City, Utah, USA: NACE International.

35. Maruthamuthu, S., T. Nagendran, B. Anandkumar, M. Karthikeyan, N. Palaniswamy, and G. Narayanan, *Microbiologically influenced corrosion on rails.* Current Science, 2011. **100**(6): p. 870-880.

36. Chang, J.I. and C.-C. Lin, *A study of storage tank accidents.* Journal of loss prevention in the process industries, 2006. **19**(1): p. 51-59.

37. Jacobson, G.A., *Corrosion at Prudhoe Bay: a lesson on the line.* Materials performance, 2007. **46**(8).

38. Robertson, T.L., E. DeCola, and L. Pearson, *Alaska North Slope spills analysis: Final report on North Slope spills analysis and expert panel recommendations on mitigation measures*. 2010: Alaska Department of Environmental Conservation.

39. Abdullah, A., N. Yahaya, N. Md Noor, and R. Mohd Rasol, *Microbial corrosion of API 5L X-70 carbon steel by ATCC 7757 and consortium of sulfate-reducing bacteria.* Journal of Chemistry, 2014. **2014**.

40. Sustaita, M. *Cause of deadly Pemex Abkatun fire determined*. Offshore Engineer 2015 19 October 2015 [cited 2016 31 August]; Available from: http://www.oedigital.com/component/k2/item/10636-cause-of-deadly-pemex-abkatun-fire-found.

41. Rajasekar, A., W. Xiao, M. Sethuraman, P. Parthipan, and P. Elumalai, *Airborne bacteria associated with corrosion of mild steel 1010 and aluminum alloy 1100.* Environmental Science and Pollution Research, 2017: p. 1-17.

42. Dong, Z.H., W. Shi, H.M. Ruan, and G.A. Zhang, *Heterogeneous corrosion of mild steel under SRB-biofilm characterised by electrochemical mapping technique.* Corrosion Science, 2011. **53**(9): p. 2978-2987.

43. Zhang, T., H. Fang, and B. Ko, *Methanogen population in a marine biofilm corrosive to mild steel.* Applied microbiology and biotechnology, 2003. **63**(1): p. 101-106.

44. Luo, J., P. Angell, D. White, and I. Vance. *MIC of mild steel in oilfield produced water*. in Corrosion-National association of corrosion engineers annual conference. 1994. NACE.

45. McBeth, J.M., B.J. Little, R.I. Ray, K.M. Farrar, and D. Emerson, *Neutrophilic iron-oxidizing "Zetaproteobacteria" and mild steel corrosion in nearshore marine environments.* Applied and Environmental Microbiology, 2011. **77**(4): p. 1405-1412.

46. Lee, A.K., M.G. Buehler, and D.K. Newman, *Influence of a dual-species biofilm on the corrosion of mild steel.* Corrosion Science, 2006. **48**(1): p. 165-178.

47. Fonseca, I.T., M.J. Feio, A.R. Lino, M. Reis, and V.L. Rainha, *The influence of the media on the corrosion of mild steel by Desulfovibrio desulfuricans bacteria: an electrochemical study.* Electrochimica Acta, 1998. **43**(1): p. 213-222.

48. Wang, H., L.-K. Ju, H. Castaneda, G. Cheng, and B.-m.Z. Newby, *Corrosion of carbon steel C1010 in the presence of iron oxidizing bacteria Acidithiobacillus ferrooxidans.* Corrosion Science, 2014. **89**: p. 250-257.

49. Binkauskiene, E., A. Lugauskas, I. Prosyčevas, V. Pakštas, A. Selskiene, D. Bučinskiene, and A. Ručinskiene, *The Impact of Microscopic Fungi on the Morphological and Structural Properties of Carbon Steel.* Journal of Surface Engineered Materials and Advanced Technology, 2014. **2014**.

50. Pérez, E.J., R. Cabrera-Sierra, I. González, and F. Ramírez-Vives, *Influence of Desulfovibrio sp. biofilm on SAE 1018 carbon steel corrosion in synthetic marine medium.* Corrosion Science, 2007. **49**(9): p. 3580-3597.

51. Sarioğlu, F., R. Javaherdashti, and N. Aksöz, *Corrosion of a drilling pipe steel in an environment containing sulphate-reducing bacteria.* International journal of pressure vessels and piping, 1997. **73**(2): p. 127-131.

52. Jia, R., J.L. Tan, P. Jin, D.J. Blackwood, D. Xu, and T. Gu, *Effects of biogenic H2S on the microbiologically influenced corrosion of C1018 carbon steel by sulfate reducing Desulfovibrio vulgaris biofilm.* Corrosion Science, 2018. **130**: p. 1-11.

53. Jia, R., D. Yang, J. Xu, D. Xu, and T. Gu, *Microbiologically influenced corrosion of C1018 carbon steel by nitrate reducing Pseudomonas aeruginosa biofilm under organic carbon starvation.* Corrosion Science, 2017. **127**: p. 1-9.

54. Bao, Q., D. Zhang, D. Lv, and P. Wang, *Effects of two main metabolites of sulphate-reducing bacteria on the corrosion of Q235 steels in 3.5 wt.% NaCl media.* Corrosion Science, 2012. **65**: p. 405-413.

55. Xu, J., K. Wang, C. Sun, F. Wang, X. Li, J. Yang, and C. Yu, *The effects of sulfate reducing bacteria on corrosion of carbon steel Q235 under simulated disbonded coating by using electrochemical impedance spectroscopy.* Corrosion Science, 2011. **53**(4): p. 1554-1562.

56. Liu, T. and Y.F. Cheng, *The influence of cathodic protection potential on the biofilm formation and corrosion behaviour of an X70 steel pipeline in sulfate reducing bacteria media.* Journal of Alloys and Compounds, 2017. **729**: p. 180-188.

57. Wan, H., D. Song, D. Zhang, C. Du, D. Xu, Z. Liu, D. Ding, and X. Li, *Corrosion effect of Bacillus cereus on X80 pipeline steel in a Beijing soil environment.* Bioelectrochemistry, 2017.

58. George, R., P. Muraleedharan, K. Sreekumari, and H. Khatak, *Influence of surface characteristics and microstructure on adhesion of bacterial cells onto a type 304 stainless steel.* Biofouling, 2003. **19**(1): p. 1-8.

59. Jia, R., D. Yang, D. Xu, and T. Gu, *Anaerobic corrosion of 304 stainless steel caused by the Pseudomonas aeruginosa biofilm.* Frontiers in microbiology, 2017. **8**.

60. Zhou, E., H. Li, C. Yang, J. Wang, D. Xu, D. Zhang, and T. Gu, *Accelerated corrosion of 2304 duplex stainless steel by marine Pseudomonas aeruginosa biofilm.* International Biodeterioration & Biodegradation, 2018. **127**: p. 1-9.

61. Li, H., E. Zhou, D. Zhang, D. Xu, J. Xia, C. Yang, H. Feng, Z. Jiang, X. Li, and T. Gu, *Microbiologically influenced corrosion of 2707 hyper-duplex stainless steel by marine Pseudomonas aeruginosa biofilm.* Scientific reports, 2016. **6**: p. 20190.

62. Song, W., X. Chen, C. He, X. Li, and C. Liu, *Microbial Corrosion of 2205 Duplex Stainless Steel in Oilfield-Produced Water.* Int. J. Electrochem. Sci, 2018. **13**: p. 675-689.

63. Dec, W., M. Jaworska-Kik, W. Simka, and J. Michalska, *Corrosion behaviour of 2205 duplex stainless steel in pure cultures of sulphate reducing bacteria: SEM studies, electrochemical characterisation and biochemical analyses.* Materials and Corrosion, 2018. **69**(1): p. 53-62.

64. Moradi, M., Z. Song, L. Yang, J. Jiang, and J. He, *Effect of marine Pseudoalteromonas sp. on the microstructure and corrosion behaviour of 2205 duplex stainless steel.* Corrosion Science, 2014. **84**: p. 103-112.

65. Xu, D., J. Xia, E. Zhou, D. Zhang, H. Li, C. Yang, Q. Li, H. Lin, X. Li, and K. Yang, *Accelerated corrosion of 2205 duplex stainless steel caused by marine aerobic Pseudomonas aeruginosa biofilm.* Bioelectrochemistry, 2017. **113**: p. 1-8.

66. Li, P., Y. Zhao, Y. Liu, Y. Zhao, D. Xu, C. Yang, T. Zhang, T. Gu, and K. Yang, *Effect of Cu addition to 2205 duplex stainless steel on the resistance against pitting corrosion by the Pseudomonas aeruginosa biofilm.* Journal of Materials Science & Technology, 2017. **33**(7): p. 723-727.

67. Liu, H., D. Xu, K. Yang, H. Liu, and Y.F. Cheng, *Corrosion of antibacterial Cu-bearing 316L stainless steels in the presence of sulfate reducing bacteria.* Corrosion Science, 2017.

68. Abraham, G., V. Kain, and G. Dey, *MIC failure of type 316l seawater pipeline.* Mater Perform, 2009. **48**: p. 64-69.

69. Sun, Z., M. Moradi, Y. Chen, R. Bagheri, P. Guo, L. Yang, Z. Song, and C. Xu, *Simulation of the marine environment using bioreactor for investigation of 2507 duplex stainless steel corrosion in the presence of marine isolated Bacillus Vietnamensis bacterium.* Materials Chemistry and Physics, 2018. **208**: p. 149-156.

70. Rosales, B.M. and M. Iannuzzi, *Aluminium AA2024 T351 aeronautical alloy: Part 1. Microbial influenced corrosion analysis.* Materials Science and Engineering: A, 2008. **472**(1): p. 15-25.

71. Smirnov, V., D. Belov, T. Sokolova, O. Kuzina, and V. Kartashov, *Microbiological corrosion of aluminum alloys.* Applied biochemistry and microbiology, 2008. **44**(2): p. 192-196.

72. De Romero, M., Z. Duque, O. De Rincón, O. Perez, I. Araujo, and A. Martinez, *Online Monitoring systems of microbiologically influenced corrosion on Cu-10% Ni alloy in chlorinated, brackish water.* Corrosion, 2000. **56**(8): p. 867-876.

73. Li, H., C. Yang, E. Zhou, C. Yang, H. Feng, Z. Jiang, D. Xu, T. Gu, and K. Yang, *Microbiologically influenced corrosion behavior of S32654 super austenitic stainless steel in the presence of marine Pseudomonas aeruginosa biofilm.* Journal of Materials Science & Technology, 2017. **33**(12): p. 1596-1603.

74. Larsen, J., K. Rasmussen, H. Pedersen, K. Sørensen, T. Lundgaard, and T.L. Skovhus. *Consortia of MIC bacteria and archaea causing pitting corrosion in top side oil production facilities*. in *CORROSION 2010*. 2010. San Antonio, Texas, USA: NACE International.

75. Skovhus, T.L., L. Holmkvist, K. Andersen, J. Larsen, and H. Pedersen. *MIC risk assessment of the Halfdan Oil Export Spool*. in *SPE International Conference & Workshop on Oilfield Corrosion*. 2012. Society of Petroleum Engineers.

76. Geissler, B., R. De Paula, C. Keller-Schultz, J. Lilley, and V. Keasler. *Data Mining to Prevent Microbiologically Influenced Corrosion?* in *CORROSION 2014*. 2014. San Antonio, Texas, USA: NACE International.

77. Zuo, R., *Biofilms: strategies for metal corrosion inhibition employing microorganisms.* Applied microbiology and biotechnology, 2007. **76**(6): p. 1245-1253.

78. Videla, H.A. and L.K. Herrera, *Understanding microbial inhibition of corrosion. A comprehensive overview.* International Biodeterioration & Biodegradation, 2009. **63**(7): p. 896-900.

79. Elsener, B., *Corrosion inhibitors for steel in concrete: state of the art report*. Vol. 773. 2001: Maney Pub.

80. Hasson, D., H. Shemer, and A. Sher, *State of the art of friendly "green" scale control inhibitors: a review article.* Industrial & Engineering Chemistry Research, 2011. **50**(12): p. 7601-7607.

81. Costerton, J., G. Geesey, and P. Jones, *Bacterial biofilms in relation to internal corrosion monitoring and biocide strategies*. 1987, National Assoc. of Corrosion Engineers, Houston, TX.

82. Zheludkevich, M.L., D.G. Shchukin, K.A. Yasakau, H. Möhwald, and M.G. Ferreira, *Anticorrosion coatings with self-healing effect based on nanocontainers impregnated with corrosion inhibitor.* Chemistry of Materials, 2007. **19**(3): p. 402-411.

83. Little, B., J. Lee, and R. Ray, *A review of 'green'strategies to prevent or mitigate microbiologically influenced corrosion.* Biofouling, 2007. **23**(2): p. 87-97.

84. Whitby, C. and T.L. Skovhus, *Applied microbiology and molecular biology in oilfield systems*. 2011: Springer.

85. Gu, T., K. Zhao, and S. Nesic, *A new mechanistic model for MIC based on a Biocatalytic Cathodic Sulfate Reduction Theory.* NACE Corrosion/09, paper, 2009(390).

86. Wan, Y., D. Zhang, Y. Wang, and B. Hou, *A 3D-impedimetric immunosensor based on foam Ni for detection of sulfate-reducing bacteria.* Electrochemistry Communications, 2010. **12**(2): p. 288-291.

87. Wan, Y., D. Zhang, Y. Wang, P. Qi, and B. Hou, *Direct immobilisation of antibodies on a bioinspired architecture as a sensing platform.* Biosensors and Bioelectronics, 2011. **26**(5): p. 2595-2600.

88. Chen, Y., R. Howdyshell, B.-M.Z. Newby, H. Castaneda, L.-K. Ju, X. He, S. Howdyshell, G. Cheng, and J.M. Senko. *Severe Pitting Corrosion Caused by a Starving Sulfate-Reducing Bacterium Surviving on Carbon Steel and Effect of Surface Roughness*. in *CORROSION 2013*. 2013. Orlando, Florida, USA: NACE International.

89. Kane, R.D. and S. Campbell. *Real-time corrosion monitoring of steel influenced by microbial activity (SRB) in simulated seawater injection environments*. in *CORROSION 2004*. 2004. New Orleans, Louisiana, USA: NACE International.

90. Power, M., J. Araujo, J. Van Der Meer, H. Harms, and O. Wanner, *Monitoring sulfate-reducing bacteria in heterotrophic biofilms.* Water science and technology, 1999. **39**(7): p. 49-56.

91. Al-Shamari, A.R., A.W. Al-Mithin, S. Prakash, M. Islam, A.J. Biedermann, and A. Mathew. *Some Empirical Observations About Bacteria Proliferation and Corrosion Damage Morphology in Kuwait Oilfield Waters*. in *CORROSION 2013*. 2013. Orlando, Florida, USA: NACE International.

92. Little, B.B., R.I. Ray, and R.K. Pope, *The Relationship Between Corrosion and the Biological Sulfur Cycle*. 2000, DTIC Document.

93. Bryant, R.D., W. Jansen, J. Boivin, E.J. Laishley, and J.W. Costerton, *Effect of hydrogenase and mixed sulfate-reducing bacterial populations on the corrosion of steel.* Applied and environmental microbiology, 1991. **57**(10): p. 2804-2809.

94. Cord-Ruwisch, R., W. Kleinitz, and F. Widdell, *Sulfate-reducing bacteria and their activities in oil production.* J. Pet. Technol.;(United States), 1987. **39**(1).

95. Hamilton, W.A., *Sulphate-reducing bacteria and anaerobic corrosion.* Annual Reviews in Microbiology, 1985. **39**(1): p. 195-217.

96. Hao, O.J., J.M. Chen, L. Huang, and R.L. Buglass, *Sulfate-reducing bacteria.* Critical reviews in environmental science and technology, 1996. **26**(2): p. 155-187.

97. Samant, A. and S. Singh. *Role of Microbial Induced Corrosion in Subsea Water Pipeline Failure*. in *CORROSION 98*. 1998. San Diego, California, USA: NACE international.

98. Setareh, M. and R. Javaherdashti, *Evaluation of sessile microorganisms in pipelines and cooling towers of some Iranian industries.* Journal of materials engineering and performance, 2006. **15**(1): p. 5-8.

99. Olson, M.E., H. Ceri, D.W. Morck, A.G. Buret, and R.R. Read, *Biofilm bacteria: formation and comparative susceptibility to antibiotics.* Canadian Journal of Veterinary Research, 2002. **66**(2): p. 86.

100. Costerton, J.W., Z. Lewandowski, D.E. Caldwell, D.R. Korber, and H.M. Lappin-Scott, *Microbial biofilms.* Annual Reviews in Microbiology, 1995. **49**(1): p. 711-745.

101. Nivens, D.E., J.Q. Chambers, T.R. Anderson, and D.C. White, *Long-term, on-line monitoring of microbial biofilms using a quartz crystal microbalance.* Analytical Chemistry, 1993. **65**(1): p. 65-69.

102. Denkhaus, E., S. Meisen, U. Telgheder, and J. Wingender, *Chemical and physical methods for characterisation of biofilms.* Microchimica Acta, 2007. **158**(1-2): p. 1-27.

103. Flemming, H.-C., *Microbial biofouling: Unsolved problems, insufficient approaches, and possible solutions*, in *Biofilm highlights*. 2011, Springer. p. 81-109.

104. Muyzer, G. and A.J. Stams, *The ecology and biotechnology of sulphate-reducing bacteria.* Nature Reviews Microbiology, 2008. **6**(6): p. 441-454.

105. Chen, Y., Q. Tang, J.M. Senko, G. Cheng, B.-m.Z. Newby, H. Castaneda, and L.-K. Ju, *Long-term survival of Desulfovibrio vulgaris on carbon steel and associated pitting corrosion.* Corrosion Science, 2015. **90**: p. 89-100.

106. Roberts, D.J., D. Nica, G. Zuo, and J.L. Davis, *Quantifying microbially induced deterioration of concrete: initial studies.* International Biodeterioration & Biodegradation, 2002. **49**(4): p. 227-234.

107. Flemming, H.-C., J. Wingender, U. Szewzyk, P. Steinberg, S.A. Rice, and S. Kjelleberg, *Biofilms: an emergent form of bacterial life.* Nature Reviews Microbiology, 2016. **14**(9): p. 563.

108. Eckert, R., *Emphasis on biofilms can improve mitigation of microbiologically influenced corrosion in oil and gas industry.* Corrosion Engineering, Science and Technology, 2015. **50**(3): p. 163-168.

109. Zarasvand, K.A. and V.R. Rai, *Microorganisms: induction and inhibition of corrosion in metals.* International Biodeterioration & Biodegradation, 2014. **87**: p. 66-74.

110. Vigneron, A., E.B. Alsop, B. Chambers, B.P. Lomans, I.M. Head, and N. Tsesmetzis, *Complementary microorganisms in highly corrosive biofilms from an offshore oil production facility.* Applied and environmental microbiology, 2016. **82**(8): p. 2545-2554.

111. Vigneron, A., I.M. Head, and N. Tsesmetzis, *Damage to offshore production facilities by corrosive microbial biofilms.* Applied microbiology and biotechnology, 2018. **102**(6): p. 2525-2533.

112. Usher, K., A. Kaksonen, I. Cole, and D. Marney, *Critical review: Microbially influenced corrosion of buried carbon steel pipes.* International Biodeterioration & Biodegradation, 2014. **93**: p. 84-106.

113. Larsen, J., L. Holmkvist, K. Sørensen, and T.L. Skovhus. *Identification and quantification of microorganisms involved in downhole MIC in a Dan oil producing well*. in *CORROSION 2011*. 2011. Houston, Texas, USA: NACE International.

114. Conlette, O.C., N.E. Emmanuel, and O.G. Chijoke, *Methanogen Population of an Oil Production Skimmer Pit and the Effects of Environmental Factors and Substrate Availability on Methanogenesis and Corrosion Rates.* Microbial ecology, 2016. **72**(1): p. 175-184.

115. Silva, A., T. Santiago, C. Alves, M. Guedes, J. Freire, R. Vieira, and R. Da Silva, *An evaluation of the corrosion behavior of aluminum surfaces in presence of fungi using atomic force microscopy and other tests.* Anti-Corrosion Methods and Materials, 2007. **54**(5): p. 289-293.

116. Qu, Q., L. Wang, L. Li, Y. He, M. Yang, and Z. Ding, *Effect of the fungus, Aspergillus niger, on the corrosion behaviour of AZ31B magnesium alloy in artificial seawater.* Corrosion Science, 2015. **98**: p. 249-259.

117. Mohanan, S., A. Rajasekar, N. Muthukumar, S. Maruthamuthu, and N. Palaniswamy, *The role of fungi on diesel degradation, and their influence on corrosion of API 5LX steel.* Corrosion Prevention and Control, 2005. **52**(4): p. 123-130.

118. Li, B., X. Luo, H. Zhang, and Y. Tang, *Different effects of three soil microfloras on the corrosion of copper*. RSC Advances, 2016. **6**(44): p. 37544-37554.

119. Mansouri, H., S. Alavi, and M. Yari. *A Study of Pseudomonas Aeruginosa Bacteria in Microbial Corrosion*. in *2nd International Conference on Chemical, Ecology and Environmental Sciences (ICCEES'2012) Singapore*. 2012.

120. Dinh, H.T., J. Kuever, M. Mußmann, A.W. Hassel, M. Stratmann, and F. Widdel, *Iron corrosion by novel anaerobic microorganisms.* Nature, 2004. **427**(6977): p. 829-832.

121. Sanchez-Silva, M. and D.V. Rosowsky, *Biodeterioration of construction materials: state of the art and future challenges.* Journal of Materials in Civil Engineering, 2008.

122. Liu, H.-C., J.-L. Xia, Z.-Y. Nie, A.-A. Peng, C.-Y. Ma, L. Zheng, and Y.-D. Zhao, *Comparative study of sulfur utilization and speciation transformation of two elemental sulfur species by thermoacidophilic Archaea Acidianus manzaensis YN-25.* Process Biochemistry, 2013. **48**(12): p. 1855-1860.

123. Kip, N. and J.A. van Veen, *The dual role of microbes in corrosion.* The ISME journal, 2015. **9**(3): p. 542-551.

124. Romero, M., L. Rodriguez, Z. Duque, M.A. Mendez, O. de Rincon, O. Perez, and I. Araujo. *A study of Microbiologically Induced Corrosion by SRB on Carbon Steel using Hydrogen Permeation*. in *CORROSION 2003*. 2003. San Diego, California, USA.

125. Wrangham, J.B., J.E. Penkala, S. D'Imperio, B.M. Peyton, and K.G. Wunch. *Utilization Of A 16S Rrna Gene Microarray To Analyze The Efficacy Of Oil And Gas Industry Bacteria Culture Media*. in *CORROSION 2010*. 2010. San Antonio, Texas, USA.

126. Grigoryan, A., A. Lambo, S. Lin, S. Cornish, T. Jack, and G. Voordouw, *Souring remediation by field-wide nitrate injection in an Alberta oil field.* Journal of Canadian Petroleum Technology, 2009. **48**(05): p. 58-61.

127. Johnson, R.J., B.D. Folwell, A. Wirekoh, M. Frenzel, and T.L. Skovhus, *Reservoir Souring–Latest developments for application and mitigation.* Journal of biotechnology, 2017. **256**: p. 57-67.

128. Gieg, L.M., T.R. Jack, and J.M. Foght, *Biological souring and mitigation in oil reservoirs.* Applied microbiology and biotechnology, 2011. **92**(2): p. 263-282.

129. Jansen, S., M. van Burgel, J. Gerritse, and M. Büchler. *Cathodic Protection and MIC-Effects of Local Electrochemistry*. in *CORROSION 2017*. 2017. NACE International.

130. Iverson, W.P., *Direct evidence for the cathodic depolarization theory of bacterial corrosion*. 1965, DTIC Document.

131. Telegdi, J., A. Shaban, and L. Trif, *Microbiologically influenced corrosion (MIC)*, in *Trends in Oil and Gas Corrosion Research and Technologies*. 2017, Elsevier. p. 191-214.

132. Xu, D. and T. Gu, *Bioenergetics explains when and why more severe MIC pitting by SRB can occur*. Corrosion/2011 Paper, 2011(11426).

133. Li, Y., D. Xu, C. Chen, X. Li, R. Jia, D. Zhang, W. Sand, F. Wang, and T. Gu, *Anaerobic Microbiologically Influenced Corrosion Mechanisms Interpreted Using Bioenergetics and Bioelectrochemistry: A Review.* Journal of Materials Science & Technology, 2018.

134. Gu, T. and D. Xu, *Demystifying MIC mechanisms*. 2010, National Association of Corrosion Engineers, P. O. Box 218340 Houston TX 77084 USA.

135. Xu, D., Y. Li, and T. Gu, *Mechanistic modeling of biocorrosion caused by biofilms of sulfate reducing bacteria and acid producing bacteria.* Bioelectrochemistry, 2016. **110**: p. 52-58.

136. Jia, R., D. Yang, D. Xu, and T. Gu, *Electron transfer mediators accelerated the microbiologically influence corrosion against carbon steel by nitrate reducing Pseudomonas aeruginosa biofilm.* Bioelectrochemistry, 2017. **118**: p. 38-46.

137. Zhang, P., D. Xu, Y. Li, K. Yang, and T. Gu, *Electron mediators accelerate the microbiologically influenced corrosion of 304 stainless steel by the Desulfovibrio vulgaris biofilm.* Bioelectrochemistry, 2015. **101**: p. 14-21.

138. Xu, D., Y. Li, F. Song, and T. Gu, *Laboratory investigation of microbiologically influenced corrosion of C1018 carbon steel by nitrate reducing bacterium Bacillus licheniformis.* Corrosion Science, 2013. **77**: p. 385-390.

139. Javed, M., P. Stoddart, and S. Wade, *Corrosion of carbon steel by sulphate reducing bacteria: Initial attachment and the role of ferrous ions.* Corrosion Science, 2015. **93**: p. 48-57.

140. Enning, D. and J. Garrelfs, *Corrosion of iron by sulfate-reducing bacteria: new views of an old problem.* Applied and environmental microbiology, 2014. **80**(4): p. 1226-1236.

141. Iverson, W.P., *Research on the mechanisms of anaerobic corrosion.* International biodeterioration & biodegradation, 2001. **47**(2): p. 63-70.

142. Huttunen-Saarivirta, E., P. Rajala, M. Bomberg, and L. Carpén, *EIS study on aerobic corrosion of copper in ground water: influence of micro-organisms.* Electrochimica Acta, 2017. **240**: p. 163-174.

143. Jogdeo, P., R. Chai, S. Shuyang, M. Saballus, F. Constancias, S.L. Wijesinghe, D. Thierry, D.J. Blackwood, D. McDougald, and S.A. Rice, *Onset of Microbial Influenced Corrosion (MIC) in Stainless Steel Exposed to Mixed Species Biofilms from Equatorial Seawater.* Journal of The Electrochemical Society, 2017. **164**(9): p. C532-C538.

144. Xu, D., E. Zhou, Y. Zhao, H. Li, Z. Liu, D. Zhang, C. Yang, H. Lin, X. Li, and K. Yang, *Enhanced resistance of 2205 Cu-bearing duplex stainless steel towards microbiologically influenced corrosion by marine aerobic Pseudomonas aeruginosa biofilms.* Journal of Materials Science & Technology, 2017.

145. Yuan, S. and S. Pehkonen, *Microbiologically influenced corrosion of 304 stainless steel by aerobic Pseudomonas NCIMB 2021 bacteria: AFM and XPS study*. Colloids and Surfaces B: Biointerfaces, 2007. **59**(1): p. 87-99.

146. Scotto, V., R.D. Cintio, and G. Marcenaro, *The influence of marine aerobic microbial film on stainless steel corrosion behaviour.* Corrosion Science, 1985. **25**(3): p. 185-194.

147. Sreekumari, K.R., K. Nandakumar, and Y. Kikuchi, *Bacterial attachment to stainless steel welds: significance of substratum microstructure.* Biofouling, 2001. **17**(4): p. 303-316.

148. G3-89, A., *Standard Practice for Conventions Applicable to Electrochemical Measurements in Corrosion Testing.* 2010.

149. Sooknah, R., S. Papavinasa, and R.W. Revie. *Modelling the occurrence of microbiologically influenced corrosion*. in *CORROSION 2007*. 2007. Nashville, Tennessee, USA: NACE International.

150. Inc., A.S.P. *BioGeorge, Biofilm activity monitoring system*. [cited 2018 FEB 25]; Available from: http://www.alspi.com/biogeorge.htm.

151. Kilbane, J. *Effect of Sample Storage Conditions on Oilfield Microbiological Samples*. in *CORROSION 2014*. 2014. San Antonio, Texas, USA: NACE International.

152. Sooknah, R., S. Papavinasam, and R.W. Revie, *Monitoring Microbiologically Influenced Corrosion: A Review Of Techniques*. NACE International.

153. Beech, I.B., *Corrosion of technical materials in the presence of biofilms—current understanding and state-of-the art methods of study.* International Biodeterioration & Biodegradation, 2004. **53**(3): p. 177-183.

154. Surman, S., J. Walker, D. Goddard, L. Morton, C. Keevil, W. Weaver, A. Skinner, K. Hanson, D. Caldwell, and J. Kurtz, *Comparison of microscope techniques for the examination of biofilms.* Journal of Microbiological Methods, 1996. **25**(1): p. 57-70.

155. Romero, M., O. de Rincon, D. Zoilabet, J. Araujo, and O. Perez. *Hydrogen Permeation Study with Palladium in a Sulfate-Reducing Culture*. in *CORROSION 2001*. 2001. Houston, Texas, USA: NACE International.

156. Bairamov, A.K., T. Ahmed, M.N. Al-Sonidah, J. Liang, and R. Bradley. *Excessive Rate of MIC on 316 SS in Seawater*. in *CORROSION 2002*. 2002. Denver, Colorado, USA: NACE International.

157. Song, X., Y. Yang, D. Yu, G. Lan, Z. Wang, and X. Mou, *Studies on the impact of fluid flow on the microbial corrosion behavior of product oil pipelines.* Journal of Petroleum Science and Engineering, 2016. **146**: p. 803-812.

158. Paddock, S.W., *Confocal laser scanning microscopy.* Biotechniques, 1999. **27**: p. 992-1007.

159. Neu, T.R. and J.R. Lawrence, *Development and structure of microbial biofilms in river water studied by confocal laser scanning microscopy.* FEMS Microbiology Ecology, 1997. **24**(1): p. 11-25.

160. Chen, S., Y.F. Cheng, and G. Voordouw, *A comparative study of corrosion of 316L stainless steel in biotic and abiotic sulfide environments.* International Biodeterioration & Biodegradation, 2017. **120**: p. 91-96.

161. Javed, M., B. Borges, V. Cirino, A. Osman, and S. Wade, *Effect of metal substrate on initial attachment of E. coli bacteria and subsequent microbiologically influenced corrosion.* Corrosion and Prevention, 2015.

162. Parthipan, P., P. Rahman, and A. Rajasekar, *Characterization of hydrocarbon degrading bacteria isolated from Indian crude oil reservoir and their influence on biocorrosion of carbon steel API 5LX.* International Biodeterioration and Biodegradation, 2018.

163. Zhu, R., D.T. Tan, and D. Shuai, *Research highlights: applications of atomic force microscopy in natural and engineered water systems.* Environmental Science: Water Research & Technology, 2016. **2**(3): p. 415-420.

164. Steele, A., D. Goddard, and I. Beech, *An atomic force microscopy study of the biodeterioration of stainless steel in the presence of bacterial biofilms.* International biodeterioration & biodegradation, 1994. **34**(1): p. 35-46.

165. Fang, H.H., K.-Y. Chan, and L.-C. Xu, *Quantification of bacterial adhesion forces using atomic force microscopy (AFM).* Journal of microbiological methods, 2000. **40**(1): p. 89-97.

166. Beech, I.B., J.R. Smith, A.A. Steele, I. Penegar, and S.A. Campbell, *The use of atomic force microscopy for studying interactions of bacterial biofilms with surfaces.* Colloids and surfaces B: Biointerfaces, 2002. **23**(2): p. 231-247.

167. Beech, I.B., *The potential use of atomic force microscopy for studying corrosion of metals in the presence of bacterial biofilms—an overview.* International biodeterioration & biodegradation, 1996. **37**(3): p. 141-149.

168. Mehanna, M., R. Basseguy, M.-L. Delia, R. Gubner, N. Sathirachinda, and A. Bergel, *Geobacter species enhances pit depth on 304L stainless steel in a medium lacking with electron donor.* Electrochemistry Communications, 2009. **11**(7): p. 1476-1481.

169. Nichols, P.D., J.M. Henson, J.B. Guckert, D.E. Nivens, and D.C. White, *Fourier transform-infrared spectroscopic methods for microbial ecology: analysis of bacteria, bacteri-polymer mixtures and biofilms.* Journal of microbiological methods, 1985. **4**(2): p. 79-94.

170. Chakraborty, J. and S. Das, *Application of spectroscopic techniques for monitoring microbial diversity and bioremediation.* Applied Spectroscopy Reviews, 2017. **52**(1): p. 1-38.

171. Kagarise, C., J.R. Vera, and R.B. Eckert, *The Importance of Deposit Characterization in Mitigating UDC and MIC in Dead Legs*, in *CORROSION 2017*. 2017, NACE International: New Orleans, Louisiana, USA.

172. Rodrigues, E. and R. Akid, *Internal Corrosion Assessment of the Otter Oil Production Spool*, in *SPE International Oilfield Corrosion Conference and Exhibition*. 2014, Society of Petroleum Engineers: Aberdeen, Scotland.

173. Been, J., E. Bloomfield, and Y. Jacob, *Root Cause Analysis of an Upstream Pipeline Failure Indicating the Contribution and Interaction of Multiple Factors*, in *CORROSION 2017*. 2017, NACE International: New Orleans, Louisiana, USA.

174. Larsen, J. and L.R. Hilbert, *Investigation into Under Deposit Corrosion in Halfdan Production Tubulars*, in *CORROSION 2014*. 2014, NACE International: San Antonio, Texas, USA.

175. Burns, M.G., *The Tales That Rust Can Tell: The Use of Corrosion Product Analyses In Corrosion Failure Investigations*, in *SPE International Oilfield Corrosion Conference and Exhibition*. 2016, Society of Petroleum Engineers: Aberdeen, Scotland, UK.

176. Huttunen-Saarivirta, E., M. Honkanen, T. Lepistö, V.T. Kuokkala, L. Koivisto, and C.G. Berg, *Microbiologically influenced corrosion (MIC) in stainless steel heat exchanger.* Applied Surface Science, 2012. **258**(17): p. 6512-6526.

177. El Hajj, H., A. Abdelouas, Y. El Mendili, G. Karakurt, B. Grambow, and C. Martin, *Corrosion of carbon steel under sequential aerobic–anaerobic environmental conditions.* Corrosion Science, 2013. **76**(0): p. 432-440.

178. Miranda, E., M. Bethencourt, F. Botana, M. Cano, J. Sánchez-Amaya, A. Corzo, J.G. De Lomas, M.-L. Fardeau, and B. Ollivier, *Biocorrosion of carbon steel alloys by an hydrogenotrophic sulfate-reducing bacterium Desulfovibrio capillatus isolated from a Mexican oil field separator.* Corrosion Science, 2006. **48**(9): p. 2417-2431.

179. Ilhan-Sungur, E. and A. Çotuk, *Microbial corrosion of galvanized steel in a simulated recirculating cooling tower system.* Corrosion Science, 2010. **52**(1): p. 161-171.

180. Skovhus, T.L., S.M. Caffrey, and C.R. Hubert, *Applications of Molecular Microbiological Methods*. 2014: Caister Academic Press.

181. Liang, R., D.F. Aktas, E. Aydin, V. Bonifay, J. Sunner, and J.M. Suflita, *Anaerobic biodegradation of alternative fuels and associated biocorrosion of carbon steel in marine environments.* Environmental science & technology, 2016. **50**(9): p. 4844-4853.

182. Beale, D.J., A.V. Karpe, S. Jadhav, T.H. Muster, and E.A. Palombo, *Omics-based approaches and their use in the assessment of microbial-influenced corrosion of metals.* Corrosion Reviews, 2016. **34**(1-2): p. 1-15.

183. Klein, D., *Quantification using real-time PCR technology: applications and limitations.* Trends in molecular medicine, 2002. **8**(6): p. 257-260.

184. Fierer, N., J.A. Jackson, R. Vilgalys, and R.B. Jackson, *Assessment of soil microbial community structure by use of taxon-specific quantitative PCR assays.* Applied and environmental microbiology, 2005. **71**(7): p. 4117-4120.

185. Summer, E.J., S. Duggleby, C. Janes, and M. Liu, *Microbial Populations in the O&G: Application of this Knowledge*, in *CORROSION 2014*. 2014, NACE International: San Antonio, Texas, USA.

186. Geurkink, B., S. Doddema, H. de Vries, G.J. Euverink, and E. Croese, *Value of Next Generation Sequencing as Monitoring Tool For Microbial Corrosion - A Practical Case from Bioprophyling to Tailor made MMM Analysis*, in *CORROSION 2016*. 2016, NACE International: Vancouver, British Columbia, Canada.

187. Bartling, C., K.H. Kucharzyk, L. Mullins, A. Minard-Smith, and J. Busch-Harris, *Interpreting Omic Data for Microbially Influenced Corrosion: Lessons from a Case Study Involving a Seawater Injection System*, in *CORROSION 2017*. 2017, NACE International: New Orleans, Louisiana, USA.

188. Mand, J., T.R. Jack, G. Voordouw, and H. Hoffmann, *Use of molecular methods (pyrosequencing) for evaluating MIC potential in water systems for oil production in the North Sea*, in *SPE International Oilfield Corrosion Conference and Exhibition*. 2014, Society of Petroleum Engineers: Aberdeen, Scotland.

189. Demeter, M., K. Dockens, S. Johnston, and R.J. Turner, *Molecular MIC Diagnoses from ATP Field Test: Streamlined Workflow from Field to 16S RRNA Gene Metagenomics Results*, in *CORROSION 2017*. 2017, NACE International: New Orleans, Louisiana, USA.

190. Johnson, R., *Sequencing the Oil Field Microbiome – Can Metagenomics Help Combat MIC?*, in *CORROSION 2015*. 2015, NACE International: Dallas, Texas.

191. Muyzer, G., E.C. De Waal, and A.G. Uitterlinden, *Profiling of complex microbial populations by denaturing gradient gel electrophoresis analysis of polymerase chain reaction-amplified genes coding for 16S rRNA.* Applied and environmental microbiology, 1993. **59**(3): p. 695-700.

192. Teng, F., Y. Guan, and W. Zhu, *Effect of biofilm on cast iron pipe corrosion in drinking water distribution system: corrosion scales characterization and microbial community structure investigation.* Corrosion science, 2008. **50**(10): p. 2816-2823.

193. Carvalho, M.L., J. Doma, M. Sztyler, I. Beech, and P. Cristiani, *The study of marine corrosion of copper alloys in chlorinated condenser cooling circuits: The role of microbiological components.* Bioelectrochemistry, 2014. **97**: p. 2-6.

194. Moniee, M., X. Zhu, L. Tang, S. Juhler, F.I. Nuwaiser, P.F. Sanders, and F. Abeedi, *Optimization of DNA Staining Technology for Development of Autonomous Microbe Sensor for Injection Seawater Systems.* Journal of Sensor Technology, 2016. **6**(03): p. 27.

195. Zhu, X., J.I. Kilbane, A. Ayala, and H. Modi. *Application of quantitative, real-time PCR in monitoring microbiologically influenced corrosion (MIC) in gas pipelines*. in *CORROSION 2005*. 2005. NACE International.

196. Zhu, X., H. Modi, A. Ayala, and J. Kilbane, *Rapid detection and quantification of microbes related to microbiologically influenced corrosion using quantitative polymerase chain reaction.* Corrosion, 2006. **62**(11): p. 950-955.

197. Murali Mohan, A., A. Hartsock, K.J. Bibby, R.W. Hammack, R.D. Vidic, and K.B. Gregory, *Microbial community changes in hydraulic fracturing fluids and produced water from shale gas extraction.* Environmental science & technology, 2013. **47**(22): p. 13141-13150.

198. Zhang, T. and H. Fang, *Phylogenetic diversity of a SRB-rich marine biofilm.* Applied microbiology and biotechnology, 2001. **57**(3): p. 437-440.

199. Amann, R., J. Stromley, R. Devereux, R. Key, and D. Stahl, *Molecular and microscopic identification of sulfate-reducing bacteria in multispecies biofilms.* Applied and Environmental Microbiology, 1992. **58**(2): p. 614-623.

200. Schmeisser, C., I. Krohn-Molt, and W.R. Streit, *Metagenome Analyses of Multispecies Microbial Biofilms: First Steps Toward Understanding Diverse Microbial Systems on Surfaces,* in *Functional Metagenomics: Tools and Applications*. 2017, Springer. p. 201-215.

201. Upreti, M.K., *Development of PCR based methodology for quick detection of microbiologically influenced corrosion.*

202. Zhu, X.Y., J. Lubeck, and J.J. Kilbane, *Characterization of microbial communities in gas industry pipelines.* Applied and Environmental Microbiology, 2003. **69**(9): p. 5354-5363.

203. Jan-Roblero, J., A. Posadas, J.Z.D. de la Serna, R. García, and C. Hernández-Rodríguez, *Phylogenetic characterization of bacterial consortia obtained of corroding gas pipelines in Mexico.* World Journal of Microbiology and Biotechnology, 2008. **24**(9): p. 1775-1784.

204. Duncan, K.E., L.M. Gieg, V.A. Parisi, R.S. Tanner, S.G. Tringe, J. Bristow, and J.M. Suflita, *Biocorrosive thermophilic microbial communities in Alaskan North Slope oil facilities.* Environmental science & technology, 2009. **43**(20): p. 7977-7984.

205. Dahle, H., F. Garshol, M. Madsen, and N.-K. Birkeland, *Microbial community structure analysis of produced water from a high-temperature North Sea oil-field.* Antonie van Leeuwenhoek, 2008. **93**(1-2): p. 37-49.

206. Penner, T.J., J.M. Foght, and K. Budwill, *Microbial diversity of western Canadian subsurface coal beds and methanogenic coal enrichment cultures.* International Journal of Coal Geology, 2010. **82**(1): p. 81-93.

207. Jan-Roblero, J., J. Romero, M. Amaya, and S. Le Borgne, *Phylogenetic characterization of a corrosive consortium isolated from a sour gas pipeline.* Applied microbiology and biotechnology, 2004. **64**(6): p. 862-867.

208. Skovhus, T.L., K. Sorensen, J. Larsen, K. Rasmussen, and M. Jensen. *Rapid determination of MIC in oil production facilities with a DNA-based diagnostic kit*. in *SPE International Conference on Oilfield Corrosion*. 2010. Society of Petroleum Engineers.

209. Geurkink, B., H. de Vries, S. Doddema, G.J. Euverink, and E. Croese. *Value of Next Generation Sequencing as monitoring tool for microbial corrosion: A practical case from bioprophyling to tailor made MMM analysis*. in *NACE International Corrosion Conference Proceedings*. 2016. NACE International.

210. Park, H.S., J. Mand, T.R. Jack, and G. Voordouw, *Next-generation Sequencing Approach to Understand Pipeline Biocorrosion.* Applications of Molecular Microbiological Methods, 2014: p. 33.

211. Celikkol-Aydin, S., C.C. Gaylarde, T. Lee, R.E. Melchers, D.L. Witt, and I.B. Beech, *16S rRNA gene profiling of planktonic and biofilm microbial populations in the Gulf of Guinea using Illumina NGS.* Marine environmental research, 2016. **122**: p. 105-112.

212. Chiu, C. and S. Miller, *Next-generation sequencing*, in *Molecular Microbiology*. 2016, American Society of Microbiology. p. 68-79.

213. An, D., X. Dong, A. An, H.S. Park, M. Strous, and G. Voordouw, *Metagenomic analysis indicates epsilonproteobacteria as a potential cause of microbial corrosion in pipelines injected with bisulfite.* Frontiers in microbiology, 2016. **7**: p. 28.

214. Tsesmetzis, N., E.B. Alsop, A. Vigneron, F. Marcelis, I.M. Head, and B.P. Lomans, *Microbial community analysis of three hydrocarbon reservoir cores provides valuable insights for the assessment of reservoir souring potential.* International Biodeterioration & Biodegradation, 2018. **126**: p. 177-188.

215. Muyzer, G. and F. Marty, *Molecular Methods in Microbiologically Influenced Corrosion Research, Monitoring and Control.* 2014.

216. VanLear, G. and F. McLafferty, *Biochemical aspects of high-resolution mass spectrometry.* Annual review of biochemistry, 1969. **38**(1): p. 289-322.

217. Brauer, J.I., I.B. Beech, and J. Sunner, *Mass Spectrometric Imaging Using Laser Ablation and Solvent Capture by Aspiration (LASCA).* Journal of The American Society for Mass Spectrometry, 2015. **26**(9): p. 1538-1547.

218. Brauer, J.I., Z. Makama, V. Bonifay, E. Aydin, E.D. Kaufman, I.B. Beech, and J. Sunner, *Mass spectrometric metabolomic imaging of biofilms on corroding steel surfaces using laser ablation and solvent capture by aspiration.* Biointerphases, 2015. **10**(1): p. 019003.

219. Gutarowska, B., S. Celikkol-Aydin, V. Bonifay, A. Otlewska, E. Aydin, A.L. Oldham, J.I. Brauer, K.E. Duncan, J. Adamiak, and J.A. Sunner, *Metabolomic and high-throughput sequencing analysis—modern approach for the assessment of biodeterioration of materials from historic buildings.* Frontiers in microbiology, 2015. **6**.

220. Javed, M., W. Neil, G. McAdam, and S. Wade, *Effect of sulphate-reducing bacteria on the microbiologically influenced corrosion of ten different metals using constant test conditions.* International Biodeterioration & Biodegradation, 2017. **125**: p. 73-85.

221. Cheng, S., J. Tian, S. Chen, Y. Lei, X. Chang, T. Liu, and Y. Yin, *Microbially influenced corrosion of stainless steel by marine bacterium Vibrio natriegens:(I) Corrosion behavior.* Materials Science and Engineering: C, 2009. **29**(3): p. 751-755.

222. Beese-Vasbender, P.F., S. Nayak, A. Erbe, M. Stratmann, and K.J. Mayrhofer, *Electrochemical characterization of direct electron uptake in electrical microbially influenced corrosion of iron by the lithoautotrophic SRB Desulfopila corrodens strain IS4.* Electrochimica Acta, 2015. **167**: p. 321-329.

223. Brauer, J.I., S. Celikkol-Aydin, J.A. Sunner, C.C. Gaylarde, and I.B. Beech, *Metabolomic imaging of a quaternary ammonium salt within a marine bacterial biofilm on carbon steel.* International Biodeterioration & Biodegradation, 2017. **125**: p. 33-36.

224. Pourbaix, M., *Applications of electrochemistry in corrosion science and in practice.* Corrosion Science, 1974. **14**(1): p. 25-82.

225. Pourbaix, M., *A comparative review of electrochemicalmethods of assessing corrosion and the behaviour in practice of corrodible material.* Corrosion Science, 1965. **5**(10): p. 677-700.

226. Schmitt, G., *Sophisticated Electrochemical methods for MIC investigation and monitoring.* Materials and Corrosion, 1997. **48**(9): p. 586-601.

227. Padilla-Viveros, A., E. Garcia-Ochoa, and D. Alazard, *Comparative electrochemical noise study of the corrosion process of carbon steel by the sulfate-reducing bacterium Desulfovibrio alaskensis under nutritionally rich and oligotrophic culture conditions.* Electrochimica Acta, 2006. **51**(18): p. 3841-3847.

228. Jamali, S.S. and D.J. Mills, *A critical review of electrochemical noise measurement as a tool for evaluation of organic coatings.* Progress in Organic Coatings, 2016. **95**: p. 26-37.

229. Homborg, A., R. Cottis, and J. Mol, *An integrated approach in the time, frequency and time-frequency domain for the identification of corrosion using electrochemical noise.* Electrochimica Acta, 2016. **222**: p. 627-640.

230. Chandrasatheesh, C., J. Jayapriya, R. George, and U.K. Mudali, *Detection and analysis of microbiologically influenced corrosion of 316 L stainless steel with electrochemical noise technique.* Engineering Failure Analysis, 2014. **42**: p. 133-142.

231. Homborg, A., C.L. Morales, T. Tinga, J. De Wit, and J. Mol, *Detection of microbiologically influenced corrosion by electrochemical noise transients.* Electrochimica acta, 2014. **136**: p. 223-232.

232. Miller II, R.B., A. Sadek, A. Rodriguez, M. Iannuzzi, C. Giai, J.M. Senko, and C.N. Monty, *Use of an electrochemical split cell technique to evaluate the influence of Shewanella oneidensis activities on corrosion of carbon steel.* PloS one, 2016. **11**(1): p. e0147899.

233. Smart, N., A. Rance, B. Reddy, L. Hallbeck, K. Pedersen, and A. Johansson, *In situ evaluation of model copper-cast iron canisters for spent nuclear fuel: a case of microbiologically influenced corrosion (MIC).* Corrosion Engineering, Science and Technology, 2014. **49**(6): p. 548-553.

234. Homborg, A.M., C.F. Leon Morales, T. Tinga, J.H.W. de Wit, and J.M.C. Mol, *Detection of microbiologically influenced corrosion by electrochemical noise transients.* Electrochimica Acta, 2014. **136**: p. 223-232.

235. Loto, C.A., *Electrochemical noise measurement technique in corrosion research.* International Journal of Electrochemical Science, 2012. **7**(10): p. 9248-9270.

236. Homborg, A.M., T. Tinga, X. Zhang, E.P.M. van Westing, P.J. Oonincx, G.M. Ferrari, J.H.W. de Wit, and J.M.C. Mol, *Transient analysis through Hilbert spectra of electrochemical noise signals for the identification of localized corrosion of stainless steel.* Electrochimica Acta, 2013. **104**: p. 84-93.

237. Loto, C.A., *Electrochemical noise evaluation and data statistical analysis of stressed aluminium alloy in NaCl solution.* Alexandria Engineering Journal, 2017.

238. Men, H., J. Zhang, and L. Zhang, *Intelligent Recognition for Microbiologically Influenced Corrosion Based On Hilbert-huang Transform and BP Neural Network.* JCP, 2012. **7**(9): p. 2283-2291.

239. Little, B.J. and J.S. Lee, *Microbiologically influenced corrosion: an update.* International Materials Reviews, 2014. **59**(7): p. 384-393.

240. Li, H., E. Zhou, D. Zhang, D. Xu, J. Xia, C. Yang, H. Feng, Z. Jiang, X. Li, T. Gu, and K. Yang, *Microbiologically Influenced Corrosion of 2707 Hyper-Duplex Stainless Steel by Marine Pseudomonas aeruginosa Biofilm.* Scientific Reports, 2016. **6**: p. 20190.

241. Holthe, R., Bardal, E., Gartland, and P. O., *Time dependence of cathodic properties of materials in seawater. Stainless steel, titanium, platinum and 90/10 CuNi*. Vol. 28. 1989, Houston, TX, ETATS-UNIS: National Association of Corrosion Engineers.

242. Motoda, S., Y. Suzuki, T. Shinohara, and S. Tsujikawa, *The effect of marine fouling on the ennoblement of electrode potential for stainless steels.* Corrosion Science, 1990. **31**: p. 515-520.

243. Mollica, A., *Biofilm and corrosion on active-passive alloys in seawater.* International Biodeterioration & Biodegradation, 1992. **29**(3): p. 213-229.

244. Zhang, H.J. and S.C. Dexter, *Effect of Biofilms on Crevice Corrosion of Stainless Steels in Coastal Seawater.* CORROSION, 1995. **51**(1): p. 56-66.

245. Debuy, S., S. Pecastaings, A. Bergel, and B. Erable, *Oxygen-reducing biocathodes designed with pure cultures of microbial strains isolated from seawater biofilms.* International Biodeterioration & Biodegradation, 2015. **103**: p. 16-22.

246. Dexter, S.C. and G.Y. Gao, *Effect of Seawater Biofilms on Corrosion Potential and Oxygen Reduction of Stainless Steel.* CORROSION, 1988. **44**(10): p. 717-723.

247. Searson, P. and J. Dawson, *Analysis of electrochemical noise generated by corroding electrodes under open-circuit conditions.* Journal of the Electrochemical Society, 1988. **135**(8): p. 1908-1915.

248. Jarragh, A., A.R. Al-Shamari, M. Islam, S. Al-Sulaiman, B. Lenka, and S. Prakash, *Evaluation of the Effectiveness of Online Corrosion Monitoring Utilizing ER/LPR Probes and Coupon within Hydrocarbon Systems*, in *CORROSION 2014*. 2014, NACE International: San Antonio, Texas, USA.

249. Nikam, V.V., H. Mackey, C. Lane, J. Wade, and K. Cloke, *Evaluation of CMAS Probe in Field Simulated MIC Conditions*, in *CORROSION 2014*. 2014, NACE International: San Antonio, Texas, USA.

250. Rajala, P., E. Huttunen-Saarivirta, M. Bomberg, and L. Carpén, *Corrosion of Stainless Steels AISI 304 and AISI 316 Induced by Sulfate Reducing Bacteria in Anoxic Groundwater*, in *CORROSION 2017*. 2017, NACE International: New Orleans, Louisiana, USA.

251. Birketveit, ø. and M. Stipanicev, *Insight in Sidestream Corrosion Field-testing from the North Sea: Experiences, Benefits and Pitfalls*, in *CORROSION 2016*. 2016, NACE International: Vancouver, British Columbia, Canada.

252. Islam, M., A.R. Al-Shamari, S. Al-Sulaiman, S. Prakash, and A. Biedermann, *Premature Failure of Access Fittings Installed on High Pressure Effluent Water Lines Due to*

Microbiologically Induced Corrosion, in *CORROSION 2016*. 2016, NACE International: Vancouver, British Columbia, Canada.

253. Okoro, C.C., O. Samuel, and J. Lin, *The effects of Tetrakis-hydroxymethyl phosphonium sulfate (THPS), nitrite and sodium chloride on methanogenesis and corrosion rates by methanogen populations of corroded pipelines.* Corrosion Science, 2016. **112**: p. 507-516.

254. Beese, P., H. Venzlaff, J. Srinivasan, J. Garrelfs, M. Stratmann, and K.J. Mayrhofer, *Monitoring of anaerobic microbially influenced corrosion via electrochemical frequency modulation.* Electrochimica Acta, 2013. **105**: p. 239-247.

255. Deng, B., Z. Wang, Y. Jiang, H. Wang, J. Gao, and J. Li, *Evaluation of localized corrosion in duplex stainless steel aged at 850 C with critical pitting temperature measurement.* Electrochimica Acta, 2009. **54**(10): p. 2790-2794.

256. Jeffers, K.E., *Electrochemical impedance spectroscopy for the characterization of corrosion and cathodic protection of buried pipelines*. 1999, Citeseer.

257. Kotu, S.P., C. Erbay, N. Sobahi, A. Han, S. Mannan, and A. Jayaraman. *Integration of electrochemical impedance spectroscopy and microfluidics for investigating microbially influenced corrosion using co-culture biofilms*. in *CORROSION 2016*. 2016. NACE International.

258. San, N.O., H. Nazır, and G. Dönmez, *Microbially influenced corrosion and inhibition of nickel–zinc and nickel–copper coatings by Pseudomonas aeruginosa.* Corrosion Science, 2014. **79**: p. 177-183.

259. Liu, H., M. Sharma, J. Wang, Y.F. Cheng, and H. Liu, *Microbiologically influenced corrosion of 316L stainless steel in the presence of Chlorella vulgaris.* International Biodeterioration & Biodegradation, 2018. **129**: p. 209-216.

260. Qu, Q., Y. He, L. Wang, H. Xu, L. Li, Y. Chen, and Z. Ding, *Corrosion behavior of cold rolled steel in artificial seawater in the presence of Bacillus subtilis C2.* Corrosion Science, 2015. **91**: p. 321-329.

261. Yousaf, M., I. Ali, M. Arif, G. Mustafa, S. Ahmad, N. Afzal, and I. Ghauri, *Effects of microbiologically influenced corrosion by Bacillus Megaterium bacteria on the mechanical properties of Al-Cu Alloy.* Materials Today: Proceedings, 2015. **2**(10): p. 5669-5673.

262. Liu, H., C. Fu, T. Gu, G. Zhang, Y. Lv, H. Wang, and H. Liu, *Corrosion behavior of carbon steel in the presence of sulfate reducing bacteria and iron oxidizing bacteria cultured in oilfield produced water.* Corrosion Science, 2015. **100**: p. 484-495.

263. Castaneda, H. and X.D. Benetton, *SRB-biofilm influence in active corrosion sites formed at the steel-electrolyte interface when exposed to artificial seawater conditions.* Corrosion Science, 2008. **50**(4): p. 1169-1183.

264. Chabowski, K., A.F. Junka, T. Piasecki, D. Nowak, K. Nitsch, D. Smutnicka, M. Bartoszewicz, M. Moczała, and P. Szymczyk, *Impedance Sensors Made in PCB and LTCC Technologies for Monitoring Growth and Degradation of Pseudomonal Biofilm.* Metrology and Measurement Systems, 2017. **24**(2): p. 369-380.

265. Zhao, Y., E. Zhou, Y. Liu, S. Liao, Z. Li, D. Xu, T. Zhang, and T. Gu, *Comparison of different electrochemical techniques for continuous monitoring of the microbiologically influenced corrosion of 2205 duplex stainless steel by marine Pseudomonas aeruginosa biofilm.* Corrosion Science, 2017. **126**: p. 142-151.

266. Obot, I. and I.B. Onyeachu, *Electrochemical frequency modulation (EFM) technique: Theory and recent practical applications in corrosion research.* Journal of Molecular Liquids, 2017.

267. Malard, E., D. Kervadec, O. Gil, Y. Lefevre, and S. Malard, *Interactions between steels and sulphide-producing bacteria—Corrosion of carbon steels and low-alloy steels in natural seawater.* Electrochimica Acta, 2008. **54**(1): p. 8-13.

268. Xu, C., Y. Zhang, G. Cheng, and W. Zhu, *Localized corrosion behavior of 316L stainless steel in the presence of sulfate-reducing and iron-oxidizing bacteria.* Materials Science and Engineering: A, 2007. **443**(1): p. 235-241.

269. Dec, W., M. Mosiałek, R.P. Socha, M. Jaworska-Kik, W. Simka, and J. Michalska, *The effect of sulphate-reducing bacteria biofilm on passivity and development of pitting on 2205 duplex stainless steel.* Electrochimica Acta, 2016. **212**: p. 225-236.

270. Xu, F.-l., J.-z. Duan, C.-g. Lin, and B.-r. Hou, *Influence of marine aerobic biofilms on corrosion of 316L stainless steel.* Journal of Iron and Steel Research, International, 2015. **22**(8): p. 715-720.

271. Batmanghelich, F., L. Li, and Y. Seo, *Influence of multispecies biofilms of Pseudomonas aeruginosa and Desulfovibrio vulgaris on the corrosion of cast iron.* Corrosion Science, 2017. **121**: p. 94-104.

272. Mudali, U.K., B. Anandkumar, and R. George. *Metal-Microbe Synergy in Pitting Corrosion of Stainless Steels*. in *NACE International Corrosion Conference Proceedings*. 2016. NACE International.

273. Whitfield, M.J., D. Bono, L. Wei, and K.J. Van Vliet, *High-throughput corrosion quantification in varied microenvironments.* Corrosion Science, 2014. **88**: p. 481-486.

274. Brossia, C.S. and L.S. Yang, *Studies of microbiologically influenced corrosion using a coupled multielectrode array sensor.* CORROSION 2003, 2003.

275. Pavanello, G., M. Faimali, M. Pittore, A. Mollica, A. Mollica, and A. Mollica, *Exploiting a new electrochemical sensor for biofilm monitoring and water treatment optimization.* Water research, 2011. **45**(4): p. 1651-1658.

276. Beltrami, L.V., M. Beltrami, M. Roesch-Ely, S.R. Kunst, F.P. Missell, E.J. Birriel, and C.d.F. Malfatti, *Magnetoelastic sensors with hybrid films for bacteria detection in milk.* Journal of Food Engineering, 2017. **212**: p. 18-28.

277. Chee, R., J. Chua, A. Agarwal, S. Wong, and G. Zhang. *Label-free detection of proteins with surface-functionalized silicon nanowires*. in *13th International Conference on Biomedical Engineering*. 2009. Springer.

278. Cui, Y., Q. Wei, H. Park, and C.M. Lieber, *Nanowire nanosensors for highly sensitive and selective detection of biological and chemical species.* Science, 2001. **293**(5533): p. 1289-1292.

279. Prasad, S., A.P. Selvam, R.K. Reddy, and A. Love, *Silicon nanosensor for diagnosis of cardiovascular proteomic markers.* Journal of laboratory automation, 2013. **18**(2): p. 143-151.

280. Lin, S.-P., C.-Y. Pan, K.-C. Tseng, M.-C. Lin, C.-D. Chen, C.-C. Tsai, S.-H. Yu, Y.-C. Sun, T.-W. Lin, and Y.-T. Chen, *A reversible surface functionalized nanowire transistor to study protein–protein interactions.* Nano Today, 2009. **4**(3): p. 235-243.

281. Stern, E., A. Vacic, and M.A. Reed, *Semiconducting nanowire field-effect transistor biomolecular sensors.* Electron Devices, IEEE Transactions on, 2008. **55**(11): p. 3119-3130.

282. Liu, J., C. Guo, C.M. Li, Y. Li, Q. Chi, X. Huang, L. Liao, and T. Yu, *Carbon-decorated ZnO nanowire array: a novel platform for direct electrochemistry of enzymes and biosensing applications.* Electrochemistry Communications, 2009. **11**(1): p. 202-205.

283. Niepelt, R., U.C. Schröder, J. Sommerfeld, I. Slowik, B. Rudolph, R. Möller, B. Seise, A. Csaki, W. Fritzsche, and C. Ronning, *Biofunctionalization of zinc oxide nanowires for DNA sensory applications.* Nanoscale research letters, 2011. **6**(1): p. 1-7.

284. Zhao, Y., X. Yan, Z. Kang, P. Lin, X. Fang, Y. Lei, S. Ma, and Y. Zhang, *Highly sensitive uric acid biosensor based on individual zinc oxide micro/nanowires.* Microchimica Acta, 2013. **180**(9-10): p. 759-766.

285. Kumar, N., A. Dorfman, and J.-i. Hahm, *Ultrasensitive DNA sequence detection using nanoscale ZnO sensor arrays.* Nanotechnology, 2006. **17**(12): p. 2875.

286. Park, H.-Y., H.-Y. Go, S. Kalme, R.S. Mane, S.-H. Han, and M.-Y. Yoon, *Protective antigen detection using horizontally stacked hexagonal ZnO platelets.* Analytical chemistry, 2009. **81**(11): p. 4280-4284.

287. Kim, J.S., W.I. Park, C.-H. Lee, and G.-C. Yi, *ZnO nanorod biosensor for highly sensitive detection of specific protein binding.* 2006.

288. Qi, P., D. Zhang, and Y. Wan, *Determination of sulfate-reducing bacteria with chemical conversion from ZnO nanorods arrays to ZnS arrays.* Sensors and Actuators B: Chemical, 2013. **181**: p. 274-279.

289. Yogeswaran, U. and S.-M. Chen, *A review on the electrochemical sensors and biosensors composed of nanowires as sensing material.* Sensors, 2008. **8**(1): p. 290-313.

290. Lei, Y., W. Chen, and A. Mulchandani, *Microbial biosensors.* Analytica Chimica Acta, 2006. **568**(1): p. 200-210.

291. Wang, J., *Electrochemical biosensors: towards point-of-care cancer diagnostics.* Biosensors and Bioelectronics, 2006. **21**(10): p. 1887-1892.

292. Kerger, B.D., P.D. Nichols, W. Sand, E. Bock, and D.C. White, *Association of acid-producing thiobacilli with degradation of concrete: analysis by 'signature'fatty acids from the polar lipids and lipopolysaccharide.* Journal of Industrial Microbiology, 1987. **2**(2): p. 63-69.

293. Smith, C.A., C.B. Phiefer, S.J. Macnaughton, A. Peacock, R.S. Burkhalter, R. Kirkegaard, and D.C. White, *Quantitative lipid biomarker detection of unculturable microbes and chlorine exposure in water distribution system biofilms.* Water Research, 2000. **34**(10): p. 2683-2688.

294. White, D.C., J.S. Gouffon, A.D. Peacock, R. Geyer, A. Biernacki, G.A. Davis, M. Pryor, M.B. Tabacco, and K.L. Sublette, *Forensic analysis by comprehensive rapid detection of pathogens and contamination concentrated in biofilms in drinking water systems for water resource protection and management.* Environmental Forensics, 2003. **4**(1): p. 63-74.

295. Pang, X. *An Amperometric Sensor for Sulfide Detection Based on Carbon Nanotubes*. in *CORROSION 2016*. 2016. NACE International.

296. Taitt, C.R., G.P. Anderson, B.M. Lingerfelt, M.J. Feldstein, and F.S. Ligler, *Nine-analyte detection using an array-based biosensor.* Analytical chemistry, 2002. **74**(23): p. 6114-6120.

297. Munktell, S., M. Tydén, J. Högström, L. Nyholm, and F. Björefors, *Bipolar electrochemistry for high-throughput corrosion screening.* Electrochemistry communications, 2013. **34**: p. 274-277.

298. Bang, B.M., H. Kim, J.-P. Lee, J. Cho, and S. Park, *Mass production of uniform-sized nanoporous silicon nanowire anodes via block copolymer lithography.* Energy & Environmental Science, 2011. **4**(9): p. 3395-3399.

299. Brockway, L., M. Van Laer, Y. Kang, and S. Vaddiraju, *Large-scale synthesis and in situ functionalization of Zn 3 P 2 and Zn 4 Sb 3 nanowire powders.* Physical Chemistry Chemical Physics, 2013. **15**(17): p. 6260-6267.

300. Holmes, J.D., K.P. Johnston, R.C. Doty, and B.A. Korgel, *Control of thickness and orientation of solution-grown silicon nanowires.* Science, 2000. **287**(5457): p. 1471.

301. Kumar, V., J.H. Kim, C. Pendyala, B. Chernomordik, and M.K. Sunkara, *Gas-phase, bulk production of metal oxide nanowires and nanoparticles using a microwave plasma jet reactor.* The Journal of Physical Chemistry C, 2008. **112**(46): p. 17750-17754.

302. Vasiraju, V., Y. Kang, and S. Vaddiraju, *Non-conformal decoration of semiconductor nanowire surfaces with boron nitride (BN) molecules for stability enhancement: degradation-resistant Zn 3 P 2, ZnO and Mg 2 Si nanowires.* Physical Chemistry Chemical Physics, 2014. **16**(30): p. 16150-16157.

303. Hoxha, G., C. Di Iorio, and F. De Ferra. *Microbial Corrosion. New Investigation Techniques*. in *Abu Dhabi International Petroleum Exhibition and Conference*. 2014. Society of Petroleum Engineers.

304. Ramgir, N.S., Y. Yang, and M. Zacharias, *Nanowire-Based Sensors.* Small, 2010. **6**(16): p. 1705-1722.

305. Liu, A., *Towards development of chemosensors and biosensors with metal-oxide-based nanowires or nanotubes.* Biosensors and Bioelectronics, 2008. **24**(2): p. 167-177.

306. Hochbaum, A.I., R. Chen, R.D. Delgado, W. Liang, E.C. Garnett, M. Najarian, A. Majumdar, and P. Yang, *Enhanced thermoelectric performance of rough silicon nanowires.* Nature, 2008. **451**(7175): p. 163.

307. Shi, Y., W. Yang, X. Feng, L. Feng, G. Yue, and Y. Wang, *Bio-inspired fabrication of copper oxide nanowire films with switchable wettability via a facile thermal oxidation method.* RSC Advances, 2015. **5**(33): p. 26107-26113.

308. Akhavan, O. and E. Ghaderi, *Copper oxide nanoflakes as highly sensitive and fast response self-sterilizing biosensors.* Journal of Materials Chemistry, 2011. **21**(34): p. 12935-12940.

309. Husain, E., T.N. Narayanan, J.J. Taha-Tijerina, S. Vinod, R. Vajtai, and P.M. Ajayan, *Marine corrosion protective coatings of hexagonal boron nitride thin films on stainless steel.* ACS applied materials & interfaces, 2013. **5**(10): p. 4129-4135.

310. Behzadnasab, M., S. Mirabedini, K. Kabiri, and S. Jamali, *Corrosion performance of epoxy coatings containing silane treated ZrO2 nanoparticles on mild steel in 3.5% NaCl solution.* Corrosion Science, 2011. **53**(1): p. 89-98.

311. Cui, Z., S. Wu, S. Zhu, and X. Yang, *Study on corrosion properties of pipelines in simulated produced water saturated with supercritical CO2.* Applied Surface Science, 2006. **252**(6): p. 2368-2374.

312. Vogiatzis, C., D. Kountouras, and S. Skolianos, *Corrosion behaviour of 304 stainless steel in simulated oilfield produced water.* Corrosion Engineering, Science and Technology, 2016. **51**(1): p. 51-59.

313. Ishizaki, T., Y. Masuda, and M. Sakamoto, *Corrosion resistance and durability of superhydrophobic surface formed on magnesium alloy coated with nanostructured cerium oxide film and fluoroalkylsilane molecules in corrosive NaCl aqueous solution.* Langmuir, 2011. **27**(8): p. 4780-4788.

314. Zhang, X., Z.H. Jiang, Z.P. Yao, Y. Song, and Z.D. Wu, *Effects of scan rate on the potentiodynamic polarization curve obtained to determine the Tafel slopes and corrosion current density.* Corrosion Science, 2009. **51**(3): p. 581-587.

315. Gao, Y., S. Chen, D. Cao, G. Wang, and J. Yin, *Electrochemical capacitance of Co3O4 nanowire arrays supported on nickel foam.* Journal of Power Sources, 2010. **195**(6): p. 1757-1760.

316. de Beer, C., P.S. Barendse, P. Pillay, B. Bullecks, and R. Rengaswamy, *Classification of high-temperature PEM fuel cell degradation mechanisms using equivalent circuits.* IEEE Transactions on Industrial Electronics, 2015. **62**(8): p. 5265-5274.

317. Palapati, N.K., M.R.A. Shikder, B.W. Byles, E. Pomerantseva, and A. Subramanian. *Electrochemically-correlated measurement of electronic transport in battery nanoelectrodes using single nanowire devices*. in *Nano/Micro Engineered and Molecular Systems (NEMS), 2017 IEEE 12th International Conference on*. 2017. IEEE.

318. Rogers, J.A., Q. Cao, M. Alam, and N. Pimparkar, *Medium scale carbon nanotube thin film integrated circuits on flexible plastic substrates*. 2015, Google Patents.

319. Li, G., Y. Wang, and Q. Tao, *Modeling and Simulation of Silicon Nanowire–Based Biosensors.* Modeling and Control for Micro/Nano Devices and Systems, 2017: p. 22.

320. Ray, P.C., *Size and Shape Dependent Second Order Nonlinear Optical Properties of Nanomaterials and Their Application in Biological and Chemical Sensing.* Chemical Reviews, 2010. **110**(9): p. 5332-5365.

321. Ali, A., Y. Chen, V. Vasiraju, and S. Vaddiraju, *Nanowire-based thermoelectrics.* Nanotechnology, 2017. **28**(28): p. 282001.

322. Yoon, H. and J. Jang, *Conducting-polymer nanomaterials for high-performance sensor applications: issues and challenges.* Advanced Functional Materials, 2009. **19**(10): p. 1567-1576.

323. Chen, X., C.K. Wong, C.A. Yuan, and G. Zhang, *Nanowire-based gas sensors.* Sensors and Actuators B: Chemical, 2013. **177**: p. 178-195.

324. Cui, Y. and C.M. Lieber, *Functional nanoscale electronic devices assembled using silicon nanowire building blocks.* Science, 2001. **291**(5505): p. 851-853.

325. Goldberger, J., A.I. Hochbaum, R. Fan, and P. Yang, *Silicon vertically integrated nanowire field effect transistors.* Nano letters, 2006. **6**(5): p. 973-977.

326. Black, C., *Self-aligned self assembly of multi-nanowire silicon field effect transistors.* Applied Physics Letters, 2005. **87**(16): p. 163116.

327. Yuhas, B.D. and P. Yang, *Nanowire-based all-oxide solar cells.* Journal of the American Chemical Society, 2009. **131**(10): p. 3756-3761.

328. Gudiksen, M.S., L.J. Lauhon, J. Wang, D.C. Smith, and C.M. Lieber, *Growth of nanowire superlattice structures for nanoscale photonics and electronics.* Nature, 2002. **415**(6872): p. 617-620.

329. Zhou, Z., C. Zhan, Y. Wang, Y. Su, Z. Yang, and Y. Zhang, *Rapid mass production of ZnO nanowires by a modified carbothermal reduction method.* Materials Letters, 2011. **65**(5): p. 832-835.

330. Ying, J.Y., Z. Zhang, L. Zhang, and M.S. Dresselhaus, *Nanowire arrays*. 2002, Google Patents.

331. Brockway, L., V. Vasiraju, H. Asayesh-Ardakani, R. Shahbazian-Yassar, and S. Vaddiraju, *Thermoelectric properties of large-scale Zn3 P2 nanowire assemblies.* Nanotechnology, 2014. **25**(14): p. 145401.

332. Peng, K.-Q., X. Wang, L. Li, Y. Hu, and S.-T. Lee, *Silicon nanowires for advanced energy conversion and storage.* Nano Today, 2013. **8**(1): p. 75-97.

333. Nair, P.R. and M.A. Alam, *Design considerations of silicon nanowire biosensors.* IEEE Transactions on Electron Devices, 2007. **54**(12): p. 3400-3408.

334. Kaur, M., K. Muthe, S. Despande, S. Choudhury, J. Singh, N. Verma, S. Gupta, and J. Yakhmi, *Growth and branching of CuO nanowires by thermal oxidation of copper.* Journal of Crystal Growth, 2006. **289**(2): p. 670-675.

335. Jiang, X., T. Herricks, and Y. Xia, *CuO nanowires can be synthesized by heating copper substrates in air.* Nano Letters, 2002. **2**(12): p. 1333-1338.

336. Chen, J., F. Zhang, J. Wang, G. Zhang, B. Miao, X. Fan, D. Yan, and P. Yan, *CuO nanowires synthesized by thermal oxidation route.* Journal of Alloys and Compounds, 2008. **454**(1): p. 268-273.

337. Yuan, L. and G. Zhou, *Enhanced CuO nanowire formation by thermal oxidation of roughened copper.* Journal of The Electrochemical Society, 2012. **159**(4): p. C205-C209.

338. Gonçalves, A., L. Campos, A. Ferlauto, and R. Lacerda, *On the growth and electrical characterization of CuO nanowires by thermal oxidation.* Journal of applied physics, 2009. **106**(3): p. 034303.

339. Mema, R., L. Yuan, Q. Du, Y. Wang, and G. Zhou, *Effect of surface stresses on CuO nanowire growth in the thermal oxidation of copper.* Chemical Physics Letters, 2011. **512**(1): p. 87-91.

340. Xu, C., C. Woo, and S. Shi, *The effects of oxidative environments on the synthesis of CuO nanowires on Cu substrates.* Superlattices and Microstructures, 2004. **36**(1): p. 31-38.

341. Zhang, K., C. Rossi, C. Tenailleau, P. Alphonse, and J.-Y. Chane-Ching, *Synthesis of large-area and aligned copper oxide nanowires from copper thin film on silicon substrate.* Nanotechnology, 2007. **18**(27): p. 275607.

342. Liao, L., Z. Zhang, B. Yan, Z. Zheng, Q. Bao, T. Wu, C. Li, Z. Shen, J. Zhang, and H. Gong, *Multifunctional CuO nanowire devices: p-type field effect transistors and CO gas sensors*. Nanotechnology, 2009. **20**(8): p. 085203.

343. Kang, Y. and S. Vaddiraju, *Solid-state phase transformation as a route for the simultaneous synthesis and welding of single-crystalline Mg2Si nanowires.* Chemistry of Materials, 2014. **26**(9): p. 2814-2819.

344. Ozdemir, B., M. Kulakci, R. Turan, and H.E. Unalan, *Effect of electroless etching parameters on the growth and reflection properties of silicon nanowires.* Nanotechnology, 2011. **22**(15): p. 155606.

345. Piscanec, S., M. Cantoro, A. Ferrari, J. Zapien, Y. Lifshitz, S. Lee, S. Hofmann, and J. Robertson, *Raman spectroscopy of silicon nanowires.* Physical Review B, 2003. **68**(24): p. 241312.

346. Yu, T., X. Zhao, Z.X. Shen, Y.H. Wu, and W.H. Su, *Investigation of individual CuO nanorods by polarized micro-Raman scattering.* Journal of Crystal Growth, 2004. **268**(3–4): p. 590-595.

347. Hoa, N.D., N. Van Quy, H. Jung, D. Kim, H. Kim, and S.-K. Hong, *Synthesis of porous CuO nanowires and its application to hydrogen detection.* Sensors and Actuators B: Chemical, 2010. **146**(1): p. 266-272.

348. Filipič, G. and U. Cvelbar, *Copper oxide nanowires: a review of growth.* Nanotechnology, 2012. **23**(19): p. 194001.

349. Song, L., L. Ci, H. Lu, P.B. Sorokin, C. Jin, J. Ni, A.G. Kvashnin, D.G. Kvashnin, J. Lou, and B.I. Yakobson, *Large scale growth and characterization of atomic hexagonal boron nitride layers.* Nano letters, 2010. **10**(8): p. 3209-3215.

350. Nešić, S., *Key issues related to modelling of internal corrosion of oil and gas pipelines–A review*. Corrosion science, 2007. **49**(12): p. 4308-4338.

351. Yersak, A.S., R.J. Lewis, L.-A. Liew, R. Wen, R. Yang, and Y.-C. Lee, *Atomic Layer Deposited Coatings on Nanowires for High Temperature Water Corrosion Protection.* ACS applied materials & interfaces, 2016. **8**(47): p. 32616-32623.

352. Zhou, Y., B. Zhang, S. Zheng, J. Wang, X. San, and X. Ma, *Atomic-scale decoration for improving the pitting corrosion resistance of austenitic stainless steels.* Scientific reports, 2014. **4**: p. 3604.

353. Chen, Y.W., J.D. Prange, S. Dühnen, Y. Park, M. Gunji, C.E. Chidsey, and P.C. McIntyre, *Atomic layer-deposited tunnel oxide stabilizes silicon photoanodes for water oxidation.* Nature materials, 2011. **10**(7): p. 539.

354. Alper, J.P., M. Vincent, C. Carraro, and R. Maboudian, *Silicon carbide coated silicon nanowires as robust electrode material for aqueous micro-supercapacitor*. Applied Physics Letters, 2012. **100**(16): p. 163901.

355. Icenhower, J.P. and P.M. Dove, *The dissolution kinetics of amorphous silica into sodium chloride solutions: effects of temperature and ionic strength.* Geochimica et Cosmochimica Acta, 2000. **64**(24): p. 4193-4203.

356. Rimstidt, J.D. and H. Barnes, *The kinetics of silica-water reactions.* Geochimica et Cosmochimica Acta, 1980. **44**(11): p. 1683-1699.

357. Li, H., S. Yu, and X. Han, *Fabrication of CuO hierarchical flower-like structures with biomimetic superamphiphobic, self-cleaning and corrosion resistance properties.* Chemical Engineering Journal, 2016. **283**: p. 1443-1454.

358. Ambat, R., N.N. Aung, and W. Zhou, *Evaluation of microstructural effects on corrosion behaviour of AZ91D magnesium alloy.* Corrosion science, 2000. **42**(8): p. 1433-1455.

359. Redondo, M. and C.B. Breslin, *Polypyrrole electrodeposited on copper from an aqueous phosphate solution: Corrosion protection properties.* Corrosion science, 2007. **49**(4): p. 1765-1776.

360. Pyun, C.H. and S.M. Park, *In situ spectroelectrochemical studies on anodic oxidation of copper in alkaline solution.* Journal of The Electrochemical Society, 1986. **133**(10): p. 2024-2030.

361. Heakal, F.E.-T. and S. Haruyama, *Impedance studies of the inhibitive effect of benzotriazole on the corrosion of copper in sodium chloride medium.* Corrosion science, 1980. **20**(7): p. 887-898.

362. Bunker, B., *Molecular mechanisms for corrosion of silica and silicate glasses.* Journal of Non-Crystalline Solids, 1994. **179**: p. 300-308.

363. Datta, N., N.S. Ramgir, S. Kumar, P. Veerender, M. Kaur, S. Kailasaganapathi, A. Debnath, D. Aswal, and S. Gupta, *Role of various interfaces of CuO/ZnO random nanowire networks in H 2 S sensing: An impedance and Kelvin probe analysis.* Sensors and Actuators B: Chemical, 2014. **202**: p. 1270-1280.

364. Ruffo, R., S.S. Hong, C.K. Chan, R.A. Huggins, and Y. Cui, *Impedance analysis of silicon nanowire lithium ion battery anodes.* The Journal of Physical Chemistry C, 2009. **113**(26): p. 11390-11398.

365. Xu, L., Q. Yang, X. Liu, J. Liu, and X. Sun, *One-dimensional copper oxide nanotube arrays: biosensors for glucose detection.* RSC Advances, 2014. **4**(3): p. 1449-1455.

366. Williams, E.H., J.A. Schreifels, M.V. Rao, A.V. Davydov, V.P. Oleshko, N.J. Lin, K.L. Steffens, S. Krylyuk, K.A. Bertness, and A.K. Manocchi, *Selective streptavidin bioconjugation on silicon and silicon carbide nanowires for biosensor applications.* Journal of Materials Research, 2013. **28**(01): p. 68-77.

367. Dawood, M., L. Zhou, H. Zheng, H. Cheng, G. Wan, R. Rajagopalan, H. Too, and W. Choi, *Nanostructured Si-nanowire microarrays for enhanced-performance bio-analytics.* Lab on a Chip, 2012. **12**(23): p. 5016-5024.

368. Baumgartner, S., M. Vasicek, A. Bulyha, and C. Heitzinger, *Optimization of nanowire DNA sensor sensitivity using self-consistent simulation.* Nanotechnology, 2011. **22**(42): p. 425503.

369. Stern, E., R. Wagner, F.J. Sigworth, R. Breaker, T.M. Fahmy, and M.A. Reed, *Importance of the Debye screening length on nanowire field effect transistor sensors.* Nano letters, 2007. **7**(11): p. 3405-3409.

370. Khan, S.B., M. Faisal, M.M. Rahman, I. Abdel-Latif, A.A. Ismail, K. Akhtar, A. Al-Hajry, A.M. Asiri, and K.A. Alamry, *Highly sensitive and stable phenyl hydrazine chemical sensors based on CuO flower shapes and hollow spheres.* New Journal of Chemistry, 2013. **37**(4): p. 1098-1104.

371. Bunimovich, Y.L., G. Ge, K.C. Beverly, R.S. Ries, L. Hood, and J.R. Heath, *Electrochemically programmed, spatially selective biofunctionalization of silicon wires.* Langmuir, 2004. **20**(24): p. 10630-10638.

372. Bayer, E.A., H. Ben-Hur, Y. Hiller, and M. Wilchek, *Postsecretory modifications of streptavidin.* Biochemical Journal, 1989. **259**(2): p. 369-376.

373. Weber, P.C., D. Ohlendorf, J. Wendoloski, and F. Salemme, *Structural origins of high-affinity biotin binding to streptavidin.* Science, 1989. **243**(4887): p. 85-88.

374. Skovhus, T., H.-E. Berge, R. Bruce Eckert, and G. Koch, *Introducing a Corrosion Management Approach to MIC Assessment, Control and Monitoring in the Oil and Gas Industry*. 2014.

375. Eckert, R.B., T.L. Skovhus, and B. Graver. *Corrosion management of MIC contributes to pipeline integrity*. in *CORROSION 2015*. 2015. NACE International.

376. Eckert, R.B. and T.L. Skovhus, *Advances in the application of molecular microbiological methods in the oil and gas industry and links to microbiologically influenced corrosion.* International Biodeterioration & Biodegradation, 2018. **126**: p. 169-176.

377. Zhu, X. and J. Kilbane. *Faster and more accurate data collection for microbiologically influenced corrosion*. in *SPE International Symposium on Oilfield Chemistry*. 2005. Society of Petroleum Engineers.

378. Wade, S., M. Javed, E. Palombo, S. McArthur, and P. Stoddart, *On the need for more realistic experimental conditions in laboratory-based microbiologically influenced corrosion testing.* International Biodeterioration & Biodegradation, 2017. **121**: p. 97-106.

379. Lafleur, J.P., A. Jönsson, S. Senkbeil, and J.P. Kutter, *Recent advances in lab-on-a-chip for biosensing applications.* Biosensors and Bioelectronics, 2016. **76**: p. 213-233.

380. Mohammed, M.I., S. Haswell, and I. Gibson, *Lab-on-a-chip or Chip-in-a-lab: Challenges of Commercialization Lost in Translation.* Procedia Technology, 2015. **20**: p. 54-59.

381. Liu, F., A. Nordin, F. Li, and I. Voiculescu, *A lab-on-chip cell-based biosensor for label-free sensing of water toxicants.* Lab on a Chip, 2014. **14**(7): p. 1270-1280.

382. Romao, V.C., S.A. Martins, J. Germano, F.A. Cardoso, S. Cardoso, and P.P. Freitas, *Lab-on-Chip Devices: Gaining Ground Losing Size.* ACS nano, 2017. **11**(11): p. 10659-10664.

383. Yasri, M., B. Lescop, F. Gallée, E. Diler, D. Thierry, and S. Rioual. *Microwave characterization of materials during corrosion: Application to wireless sensors*. in *Microwave Conference (EuMC), 2015 European*. 2015. IEEE.

384. Skovhus, T.L., E.S. Andersen, and E. Hillier, *Management of Microbiologically Influenced Corrosion in Risk-Based Inspection Analysis.* SPE Production & Operations, 2017.

385. Singh, M. and M. Pokhrel, *A Fuzzy logic-possibilistic methodology for risk-based inspection (RBI) planning of oil and gas piping subjected to microbiologically influenced corrosion (MIC).* International Journal of Pressure Vessels and Piping, 2018. **159**: p. 45-54.

386. Qu, H., A.T. Csordas, J. Wang, S.S. Oh, M.S. Eisenstein, and H.T. Soh, *Rapid and label-free strategy to isolate aptamers for metal ions.* ACS nano, 2016. **10**(8): p. 7558-7565.

387. Gotrik, M., G. Sekhon, S. Saurabh, M. Nakamoto, M. Eisenstein, and H.T. Soh, *Direct Selection of Fluorescence-Enhancing RNA Aptamers.* Journal of the American Chemical Society, 2018. **140**(10): p. 3583-3591.

388. Lomans, B.P., R. de Paula, B. Geissler, C.A. Kuijvenhoven, and N. Tsesmetzis. *Proposal of Improved Biomonitoring Standard for Purpose of Microbiologically Influenced Corrosion Risk Assessment*. in *SPE International Oilfield Corrosion Conference and Exhibition*. 2016. Society of Petroleum Engineers.

389. Zhu, C., G. Yang, H. Li, D. Du, and Y. Lin, *Electrochemical sensors and biosensors based on nanomaterials and nanostructures.* Analytical chemistry, 2014. **87**(1): p. 230-249.

390. Govindhan, M., B.-R. Adhikari, and A. Chen, *Nanomaterials-based electrochemical detection of chemical contaminants.* RSC Advances, 2014. **4**(109): p. 63741-63760.

391. Gong, S., W. Schwalb, Y. Wang, Y. Chen, Y. Tang, J. Si, B. Shirinzadeh, and W. Cheng, *A wearable and highly sensitive pressure sensor with ultrathin gold nanowires.* Nature communications, 2014. **5**: p. 3132.

392. Hsu, C.-L., J.-Y. Tsai, and T.-J. Hsueh, *Ethanol gas and humidity sensors of CuO/Cu2O composite nanowires based on a Cu through-silicon via approach.* Sensors and Actuators B: Chemical, 2016. **224**: p. 95-102.

393. Gao, N., W. Zhou, X. Jiang, G. Hong, T.-M. Fu, and C.M. Lieber, *General strategy for biodetection in high ionic strength solutions using transistor-based nanoelectronic sensors.* Nano letters, 2015. **15**(3): p. 2143-2148.

394. Jensen, M.L., T. Lundgaard, J. Jensen, and T.L. Skovhus. *Improving Risk Based Inspection with Molecular Microbiological Methods*. in *CORROSION 2013*. 2013. Orlando, Florida, USA: NACE International.

395. Skovhus, T.L., R.B. Eckert, and E. Rodrigues, *Management and control of microbiologically influenced corrosion (MIC) in the oil and gas industry—Overview and a North Sea case study.* Journal of biotechnology, 2017. **256**: p. 31-45.

396. Flitton, M.A., R. Mizia, and C. Bishop, *Underground Corrosion of Activated Metals in an Arid Vadose Zone Environment.* 2002., 2002.

397. Li, S.Y., Y.G. Kim, Y.T. Kho, and T. Kang. *Corrosion Behavior of Carbon Steel Influenced by Sulfate Reducing Bacteria in Soil Environments*. in *CORROSION 2003*. 2003. San Diego, California, USA: NACE International.

398. Machuca, L.L., S.I. Bailey, R. Gubner, E.L. Watkin, M.P. Ginige, A.H. Kaksonen, and K. Heidersbach, *Effect of oxygen and biofilms on crevice corrosion of UNS S31803 and UNS N08825 in natural seawater.* Corrosion Science, 2013. **67**: p. 242-255.

399. Zhao, K., T. Gu, I. Cruz, and A. Kopliku. *Laboratory investigation of MIC in hydrotesting using seawater*. in *CORROSION 2010*. 2010. San Antonio, Texas, USA.

400. Hamdy, A.S., E. El-Shenawy, and T. El-Bitar, *Electrochemical impedance spectroscopy study of the corrosion behavior of some niobium bearing stainless steels in 3.5% NaCl.* International Journal of Electrochemical Science, 2006. **1**(4): p. 171-80.

401. Walker, J., K. Hanson, D. Caldwell, and C. Keevil, *Scanning confocal laser microscopy study of biofilm induced corrosion on copper plumbing tubes.* 1998.

402. Słomczyński, T. and M. Łebkowska, *Role of micro-organisms present in diesel fuel in the microbiological corrosion of carbon steel St3S.* Desalination and Water Treatment, 2015: p. 1-11.

403. Nan, L., D. Xu, T. Gu, X. Song, and K. Yang, *Microbiological influenced corrosion resistance characteristics of a 304L-Cu stainless steel against Escherichia coli.* Materials Science and Engineering: C, 2015. **48**: p. 228-234.

404. Rajasekar, A. and Y.-P. Ting, *Microbial corrosion of aluminum 2024 aeronautical alloy by hydrocarbon degrading bacteria Bacillus cereus ACE4 and Serratia marcescens ACE2.* Industrial & Engineering Chemistry Research, 2010. **49**(13): p. 6054-6061.

405. Javed, M., P. Stoddart, S. McArthur, and S. Wade, *The effect of metal microstructure on the initial attachment of Escherichia coli to 1010 carbon steel.* Biofouling, 2013. **29**(8): p. 939-952.

406. Liu, H., D. Xu, A.Q. Dao, G. Zhang, Y. Lv, and H. Liu, *Study of corrosion behavior and mechanism of carbon steel in the presence of Chlorella vulgaris.* Corrosion Science, 2015. **101**: p. 84-93.

407. Machuca, L.L., S.I. Bailey, R. Gubner, E.L. Watkin, M.P. Ginige, and A.H. Kaksonen. *Crevice corrosion of duplex stainless steels in the presence of natural marine biofilms*. in *CORROSION 2012*. 2012. Salt Lake City, Utah, USA: NACE International.

408. Witt, D., K.-T. Ma, T. Lee, C. Gaylarde, S. Celikkol, Z. Makama, and I. Beech. *Field Studies of Microbiologically Influenced Corrosion of Mooring Chains*. in *Offshore Technology Conference*. 2016. Offshore Technology Conference.

409. Aktas, D.F., J.S. Lee, B.J. Little, R.I. Ray, I.A. Davidova, C.N. Lyles, and J.M. Suflita, *Anaerobic metabolism of biodiesel and its impact on metal corrosion.* Energy & Fuels, 2010. **24**(5): p. 2924-2928.

410. Güngör, N.D., A. Çotuk, and D. Dışpınar, *The Effect of Desulfovibrio sp. Biofilms on Corrosion Behavior of Copper in Sulfide-Containing Solutions.* Journal of Materials Engineering and Performance, 2015. **24**(3): p. 1357-1364.

411. San, N.O., H. Nazır, and G. Dönmez, *Evaluation of microbiologically influenced corrosion inhibition on Ni–Co alloy coatings by Aeromonas salmonicida and Clavibacter michiganensis.* Corrosion Science, 2012. **65**: p. 113-118.

412. Huttunen-Saarivirta, E., M. Honkanen, T. Lepistö, V.-T. Kuokkala, L. Koivisto, and C.-G. Berg, *Microbiologically influenced corrosion (MIC) in stainless steel heat exchanger.* Applied Surface Science, 2012. **258**(17): p. 6512-6526.

413. Reyes, A., M. Letelier, R. De la Iglesia, B. González, and G. Lagos, *Microbiologically induced corrosion of copper pipes in low-pH water*. International Biodeterioration & Biodegradation, 2008. **61**(2): p. 135-141.

414. Kuang, F., J. Wang, L. Yan, and D. Zhang, *Effects of sulfate-reducing bacteria on the corrosion behavior of carbon steel.* Electrochimica Acta, 2007. **52**(20): p. 6084-6088.

415. Starosvetsky, D., R. Armon, J. Yahalom, and J. Starosvetsky, *Pitting corrosion of carbon steel caused by iron bacteria.* International biodeterioration & biodegradation, 2001. **47**(2): p. 79-87.

416. Xu, L.C., H.H. Fang, and K.Y. Chan, *Atomic force microscopy study of microbiologically influenced corrosion of mild steel.* Journal of the Electrochemical Society, 1999. **146**(12): p. 4455-4460.

417. McNeil, M., J. Jones, and B. Little, *Production of sulfide minerals by sulfate-reducing bacteria during microbiologically influenced corrosion of copper.* Corrosion, 1991. **47**(9): p. 674-677.

418. El Hajj, H., A. Abdelouas, B. Grambow, C. Martin, and M. Dion, *Microbial corrosion of P235GH steel under geological conditions.* Physics and Chemistry of the Earth, Parts A/B/C, 2010. **35**(6): p. 248-253.

419. Nivens, D., P. Nichols, J. Henson, G. Geesey, and D. White, *Reversible acceleration of the corrosion of AISI 304 stainless steel exposed to seawater induced by growth and secretions of the marine bacterium Vibrio natriegens.* Corrosion, 1986. **42**(4): p. 204-210.

420. Franklin, M., D. Nivens, A. Vass, M. Mittelman, R. Jack, N. Dowling, and D. White, *Effect of chlorine and chlorine/bromine biocide treatments on the number and activity of biofilm bacteria and on carbon steel corrosion.* Corrosion, 1991. **47**(2): p. 128-134.

421. Bhosle, N. and A. Wagh, *The effect of organic matter associated with the corrosion products on the corrosion of mild steel in the Arabian Sea.* Corrosion science, 1992. **33**(5): p. 647-655.

422. Carpen, L., L. Raaska, K. Mattila, M. Salkinoja-Salonen, and T. Hakkarainen, *Electrochemical and microbiological characterization of biofilm formation on stainless steels in Baltic seawater*. 1997, NACE International, Houston, TX (United States).

423. Vester, F. and K. Ingvorsen, *Improved most-probable-number method to detect sulfate-reducing bacteria with natural media and a radiotracer.* Applied and environmental microbiology, 1998. **64**(5): p. 1700-1707.

424. Kumar, A.R., R. Singh, and R. Nigam, *Mössbauer spectroscopy of corrosion products of mild steel due to microbiologically influenced corrosion.* Journal of Radioanalytical and Nuclear Chemistry, 1999. **242**(1): p. 131-137.

425. Ibars, J., J. Polo, D. Moreno, C. Ranninger, and J. Bastidas, *An impedance study on admiralty brass dezincification originated by microbiologically influenced corrosion.* Biotechnology and bioengineering, 2004. **87**(7): p. 855-862.

426. Gayosso, M.H., G.Z. Olivares, N.R. Ordaz, C.J. Ramirez, R.G. Esquivel, and A.P. Viveros, *Microbial consortium influence upon steel corrosion rate, using polarisation resistance and electrochemical noise techniques.* Electrochimica acta, 2004. **49**(25): p. 4295-4301.

427. Ilhan-Sungur, E., N. Cansever, and A. Cotuk, *Microbial corrosion of galvanized steel by a freshwater strain of sulphate reducing bacteria (Desulfovibrio sp.).* Corrosion Science, 2007. **49**(3): p. 1097-1109.

428. Rajasekar, A., T.G. Babu, S.K. Pandian, S. Maruthamuthu, N. Palaniswamy, and A. Rajendran, *Biodegradation and corrosion behavior of manganese oxidizer Bacillus cereus ACE4 in diesel transporting pipeline.* Corrosion Science, 2007. **49**(6): p. 2694-2710.

429. Javaherdashti, R., R.S. Raman, C. Panter, and E. Pereloma, *Microbiologically assisted stress corrosion cracking of carbon steel in mixed and pure cultures of sulfate reducing bacteria.* International biodeterioration & biodegradation, 2006. **58**(1): p. 27-35.

430. Rajasekar, A., T.G. Babu, S.T.K. Pandian, S. Maruthamuthu, N. Palaniswamy, and A. Rajendran, *Role of Serratia marcescens ACE2 on diesel degradation and its influence on corrosion.* Journal of industrial microbiology & biotechnology, 2007. **34**(9): p. 589-598.

431. Beech, I.B. and S.A. Campbell, *Accelerated low water corrosion of carbon steel in the presence of a biofilm harbouring sulphate-reducing and sulphur-oxidising bacteria recovered from a marine sediment.* Electrochimica acta, 2008. **54**(1): p. 14-21.

432. Doğruöz, N., D. Göksay, E. Ilhan-Sungur, and A. Cotuk, *Pioneer colonizer microorganisms in biofilm formation on galvanized steel in a simulated recirculating cooling-water system.* Journal of basic microbiology, 2009. **49**(S1).

433. Sherar, B., I. Power, P. Keech, S. Mitlin, G. Southam, and D. Shoesmith, *Characterizing the effect of carbon steel exposure in sulfide containing solutions to microbially induced corrosion.* Corrosion Science, 2011. **53**(3): p. 955-960.

434. San, N.O., H. Nazır, and G. Dönmez, *Microbial corrosion of Ni–Cu alloys by Aeromonas eucrenophila bacterium.* Corrosion Science, 2011. **53**(6): p. 2216-2221.

435. De Turris, A., M. de Romero, T.G. Haile, S. Papavinasam, and W.D. Gould. *Correlation Between The Growth Of A Mixed Culture Of Sulphate-Reducing Bacteria Isolated From Produced Water And The Corrosion Of Carbon Steel*. in *CORROSION 2012*. 2012. Salt Lake City, Utah, USA: NACE International.

436. El Hajj, H., A. Abdelouas, Y. El Mendili, G. Karakurt, B. Grambow, and C. Martin, *Corrosion of carbon steel under sequential aerobic–anaerobic environmental conditions.* Corrosion Science, 2013. **76**: p. 432-440.

437. Chen, Y., X. He, R. Howdyshell, S. Howdyshell, B. Newby, G. Cheng, H. Castaneda, J. Senko, and L. Ju. *Severe pitting corrosion caused by a starving sulfate-reducing bacterium surviving on carbon steel and effect of surface roughness*. in *CORROSION 2013*. 2013. NACE International.

438. Xu, D. and T. Gu, *Carbon source starvation triggered more aggressive corrosion against carbon steel by the Desulfovibrio vulgaris biofilm.* International Biodeterioration & Biodegradation, 2014. **91**: p. 74-81.

439. Beech, I.B., C.S. Cheung, D.B. Johnson, and J.R. Smith, *Comparative studies of bacterial biofilms on steel surfaces using atomic force microscopy and environmental scanning electron microscopy.* Biofouling, 1996. **10**(1-3): p. 65-77.

440. Stipanicev, M., F. Turcu, L. Esnault, O. Rosas, R. Basseguy, M. Sztyler, and I.B. Beech, *Corrosion of carbon steel by bacteria from North Sea offshore seawater injection systems: laboratory investigation.* Bioelectrochemistry, 2014. **97**: p. 76-88.

441. Cote, C., O. Rosas, M. Sztyler, J. Doma, I. Beech, and R. Basseguy, *Corrosion of low carbon steel by microorganisms from the 'pigging'operation debris in water injection pipelines.* Bioelectrochemistry, 2014. **97**: p. 97-109.

442. Lee, J.S., R.I. Ray, and B.J. Little, *Corrosion-related consequences of biodiesel in contact with natural seawater*. 2010, DTIC Document.

443. Davidova, I.A., K.E. Duncan, B.M. Perez-Ibarra, and J.M. Suflita, *Involvement of thermophilic archaea in the biocorrosion of oil pipelines.* Environmental microbiology, 2012. **14**(7): p. 1762-1771.

444. Bento, F.M., I.B. Beech, C.C. Gaylarde, G.E. Englert, and I.L. Muller, *Degradation and corrosive activities of fungi in a diesel–mild steel–aqueous system.* World Journal of Microbiology and Biotechnology, 2005. **21**(2): p. 135-142.

445. de Romero, M.F., L. Ocando, A. De Turris, L.-P. INCORS, and L.L. Machuca. *Evaluation of Non-oxidizing Biocides to Control Sulfate-Reducing Bacteria on a Produced Water Injection Plant*. in *CORROSION 2015*. 2015. Dallas, Texas, USA: NACE International.

446. Machuca, L.L., R. Jeffrey, S.I. Bailey, R. Gubner, E.L. Watkin, M.P. Ginige, A.H. Kaksonen, and K. Heidersbach, *Filtration–UV irradiation as an option for mitigating the risk of microbiologically influenced corrosion of subsea construction alloys in seawater.* Corrosion Science, 2014. **79**: p. 89-99.

447. Mori, K., H. Tsurumaru, and S. Harayama, *Iron corrosion activity of anaerobic hydrogen-consuming microorganisms isolated from oil facilities.* Journal of bioscience and bioengineering, 2010. **110**(4): p. 426-430.

448. Nithila, S.R., B. Anandkumar, S. Vanithakumari, R. George, U.K. Mudali, and R. Dayal, *Studies to control biofilm formation by coupling ultrasonication of natural waters and anodization of titanium.* Ultrasonics sonochemistry, 2014. **21**(1): p. 189-199.

449. Liu, H., T. Gu, G. Zhang, Y. Cheng, H. Wang, and H. Liu, *The effect of magneticfield on biomineralization and corrosion behavior of carbon steel induced by iron-oxidizing bacteria.* Corrosion Science, 2016. **102**: p. 93-102.

450. Tan, J., P.C. Goh, and D. Blackwood, *Influence of H2S-producing chemical species in culture medium and energy source starvation on carbon steel corrosion caused by methanogens.* Corrosion Science, 2017. **119**: p. 102-111.

451. Machuca, L.L., K. Lepkova, and A. Petroski, *Corrosion of carbon steel in the presence of oilfield deposit and thiosulphate-reducing bacteria in CO2 environment.* Corrosion Science, 2017. **129**: p. 16-25.

452. Wang, X. and R.E. Melchers, *Corrosion of carbon steel in presence of mixed deposits under stagnant seawater conditions.* Journal of Loss Prevention in the Process Industries, 2017. **45**: p. 29-42.

APPENDIX A

POLARIZATION PLOTS

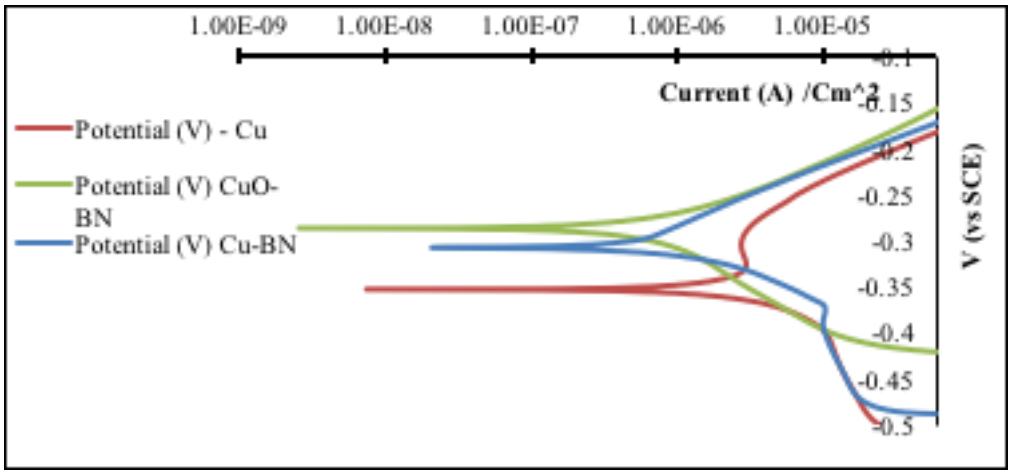

Figure 42. Polarization scan at 12-hour immersion in a 3 - electrode setup using SCE reference

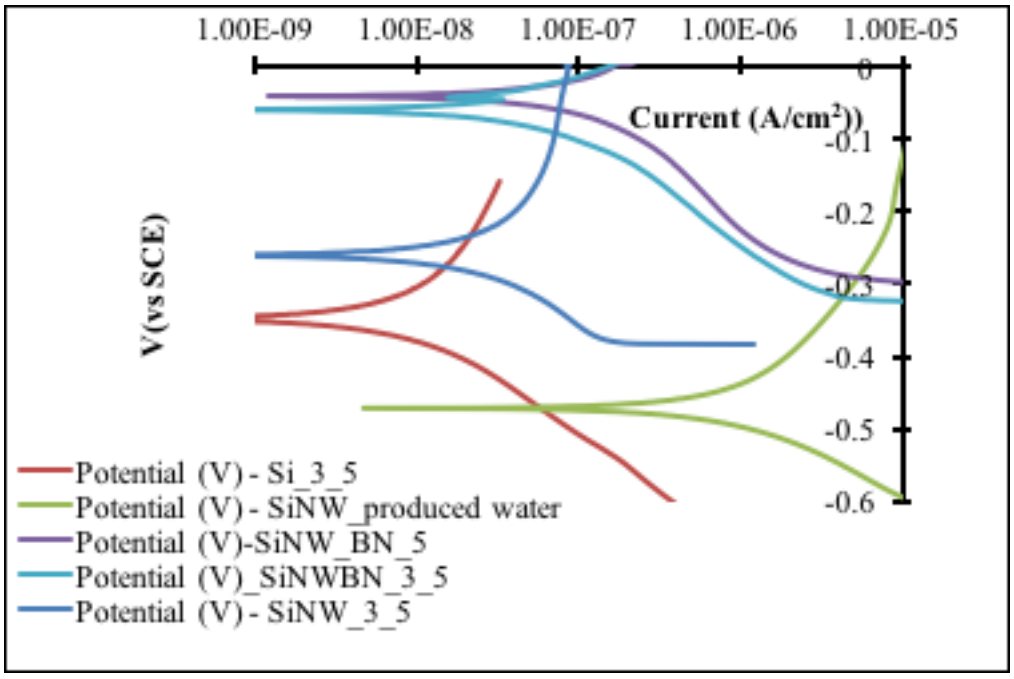

Figure 43. Polarization scan at 12-hour immersion in a 3 - electrode setup using SCE reference

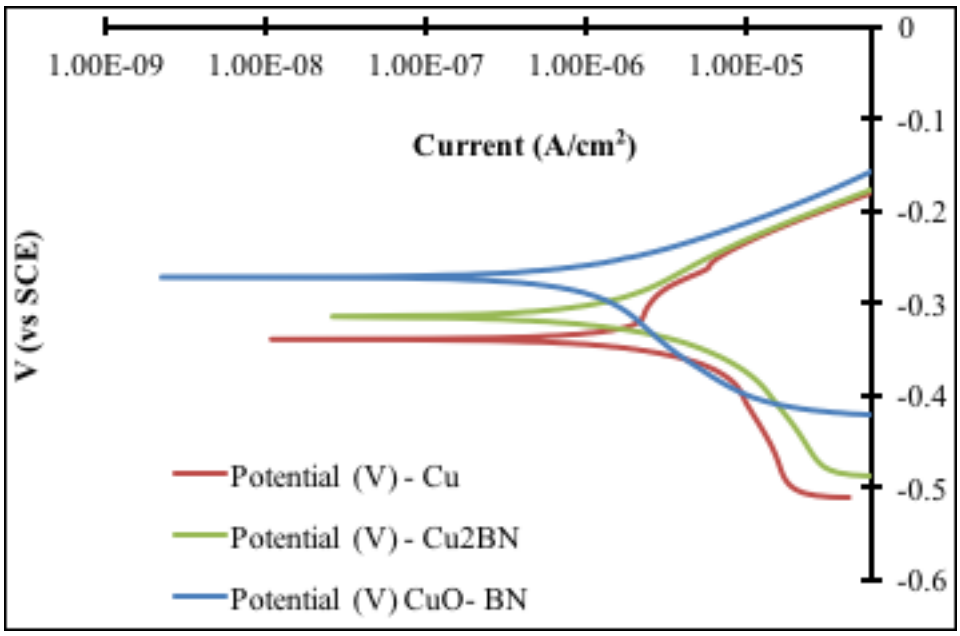

Figure 44. Polarization scan at 24-hour immersion in a 3 - electrode setup using SCE reference

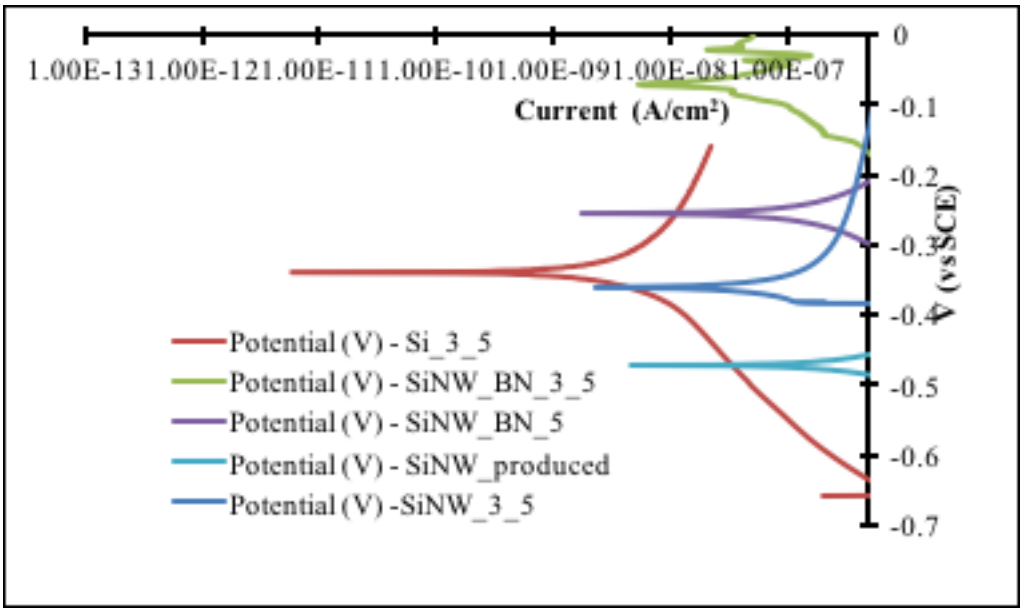

Figure 45. Polarization scan at 24-hour immersion in a 3 - electrode setup using SCE reference

APPENDIX B

ELECTROCHEMICAL IMPEDANCE SPECTROSCOPY AND EQUIVALENT CIRCUITS

FITTING USING ZSIMPWIN

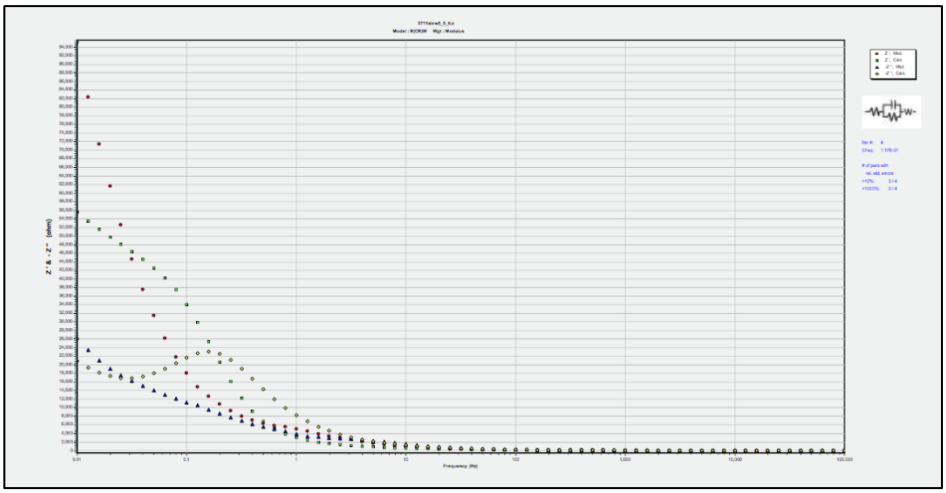

Figure 46. Example of a Bode phase and magnitude plot fitting with experimental impedance data fitting using Zsimpwin 3.60 with RCRW model

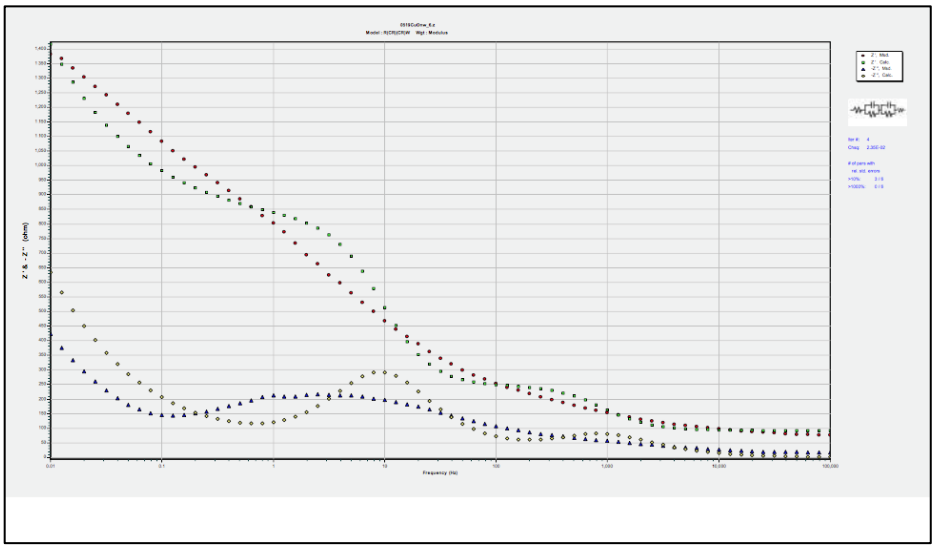

Figure 47. Example of the fitting of an equivalent circuit with experimental impedance data to a RCRCRW circuit with the deviation between experimental and calculated values observed at lower frequencies

APPENDIX C

SUMMARY OF RESULTS FROM ANALYTICAL TOOLS EMPLOYED FOR MIC STUDY OF ENGINEERING MATERIALS USED IN THE OIL AND GAS INDUSTRY WITH RESULTS FROM THE CHARACTERIZATION AND THE INFERRED CONCLUSIONS OF 23 STUDIES.

No.	Material	Type of Characterization	Result from the Characterization	Overall Conclusion
1	2304 DSS[60]	Morphological	FESEM was used to characterize the adhesion of *P.aeruginosa* cells on the coupon. The rod-shaped cells were 1 -3 µm in length and pitting was observed below the biofilm after 14 days. CLSM images after live/dead staining showed dense biofilms at 7 –days, with increase in sparseness and porosity at 14 days with a reduction in thickness from 59.1 µm to 47.5 µm. The average pit depth in the biotic environment was 5.6+/-2.4 µm as compared to 3.1 +/- 1.0 µm in the abiotic control	The presence of aerobic marine *P.aeruginosa* biofilm was implicated in the MIC of 2304 DSS. It was concluded that the formation of hexavalent chromium by the catalysis enabled by the biofilm as a contributing cause of severe pitting corrosion.
		Chemical/Instrumented	EDS analysis showed elemental content in not change after 14 days of immersion indicating stable passive films, with increase in organic elements on the surface (C/N) due to the biofilm proliferation. HR-XPS spectra indicated the presence of hexavalent chromium in the abiotic coupon, and a relative increase of Fe from 9.5% to 34.7 % in the biotic sample	
		Electrochemical	Polarization resistance testing provide a R_P value of 10kΩ cm^2 in the presence of *P.aeruginosa* indicating severe MIC attack. EFM monitoring indicated an increase from 0.029 mm/year to 0.216 mm/year corrosion rate for the biotic environment validating the polarization results. EIS analysis indicated an increased diameter in the capacitive semi circles at the 4-7 and	

			14-day time points, indicating influence of the biofilm on the surface. Polarization curves indicating a significant increase (76.5 times higher) of the corrosion current density in the presence of *P.aeruginosa* as compared to the abiotic control. Pitting potential also shifted in the negative direction indicating film breakdown.	
2	2707 HDSS[61]	Morphological	Optical micrograph revealed the microstructures containing 50% of austenite and ferrite phases. CLSM and SEM images indicated dense biofilm coverage after 7 days with decrease in coverage at 14 days. Average pit depth at 7 days was 0.42 +/- µm and 0.52 +/- µm at 14 days.	Aggressive MIC pitting corrosion was found on the surface of 2707 HDSS but was found to be more resistant as compared to 2205 DSS.
		Electrochemical	OCP vs. time data revealed significant variations in OCP in the initial 24 hours, with E_{OCP} stable at ~-228 mV (vs. SCE) for the *P.aeruginosa* exposed coupon compared to -442 mV (Vs.SCE) for the abiotic control. Corrosion rate obtained with polarization curves determined the corrosion current density for the biotic environment to be four times the abiotic sample (0.328 vs. 0.087 µA cm^{-2}). LPR study revealed a iCorr value for the *P.aeruginosa* was higher by 1 order of magnitude as compared to the abiotic control. EIS analysis revealed a decrease in the Nyquist loop diameter in the presence of *P.aeruginosa.* An increase in total impedance magnitude was observed in the Bode plots.	
		Chemical/Instrumented	EDS analysis revealed higher amounts of C,N,O,P in the biofilm and corrosion products as compared to the bare metal. High levels of Cr and Fe in the biofilm indicated loss of metal due to corrosion. XPS analysis revealed the presence of Cr^{6+} and a relatively higher portion of $Cr(OH)_3$ beneath the biofilm as compared to the abiotic coupons.	
3	2205 DSS[64]	Morphological	FESEM revealed bacterial adhesion in specific regions with complete coverage by biofilm in 30 days.	2205 DSS alloys were observed to be susceptible to MIC by *Pseudoalteromonas sp*
		Electrochemical	E_{OCP} in the presence of bacteria *(Pseudoalteromonas sp)* showed an initial shift towards negative direction reaching a	

			constant value of -0.41V vs.SCE after 5 days.	in artificial sea water environment.
		Chemical/Instrumented	**EDS analysis revealed high carbon concentrations and low Cr concentration in the biofilm. Depletion in Cr and Fe in cracks revealed the effect of biofilms on the alloy microstructure.**	
4	Pd [155]	Morphological	SEM was used to characterize the *D.desulfuricans* morphologically, involved sample preparation including fixing of biofilm with glutaraldehyde and osmium tetroxide, followed by dehydration and the metallized with gold. The characterization was used to show that the biofilm development was efficient, regardless of polarization. The combination of SEM and EDS showed high sulfur content and small heaps with the compound kansite which has poor protective properties.	SRB activity was evaluated using the hydrogen permeation technique and is shown to be useful for mechanism studies. It increases hydrogen permeation significantly and the electrode is susceptible to hydrogen embrittlement
		Electrochemical	Permeation current measurement was done using oxidation at 300 mV vs. standard calomel electrode.	
5	316 SS [156]	Morphological	SEM and EDS together of the bottom surfaces of the pits (Along the cross section of the sample) covered with a layer consisting of fiber like long rod shaped particles. The SEM observation allowed to observe the bottom surface and the rod like particles, The EDS analysis showed large amounts of organic matter in the slime, the SEM showed that the typical seawater bacteria was only observed, The EDS analysis with the high concentration of S and Fe indicated the type of microorganism may *be desulfovibrio desulfuricans* as well cited in the literature	Based on the combined FTIR, SEM and EDS measurement along with the severe positive in the microbiological assay it was implied that MIC had a role to play in the corrosion of the plugs.
		Biological	FGS Microbiological test kit analysis was done and it registered a severe level of anaerobic bacteria condition,	
		Instrumented/Materials characterization	FTIR analysis was done on the scale deposit at the bottom of the heat exchanger, The analysis showed typical bond presence of the calcium carbonate and calcium chloride	

6	C-Steel[27]	Electrochemical	Surface mapping was carried out using two microelectrodes for measuring current around corrosion pits. The carbon steel coupon was incubated in a SRB culture and the mapping of the surface current density was carried out periodically to generate maps	The utilization of the probe allows for the detection of bio-corrosion pits and accurate corrosion rate determination
7	Type 304L SS, Type 316L SS, Ni-Cr Alloy (UNS No.7718) Beryllium, Aluminum 6061-T6, Zirconium alloy (UNS 60804), Carbon steel and duplex SS (UNS S32550) [396]	Biological	Examination of the coupons and the soil showed the presence of heterotrophs (1 year coupons), which produce organic acid. SRB was found in the soil but not on the coupon, for the 3 year coupon there was colonizing by the SRB on some of the carbon steel, aluminum and beryllium coupons	Carbon steel and beryllium showed highest corrosion rates, corrosion rate of aluminum, austenitic S.S (type 304 L and type 316 L), Ni-Cr alloy and duplex S.S was low but detectable after 3 years. Corrosion rates of Zr alloy were very low and below detection limits. Pit characterization was not performed. By inference it was concluded that MIC potential was there, since there was organic acids and colonization
		Instrumented/Materials characterization	Environmental factors such as soil resistivity (ASTM G 57) were reported, soil was found to be mildly alkaline. Temperature was also measured at around 40 F	
8	Carbon steel [397]	Morphological	Surface analysis was performed with SEM and EDS, to observe the surface of the steel coupons, Dense sulphide film observed after 148 days, bacterial cells on the surface, further removal of the film exposed large pits	Multidisciplinary approach required combining microbiological, electrochemical and microscopic approach
		Modeling	The Cathodic protection used to protect the pipe was disbonded and numerical modeling using two dimensional boundary element method was done	

		Electrochemical	TFER probe used to monitor the corrosion in the buried soil environment ,It was observed on the basis of data the larger the population of the bacteria more is the corrosion rate, MIC risk assessed in short term	
9	Stainless steel (UNS S31803) Nickel alloy (UNS N08825)[398]	Morphological	Fluorescence microscopy images revealed the attachment of biological material that was distributed along the outer edge of the crevice area, with limited attachment in the crevice area. Microbial colonization was found to be patchy	The crevice corrosion was found to be affected by the biofilm in the presence of oxygen. Biofilms developed under anaerobic conditions were found to be more potent than aerobically grown biofilms
		Electrochemical	The alloys maintained under open circuit conditions did not lead to corrosion initiation regardless of oxygen concentration or biofilm coverage. Ennoblement of the nickel alloy likely initiated crevice corrosion, where the stainless steel remained protected until a trans-passive region was reached	
		Biological	PCR-DGGE analysis and DNA sequencing data indicated that biofilm diversity was higher under aerobic conditions than under anaerobic conditions. The stainless steel alloy showed higher biodiversity in aerobic conditions and the nickel alloy showed higher biodiversity under anaerobic conditions	
10	X65 carbon steel coupons [399]	Morphological	SEM images of the incubated coupons showed kidney bean shaped Srb cells and an EDS analysis showed the presence of Iron sulfide- pits characteristic of the MIC attack was seen after cleaning the coupon	A framework for laboratory testing of hydro testing water was developed. Offshore seawater samples was found to have insufficient inoculum, and hence enriched inoculum was used in the lab scale environment for accelerated testing
		Biological	The total organic carbon was measured in the seawater and it was found in the range of 1 to 2 ppm for typical seawater, the Qurrayah (SA) water had organic content 500 times higher than comparable seawater	
		Modeling	By using charge transfer and mass transfer theories and electrochemical kinetics a mechanistic model has been created and solved numerically. A single pit depth was used to model the biofilm aggressiveness, further validations required	

11	API 5L X-70 carbon steel [39]	Morphological	FESEM was used to after drying with supercritical CO2 and gold coating. Typical SRB cells (1.5 to 2.0 micrometer samples were observed) and the cleaned surface analysis showed pits of 20 micrometer. EDS analysis of the corrosion product revealed sulfur and iron peaks and oxygen peaks, Pitting corrosion was observed and the SRB could be seen on the surface	The SRB activity was more related to corrosion than the SRB itself, the ennoblement of the surface was observed along with pitting corrosion morphologies. The study allows for the use of a laboratory strain to observe similar results as the field
		Biological	Cell counts were taken with planktonic cell enumeration done to enumerate the growth of the bacteria	
		Electrochemical	Open circuit potential was obtained and the experiments were conducted in an ASTM standard cell. Polarization curves were also taken and extrapolated to observe the effect on the corrosion, SRB growth shifted the E_{corr} to a more positive value - ennoblement of the surface was observed - Polarization curves (tafel plots) showed increase in I_{corr} with time (21 days more than 7)	
12	SAE 1018 carbon steel corrosion [50]	Morphological	SEM was used to study the biofilms after varied times of incubation, Morphological analysis showed well defined architecture with protection of the cells by the EPS	Study of biofilm production was done and it was observed that biofilm production was enhanced is dissimilative conditions - analysis of equivalent circuits helped propose mechanisms of steel oxidation - strong adhesion to carbon steel
		Instrumented/Materials characterization	EIS was done to study evolution of the electrochemical interfaces to compare the polished S.S and S.S in incubated medium. 3 cell configuration was used, Nyquist plots to obtain the impedance values and bod phase angle plots were generated, observations include an increase in the impedance values with biofilm growth which may indicate passivation or steel surface modification, observations such as biofilm aging were also obtained.	

13	316 L seawater pipeline [68]	Morphological	Visual examination - shallow pits at the weld (heat affected zone) , leaky regions confined to 5 to 7 PM position in ID ,Pit morphology (shallow pits) clearly indicated MIC, sulfide stringers indicate favorable sites for attack	EPMA allowed for chemical signature of the pit to be obtained and inferred that it was MIC in action
		Biological	Microbial analysis using bacterial culturing indicated SRB apart from nitrogen manganese and iron oxidizing bacteria	
		Electrochemical	Electron probe microanalysis was done across the cross section of the pitted region, Profiles indicated decrease in chromium content within the pit and decrease in iron content at the edge of the pit	
14	Cu - 10 % Nickel alloy [72]	Morphological	SEM analysis was done, dense populations of various kinds of bacterial cells bacilli, vibrio's and filamentous bacilli was entrapped amongst the corrosion products , EDX analysis was also performed, SEM analysis showed that chlorine had an important effect on Cu_2O development. Hemispherical MIC holes were seen , chlorinated water showed severe localized and general corrosion , EDX analysis reveals sloughing off of the deposits	Chlorination increased corrosion by increasing oxidative capacity, and should be restricted for treatment of MIC of copper alloys
		Biological	Pretreatment planktonic and sessile counts were taken, also the sulphate concentrations indicated high loads (223 to 720 ppm) which provide for a good environment for the heightened activity	
		Electrochemical	Open circuit potential, cyclic polarization and the polarization resistance were measured ,OCP showed peak movement -may be attributed to biofilm movement , and localized corrosion dynamics , PR in untreated water is less than treated water, CP tests negative hysteresis at high current density (10 micrometer/cm2. greater corrosion density in chlorinated water as compared to un chlorinated water	

15	Carbon steel [24]	Morphological	The cleaned surfaces were examined using optical micrographs at various magnifications (50 100 X), laser profilometer and also SEM,SEM photographs do show the pit formation and the biofilm which was produced	Carbon steel susceptible to corrosion in synthetic produced water and in water containing dissolved CO2 alone or SRB alone , susceptibility for synergistic effect was seen maximum at 10 % concentration CO2
		Biological	Bacteria was counted using serial dilution technique by detaching the biofilm from the coupon, also by enumerating the SRB concentration from produced water and planktonic initial and final and sessile final was taken from each of the runs, Synergistic effect observed at a concentration of 10 percent CO_2 , CO_2 concentration was seen affecting the SRB growth at higher concentrations and at no CO_2 it was primarily seen to be SRB alone	
		Instrumented/Materials characterization	Mass loss measurements were primarily taken to determine the corrosion rates, concentration of sulphates pH sulphide calcium and magnesium, iron were also measured. EDS was taken , XRD also showed the elemental composition of the coupons, EDS showed the presence of FeS $CaCO_3$ and $MgCO_3$, XRD showed the elemental composition of the coupons change with the change in the environment, with $MgCO_3$ formation in CO_2 only and FeS formation in the sulfide SRB inoculated and SRB + CO_2 inoculated	
16	Carbon steel alloys [178]	Morphological	The study was done using an ESEM and EDS, EDS revealed that the corrosion deposits mainly contained iron and sulfur, The incubation was for between 7 and 42 days. It was seen that the pits were of more depth in the 5XL52 alloys	It was seen form the three pronged analysis that the ENM, EIS was in good agreement with

		Instrumented/Materials characterization	The Ecorr was monitored for the first 7 days and it was observed that there was a steep decrease after the first 40 - 54 hours, EIS was also performed to obtain the bode and Nyquist plots, Ecorr decrease This was attributed to the establishment of the biofilm, accumulation of the metabolic products - The data from the EIS showed that there were other electrochemical transfer processes in play other than metal oxidation and sulfides or some other metabolic product accelerated the anodic reaction.	the Ecorr and Rp techniques and that that there was susceptibility for corrosion of the API 5XL52 alloy. Moreover EIS was able to differentiate the corrosion process taking place in different media
17	Niobium bearing stainless steel [400]	Morphological	SEM and XRD were performed to get an insight into the change in the surface- Chloride solutions pit the surface and hence this had to be analyzed, The SEM showed that the surface distribution improved with the addition of niobium, with no pitting cracking found after two weeks of immersion in 3.5% Sodium Chloride (NaCl)	The cold deformation increased corrosion resistance up to 23% and the percentage of niobium increased corrosion protection of austenitic stainless steel
		Electrochemical	EIS and polarization curves were generated, EIS data showed that the 1.24% niobium metal had the best corrosion protection	
18	Mild steel [47]	Morphological	SEM was performed along with EDS and on samples which were incubated over 21 days after the removal of the deposits, The pits generated in the lactate/sulfate were uniform in shape and the lactate/nitrate medium was bigger in size and more random	Lab scale studies to identify the effect of the media
		Electrochemical	Open circuit potential was measured / potentiodynamic measurements and redox measurements were also taken, OCV showed that the increase is more rapid in the lactate nitrate media and slower in the lactate sulphate media - Potentiodynamic measurements showed that the Ecorr and Icorr changed dramatically in the lactate/nitrate media as compared to the lactate/sulfate media	

19	Copper tubing [401]	Morphological	The surface analysis was performed using a CLSM, the bacterial samples were stained and then used, The CLSM allowed for study both of the substrate and the biofilm formation in tandem (as against the SEM in which the biofilm needs to be removed in order to study the base layer)	The images confirmed the heterogeneity of the biofilm and the CLSM presented a good way to look at the microenvironment as against the techniques such as SEM and AFM
		Biological	Bacterial metabolic activity was analyzed using CDF and RITC to analyses the bacteria	
			The biofilm samples were collected from 21 sites and DNA extraction was performed and PCR was performed. Screening of functional genes and specific bacterial groups were identified,2500 sequences were analyzed representing one of the largest surveys - proteobacteria was the most abundant phylum present, there was also archaea and fungi identified apart from methanotrophs - the phylogenetic diversity was connected to the metabolic diversity	
20	Carbon steel st3S[402]	Morphological	SEM images were taken of the coupons - placed at various locations- EDS analysis was also performed on the corrosion products, The at the water fuel interphase showed the most aggressive corrosion (uniform) EDS analysis showed the presence of iron in the products - over a period of 47 days the tests was performed - at the water fuel interphase Surface of the coupons characterized by pits up to 130 micrometer deep	Studies on the corrosion of the steel using feel water interface was studied and it was recommended that the tanks should be mixed and cleaned well - and the whole installation needs to be maintained well
		Biological	Chemical analysis of the water followed various parameters such as COD, ether extract, and total nitrogen. The microbiological assay detection was done on the basis of the standards such as API 20E, API 20NE and API STAPH ,The microbiological assay showed various species such as iron bacteria, fungi and SRB (only CFU/ml) values were available	

21	304L - Cu SS [403]	Morphological	SEM image was taken also the maximum pit depth profiles was taken with a CLSM , XPS was also taken ,SEM image of the surface showed a maximum pit depth reduction of 38% for the copper alloyed SS. The surface roughness was two times as the 304LSS cu alloys. There was a change in the valence state of Cu which may indicate why the corrosion process had slowed down Possible causes for the prevention of corrosion is the release of copper ions or the presence of a Cu_2O layer which was formed on the surface	The presence of Cu resulted in less formation of *E.coli* and pitting corrosion - The passivation is linked to formation of oxide - significant reduction in the risk of bio corrosion
		Electrochemical	OCV values were taken and also polarization techniques were used to analyses the sample, The open circuit voltage used to characterize the MIC behavior showed that the value was 100 mV higher for the 304L-Cu SS than for the 304L- Cu. Potentiodynamic curves showed that the Ecorr value decreased rapidly for the sample without Cu than for the sample with Cu	
22	1018 Carbon Steel [219]	Biological	LASCA mass spectroscopic imaging combined with metabolomic HPLC was obtained with 3000 features for anaerobic incubation and 1500 features for aerobic incubation. Spatial distributions of metabolites/organic residues were obtained to identify localized concentrations. Abundances of glycophospholipids, as well as metabolites relating to amino acid metabolism were observed.	In the anaerobic exposure study strong correlations were observed between the biofilm metabolome and the occurrence of corrosion, and no correlation was detected for the aerobic sample
		Instrumented	3D non-contact axial chromatism profilometry was performed and roughness in the range of 0 to 260 μm was observed on the anaerobically incubated sample and 0 to 35 μm was observed for the aerobically incubated sample	

23	Stainless steel alloys UNS S31803 UNS N08825 [168]	Electrochemical	Cyclic polarization scans were conducted with a final voltage of -0.1 V vs. E_{corr}. Under anaerobic conditions a shift of E_{corr} towards negative values over 30 days (300 mV lower) was observed. On exposure to aerated water the E_{corr} showed stability. For UNS N08825 alloys the anaerobic test yielded negative values of -100 mV, however under aerobic conditions it moved towards positive values. The cyclic polarization curve for UNS 31803 alloy under anaerobic conditions yielded linear increase with potential in the anodic scan. In the case of UNS N08825 alloys no passivation region was observed.	Passivity breakdown was observed due to crevice corrosion and it was found to be initiated by the ennoblement of the E_{corr}. Crevice corrosion was found to be more severe under total anaerobic conditions and was exacerbated by the biofilm only under external polarization
		Morphological	Surface images obtained by optical microscopy indicated crevice attack was restricted to border areas, and anaerobic conditions were found to be more aggressive than aerobic conditions	
		Biological	PCR-DGGE analysis of the 16S rRNA gene fragments was carried out along with DNA sequencing. The biofilm composition was strongly dependent on the oxygen concentration of the environment and only *Marinovum algicola* was encountered in both the samples with all other populations highly specific to their microenvironments	

APPENDIX D

SUMMARY OF ANALYTICAL TECHNIQUES USED FOR THE STUDY OF MICROBIOLOGICALLY INFLUENCED CORROSION IN MATERIALS/SYSTEMS DEPLOYED IN THE OIL AND GAS INDUSTRY

Study/(Title of the paper/report)	**Substr-ate**	***Microbiota***	**Context**	**Year**	**SEM**	**EDS/EDAX**	**IR/FTIR/Raman/UV - Vis**	**XPS**	**TEM**	**XRD**	**PCR**	**MPN**	**CLSM/Fluorescence microscopy**	**Gravimetric**	**OCV**	**EIS**	**Potentiodynamic**	**EN**	**Profilometer**	**Others (Specialized techniques)**
Microbial Corrosion of 2205 Duplex Stainless Steel in Oilfield Produced Water[62]	2205 Duplex stainless steel	*Oilfield produced water*	Investigation of MIC of SS in simulated oilfield produced water	2017	1	1									1	1	1			Optical micrograph
Corrosion behaviour of 2205 duplex stainless steel in pure cultures of sulphate reducing bacteria: SEM studies, electrochemical characterisation and biochemical analyses[63]	2205 Duplex stainless steel	*Desulfovibrio desulfuricans*	Effect of biofilm and corrosion behavior on stainless steel	2017	1										1		1			Total protein concentration
Microbial corrosion of AL 2024 alloy[404]	Aluminum alloy - AA 2024	*Bacillus Cereus ACE4 and Serratia Marcescens ACE2*	MIC and electrochemical behavior of Aluminum alloy in presence of hydrocarbon degrading bacteria	2010															1	Bacterial adhesion to hydrocarbon assay

MIC of 304 Stainless steel [145]	304 stainless steel	*Aerobic pseudomonas NCIMB2021*	MIC study of stainless steel under aerobic conditions with pseudomonas	2007																
Corrosion of antibacterial Cu-bearing 316L stainless steels in the presence of sulfate reducing bacteria[67]	Cu-bearing 316L stainless steel	*Sulfate reducing bacteria*	Evaluation of corrosion resistance to SRB	2018	1	1		1							1	1	1			
A comparative study of corrosion of 316L stainless steel in biotic and abiotic sulfide environments[160]	316 L Stainless steel	*SRB media (extracted from oil sludge)*	Comparison of corrosion in biotic and abiotic environments	2017	1	1							1				1		1	Cyclic voltammograms
Geo bacter enhances pit depth on 304L stainless steel in an electron donor scarce media[168]	304 L stainless steel	*Geobacter sulfurreducens*	The effect on the corrosion of stainless steel in acetate rich and deficient media was evaluated to explain pitting corrosion observed	2009																
Anaerobic Corrosion of 304 Stainless Steel Caused by the *Pseudomonas aeruginosa* Biofilm[59]	304 stainless steel	*Pseudomonas aeruginosa*	Anaerobic corrosion under *Pseudomonas aeruginosa biofilm*	2017	1					1		1	1			1	1			Infinite focus microscope
The effect of metal microstructure on attachment of bacteria[405]	1010 Carbon steel	*Escherichia coli*	The effect of metallurgical features on the attachment of bacteria to metal surfaces was studied	2013																Optical microscopy
Corrosion behavior of carbon steel in the presence of algae[406]	Carbon steel (Q235)	*Chlorella vulgaris*	The investigation of algae on the corrosion rate was performed and the impact of photosynthetic mechanisms on corrosion was observed	2015																
Crevice corrosion in duplex stainless steel [398, 407]	Duplex stainless steel (UNS S31803)	*Naturally occurring marine bacteria*	Artificially creviced stainless steel was used in an immersion test to	2012																DGGE, Optical micrograph

			investigate the impact of naturally formed biofilm on crevice corrosion																	
Field study of MIC in mooring chains[408]	Steel (C0100)	*Gulf of guinea sea water*	A case study of MIC of mooring chains to develop mitigation methods using a microbial baiting kit	2016																DGGE
Effect of soil microfloras on copper corrosion[118]	Copper	*Actinomyces, fungi and bacteria from enrichment cultivation*	Copper corrosion was compared between three micro floras. Pitting and cratering was observed with bacterial groups showing aggressive behavior	2016																
Corrosion of carbon steel C1010 by iron oxidizing bacteria[48]	Carbon steel C1010	*Acidithiobacillus ferrooxidans*	Corrosion behavior was investigated with severe pitting observed on the surface of the C1010 coupons	2014																pH measurement, confocal microscopy, Ion determination assay
Anaerobic metabolism of biodiesel and its impact on corrosion[409]	Carbon steel	*Aquifer sediments, alkane degrading consortia, marine oil degrading consortia, unenriched natural ballast water, natural coastal seawater*	The suspectibility of biodiesel in anaerobic conditions was evaluated for a time period of 1 month in naturally occurring microbial consortia	**2010**																**GC-MS, H_2S concentration measurement**
Corrosion behavior of copper in sulfide containing solutions[410]	Copper	*Desulfovibrio sp*	Effect of SRB on corrosion behavior of copper in sulfide containing solutions	2015																Copper - inductively coupled plasma, EPS extraction

																			and carbohydrate analysis
Evaluation of MIC inhibition on Ni-Co coatings [411]	Ni-Co alloy coatings	*Aeromonas Salmonicida and Clavibacter michiganensis*	MIC inhibition study on Ni-Co alloy	2012															Quartz crystal microbalance (QCM)
MIC in stainless heat exchanger[412]	Stainless steel	*SRB*	MIC in a stainless steel heat exchanger was investigated (microstructural analysis)	2012															Optical microscopy
Effect of SRB on corrosion of carbon steel Q235[55]	Carbon steel Q235	*Soil extract solutions*	Study of SRB on the corrosion of the carbon steel under simulated disbonded coating in the soil extract solutions	2011															
MIC of copper pipes in low pH water[413]	Copper pipes	*Water sampled from Talca city, Chile*	Influence of microbial biofilms on the high copper levels measured in the drinking	2008															
Effect of biofilm on cast iron pipeline corrosion[192]	Cast iron	*Iron bacteria and iron reducing bacteria*	Cast iron pipeline corrosion by biofilms	2008															DGGE
Effect of SRB on the corrosion behavior of carbon steel[414]	D36 carbon steel	*Mixed SRB culture*	The effect of mixed culture SRB on carbon steel was studied	2007															pH monitoring
Microbiological corrosion of aluminum alloys[71]	Aluminum alloys - V65,D16 and D16T alloys	*Fungi and bacteria*	The bio corrosion was investigated on aluminum alloys from several fungi and bacteria	2006															Visual examination of corrosion and corrosion products, pH monitoring was conducted,

Pitting corrosion of carbon steel caused by iron bacteria[415]	1020 AISI Carbon steel	*Mixed Culture of iron oxidising bacteria*	Corrosion mechanism of 1020 AISI carbon steel in iron contaminated water	2001																	
AFM study of MIC of mild steel [416]	Mild steel	*Seawater from Victoria Harbor Hong Kong*	AFM study of MIC on corrosion of mild steel in a natural mixed culture media	1999																	
Corrosion of a drilling pipe steel in an environment SRB[51]	N-80 Steel	*Desulphovibrio sp*	MIC by SRB on drill pipe steel	1997																	
Production of sulfide minerals by SRB during MIC of copper[417]	99 Copper, 90Cu:10Ni, 70Cu:30Ni	*Mixed culture of facultative and obligate anaerobic bacteria*	Study of sulfide minerals by sulphate reducing bacteria during MIC of copper	1991																	
Effect of hydrogenase and mixed SRB on the corrosion of steel[93]	Steel	*Sulphate reducing bacteria (Mixed culture)*	Hydrogenase and mixed SRB culture effect on steel	1991																	Robbins Device/Active hydrogenase kit
Detection and mapping of SRB influenced corrosion of C-steel[27]	API 5L Carbon steel	*Desulfovibio gabonensis*	SRB influenced corrosion of carbon steel study	2002																	
Microbial corrosion of P235GH steel under geological conditions[418]	P235GH Steel	*SRB isolated form clay rock*	Corrosion of steel used for nuclear waste disposal	2010																	
EN noise study on the corrosion process of carbon steel by SRB [227]	SAE 1010 Carbon steel	*Desulfovibrio alaskensis*	EN noise study of the corrosion process of carbon steel by the SRB in a nutritionally rich and oligotrophic culture medium	2006																	
Effect of SRB metabolites on the corrosion of Q235 steels in 3.5% NaCl media[54]	Q235 steel	*EPS, sulfides*	The direct influence of two metabolites were investigated	2012																	

Aluminum AA2024 T351 aeronautical alloy - part 1 - MIC analysis[70]	Aluminum AA2024 T351 aeronautical alloy	*Hormoconis .resinae fungus*	Study of the elemental distribution of alloy elements with the MIC attack morphology	2008																	Drop test
Reversible acceleration of corrosion of stainless steel exposed to seawater induced growth [419]	AISI 304 Stainless steel	*V.natriegens, V.anguillarum*	The reversible corrosion of stainless steel by extracellular accumulations of SS exposed to seawater and non SR – marine bacteria	1986																	
Effect of chlorine bromine biocide treatment on carbon steel - srb[420]	Carbon steel	*SRB*	The effect of chlorine and bromine as biocide for carbon steel	1991																	
The effect of organic matter associated with the corrosion products on the corrosion of mild steel in the Arabian Sea[421]	Mild steel	*Arabian Sea (Natural culture)*	Effect of organic matter associated with corrosion of mild steel in the Arabian sea	1992																	Carbohydrate analysis, Water sampling (Titration)
Electrochemical and microbiological characterization of biofilm formation on stainless steel in Baltic seawater[422]	Austenitic stainless steel, Duplex stainless steel	*Mixed culture (Baltic seawater)*	Baltic seawater environment on stainless steel	1997																	
Improved Most-Probable-Number Method To Detect Sulfate- Reducing Bacteria with Natural Media and a Radiotracer[423]		*Desulfobulbus propionicus*	The MPN method was modified using a radio tracer, only the sediments were evaluated	1998																	

Mossbauer spectroscopy of corrosion products of mild steel due to MIC[424]	Mild steel	*Hydrogenase positive strain - Desulfovibrio desulfuricans and desulfovibrio vulgaris Hydrogenase negative strain - Desulfotomaculum orientis and Desulfotomaculum nigrificans*	Mossbauer spectroscopy of corrosion products of mild steel due to MIC	1999																Mossbauer spectroscopy
Influence of surface characteristics and microstructure on adhesion of bacterial cells on a type 304 S[58]	AISI 304 stainless steel	*Pseudomonas sp.*	Influence of surface characteristics and microstructure on bacterial adhesion	2002																Electrochemical potentiokinetic reactivation
Methanogen population in a marine biofilm corrosive carbon steel[43]	Mild steel	*Methanogens*	Methanogen population study in a corrosive mild steel	2003																FISH - Fluorescence in situ hybridization
Corrosion behavior of carbon steel influenced by SRB in soil environments[397]	X65 Carbon steel	*SRB active soil*	MIC study in soil environments induced by SRB	2003																Linear polarization resistance, and Corrosion potential/ Thin film electrical resistance
An impedance study on admiralty brass dezincification originated MIC[425]	Admiralty Brass (UNS C44500)	*Fresh water media from River Tagus in Spain*	Impedance study on dezincification of admiralty brass typically used in heat exchangers	2004																Kamers Kronig transforms for EIS study, Polarization resistance

Microbial consortium influence upon steel corrosion rate using polarization resistance and EN[426]	API XL52 steel coupons	*Mixed culture from marine region of PEMEX*	Electrochemical noise and polarization resistance techniques for microbial consortium influence on steel corrosion rate	2004																	
Influence of a dual species biofilm on the corrosion of mild steel [46]	1018 Mild steel coupons	*S.oneidensis MR-1 and D.desulfuricans*	The effect of a dual species biofilm on the corrosion of carbon steel using an iron reducer and sulfate reducer	2005																	
Microbial corrosion of galvanized steel by a freshwater strain of sulphate reducing bacteria [427]	Galvanized steel	*Desulfovibrio sp (isolated from cooling towers)*	The study of SRB on galvanized steel by corrosion coupons in anaerobic lab scale	2006																	Carbohydrate analysis
Biodegradation and corrosion behavior of manganese oxidizer *Bacillus Cereus* in diesel transporting pipeline[428]	API 5LX Steel	*Bacillus Cereus*	Study of manganese oxidizer bacteria in diesel transporting pipeline	2006																	
Bio corrosion of carbon steel alloys by an hydrogenotrophic SRB [178]	API - 5XL52 steel alloy and st-35.8 steel alloy	*Desulfovibrio capillatus*	Bio corrosion of carbon steel alloy from a SRB isolated from the field	2006																	Ecorr measurement
Microbial assisted SCC of carbon steel in mixed and pure culture of SRB[429]	Carbon steel	*Mixed and pure culture from Merimbula river estuary, Australia*	Microbiological environments containing pure and mixed cultures of SRB in SCC of carbon steel in biotic and abiotic environments was investigated	2006																	Slow strain rate tests/reflected light microscopy

Role of serratia marcescens ACE2 on diesel degradation and its influence on corrosion[430]	API 5LX steel	*Serratia Marcescens ACE2*	The effect of biota isolated from diesel pipeline	2007																GC-MS/Hydrogen peroxide and pH
Srb biofilm influence on active corrosion sites in steel electrolyte interface[263]	SAE Carbon steel - 1018	*Mixed culture of Desulfovibrio gabonensis and D. Capillatus*	Interface study of carbon steel exposed to artificial seawater with mixed SRB culture	2008																Gas secondary electrons detector for environmental mode
Accelerated low water corrosion of carbon steel in the presence of a biofilm harboring sulphate reducing and sulphate oxidising bacteria recovered from a marine sediment [431]	43 A - Carbon steel	*Sulphate reducing bacteria and sulphate oxidising bacteria*	Accelerated low water corrosion of carbon steel in the presence of a biofilm	2008																Linear polarization resistance and Inductively coupled plasma
Corrosion behavior of low alloy steel ion the presence of *desulfomaculum sp*[31]	Low alloy steel	*Desulfotomaculum sp*	Effect of SRB on corrosion of low alloy steel	2009																
Microbial corrosion of galvanized steel in a simulated recirculating cooling tower system[432]	Galvanized steel	*Mixed SRB culture*	Study of microbial corrosion of steel used in cooling towers over 10 month in a simulated environment	2009																Absorbance spectra (Biofilm quantification), Carbohydrate analysis
Characterizing the effect of carbon steel exposure in sulfide containing solutions[433]	Carbon steel	*Bacterial consortium*	Comparison between biotic and abiotic sulfide on carbon steel corrosion	2011																
Heterogeneous corrosion of mild steel under SRB biofilm characterized by electrochemical mapping[42]	Mild steel	*SRB*	Heterogeneous corrosion by SRB was studied	2011															1	

Characterizing the effect of carbon steel exposure in sulfide containing solutions to MIC[433]	X65 Carbon steel	*SRB consortia from oil well in western Canadian sedimentary basin*	A study of the electrochemical effects induced by inorganic sulfide and sulfate reducing bacteria on the corrosion of carbon steel	2011																	Optical microscopy
Microbial corrosion of Ni-Cu alloys by aeromonas eucrenophilia bacterium[434]	Ni - Cu alloy	*Aeromonas eucrenophilia*	Corrosion behavior of Ni - Cu alloys by aeromonas eucrenophilia bacterium	2011																	pH monitoring/ Quartz crystal microbalance
Neutrophilic IO and Mils steel corrosion in near shore marine environments[45]	Mild steel	*Zetaproteobacteria - Enriched from isolate obtained from Great salt bay, Newcastle*	Examination of a marine Iron oxidizing bacteria is involved in MIC	2011																	pH measurements Fe concentration/Eh redox potential
Correlation between the growth of mixed culture of SRB in produced water and the corrosion of carbon steel[435]	Carbon steel	*D.desulfuricans*	Produced water carbon steel corrosion	2012																	Rotating cage /optical microscopy
Corrosion of carbon steel under sequential aerobic and anaerobic conditions[436]	Carbon steel		Sequential aerobic - anaerobic conditions	2013																	Ion - Chromatography
Severe pitting corrosion caused by SRB on carbon steel and effect of surface roughness[437]	Carbon steel (UNS G10100)	*Desulfovibrio Vulgaris ATCC 7757*	Study of severe pitting corrosion by starving SRB on carbon steel including surface roughness	2013																	IFM - infinite focus microscopy and HPLC - supernatant
Long term desulfovibrio vulgaris on carbon steel and associated pitting corrosion[105]	Carbon steel	*Desulfovibrio vulgaris*	Long term SRB survival study under electron donor starvation	2015																	Ion exchange chromatography - for ion detection/Biofilm viability kit/pH measurement

Carbon source starvation triggered more aggressive corrosion against carbon steel by the desulfovibrio vulgaris biofilm[438]	C1018 Carbon steel	*Desulfovibrio Vulgaris (ATCC 7757)*	MIC mechanism study by using carbon source starvation triggering aggressive SRB related corrosion	2014																Infinite focus microscope profilometer/pH Measurement
An assessment of alternative diesel fuels' corrosion and microbiological contamination[409]	Carbon steel (C1020) Stainless steel (SS304L) Aluminum alloy (AA 5052)	*Niastella, Acinetobacter, Bacillus, Rhodotorula, Mycosphaerella Sphingomonas Aureobasidium Paecilomyces Rhodotorula*	Experiments were performed to evaluate nature and extent off MIC in conventional high sulfur diesels and alternative fuels including 100% biodiesel, ultra low sulfur diesels and blends	2010																pH measurements, DGGE-qPCR, optical micrograph
Two analytical techniques (AFM and ESEM) was used for the study of biofilms on steel surfaces[439]	Mild steel and AISI 316 stainless steel	*Marine SRB isolate (Indonesia and Portsmouth) Acidophilic microbial consortia*	AFM and ESEM were compared for the observation of the surfaces to reveal surface topography and deterioration	1996																
Complementary microorganisms in highly corrosive biofilms from an offshore oil production facility[110]	Steel pipe	*Biofilm from pipe carrying oily seawater*	Bacterial and archaeal community were investigated using genomic techniques and microbial taza and functional genes were identified.	2016																Optical micrography Automated ribosomal intergenic spacer analysis (ARISA) Illumina M1sequencing
MIC caused by consortia of bacteria and archaea in oil production facilities[74]	Carbon steel	*SRB, SRA, methanogens*	A case study of MIC in a HP separator at an oil production facility	2010																
Carbon steel corrosion in Northsea offshore seawater injection systems[440]	S235JR Carbon steel	*Anaerobic bacterium – genus Caminicella*	A case study on the influence of the sulfidogenic bacteria on a sea	2014																LPR, DGGE

			water injection system studied in a flow bioreactor operating anaerobically for 100 days																		
Corrosion of low carbon steel from pigging debris in water injection pipelines[441]	Low carbon steel (AISI S235JR)	*SRB and Clostridiales*	Microorganisms from the pigging debris were tested to analyze the effect on carbon steel	2014																	DGGE
Corrosion consequences of biodiesel and natural sea water mixture[442]	Carbon steel (C10200)	*Native bacteria from biodiesel and seawater samples*	The corrosion behavior was examined of unprotected carbon steel with pure diesel in the presence of natural coastal waters	2010																	LPR
The involvement of thermophilic archaea in the biocorrosion of pipelines was investigated [443]	-	*Thermophilic archaea strain PK and strain MG*	The physiological characteristics were investigated to reveal possible corrosive mechanisms	2012																	Ion Chromatography, Gas chromatography
Corrosive activities of fungi in a diesel – mild steel – aqueous system[444]	Mild steel (ASTM A 283 – 93 – C)	*Aspergillus fumigatus, Hormoconis resinae, Candida silvicola*	The degradation ability of the fungus along with the corrosion study of the metal substrate was investigated for 60 day incubation period	2005																	Solid phase micro extraction (SPME), GC-MS
Effect of fungus on magnesium alloy corrosion in artificial sea water [116]	Magnesium alloy AZ31B	*Aspergillus Niger*	The fungal threat to magnesium alloys was evaluated and pitting corrosion was observed	2015																	pH measurements
Effect of non-oxidizing biocides was evaluated in a produced water injection plant[445]	Carbon steel	*SRB*	The effectiveness of biocides was evaluated on	2015																	

			sessile SRB on carbon steel surfaces																	
Filtration – UV irradiation to mitigate MIC in subsea alloys in seawater [446]	Carbon steel, stainless steel, nickel base alloys	*Sea water (New South wales, Australia)*	The effect of filtration – UV irradiation of sea water on biofilm activity was evaluated	2013																DGGE, optical microscopy
Iron corrosion activity of anaerobic hydrogen consuming microorganisms isolated from oil facilities [447]	Iron granules	*Acetogens, sulphate reducing bacteria, methanogens isolated from oil facilities*	The study was used to establish that hydrogen consumption foes not strongly stimulate iron corrosion	2010																Gas chromatography
Online monitoring of corrosion behavior of alloys in a chlorinated condenser cooling circuit[193]	CuNi 70:30 and Al brass alloys	*Marinobacter, alteromonas, pseudomonas*	A case study of the role of microbiological components and the role played by biofouling deposition against passivity of the alloys																	BIOX electrochemical probe, DGGE, LPR
Biofilm formation prevention by ultra-sonication of natural waters[448]	Titanium	*Pseudomonas sp Flavobacterium sp Bacillus sp Micrococcus sp*	Investigation of anodization of titanium and biofilm formation density in ultra sonicated water	2014																
Effect of magnetic field on bio mineralization and corrosion behavior of carbon steel [449]	Carbon steel Q237	*Iron oxidizing bacteria isolate from oil field*	Investigation of magnetic field on corrosion behavior of carbon steel	2016																
Impact of fungi on morphology and structural properties of carbon steel[49]	Low carbon steel	*Penicillium palitans Arthrinium phaeospermum*	The consumption of chlorine by the fungi and the deposition of products on the surface was observed	2014																
The study of iron tubercles formed in fresh water was investigated[447]	Carbon steel	*Natural fresh water (estuary) exposure*	Structure and mineralogy of the corrosion products were investigated	2010																

Microbiologically influenced corrosion of C1018 carbon steel by nitrate reducing Pseudomonas aeruginosa biofilm under organic carbon starvation[53]	C1018 Carbon steel	*Pseudomonas aeruginosa*	The experimental data support for the BCSR theory was elicited	2017																Infinite Focus Microscope (IFM)
Microbiologically influenced corrosion behavior of S32654 super austenitic stainless steel in the presence of marine Pseudomonas aeruginosa biofilm[73]	S32654 super austenitic stainless steel	*Pseudomonas aeruginosa*	Investigation of pitting corrosion acceleration by bacteria	2017																
Onset of Microbial Influenced Corrosion (MIC) in Stainless Steel Exposed to Mixed Species Biofilms from Equatorial Seawater[143]	304 and 2507 Duplex stainless	*Equatorial seawater*	Investigation of the onset of MIC	2017																
Effect of sulphate-reducing bacteria on the microbiologically influenced corrosion of ten different metals using constant test conditions[220]	DH 36, 316, 904L, 254 SMO, 2507 SS, 2205 SS, CuNi 90:10; CuNi 70:30, Inconel 625, Titanium	*Desulfovibrio desulfuricans, in modified Baar's medium*	Study of MIC under same test conditions of alloys	2017																Optical Images
Influence of H2S-producing chemical species in culture medium and energy source starvation on carbon steel corrosion caused by methanogens[450]	Carbon steel	*Methanogens (M. barkeri, M. maripaludis)*	Biocorrosion of carbon steel by methanogens	2017																
Effects of biogenic H2S on the microbiologically influenced corrosion of C1018 carbon steel by sulfate reducing Desulfovibrio vulgaris biofilm [52]	C1018 Carbon steel	*Desulfovibrio vulgaris biofilm*	Study of biogenic sulfide	2018																Micro-GC
The influence of cathodic protection potential on	X70 Line pipe steel	*Desulfovibrio desulfuricans*	Effect of cathodic	2017																

the biofilm formation and corrosion behaviour of an X70 steel pipeline in sulfate reducing bacteria media[56]			protection on preventing MIC																	
Corrosion effect of Bacillus cereus on X80 pipeline steel in a Beijing soil environment[57]	X80 pipeline steel	*Bacillus cereus*	MIC study in a local soil environment	2018																
Corrosion of carbon steel in the presence of oilfield deposit and thiosulphate-reducing bacteria in CO2 environment[451]	Carbon steel	*Thiosulphate reducing bacteria*	MIC study with SRB in a CO_2 environment	2017																Gas Chromatography, Ion-Trap Mass Spectrometric, ICP-OES, AES
Corrosion of carbon steel in presence of mixed deposits under stagnant seawater conditions[452]	Carbon steel	*Natural sea water*	Corrosion of carbon steel under mixed deposits	2017																Linear variable differential transformer
Simulation of the marine environment using bioreactor for investigation of 2507 duplex stainless steel corrosion in the presence of marine isolated Bacillus Vietnamensis bacterium[69]	2507 Duplex stainless steel	*Bacillus Vietnamensis bacterium*	Bioreactor based study of MIC	2018																